Formation of Glycomimetics of *N*-Acetyl-D-Glucosamine, *N*-Acetyl-D-Quinavosamine, and *N*-Acetyl-D- and L-Fucosamine Using the Nitroglycal Method

By

Joseph G. Lisko

Submitted in Partial Fulfillment

of the Requirements

for the Degree of

Master of Science

in the Chemistry Program

SCHOOL OF GRADUATE STUDIES

YOUNGSTOWN STATE UNIVERSITY

May, 2002

Formation of Glycomimetics of *N*-Acetyl-D-Glucosamine, *N*-Acetyl-D-Quinavosamine, and *N*-Acetyl-D- and L-Fucosamine Using the Nitroglycal Method

Joseph G. Lisko

I hereby release this thesis to the public. I understand this thesis will be housed at the Circulation Desk of the University Library and will be available for public access. I also authorize the University or other individuals to make copies of this thesis as needed for scholarly research.

Signature: _____ 5-2-02

Joseph G. Lisko — Date

Approvals:

_____ 5/2/02

Dr. Peter Norris — Date
Thesis Advisor

_____ 5/2/02

Dr. John Jackson — Date
Committee Member

_____ May 2 '02

Dr. Jeffrey Smiley — Date
Committee Member

_____ 5/3/02

Dr. Peter J. Kasvinsky — Date
Dean of Graduate Studies

Thesis Abstract

This project involves the synthesis of amino sugar analogs that may potentially inhibit enzymes that construct the capsular polysaccharide of *Staphylococcus aureus* bacteria. Specifically, the syntheses of *N*-acetyl-D-glucosamine, *N*-acetyl-D-quinavosamine, *N*-acetyl-D-fucosamine, and *N*-acetyl-L-fucosamine analogs from readily available precursors were the targets of the research project. Methods and results for the formation of each of these compounds are described in detail.

Table of Contents

List of Schemes

List of Figures

Introduction

Staphylococcus aureus or "staph" is a bacterium most often found on the skin and in the nose and throat of over 50% of the world's population today.[1] *S. aureus* is responsible for many minor skin infections such as pimples or boils, but staph can also cause more serious and sometimes fatal infections.[2] For example, septicemia is a condition in which the blood is contaminated with bacterial toxins. If these toxins are not fought off by the immune system, septicemia can prove to be fatal. In 1991, septicemia was ranked as the 13th leading cause of death in the United States. The 2001 report of the survey of mortality in the United States showed that septicemia had moved to 10th with ~31,000 cases.[3] *S. aureus* strains can also be linked to toxic shock syndrome, which has proven to be a dangerous condition where patients in the hospital being treated for other ailments become infected with the bacterium. Because the patient's immune system is depleted, *S. aureus* infects the patient and causes further illness.[4]

Besides the many medical problems caused by "staph," strains of *S. aureus* bacteria have shown increasing resistance to traditional treatments.[5] Normally, *S. aureus* is treated with a penicillin antibiotic like methicillin or ampicillin, which prevented the construction of the bacterial cell wall. Recently, resistant strains of *S. aureus* have been found around the world. In the past when penicillins proved ineffective in treatment of *S. aureus* strains, vancomycin was prescribed. Until recently, vancomycin was considered the most versatile and effective antibiotic available, but strains of *S. aureus* are now showing resistance to this drug as well.[6] Nicolaou and coworkers have been investigating the synthesis of vancomycin analogs to combat the resistant strains of bacteria, including vancomycin-intermediate-resistant *S. aureus* (VISA). They reported significant

antibacterial activity towards those resistant strains of bacteria.[7] Although Nicolaou has found a few derivatives of vancomycin that will combat resistant strains of bacteria, continuing investigation must be performed because of the bacterias' ability to quickly become resistant to treatment.

Of the many different strains of *S. aureus*, Types 5 and 8 account for 22% and 53% of all the infections caused by the bacterium.[8] In types 5 and 8, the bacterium employs a capsular polysaccharide (CP), or protective coating that makes the bacterium undetectable by the immune system due to the inability of the immune system to make tight binding antibodies against carbohydrates. The CP of *S. aureus* types 5 and 8 is made up of repeating units (Figure 1) of amino sugar components composed of *N*-acetyl-2-amino-2-deoxy-D-mannopyranose uronic acid (D-ManAcA), *N*-acetyl-2-amino-2-deoxy-D-fucopyranose (D-FucNAc), and *N*-acetyl-2-amino-2-deoxy-L-fucopyranose (L-FucNAc) (Figure 2). Strains of types 5 and 8 differ only in the attachment points of other sugar units on the D-ManAcA residue. Although little is known about the biosynthesis of the CP of these strains of *S. aureus*, interrupting the construction of the CP may be an effective method of combating *S. aureus*. Without the protective capsular polysaccharide coating, the bacterium becomes susceptible to the immune system.

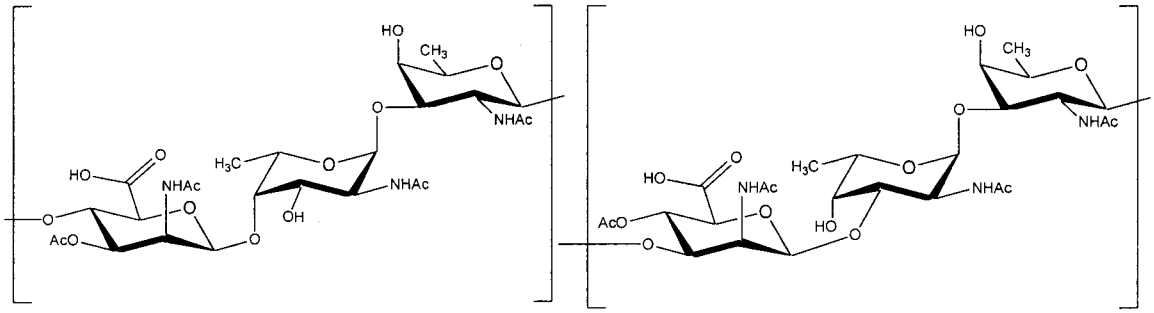

Serotype 5 Serotype 8

Figure 1: The repeating amino sugar chain of the *S. aureus* capsular polysaccharide.

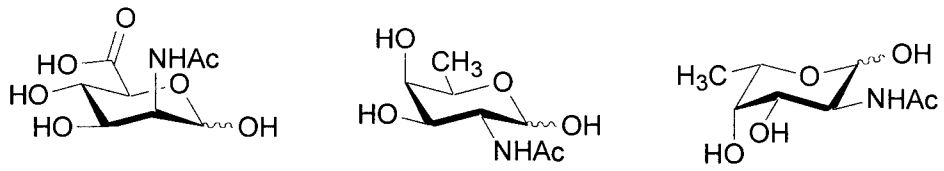

D-ManAcA D-FucNAc L-FucNAc

Figure 2: Amino sugar components of the *S. aureus* CP.

Despite the lack of information concerning the mechanism for CP construction in *S. aureus*, the biosynthesis of the CP for other bacteria has been studied extensively as part of the growing field of glycobiology. In general, the construction of the CP layer has been found to be mediated by enzymes, which include glycosyl transferases, glycosyl hydrolases and other miscellaneous enzymes. Transferases are responsible for linking carbohydrate units *via* glycosidic bonds, hydrolases selectively hydrolyze such bonds, and miscellaneous enzymes like epimerases and dehydrogenases alter functionality and stereochemical configuration on sites other than the anomeric carbon of the sugar. When working together simultaneously, these enzymes construct the CP layer with the appropriate configurations and functionalities needed by the bacterium (Scheme 1).[9, 10, 11]

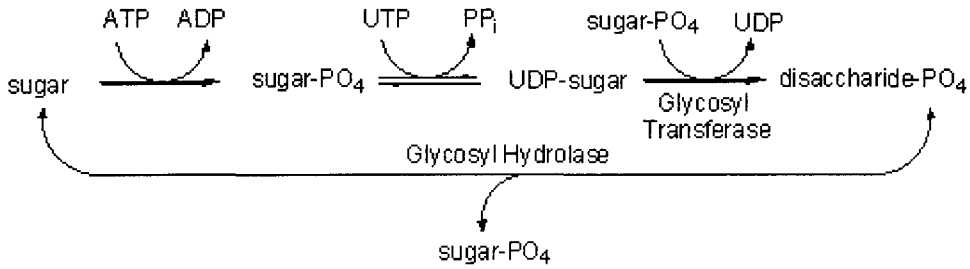

Scheme 1: Enzyme construction of biological oligiosaccharides

Because enzymes carry out the biosynthesis of the CP, these proteins become prime targets for inhibition. Glycomimetics, or sugar analogs that mimic the natural enzyme substrate, have proved to be effective in the elucidation of many enzyme mechanisms as well as the structure of those enzymes. Generally, there are two classes of mimics: those that compete with the natural substrate to be bound at the enzyme binding site, thus disrupting biosynthesis, and those that mimic the transition state formed during the formation or cleavage of the glycosidic linkage. Examples of glycomimetics include *C*-glycosides and iminosugars (often called azasugars). *C*-Glycosides employ a *C*-glycosidic bond that will not be hydrolyzed by a hydrolase, thus potentially inhibiting the biosynthetic process. Iminosugars by definition contain a nitrogen atom in the sugar ring where the oxygen atom normally lies. Unlike *C*-glycosides, iminosugars mimic the enzymatic transition state, and will bind to the enzyme and inhibit the biological process. For example, nojirimycin has been used as an effective antibiotic (Figure 3).[12] Because carbohydrate glycomimetics have shown effective biological activity, the chemistry of carbohydrates is an important area for potential drug development.

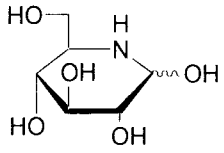

nojirimycin

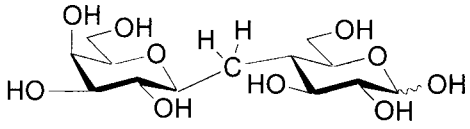

C-lactose

Figure 3: The iminosugar nojirimycin and the *C*-glycoside *C*-lactose

In the past 30 years, a surge of investigation into carbohydrates has emerged due to their importance in many biological systems. Glycoconjugates like glycoproteins and glycolipids have been shown to regulate many biochemical processes. For example,

carbohydrates play an integral role in the protective cell wall for both plant cells and bacteria. Discoveries utilizing carbohydrates extend from food additives[13] to the pharmaceutical industry.[14] Recently, researchers have constructed many important compounds containing carbohydrate backbones that have shown activity towards ailments like human immunodeficiency virus (HIV), certain types of cancer and potentially harmful bacteria. Nicolaou and associates at the Scripps Research Institute have recently discovered an efficient synthesis for D-callipeltose (shown below), a precursor for Callipeltoside A, which has been shown to protect cells infected with HIV (Figure 4).[15] Van Boom and coworkers have found an approach to synthesizing 2-azido-2-deoxy-β-D-mannosides that exhibit inhibitive properties toward a bacterium from the genus *Xanthomonas*, a gram-positive bacterium.[16] Additionally, Danishefsky and partners at the Sloan-Kettering Institute for Cancer Research has effectively synthesized polysaccharide-based compounds to be used as an anti-cancer vaccine.[17]

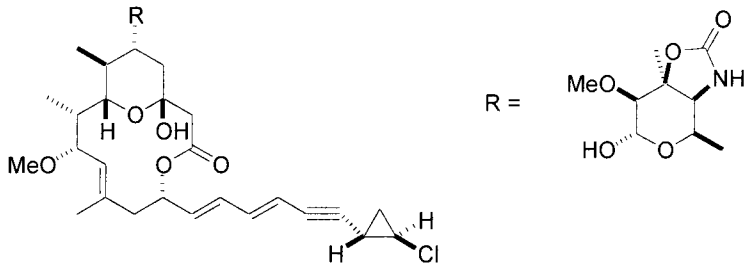

Callipeltoside A D-callipeltose

Figure 4: The research of Nicolaou and coworkers; Callipeltoside A and D-callipeltose

Biologically active carbohydrate-based discoveries are often difficult to make because of the complexity of sugar monomer units. Carbohydrates are compounds generally of the formula $C_n(H_2O)_n$, with the simple sugars being called

monosaccharides.[18] Monosaccharides exist in three main forms: the *aldehydo*, or acyclic form; the furanose ring (five-membered); and the pyranose ring (six-membered). Formation of the ring forms of carbohydrates comes from attack of the hydroxyl (-OH) at carbon 4 or 5 onto the carbonyl carbon in the *aldehydo* form (Figure **5A**). As the ring is formed, one can imagine attack of the -OH coming from the top or the bottom of the flat aldehyde functional group, resulting in either an alpha (α) (Figure **5B**,**5D**) or beta (β) (Figure **5C**,**5E**) configuration. The α configuration will provide the -OH functionality at C-1 in the axial position below the plane of the molecule and the β configuration will afford the -OH functionality in the equatorial position in the same plane as the molecule.

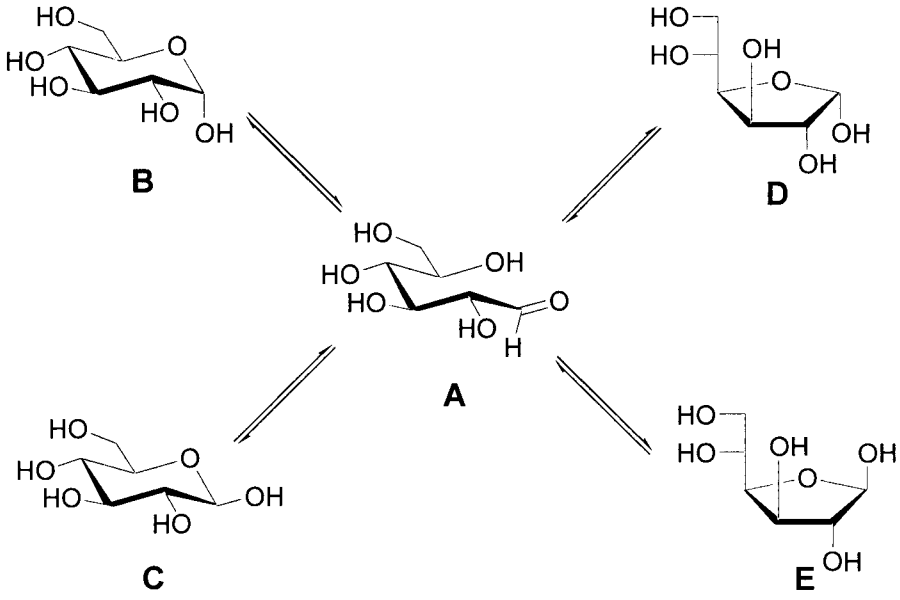

Figure 5: The configurations of D-glucose

D and L nomenclatures are often used when reporting the configuration of carbohydrates. When looking at a Fischer projection, D and L refer to the orientation of the first chiral center from the bottom of the projection. A D notation means that the hydroxyl is oriented to the right of the sugar chain and an L notation denotes a hydroxyl

group to the left of the sugar chain. The examples of D- and L- galactose are shown (Figure 6).

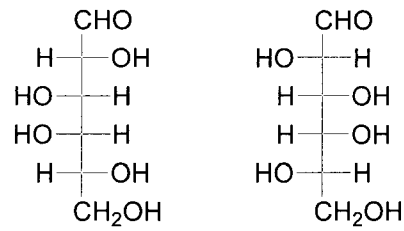

Figure 6: D-galactose and L-galactose

Carbohydrates become increasingly difficult to work with when considering the fact that a combination of all five of the different forms can exist in solution at one time. The presence of all of these forms in solution may cause many different undesired reaction pathways when conducting reactions on monomer units.

The overall class of carbohydrates can be divided into many subdivisions, three of the most important being glycosides, amino sugars and glycals. Glycosides have been shown to be abundant in nature, which makes them potential targets for synthesis. A glycoside is a sugar (or sugar chain) in which the hydroxyl at the anomeric position is replaced with any other functionality, for example *–OR*, *-CR -NR*, or *–SR*. The resulting glycosidic linkages give rise to the nomenclature of *O*-glycosides, *C*-glycosides, *N*-glycosides, or *S*-glycosides respectively.

Forming glycosidic bonds has proven to be challenging for synthetic chemists because of the anomeric effect. When a glycosidic bond is formed, the orientation of the product is controlled, in part, by the anomeric effect, which is caused by the interaction of the electronegative oxygen atom in the sugar ring with the substituent at C-1. The interaction between the two electronegative atoms causes an overlap of the non-bonding

orbital of the substituent with one of the lone pairs of the oxygen in the sugar ring. The orbital overlap will stabilize the α anomer and make it the major product because the β configuration does not provide this overlap interaction. Because of their vast importance, past investigation of glycosidic bonds has been extensive. The anomeric effect can be observed in the glycosylation of D-glucose with methanol to give primarily methyl α-D-glucopyranoside (Figure 7).[12]

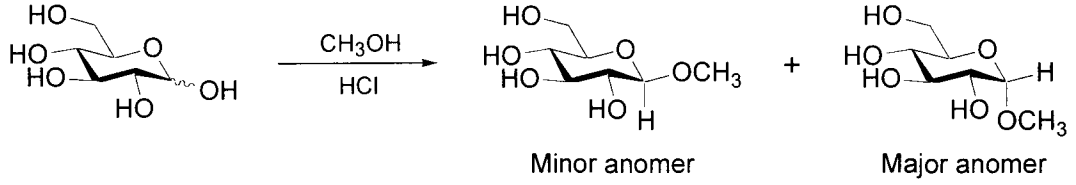

Figure 7: Glycosylation of D-glucose with methanol, an illustration of the anomeric effect

Besides glycosides, amino sugars can also be found in many natural products. Many of the sugars units found in humans are repeating chains of amino sugars. By definition, an amino sugar is a carbohydrate that contains the amino functionality anywhere on the sugar ring except the anomeric carbon. For example D-glucosamine and D-galactosamine are found in the exoskeleton of many shellfish. Also, sialic acids play a major role in biological systems.[12] Because of their importance in many natural systems, many methods have been introduced for the synthesis of amino sugars. While many procedures have been devised for the synthesis of amino sugars, some have proved more useful than others. While displacement of a leaving group is not the most extravagant method for synthesizing amino sugars, it has been widely effective. A simple example is

when a monosaccharide tosylated at C-6 is dissolved in methanol, treated with ammonia and heated under high pressure to yield an amino sugar salt in moderate yields.[19]

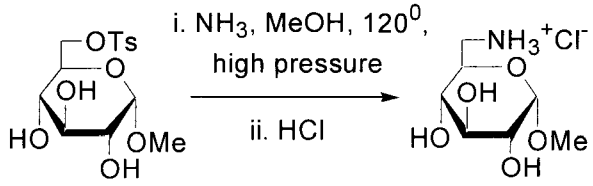

Figure 8: Tosylate displacement

Another effective displacement method for the production of amino sugars is *via* mesylate displacement. When treated sodium azide, a mesylated sugar will provide an azidosugar with inverted stereochemistry about the mesylated carbon by nucleophilic substitution. Upon addition of lithium aluminum hydride, the desired amino sugar is produced and in the example, the benzoyl protecting group is removed.[20]

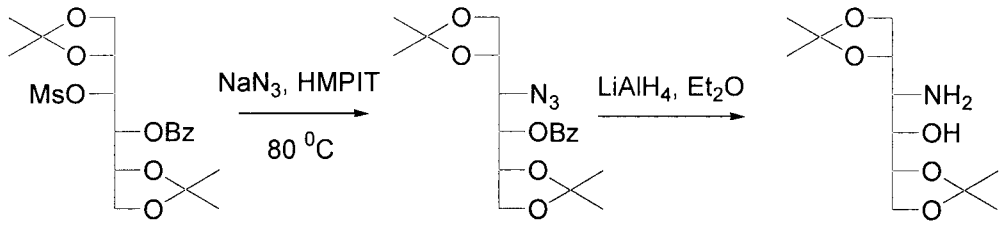

Figure 9: Mesylate displacement, followed by reduction

While synthesis of amino sugars is effective starting with saturated sugar units, the use of glycals as starting materials has been shown to be most effective in the synthesis of amino sugars because of their versatility. Glycals are sugars with a double bond between the first and second carbons of the sugar chain and no hydroxyl groups one either of those carbons. Because of the presence of a double bond, a wide range of products, including amino sugars and glycosides, may be synthesized. Lemieux

introduced a method for the synthesis of 2-azido-2-deoxy glycosyl nitrates using a method called azidonitration whereby the reaction proceeds *via* radical intermediates. An example protocol for the reaction calls for the treatment of 3,4,6-tri-*O*-acetyl-D-galactal with sodium azide and ceric ammonium nitrate in acetonitrile to produce the desired 2-azido-2-deoxy glycosyl nitrate shown below. The method for azidonitration has been applied to a wide range of glycal precursors.[21]

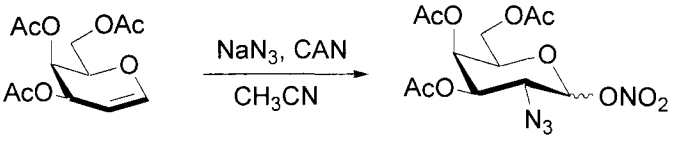

Figure 10: Azidonitration of tri-*O*-acetyl-D-galactal

Nicolaou and coworkers extended the investigation into amino sugar synthesis when they introduced a "tethered" approach to making 2-aminosugars. The method called for the treatment of C-3 glycal urethanes with *o*-iodoxybenzoic acid (IBX) and water to produce 2-aminosugars as a fused heterocyclic ring system in a single step.[22] Rojas conducted a reaction producing similar results, but he employed the use of light and an azidoformate rather than an acetamido moiety. This method provided a stereoselective method for 2-*N*-acetamido-β-allopyranosides.[23]

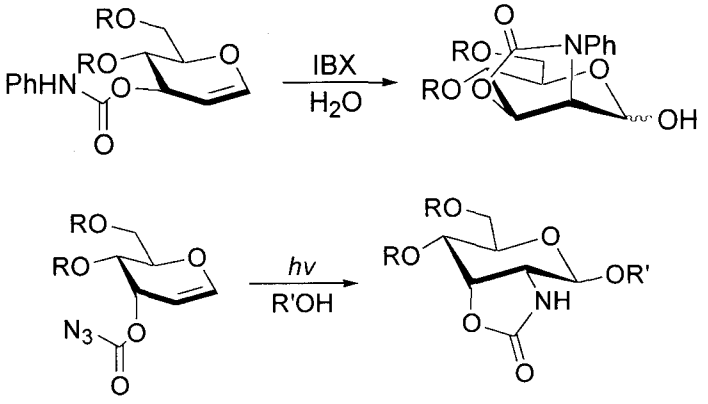

Figure 11: Tethered methods for the formation of 2-aminosugars

Recently, Gin has introduced a one-pot, stereoselective method for the synthesis of amino sugars *via* an oxazoline intermediate. Starting with a glycal precursor dissolved in chloroform, the solution is treated with thianthrene-5-oxide and triflic anhydride. Upon formation of the triflated thianthrene species, *N*-trimethylsilylacetamide and *N,N*-diethylaniline are added and an oxazoline intermediate is formed. The intermediate ring can then be opened up to the corresponding amino sugar retaining the stereochemical configuration at C-2 and producing β-anomers. The method outlined by Gin was shown to be effective for both primary and secondary alcohol nucleophiles as well as selectively deprotected sugar monosaccharide units.[24]

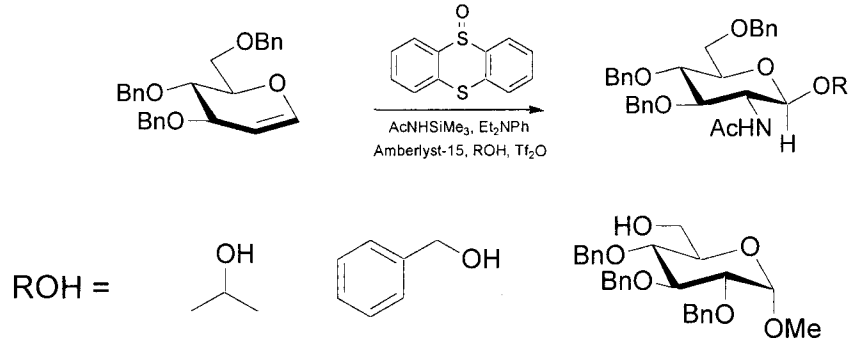

Figure 12: Gin acetamidoglycosylation for the formation of 2-aminosugars

Schmidt and Das have implemented the use of acetyl nitrate ($AcONO_2$) generated *in situ*. Upon addition of the glycal, the nitro moiety attaches at C-2 and the acetyl functionality is trapped by the positive charge at C-1. The resulting product is then treated with a base and the acetyl moiety is eliminated to provide a nitroglycal. Because of the electron-withdrawing nitro moiety and the oxygen in the ring next to C-1, C-1 has significant positive character, making it susceptible to attack from nucleophiles. The nitro moiety may then be reduced and acetylated to provide the acetamido functionality.[25]

Schmidt and Das have extended this procedure to produce a wide range of *O*- and *N*-glycosides with various biological possibilities.[26-28]

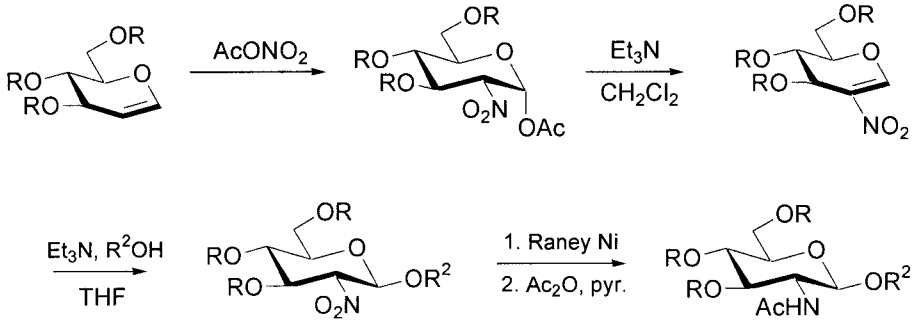

Figure 13: The Schmidt nitroglycal method for synthesis of amino sugars

The versatility of Schmidt and Das' method provides the precursors necessary for the synthesis of many amino sugar products, including those found in the capsular polysaccharide of *S. aureus*. Because the method has been applied to a wide range of sugar precursors, one could imagine its effectiveness in the synthesis of D-FucNAc, L-FucNAc and a wide range of glycomimetic analogs.

Statement of Problem

Staphylococcus aureus has shown increasing resistance to traditional methods of treatment, including the antibiotic vancomycin. Past methods of treatment effectively blocked the biosynthesis of the bacterial cell wall. Because *S. aureus* bacteria have shown increasing resistance towards traditional treatment methods, new methods for combating the bacteria must be found.

The focus of this research is to develop glycomimetics, or compounds with similar structures to those found in natural biosynthetic pathways. More specifically, the research targets the protective capsular polysaccharide coating of *S. aureus* bacteria, which is made up of a repeating chain of amino sugar units. A mimic of one of the amino sugars in the chain may disrupt the biosynthesis of the capsular polysaccharide, thus making the bacteria detectable by the human immune system.

Synthetic methods towards the formation of analogs of *N*-acetyl-2-amino-2-deoxy-D-fucosamine (D-FucNAc) and *N*-acetyl-2-amino-2-deoxy-L-fucosamine (L-FucNAc), as well as other possible amino sugar glycomimetics with the flexibility to provide many such analogs, are the goals of this research.

Results and Discussion

Model Study on Gin Acetamidoglycosylation

Gin and coworkers introduced a convenient, stereoselective, one-pot synthesis of 2-amino sugars from glycals that formed exclusively the β-anomer. The protocol was investigated to explore the application of Gin's research method to the synthesis of D-FucNAc and L-FucNAc glycomimetics.

The experimental procedure calls for the use of tri-*O*-benzyl-D-glucal as a precursor, which can be readily made from the relatively inexpensive tri-*O*-acetyl-D-glucal (**1**) by first deacetylating the protected sugar with sodium in methanol to produce D-glucal (**2**). After reacting overnight, TLC showed disappearance of the starting material and appearance of a new spot with a much lower R_f value when treated with 5% sulfuric acid/ethanol solution and heating to visualize the product. The product was then isolated from the crude mixture using a hot ethyl acetate extraction affording **2** as a white solid in 72% yield. The ^{1}H NMR spectrum showed the disappearance of the three acetate peaks at 2.1 ppm and the appearance of three doublets, one for each -OH on the sugar ring appearing at 5.11 ppm, 4.87 ppm and 4.56 ppm. Upon investigation of the ^{13}C NMR spectrum, six peaks were evident, which is the expected outcome. Two significant signals shifted to 140.4 ppm and 100.6 ppm belonged to the carbons in the glycal double bond.

Compound **2** was then treated with sodium hydride and benzyl bromide in order to protect the free hydroxyls and provide tri-*O*-benzyl-D-glucal (**3**). When examining the TLC plate, a spot that was now UV-active, due to the benzene chromophores, showed at a much higher R_f than the starting material. The ^{1}H NMR spectrum showed the

disappearance of the signals at 5.11 ppm, 4.87 ppm, and 4.56 ppm that belonged to the protons on the -OH groups and an appearance of a multiplet from 7.23 – 7.34 ppm integrating to 15 hydrogens that corresponded to the aryl protons on the benzene rings. The ^{13}C NMR spectrum provided evidence of the benzyl protecting groups with three shifts at 139.3 ppm, 139.1 ppm, and 138.9 ppm that correspond to the *ipso* carbons of the benzyl protecting groups. Also shown are the signals for the remaining twelve carbons of the benzene rings at ~128 ppm. Six peaks are shown between 70 and 80 ppm, which correspond to the methylene carbons of the benzyl protecting groups and the four carbons of the sugar ring not part of the double bond. The carbons for the double bond show at 145.7 ppm and 101.0 ppm for C-1 and C-2 respectively.

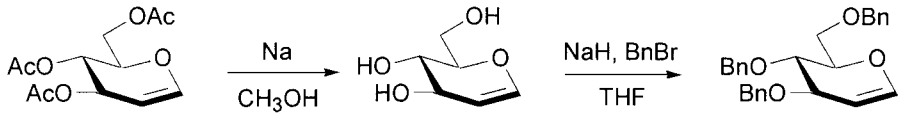

1 **2** **3**

Scheme 2: Preparation of tri-*O*-benzyl-D-glucal.

The protocol for Gin's method also called for thianthrene-5-oxide (**5**), which had to be made from one equivalent of thianthrene (**4**) and one equivalent of *m*-CPBA in methylene chloride to ensure that only one of the sulfur atoms of thianthrene was oxidized (Scheme 3). TLC of the reaction product showed a UV-active spot with a slightly lower R_f value and examination of the ^1H NMR spectrum provided a doublet of doublets at 7.93 ppm that corresponds to two equivalent protons, H-1 and H-1'. Also shown are three multiplets for the remaining six protons on the molecule. Evidence for the equivalent carbons due to symmetry is found in the ^{13}C NMR spectrum. Six signals

are found in the spectrum with the carbons next to the sulfoxide shifted furthest downfield at 142.3 ppm. The carbons next to the unoxidized sulfur atom are also shifted downfield to 134.7 ppm, and the remaining four signals for the other eight carbons are found slightly upfield at ~130 ppm. The mass spectrum of the product gives an *m/z* at 233.16 in the positive mode, which corresponds to the calculated molecular weight of 232.32.

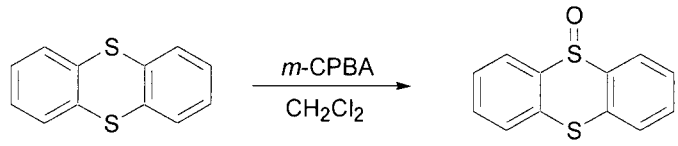

4 **5**

Scheme 3: Formation of thianthrene-5-oxide

Gin's one-pot method was then attempted in order to first make the triflate of thianthrene-5-oxide at –10 °C with tri-*O*-benzyl-D-glucal (**3**) present in the reaction mixture. The triflated species was then treated with *N*-trimethylsilylacetamide and *N,N*-diethylaniline. According to the literature, an oxazoline intermediate was supposed to be formed, but after analyzing ^{1}H and ^{13}C NMR data the intermediate was apparently not formed. 2-Propanol and Amberlyst-15 were then added to the reaction mixture, but the desired product was not formed. ^{1}H NMR studies suggested the formation of methyl 3,4,6-tri-*O*-benzyl-2-deoxy-D-glucopyranoside, without insertion of the acetamido moiety at C-2. Experimental protocol from the literature was followed using freshly distilled solvents and newly purchased reagents in carefully flame-dried flasks to ensure dryness, but the desired product was never formed. The product characterized from the NMR data was the glycosylated product without insertion of the nitrogen at C-2.

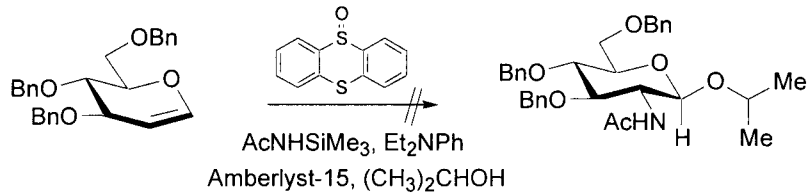

Scheme 4: The Gin Method

Investigation of the Schmidt Method: Model Study on Tri-*O*-benzyl-D-glucal

Schmidt and Das introduced the method of synthesizing 2-amino sugars *via* a nitroglycal intermediate using tri-*O*-benzyl-D-galactal. Because of the relative expense associated with tri-*O*-benzyl-D-galactal, an inexpensive alternative in the form of a benzylated D-glucal precursor was chosen instead. The system was set up similar to the manner outlined by Schmidt and Das in the literature using a benzylated D-galactal starting material. Acetyl nitrate was generated *in situ* upon addition of concentrated nitric acid to acetic anhydride. Tri-*O*-benzyl-D-glucal (**3**) was then introduced to the system, and progress of the reaction was monitored by TLC. Observation of the TLC results showed formation of a new spot with ultraviolet absorbance with an R_f value slightly less than that of the starting material, which burned on the TLC plate when treated with 5% H_2SO_4/ethanol solution. The ^1H NMR spectrum of the crude product (**6**) showed appearance of a singlet at 1.96 ppm for the formation of the acetate at C-1 and the disappearance of the doublet of doublets for the C-1 proton at 6.42 ppm of the starting material. The other peaks were observed as a multiplet ranging from ~3.50 ppm to ~4.70 ppm.

Because Schmidt and Das observed an increased yield of product by using the crude reaction material directly, the next step of the reaction scheme was run with the

crude mixture. Elimination of the C-1 acetyl moiety occurred upon treatment of **6** with triethylamine to provide the nitroglycal **7**. Inspection of the ^{1}H NMR spectrum showed a downfield shift of the proton at C-1 to 8.2 ppm, which appeared as a singlet because of the presence of the electron withdrawing oxygen neighbor as well as being part of alkene system with the nitro functionality at C-2. The region from 7.21 – 7.37 ppm integrated to account for the 15 aryl protons, and the remaining protons for the compound were located from 3.5 – 4.9 ppm. The ^{13}C NMR showed the presence of peaks at 155.4 ppm and 131.7 ppm for C-2 and C-1 respectively. Also shown were the peaks corresponding to the aryl carbons; three at ~138 ppm and 9 signals at ~129 ppm. The rest of the signals that lie between 64 and 79 ppm correspond to the remaining carbons of the sugar ring and the three methylene carbons of the benzyl protecting groups. Mass-spectral data afforded an M^{+} of 479.22, which corresponds to the calculated molecular weight (461.51) with the addition of a water molecule.

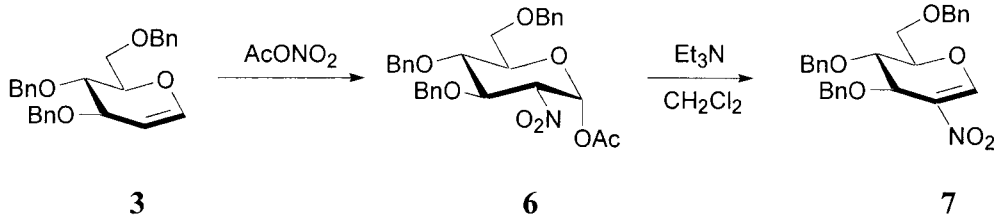

3 **6** **7**

Scheme 5: The synthesis of 3,4,6-tri-*O*-benzyl-2-nitro-D-glucal (7)

The methyl *O*-glycoside **8** was then synthesized *via* treatment of **7** with triethylamine and methanol. The TLC of the reaction mixture showed a spot that was UV-active and burned at a slightly lower R_f value than that of the starting material. Investigation of the ^{1}H NMR spectrum showed the disappearance of the singlet at 8.2 ppm that corresponded to the proton at C-1 for the starting material, and the emergence of

a doublet at 4.7 ppm with a coupling constant, J = 8.06 Hz. The J value of 8.06 Hz is consistent with formation of the β-anomer, which was the desired product. A singlet at 3.52 ppm also appears, which corresponds to the protons of the methoxy moiety. The ^{13}C NMR spectrum illustrates the disappearance of the alkene carbon signals showing C-2 and C-1 at 101.9 ppm and 90.7 ppm respectively. Aryl carbons for the product are still shown as three peaks at ~138 ppm and a cluster of signals worth nine carbons at ~129 ppm. The remaining carbons of the sugar ring and the methylene carbons of the benzyl protecting groups are located from ~58 – 82 ppm. Mass spectrometry data provided an M^+ at 511.44 in positive mode, which corresponds to the calculated molecular weight, 493.55, with the addition of a water molecule.

The methyl *O*-glycoside **8** was then first treated with Raney Nickel to reduce the nitro moiety, and then reaction with acetic anhydride in pyridine provided methyl 3,4,6-tri-*O*-benzyl-2-deoxy-2-acetamido-D-glucopyranoside (**9**) in 73% yield. ^1H NMR spectra showed the emergence of two important signals. A doublet at 5.5 ppm corresponds to the N-H proton that is split only by the proton at C-2. Also appearing in the spectrum is a singlet at 1.86 ppm integrating to the three protons that are associated with the acetyl moiety. The anomeric proton still has a coupling constant (J = 7.67 Hz) indicating the β-configuration, which is expected since there was no direct change on C-1. Examination of the ^{13}C NMR spectrum shows the appearance of a signal at 171.3 ppm, which corresponds to carbonyl carbon of the acetamido functionality. The other signals of the ^{13}C spectrum showed little change from the spectrum of the starting material. Mass spectrometry afforded an M^+ of 504.60 in negative mode, which corresponds to the calculated value of 505.60.

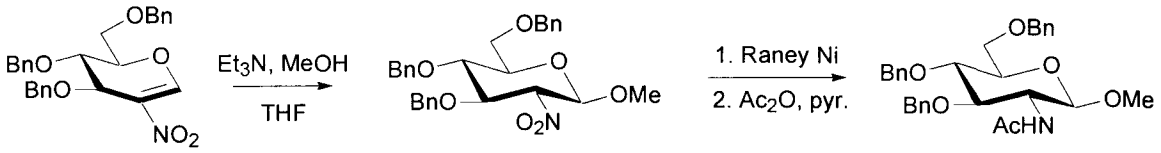

7 **8** **9**

Scheme 6: Synthesis of methyl 3,4,6-tri-*O*-benzyl-2-deoxy-2-acetamido-D-glucopyranoside

Precursor Synthesis: Model Study employing D-glucal

Fucose analogs require the presence of a methyl group at C-6, requiring reduction of the C-6 hydroxyl. To obtain the desired stereochemical configuration of D- and L-FucNAc, the manipulation of the functionalities of galactal precursors must be employed. However, the relative cost of D-galactal versus D-glucal is approximately 16x greater, so the less expensive D-glucal was chosen as a precursor to ensure the effectiveness of the devised synthetic strategy.

The first step involved in the synthetic strategy was the selective protection of the primary hydroxyl of D-glucal (**2**) to give 6-*O*-*t*-butyldiphenylsilyl-D-glucal (**10**). The reaction proceeded using 0.9 equivalents of *t*-butylchlorodiphenylsilane to ensure minimal side reactions at other hydroxyls. TLC showed a UV-active spot that also burned with a much higher R_f value than that of the starting material. The appearance of a singlet at 1.0 ppm in the ^{1}H NMR spectrum represents the nine equivalent hydrogens of the *t*-butyl group. Also appearing were the aryl protons from 7.62 – 7.67 ppm and 7.39 – 7.44 ppm that integrated to 10 protons. A doublet representing the hydroxyl that was protected at 4.55 ppm disappeared from the spectrum. The ^{13}C NMR spectrum afforded signals for the *t*-butyl moiety at 20.7 ppm and 28.3 ppm respectively. Aryl carbons appeared at 136.6 ppm, 134.5 ppm, 131.2 ppm and 129.3 ppm representing 10 carbon

atoms. Mass spectral data provided an M^+ of 383.20 in negative mode, which corresponds to the calculated value 384.54.

The *t*-butyldiphenylsilyl protected sugar **10** was then treated with sodium hydride and benzyl bromide to protect the remaining hydroxyls of the precursor in 98% yield. TLC investigations indicated the formation of a UV-active spot burning at a much larger R_f value than the starting material. After looking at the ^1H NMR spectrum, shifts at 7.21 – 7.46 ppm became more complicated because of the presence of the additional 10 aryl protons. Also shown in the spectra is a multiplet at 4.51 – 4.70 ppm integrating to four protons that represents the methylene protons of the benzyl protecting groups. The ^{13}C spectrum afforded more evidence for the formation of the product with two shifts at ~139 ppm that represent the *ipso* carbons of the benzyl protecting groups and shifts worth 7 carbons at ~129 ppm for the remaining 6 carbons of the benzyl protecting groups and one of the signals for the *t*-butyldiphenylsilyl protecting group. Mass spectrometry indicated an M^+ value of 582.33 in positive mode, which corresponds to the calculated molecular weight (564.79) of the product with the addition of a water molecule.

The primary hydroxyl of **11** was deprotected using tetra-*N*-butyl ammonium fluoride in THF at room temperature to afford **12** in 77% yield. TLC showed a UV-active spot with a lower R_f value than the starting material due to the loss of the non-polar *t*-butyldiphenylsilyl protecting group. ^1H NMR data showed the loss of the protecting group through the absence of the singlet at 1.0 ppm representing the protons of the *t*-butyl group and the multiplet at 7.67 – 7.71 ppm illustrating 5 of the aryl protons associated with the protecting group. The loss of the remaining 5 aromatic protons was only evidenced through the integration of the region from 7.26 – 7.38 ppm, which now

only integrated to the 10 remaining aryl protons. Also shown in the ^{1}H NMR spectrum is a triplet of doublets at 6.4 ppm representing the hydrogen at the anomeric position. The unusual splitting pattern can be explained by allylic splitting or splitting from the proton of the primary hydroxyl at C-6. The ^{13}C NMR spectrum also showed the disappearance of the *t*-butyl group and phenyl groups compared to the starting material. Absent from the spectra are shifts at 20.5 ppm, 28.2 ppm for the *t*-butyl group and shifts at 136.8 ppm, 134.5 ppm, 130.7 ppm and 129.4 ppm for the phenyl groups. Investigation of the mass spectral data afforded an M^{+} of 327.29 in positive mode, which corresponds to the calculated molecular weight of 326.39.

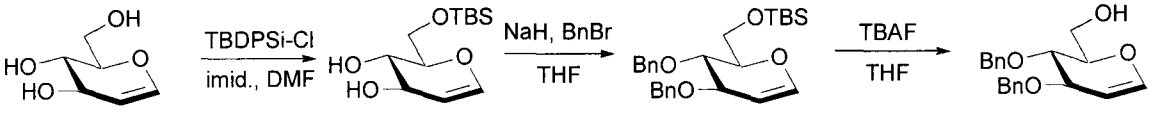

2 **10** **11** **12**

Scheme 7: Protecting group strategies for D-glucal

Reduction of the free hydroxyl at C-6 was then investigated through the employment of the Barton-McCombie method.[29] The first step was to react the free hydroxyl at C-6 by treating **12** with *N,N*-thiocarbonyldiimidazole and allowing the reaction to proceed at room temperature. TLC showed a UV-active spot that burned with an R_f value much lower than the starting material because of the polar thiocarbonylimidazoyl group. The product was isolated *via* flash column to afford the product **13** in 74% yield. The ^{1}H NMR spectrum showed evidence of the product by indicating three singlets, one for each of the protons of the imidazole ring at 8.22 ppm, 7.52 ppm, and 7.01 ppm respectively. ^{13}C NMR data provided evidence for the carbonyl

carbon of the thioimidazoyl group by showing a shift at 184.6 ppm. Also present in the ^{13}C NMR spectrum were the signals for the carbons of the imidazole ring shown at 137.9 ppm, 131.8 ppm and 118.4 ppm. In the positive mode, mass spectrometry showed an M^+ at 437.23, which corresponds to the calculated value of 436.52.

Reduction of the thiocarbonylimidazole-substituted glucal derivative **13** was attempted using tri-*n*-butyl tin hydride as a reducing agent. While TLC did show movement of a UV-active spot that burned to a larger R_f value, the desired product was not found after purification *via* flash column chromatography. Because the reaction proceeds through radical intermediates, undesired reactions may have been possible due to the presence of the electron-rich double bond of the glycal. NMR studies did not show the presence of the desired doublet for the protons of the C-6 methyl functionality.

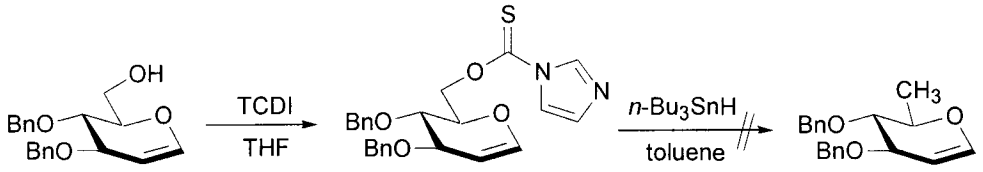

12 **13** **14**

Scheme 8: Attempted Barton-McCombie method for the reduction of C-6

Because the Barton-McCombie method did not result in the formation of the desired 6-deoxysugar, other methods were investigated. When investigating the literature, reduction *via* a tosylated intermediate suggested a possible method of reduction.[30] Compound **12** was reacted with *p*-toluenesulfonyl chloride in pyridine at room temperature under a nitrogen atmosphere. An R_f value higher than that of the starting material was shown as a single spot on the TLC plate. Investigation of the ^1H NMR data showed a doublet at 7.83 ppm integrating to two hydrogens from the *para*-

substituted tosyl group. The remaining protons of the tosyl group showed their signal in the same region as the aryl protons of the benzyl protecting groups. Also evident in the ^{1}H NMR spectrum was a singlet at 2.42 ppm for the methyl moiety of the tosylate. ^{13}C NMR data provides evidence for the tosyl group through the shifts in the aromatic region at 145.8 ppm and 130.8 ppm, as well as the signal at 22.9 ppm for the methyl group. Mass spectral data shows an M^{+} at 498.36 in the positive mode, which corresponds to the calculated molecular weight (480.57) with the addition of a water molecule. Also evident is a signal at 344.28, which corresponds to the cleavage of the tosyl group.

Reductive cleavage of the tosylated glucal derivative **15** was accomplished using lithium aluminum hydride in anhydrous THF. The reaction had to be refluxed overnight to show complete consumption of the starting material. TLC showed a spot that was UV-active and burned with an R_f value much higher than that of the starting material. Isolation of the product was achieved *via* flash column to provide 3,4-di-*O*-benzyl-D-rhamnal (**14**) in 83% yield. ^{1}H NMR experiments showed the disappearance of the doublet at 7.83 ppm that represented two of the hydrogens of the tosyl group. When integrating the region from 7.26 – 7.38 ppm, a loss of two protons is seen due to the loss of the other two protons of the benzene ring of the tosyl group. The emergence of a doublet worth three hydrogens at 1.38 ppm proves the presence of the C-6 methyl moiety. The ^{13}C NMR spectrum shows a signal at 18.8 ppm corresponding to the methyl group at the C-6 position. An M^{+} of 328.26 is observed in the positive mode, which corresponds to the calculated molecular weight (310.40) with the addition of a water molecule.

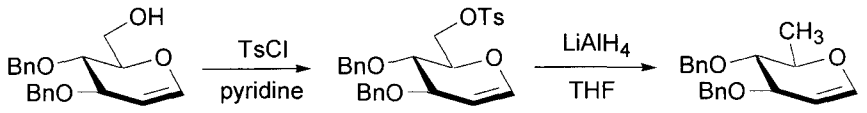

12 **15** **14**

Scheme 9: Reduction of C-6 *via* a tosylate

Application of the Schmidt Method to 3,4-di-*O*-benzyl-D-rhamnal

Although Schmidt's method proved to be effective using tri-*O*-benzyl-D-glucal (**3**) as a precursor, the protocol had not been used with a 3,4-di-*O*-benzyl-D-rhamnal (**14**) system. Investigations applying Schmidt's method to the rhamnal system were studied to ensure its versatility when applied to a wide range of starting materials, including fucal derivatives. The procedure employs the same synthetic scheme as the model system. The first step involves the use of acetyl nitrate, which is generated *in situ* by adding concentrated nitric acid to acetic anhydride under strict temperature control. The sugar **14** was then added to the system and the reaction produced **16**. The intermediate product was not isolated because the authors reported a greater overall yield of the nitroglycal **17** when using the crude product directly. The nitroglycal **17** was produced in an overall yield of 37% for both steps. TLC of the final product showed a UV-active spot that burned with a slightly lower R_f value than the intermediate **16**. ^{1}H NMR experiments showed a singlet at 8.21 ppm corresponding to the hydrogen at the anomeric position. Also evident is the doublet representing the C-6 methyl group at 1.40 ppm, which proved that the model system could be applied to other 6-deoxy glycals. ^{13}C NMR data provided shifts at 155.6 ppm and 90.87 ppm that represent C-2 and C-1 respectively, and the C-6 methyl group shows a shift at 17.4 ppm.

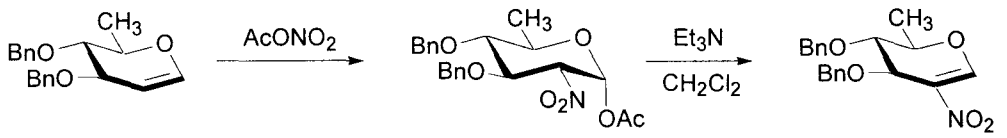

14 **16** **17**

Scheme 10: The 3,4-di-*O*-benzyl-D-rhamnal system

The nitroglycal **17** was then added to a solution of triethylamine in methanol at room temperature. TLC showed a UV-active spot that burned at a slightly lower R_f value than that of the starting material. The methyl glycoside was isolated *via* flash column to provide **18** in a 67% yield. The ^{1}H NMR spectrum showed the disappearance of the signal at 8.21 ppm for the C-1 proton, which now shows as a doublet at 4.70 ppm with a coupling constant $J = 8.06$ Hz. The large coupling constant indicates the formation of the β-anomer as the major product. Also evident in the spectrum is a singlet integrating to three protons for the methoxy group. ^{13}C NMR data shows a disappearance of the signal at 155.6 ppm due to the loss of the double bond and a new signal at 27.8 ppm for the methoxy carbon. Electrospray Ionization (ESI) mass spectrometry shows an M^+ of 405.35, which corresponds to the calculated molecular weight (387.43) with the addition of a water molecule.

The nitro moiety of the methyl glycoside **18** was then reduced using Raney nickel in ethanol and the crude mixture was treated with acetic anhydride in pyridine to provide the desired C-2 acetamido functionality in an overall yield of 19% for both steps combined. The product was isolated using flash column chromatography, but **19** had to be collected when flushing the column with methanol. ^{1}H NMR data shows the emergence of a doublet at 5.46 ppm that represents the N-H proton. Also evident is a

singlet at 1.86 ppm integrating to the three protons of the acetate functionality. The β-configuration was retained, which is proven by the doublet for the anomeric hydrogen having a coupling constant J = 8.06 Hz. The ^{13}C NMR spectrum shows the carbonyl carbon of the acetate group with a shift at 171.4 ppm and a shift at 25.0 ppm for the methyl group of the acetate. ESI mass spectra affords an M^+ of 398.49 in negative mode, which corresponds to the calculated value of 399.48.

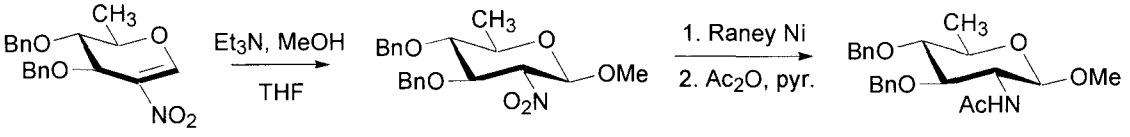

17 **18** **19**

Scheme 11: Synthesis of methyl *N*-acetyl-3,4-di-*O*-benzyl quinavosamine (**19**)

Preparation of D-fucal derivatives from tri-*O*-acetyl-D-galactal (20)

Because the Schmidt methodology for 6-deoxy amino sugars had now been established, application of the synthetic strategy to produce D-FucNAc analogs could be investigated. Precursor synthesis employed the same synthetic method as the model study. In the first step, tri-*O*-acetyl-D-galactal (**20**) was deprotected with a catalytic amount of sodium in methanol to produce D-galactal (**21**). Using a hot ethyl acetate extraction (because the sugar would have been lost to the water layer in a traditional water workup) gave the product in a 73% yield. TLC investigations showed a spot that was not UV-active but burned at a much lower R_f value than the starting material because of its polar nature. The ^1H NMR spectrum showed the disappearance of the three peaks at ~2.0 ppm representing the protons of the acetate groups. Peaks at 4.72 ppm, 4.61 ppm and 4.37 ppm represented the hydroxyl protons now present after the deprotection. ^{13}C

NMR data afforded six signals, one for each of the six carbons of the product. Shifts at 144.6 ppm and 105.2 ppm represent the carbons of the double bond. Mass spectral data provided an M^+ of 145.00 in negative mode, which corresponds to the calculated molecular weight of 146.14.

The primary hydroxyl of D-galactal was then protected with 0.9 equivalents of *t*-butylchlorodiphenylsilane. 0.9 Equivalents were used in the protection to assure minimal reactions at the secondary hydroxyls, which made isolation of the product much easier as well. The product was isolated *via* flash column to afford **22** in a 90% yield. TLC showed a UV-active spot that burned and had a much higher R_f value than the starting material due to the introduction of the non-polar *t*-butyldiphenylsilyl moiety. ^1H NMR data showed a disappearance of the signal at 4.37 ppm that represented the proton of the primary hydroxyl. Multiplets at 7.61 – 7.64 ppm and 7.39 – 7.45 ppm appear to show the presence of two phenyl groups. Also evident is a singlet integrating to 9 hydrogens for the protons of the *t*-butyl moiety. The ^{13}C NMR spectrum also provide evidence for the formation of the product through the signals at 136.6 ppm, 134.4 ppm, 131.3 ppm and 129.3 ppm, which represent the carbons of the aromatic rings. Signals at 20.5 ppm and 28.3 ppm represent the carbons of the *t*-butyl group. The ESI mass spectrum affords an M^+ of 383.65 in the negative mode, which corresponds to the calculated value of 384.54.

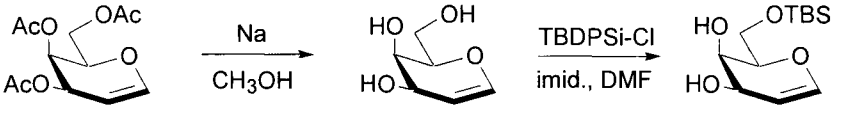

20 **21** **22**

Scheme 12: Preparation of *t*-butyldiphenylsilyl-protected D-galactal

Compound **22** was then treated with sodium hydride and benzyl bromide to protect the remaining hydroxyls. TLC studies showed a UV-active spot that burned at a much higher R_f value than the more polar starting material. Because excess benzyl bromide was used in the reaction, a flash column was used to isolate the product (**23**) in a 99% yield. The ^{1}H NMR spectrum showed the emergence of a multiplet at 7.20 – 7.44 ppm that integrated to 10 hydrogens, which represents the protons of the two benzyl protecting groups. Also present is a multiplet at 4.57 – 4.66 ppm, which represents the four methylene protons of the benzyl groups. The ^{13}C NMR spectrum showed two signals at ~139 ppm that represent the *ipso* carbons of the aromatic rings. A group of signals representing 6 carbons appeared at ~130 ppm for the remaining carbons of the benzene rings. Methylene carbon signals were found between ~63 ppm and 73 ppm. Mass spectral data showed an M^+ value of 582.46, which corresponds to the calculated value (564.79) with the addition of a water molecule.

C-6 of **23** was then deprotected using tetra-*N*-butyl ammonium fluoride to provide a primary hydroxyl. While the reaction did proceed to give the desired product, the yield was a rather low 44%. The decreased yield may be attributed to the bulky benzyl group in an axial configuration at C-4. The configuration of this substituent may block the reaction at C-6 from occurring efficiently. TLC showed a UV-active spot that burned with a much lower R_f value than the starting material due to the formation of the polar hydroxyl group at C-6. The ^{1}H NMR spectrum shows the disappearance of the *t*-butyldiphenylsilyl protecting group through the absence of the singlet at ~1.0 ppm for the *t*-butyl group and the absence of the multiplets at 7.70 – 7.73 ppm and 7.62 – 7.65 ppm representing the two phenyl substituents. Formation of the C-6 hydroxyl is evidenced by

the multiplet signal at 4.85 ppm. ^{13}C NMR data reinforces the absence of the *t*-butyldiphenylsilyl moiety through the disappearance of signals at 20.5 ppm and 28.1 ppm for the *t*-butyl group. Also, disappearance of shifts at 136.6 ppm, 134.4 ppm, 130.7 ppm and 129.5 ppm representing the carbons of the two phenyl groups provides additional evidence. Electrospray Ionization mass spectrometry shows an M^+ at 344.13, which corresponds to the calculated value (326.39) with the addition of a water molecule.

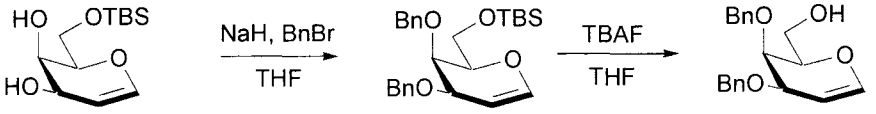

22 **23** **24**

Scheme 13: Deprotection of the C-6 hydroxyl of D-galactal

The free hydroxyl of compound **24** was then tosylated to afford a reducible species at C-6. Addition of *p*-toluenesulfonyl chloride to compound **24** in pyridine afforded 3,4-di-*O*-benzyl-6-tosyl-D-galactal (**25**) in 99% yield. The product was isolated from the crude mixture by simple aqueous workup. The ^1H NMR spectrum afforded a doublet at 7.74 ppm, which represents the signal for one of the sets of equivalent protons of the tosyl functionality. Also present is a singlet at 2.42 ppm signifying the methyl moiety of the tosyl group. The ^{13}C NMR spectrum provided signals at 23.0 ppm for the methyl moiety of the tosyl group, and shifts at 148.2 ppm, 133.8 ppm, 129.9 ppm and 129.5 ppm for the aryl carbons of the tosyl moiety. ESI mass spectra produced an M^+ of 498.29, which corresponds to the calculated molecular weight value with the addition of a water molecule.

Consistent with the synthetic strategy, compound **25** was reduced with lithium aluminum hydride to afford 3,4-di-*O*-benzyl-D-fucal (**26**). Although the reaction did produce the desired product, only a 7% yield was achieved. The low yield may be attributed to the axial configuration of the bulky benzyl moiety at C-4, which may block the attack of the hydride on C-6. The major product of the reaction was the formation of 3,4-di-*O*-benzyl-D-galactal in 36% yield (**24**). Formation of **24** may also be explained by the steric hindrance caused by the bulky benzyl group in the axial position with attack at the sulfur atom being less hindered. Despite the low yield, the product was characterized using conventional techniques. The ^{1}H NMR spectrum afforded the formation of a doublet at 1.28 ppm, which represents the C-6 methyl moiety. Disappearance of signals at 7.74 ppm, ~7.3 ppm and 2.42 ppm indicate the reduction of the tosyl group. ^{13}C NMR data illustrated the disappearance of the signals of the tosyl group and the appearance of a signal at 17.8 ppm, which represents the newly formed C-6 methyl moiety. High-resolution mass spectral data afforded an M^{+} of 310.156894461, which is consistent with calculated values. Because the devised synthetic plan was not efficient using D-galactal precursors, alternate possibilities were examined.

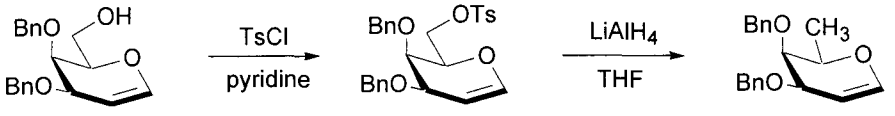

24 **25** **26**

Scheme 14: Formation of 3,4-di-*O*-benzyl-D-fucal

Direct Tosylation and Reduction of Glycals

Nicolaou and coworkers outlined a method for the direct tosylation and reduction of D-glucal (**2**) under strict reaction time and temperature control, which may be applicable to D-galactal.[15] The reaction conditions outlined for the formation of 6-*O*-tosyl-D-glucal described the treatment of D-glucal with pyridine and *p*-toluenesulfonyl chloride at 0 °C for 30 minutes. The protocol was repeated with the much cheaper D-glucal to investigate the feasibility of the experimental method. The ^{1}H NMR spectrum proved the formation of the tosylated glucal intermediate by showing signals at 7.8 ppm and 7.4 ppm as doublets corresponding to the two sets of equivalent protons of the aryl ring of the tosyl moiety. Also shown is a singlet at 2.45 ppm integrating to 3 hydrogens, which represents the methyl group of the tosylate. The ^{13}C NMR spectrum provided signals at 152.3 ppm, 138.9 ppm, 130.9 ppm and 130.1 ppm for the aryl carbons of the tosylate. Also confirming the formation of the tosylate is the shift at 22.9 ppm for the methyl group.

The tosylated glucal intermediate **27** was then treated with lithium aluminum hydride and allowed to stir at 0 °C for one hour. After quenching the reaction with water and sodium hydroxide, the product was extracted with diethyl ether and isolated *via* flash column to afford D-rhamnal (**28**) in a 45% overall yield. Investigation of the ^{1}H NMR spectrum showed the disappearance of the signals at 2.45 ppm, 7.40 ppm and 7.80 ppm and the formation of a doublet at 1.20 ppm signifying the formation of the C-6 methyl group. Inspection of the ^{13}C NMR spectrum gave a total of 6 signals, with shifts at 144.5 ppm and 106.6 ppm corresponding to C-1 and C-2 respectively. Also present was a signal at 19.2 ppm, which proves the formation of the C-6 methyl group.

Formation of 6-*O*-tosyl-D-galactal (**29**) was achieved using the same experimental method as for D-glucal. The ^{1}H NMR spectrum showed the presence of the tosyl group with shifts at 7.81 ppm and 7.35 ppm for the aryl protons and a singlet at 2.45 ppm integrating to 3 hydrogens for the methyl group. Because of product decomposition, the ^{13}C NMR spectrum did not show evidence of the product. However, it is believed that the desired product was formed but the NMR experiment was not performed soon enough after product isolation.

When treating **29** with lithium aluminum hydride, TLC showed the formation of a new spot with a higher R_f than the starting material after about one hour of reaction. Isolation of the product was then attempted using flash column chromatography. Upon inspection of the ^{1}H NMR spectrum, formation of the doublet at ~1.3 ppm for the C-6 methyl group was evident. However, signals at ~7.8 ppm, 7.4 ppm and 2.45 ppm were also present in the spectrum. The mixture was washed with saturated sodium bicarbonate to attempt to remove any excess tosyl chloride or tosyl acid present, but the method was unsuccessful. The method of washing the product also proved to be challenging because of the product's solubility in water. Therefore, the sodium hydroxide from the workup of the reaction was removed *via* filtration after dissolving the reaction mixture in THF. Because of the axial position of the hydroxyl at C-4, the hydroxyl may be tosylated because of its relatively close proximity to the desired reaction site. The desired product **31** was never isolated, therefore other methods of reduction at C-6 must be investigated.

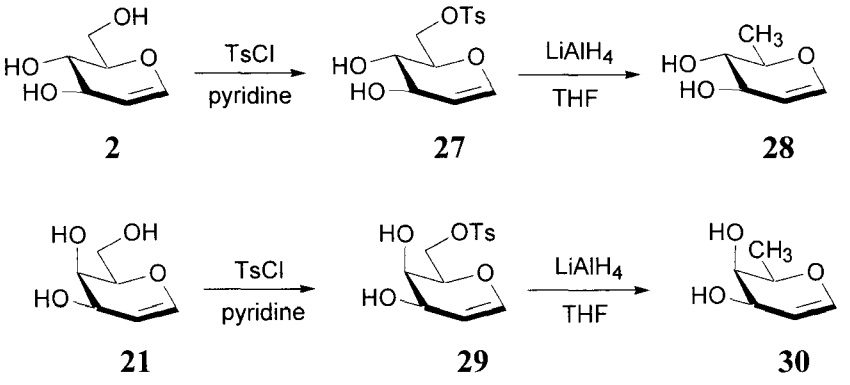

Scheme 15: Methods for the direct tosylation of D-glucal and D-galactal

Schmidt's method and 3,4-di-*O*-benzyl-6-*O*-*t*-butyldiphenylsilyl-D-galactal

Because previous methods for reduction at C-6 were unsuccessful, application of the nitroglycal methodology to compound **23** was investigated with the hope of employing a different method of reduction at C-6 after the synthesis of amino sugar analogs.

Schmidt's method has shown flexibility in its application to many types of glycal systems, which suggests the protocol would be applicable to 6-*O*-silyl-protected sugars. 6-*O*-*t*-butyldiphenylsilyl-3,4-di-*O*-benzyl-D-galactal (**23**) was treated with acetyl nitrate and triethylamine in a two step process affording (**31**) in an overall yield of 46%. The ^{1}H NMR spectrum afforded a singlet at 7.77 ppm, which represents the C-1 proton that has been shifted further downfield because of deshielding effects from the oxygen neighbor and the electron-withdrawing nitro moiety on the double bond of the sugar ring. Investigation of the ^{13}C NMR spectrum affords signals at 166.9 ppm and 88.8 ppm for C-2 and C-1 respectively. The downfield shifts of each of these signals can be explained, again by the presence of the electron-withdrawing nitro moiety at C-2.

Formation of glycosides becomes possible because of the induced positive charge on C-1 due to the presence of the surrounding electron-withdrawing groups, making C-1 a good Michael acceptor. The nitroglycal **31** was added to a solution of methanol and triethylamine and allowed to react overnight to afford **32** in 44% yield. TLC investigations showed a spot that was UV-active and burned at a slightly lower R_f value than the starting material. The ^1H NMR spectrum showed the disappearance of the singlet at 7.77 ppm for the C-1 proton, which is now represented by a doublet at 4.90 ppm with a coupling constant, $J = 8.24$ Hz. The large J value corresponds to the desired β-configuration at the anomeric position. Also present in the spectrum is a singlet at 3.43 ppm that integrates to the 3 protons of the C-1 methoxy functionality. ^{13}C NMR data also shows the disappearance of the downfield signal for C-2, which now shows at 102.1 ppm. The signal for the methoxy moiety appears at 31.2 ppm. ESI mass spectrometry provided an M^+ at 640.32 in the negative mode, which corresponds to the calculated molecular weight of 641.28.

Reduction and acetylation of **32** was attempted using Raney nickel and acetic anhydride and pyridine, but the desired product **33** was not obtained. Although TLC showed a R_f change between starting material and reaction material, investigations of ^1H NMR data did not show the desired singlet at ~2.0 ppm for the protons of the acetate group. Approximately 70 mg of unreacted starting sugar was recovered, and other fractions isolated by flash column chromatography did not indicate presence of the desired product.

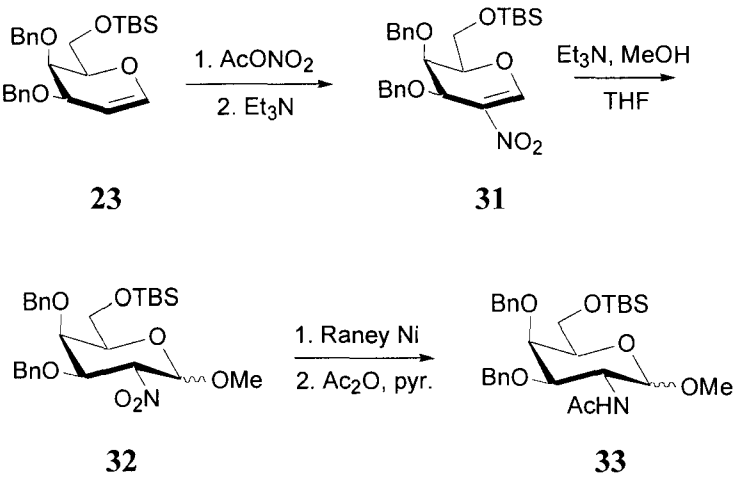

Scheme 16: Studies of the Schmidt method with *t*-butyldiphenylsilyl-protected D-galactal

Applications Towards the Synthesis of *S*-, *C*-, and *N*-glycosides.

As previously stated, C-1 of a nitroglycal becomes susceptible to nucleophilic attack because of the induced positive charge caused by the presence of the surrounding electron-withdrawing groups. Commonly, oxygen nucleophiles are used to attack C-1 to make the corresponding glycosides. However the use of sulfur, carbon and nitrogen nucleophiles may produce corresponding glycosides, which may show inhibitory properties towards enzymes that construct the CP layer of *Staphylococcus aureus*.

The synthesis of product **34** was attempted using compound **7**, benzyl mercaptan, triethylamine, in THF at room temperature. After allowing the reaction to run overnight, TLC showed an R_f difference between the starting material and reaction mixture. The spots of the TLC plate were separated and purified using a flash column, but NMR spectra and mass spectral data did not show evidence of glycoside product formation.

The method was not continued because *S*-glycosides are susceptible to reduction in the next step of the synthetic sequence.

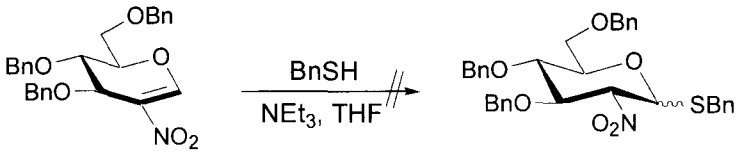

7 **34**

Scheme 17: Attempted synthesis of an *S*-glycoside

A more thorough investigation of *N*- and *C*-glycosides was conducted because of their ability to survive the remaining step of the synthetic method. Synthesis of the *C*-glycoside **35** was also attempted, providing conflicting results. Inspection of the ^{1}H NMR spectrum afforded signals for the glycosylated product, but ^{13}C NMR data did not show a shift at ~175 ppm, that should represent the two equivalent carbonyl carbons. Mass spectral data also provided the desired M^{+}, but further investigation of this compound must be conducted to ensure its presence.

Despite the problems with glycosylation, the *N*-glycoside was formed. Synthesis of **36** was achieved in 46% overall yield as a mixture α and β anomers upon the treatment of **7** with benzyl amine and triethylamine. ^{1}H NMR data afforded a doublet at 5.16 ppm, which corresponds to the N-H proton. Also present are signals for the additional benzyl group at ~7.20 ppm and ~4.35 ppm signifying the presence of the aromatic protons and the methylene protons respectively. The signal for the C-1 proton at 8.20 ppm had disappeared and is now observed at 4.49 ppm. Investigation of the ^{13}C NMR spectrum showed another shift at ~138 ppm, which corresponds to the *ipso* carbon of the benzyl amine aromatic ring, and three additional signals lie at ~129 ppm for the remaining aryl carbons. ESI mass spectral data afforded an M^{+} of 569.35 in positive mode, which

corresponds to the calculated molecular weight of 568.66. A signal at 461.36 signifies the cleavage of the benzyl amine moiety.

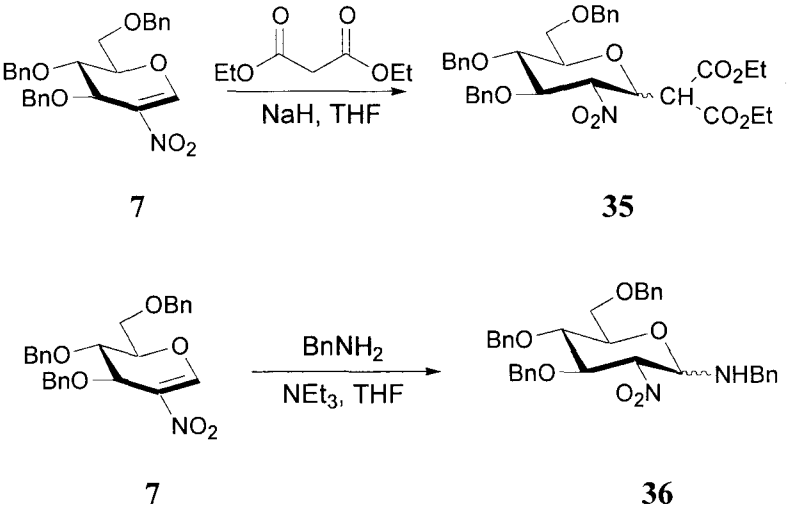

7 35

7 36

Scheme 18: Methods towards the synthesis of *C*- and *N*-glycosides

Investigations on the Formation of L-FucNAc Derivatives.

Formation of L-FucNAc was of fundamental importance in the overall project due to its presence in the capsular polysaccharide of *S. aureus*. Once a general method has been devised for the formation of L-FucNAc derivatives, many types of analogs may be synthesized and tested for possible biological activity. The strategy devised utilizes the readily available 3,4-di-*O*-acetyl-L-fucal (**37**), which would be transformed into a nitroglycal (**38**) *via* Schmidt's method. The nitroglycal **38** may then be manipulated to afford the L-FucNAc derivative **39**.

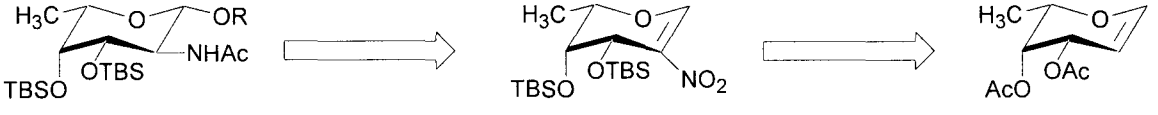

39 38 37

Figure 14: Retrosynthesis of L-FucNAc analogs

The first step of the synthesis requires deprotection of 3,4-di-*O*-acetyl-L-fucal (**37**) to afford L-fucal (**40**). Compound **37** was dissolved in methanol and treated with a catalytic amount of sodium. The reaction was allowed to stir at room temperature until TLC showed consumption of starting material and a spot that burns at a lower R_f value. The product was extracted from the crude mixture by using hot ethyl acetate to afford **40** in a 95% yield. Analysis of the ^{1}H NMR spectrum showed the disappearance of the two singlets at ~2.0 ppm that represent the protons of the acetate functionalities. The hydroxyls formed by the reaction are not present in the ^{1}H NMR spectrum, which can be explained by exchange with water in the NMR solvent. ^{13}C NMR data afforded a total of 6 signals, the shifts at 144.7 ppm and 104.8 ppm being for C-1 and C-2 respectively.

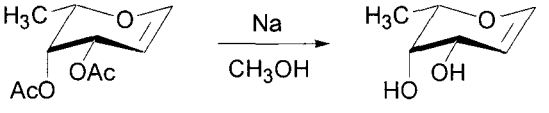

37 **40**

Scheme 19: Synthesis of L-fucal

The free hydroxyls of L-fucal (**40**) were then protected using the base-stable *t*-butyldiphenylsilyl group. Compound (**41**) was produced by adding imidazole to a solution of L-fucal (**40**) in dimethylformamide and treating the solution with two equivalents of *t*-butylchlorodiphenylsilane to afford (**41**) in a 75% yield. Appearing in the ^{1}H NMR spectrum were shifts at 7.67 – 7.79 ppm and 7.31 – 7.48 ppm integrating to 10 protons each, which prove the presence of the two *t*-butyldiphenylsilyl groups. Further evidence is shown in the form of two singlets at 1.10 ppm and 1.07 ppm referring to the two *t*-butyl groups. Investigation of the ^{13}C NMR spectrum afforded eight signals from ~129 ppm to 136 ppm corresponding to the aryl carbons of the phenyl groups. Also

appearing are two signals at ~28 ppm and ~20 ppm, which represent the tertiary carbons and methyl groups of the *t*-butyl groups respectively.

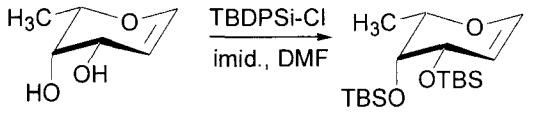

40 **41**

Scheme 20: Formation of 3,4-di-*O*-*t*-butyldiphenylsilyl-L-fucal

The *t*-butyldiphenylsilyl-protected L-fucal **41** was then added to a solution of acetyl nitrate, which was formed *in situ* by the addition of concentrated nitric acid to acetic anhydride at a reduced temperature. After reacting for 1 hour, TLC showed the disappearance of starting material. The reaction mixture was then worked up and the combined organic extracts were reduced to afford a yellow syrup. The crude mixture was then used directly in the next step because of increased yields of nitroglycal reported by Schmidt and Das. Triethylamine was added to a solution of **42** in dry methylene chloride and the reaction was allowed to proceed for ~3 hours. After workup and isolation using flash column chromatography, a 40% overall yield for both steps was achieved. ^{1}H NMR data showed the disappearance of the doublet at 6.30 ppm representing the proton at C-1; a singlet for the proton at the anomeric position is now shown at 8.16 ppm, which is explained by the surrounding electron-withdrawing functionalities. The chemical shift at 4.45 ppm for the proton at C-2 has now disappeared due to the lack of a proton at that position. The ^{13}C NMR spectrum provided evidence of the nitro group by shifting the signals for C-2 and C-1 to 154.6 ppm and 99.98 ppm respectively. Also shown in the ^{13}C

NMR spectrum is a signal at 171.6 ppm, which can be explained by the presence of acetic acid in the mixture.

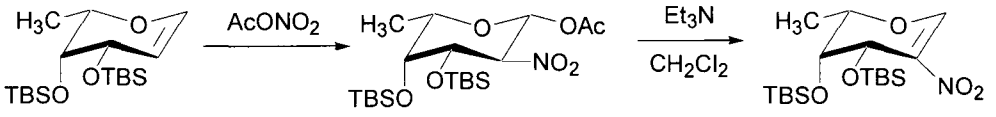

41 **42** **38**

Scheme 21: Application of the Schmidt method to protected L-fucal

The methyl glycoside of **38** was completed in an 89% yield upon the addition of **38** to a solution of triethylamine and methanol at room temperature. After allowing the reaction to proceed overnight, TLC showed a UV-active spot that no longer burned at approximately the same R_f value as the starting material. Only after isolation of the product using flash column chromatography, was the desired product **43** characterized. The ^1H NMR spectrum showed the disappearance of the singlet at 8.16 ppm representing the C-1 proton. The anomeric proton now appears at 4.5 ppm as a doublet with a coupling constant J = 8.06 Hz, which corresponds to the desired β-anomer. Also appearing in the ^1H spectrum is a singlet at 3.46 ppm for the protons of the methoxy group. The ^{13}C NMR spectrum shows large peaks for each of the carbons of the *t*-butyldiphenylsilyl protecting groups, but carbons of the sugar ring were difficult to interpret. Mass spectral data afforded an M^+ of 510.75, which corresponds to the calculated molecular weight with the addition of a water molecule and the cleavage of two phenyl groups and a *t*-butyl group. The observed cleavage is common in mass spectrometry when using silyl-protecting groups.

Manipulation of the nitro moiety was attempted to potentially provide the desired D-FucNAc analog **44**. Compound **43** was first treated with Raney nickel in ethanol at room temperature and the reaction was allowed to proceed until TLC showed disappearance of starting material. After workup, the crude reaction product was dissolved in pyridine and was treated with acetic anhydride. The reaction was once again allowed to stir until TLC showed consumption of starting material and isolation of the product was attempted *via* flash column chromatography. Inspection of the ^{1}H NMR spectrum did not afford evidence of the desired product, but rather possible decomposition. Future investigations will look at the possibility of first removing the *t*-butyldiphenylsilyl groups before acetylation.

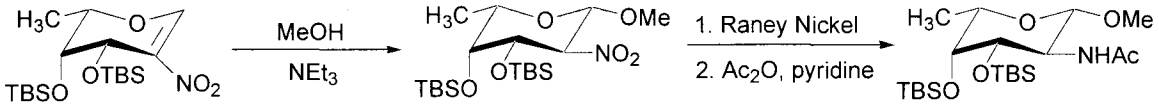

38 **43** **44**

Scheme 22: Attempted formation of D-FucNAc analogs

Future Investigations

Formation of D- and L-FucNAc analogs must be investigated further. Approaches toward the synthesis of L-FucNAc will examine the manipulation of protecting groups so as to avoid decomposition of the product. Deprotection of the *t*-butyldiphenylsilyl groups before reducing the nitro moiety may prove effective. Future considerations will also examine the reduction of C-6 of D-galactal using a more productive method such as reductive cleavage of an iodo group at C-6. Once these obstacles are overcome, a wide range of both D- and L-FucNAc analogs may be synthesized and tested for possible biological activity towards the enzymes that construct the capsular polysaccharide of *Staphylococcus aureus*.

Experimental

General Procedures

A Varian Gemini 2000 NMR system was used to obtain ^{1}H and ^{13}C NMR spectra at 400 MHz and 100 MHz respectively, using $CDCl_3$ or D_6-DMSO as solvents. Proton and carbon chemical shifts (δ) are recorded in parts per million (ppm). Multiplicities for NMR spectra are labeled as follows: s (singlet), d (doublet), dd (doublet of doublets), ddd (doublet of doublet of doublets), t (triplet), q (quartet), and m (multiplet) with coupling constants (J) measured in Hertz. A Bruker Esquire-HP 1100 mass spectrometer was used to obtain general mass spectra, and a Finnigan 8340 mass spectrometer was used to obtain high-resolution mass spectra. Flash column chromatography was performed with 32-63 μm, 60-Å silica gel.

Preparation of D-glucal (2) from tri-*O*-acetyl-D-glucal (1).

In a flame dried 500 mL round-bottom flask equipped with a septum and magnetic stir bar, tri-*O*-acetyl-D-glucal (**1**) (15.0 g, 55.6 mmol) was dissolved in methanol (235 mL). A catalytic amount of sodium (spheres, 38 mg, 2.0 mmol) was then added and the solution was allowed to stir at room temperature until TLC (100% ethyl acetate, R_f = 0.24) showed consumption of the starting material. Upon completion, excess carbon dioxide in the form of dry ice (5 g) was added to neutralize any unreacted methoxide in the solution. The mixture was then reduced and the product was extracted with hot ethyl acetate (3 x 150 mL) to yield 5.83 g of D-glucal (**2**) after evaporation of the solvent as a white powder (72%). Melting point 56-58 °C, literature melting point 57-59 °C.[31]

^{1}H NMR (D_6-DMSO): δ 6.26 (dd, J = 7.69, 4.39 Hz, 1H, H-1), 5.10 (d, J = 5.49 Hz, 1H, OH), 4.86 (d, J = 5.49 Hz, 1H, OH), 4.56 (m, 2H, OH, H-2), 3.90 (m, 1H, H-4), 3.60 (m, 1H, H-5), 3.55 (m, 1H, H-3), 3.33 (m, 2H, H-6 and H-6').

^{13}C NMR (D_6-DMSO): δ 144.2, 105.9, 80.9, 70.6, 70.0, 61.9.

Preparation of tri-*O*-benzyl-D-glucal (3) from D-glucal (2).

In a flame-dried 250 mL round-bottom flask equipped with a septum and magnetic stir bar, D-glucal (**2**) (2.35 g, 16.1 mmol) was dissolved in anhydrous tetrahydrofuran (45 mL) at room temperature. Sodium hydride (2.75 g, 69.0 mmol) was then added to the mixture slowly, and the solution was allowed to stir at room temperature for 15 minutes. Benzyl bromide (9.6 mL, 80.5 mmol) was then added *via* syringe and the mixture was refluxed until TLC (10:1 hexanes/ethyl acetate, R_f = 0.29) showed consumption of starting material (~3 hrs). Upon completion, the mixture was poured over ice water (50 mL) and washed with 5% sulfuric acid (8 mL). The product was then extracted with methylene chloride (3 x 50 mL) and the combined extracts were dried over anhydrous magnesium sulfate, filtered and reduced. The product was then recrystallized from hexanes to afford 4.24 g tri-*O*-benzyl-D-glucal (**3**) as a white powder (63%). Melting point 58-59 °C, literature melting point 57-58 °C.[32]

^{1}H NMR ($CDCl_3$): δ 7.23 – 7.34 (m, 15H, Ar-H), 6.42 (dd, J = 7.32, 4.94 Hz, 1H, H-1), 4.88 (m, 1H, H-2), 4.54 – 4.65 (m, 6H, 3 x OC$\underline{H_2}$Ph), 4.22 (m, 1H, H-5), 4.06 (m, 1H, H-3), 3.76 – 3.84 (m, 3H, H-4, H-6, H-6').

^{13}C NMR ($CDCl_3$): δ 145.7, 139.3, 139.1, 138.9, 129.43, 129.39, 129.15, 128.94, 128.81, 128.76, 128.75, 128.7, 128.67, 101.0, 76.9, 75.5, 74.9, 74.6, 71.6, 69.6.

Synthesis of thianthrene-5-oxide (5) from thianthrene (4) and *m*-CPBA.

In a flame dried 100 mL round-bottom flask equipped with a magnetic stir bar and septum inlet, thianthrene (**4**) (0.98 g, 5.6 mmol) was dissolved in methylene chloride (40 mL). The solution was then cooled to 0 °C and *m*-CPBA (77% assay) (1.2 g, 6.7 mmol) was then added. The reaction was allowed to proceed at 0 °C until TLC (100% ethyl acetate, R_f = 0.69) showed consumption of starting material. The solution was then filtered to remove *m*-chlorobenzoic acid and the filtrate was reduced to leave a white solid. The solid was purified by flash column (4:1 hexanes/ethyl acetate) to afford 1.07 g of thianthrene-5-oxide (**5**) (~100%) as a white crystalline solid. Melting point 98-100 °C.

^{1}H NMR ($CDCl_3$): δ 7.93 (dd, J = 9.15, 6.40 Hz, 2H, H-1, H-1'), 7.64 (m, 2H, H-4, H-4'), 7.54 – 7.56 (m, 2H, H-3, H-3'), 7.43 – 7.46 (m, 2H, H-2, H-2').

^{13}C NMR ($CDCl_3$): δ 142.3, 134.7, 130.9, 130.0, 129.4, 125.5.

m/z calculated: 232.32 *m/z* (APCI) observed: 233.16

Attempted acetamidoglycosylation of tri-*O*-benzyl-D-glucal with 2-propanol and *N*-trimethylsilyl acetamide.

In a flame-dried, nitrogen-flushed three-necked 50 mL round-bottom flask equipped with a magnetic stir bar and septum inlets, tri-*O*-benzyl-D-glucal (200 mg, 0.48 mmol) and thianthrene-5-oxide (224 mg, 0.96 mmol) were dissolved in 10 mL of 4:1 anhydrous chloroform : methylene chloride. The solution was then cooled to –78 °C and triflic anhydride (0.162 mL, 0.96 mmol) was added *via* syringe. After allowing the mixture to stir for 15 minutes at –78 °C, *N,N*-diethylaniline (0.304 mL, 1.92 mmol) and 0.85 M *N*-(trimethylsilyl)acetamide in chloroform (1.35 mL, 1.15 mol) were added

sequentially and the mixture was immediately brought to room temperature. The mixture was then allowed to stir at room temperature until TLC showed formation of the intermediate oxazoline product. The solution was then cooled to –78° C and Amberlyst-15 (290 mg) and 2-propanol (0.110 mL, 1.44 mmol) were sequentially added. The mixture was then brought to room temperature and was stirred until TLC showed consumption of starting material. The Amberlyst-15 was then filtered and the solution was poured over saturated sodium chloride (25 mL). The organic product was extracted using methylene chloride (3 x 20 mL) and the combined extracts were dried over anhydrous magnesium sulfate. After filtering the magnesium sulfate, the solvent was removed and the suspected product was isolated *via* flash column using 8:1 hexanes/ethyl acetate. The method described was attempted many times without success. According to ^{1}H NMR data, glycosylation occurred but insertion of the acetamide moiety was absent. Molecular sieves were employed as drying agents in the reaction mixture to ensure the water did not interfere with the desired reaction. The method was also attempted using 3,4-*O*-dibenzyl-6-*O*-*t*-butyldiphenylsilyl-D-glucal (270 mg, 0.480 mmol) and 3,4-*O*-dibenzyl-D-rhamnal (100 mg, 0.322 mmol) without success.

Preparation of 1-*O*-acetyl-3,4,6-tri-*O*-benzyl-2-deoxy-2-nitro-α-D-glucopyranoside (6) from tri-*O*-benzyl-D-glucal (3).

In a flame-dried 25 mL round-bottom flask equipped with a magnetic stir bar and septum inlet, concentrated nitric acid (0.9 mL, 14.22 mmol) was added to acetic anhydride (7 mL) at –10 °C under a nitrogen atmosphere over 30 minutes. The solution was then further cooled to –42 °C and tri-*O*-benzyl-D-glucal (**3**) (1.6 g, 3.8 mmol) in

acetic anhydride (2 mL) was added dropwise over 15 minutes. The mixture was then allowed to stir at –42 °C until TLC showed consumption of starting material. The reaction mixture was then brought to 0 °C and was poured over ice water (40 mL), mixed with saturated aqueous sodium chloride (40 mL) and extracted with diethyl ether (3 x 40 mL). The combined organic extracts were dried over magnesium sulfate, filtered and evaporated under reduced pressure. The reduced extracts yielded 2.34 g of crude yellow syrup.

Preparation of 3,4,6-tri-*O*-benzyl-2-nitro-D-glucal (7) from crude 1-*O*-acetyl-3,4,6-tri-*O*-benzyl-2-deoxy-2-nitro-α-D-glucopyranoside (6).

In a flame-dried 50 mL round-bottom flask equipped with a magnetic stir bar and septum inlet, triethylamine (1.0 mL, 5.4 mmol) was added slowly to a stirred solution of the crude 1-*O*-acetyl-3,4,6-tri-*O*-benzyl-2-deoxy-2-nitro-α-D-glucopyranoside (**6**) (2.34 g, 4.5 mmol) in freshly distilled methylene chloride (24 mL) at 0 °C under a nitrogen atmosphere. After adding the base, the cold bath was removed and the mixture was allowed to stir at room temperature until TLC (4:1 hexanes/ethyl acetate, R_f = 0.43) showed consumption of starting material. The solution was then further diluted with methylene chloride (40 mL) and washed with water (1 x 40 mL), 1M HCl (1 x 40 mL), sodium bicarbonate (1 x 40 mL) and sodium chloride (1 x 40 mL). The organic product was extracted with methylene chloride and the combined extracts were dried over magnesium sulfate. After reducing the extracts, the product was isolated *via* flash column using 10:1 hexanes/ethyl acetate to yield 980 mg of 3,4,6-tri-*O*-benzyl-2-nitro-D-glucal (**7**) as a yellow syrup (55% for both steps combined).

^{1}H NMR ($CDCl_3$): δ 8.22 (s, 1H, H-1), 7.23 – 7.37 (m, 15H, Ar-H), 4.42 – 4.72 (m, 8H, 3 x OC$\underline{H}_2$Ph, H-3, H-5), 3.87 (m, 1H, H-4), 3.73 (m, 1H, H-6), 3.60 (m, 1H, H-6').

^{13}C NMR ($CDCl_3$): δ 155.44, 138.33, 138.29, 137.81, 131.73, 129.66, 129.54, 129.50, 129.29, 129.18, 129.11, 128.94, 128.83, 128.76, 79.52, 74.56, 74.14, 72.89, 72.24, 68.85, 68.58.

m/z calculated: 461.51 *m/z* (ESI, + H_2O) observed: 479.22

Preparation of methyl 3,4,6-tri-*O*-benzyl-2-deoxy-2-nitro-D-glucopyranoside (8) from 3,4,6-tri-*O*-benzyl-2-nitro-D-glucal (7).

In a flame-dried 10 mL vial equipped with a magnetic stir bar and septum inlet, a mixture of methanol (0.11 mL, 2.1 mmol) and triethylamine (0.29 mL, 2.0 mmol) were allowed to stir at room temperature under a nitrogen atmosphere. A solution of 3,4,6-tri-*O*-benzyl-2-nitro-D-glucal (**7**) (60 mg, 0.13 mmol) in anhydrous tetrahydrofuran (1 mL) was added dropwise over 15 minutes. The mixture was allowed to stir until TLC (4:1 hexanes/ethyl acetate, R_f = 0.48) showed consumption of starting material (~5 hrs). The solution was reduced and the product was collected *via* preparative TLC using 5:1 hexanes/ethyl acetate as eluent. Methyl 3,4,6-tri-*O*-benzyl-2-deoxy-2-nitro-D-gluco-pyranoside (**8**) was isolated as 44 mg of yellow syrup (69%).

^{1}H NMR ($CDCl_3$): δ 7.16 – 7.34 (m, 15H, Ar-H), 4.78 (d, J = 10.80 Hz, 1H, H-2), 4.71 (d, J = 8.06 Hz, 1H, H-1), 4.50 - 4.65 (m, 6H, 3 x OC$\underline{H}_2$Ph), 4.26 (t, J = 9.31 Hz, 1H, H-3), 3.75 (m, 3H, H-4, H-6, H-6'), 3.55 (m, 1H, H-5), 3.52 (s, 3H, OC$\underline{H}_3$).

^{13}C NMR ($CDCl_3$): δ 138.68, 138.40, 137.88, 129.52, 129.47, 129.36, 129.24, 129.19, 129.10, 128.97, 128.89, 128.70, 101.91, 90.74, 82.44, 76.39, 76.34, 74.76, 74.73, 74.68, 69.08, 58.51.

m/z calculated: 493.55 *m/z* (ESI, + H_2O) observed: 511.44

Raney nickel reduction of methyl 3,4,6-tri-*O*-benzyl-2-deoxy-2-nitro-D-gluco-pyranoside (8).

Methyl 3,4,6-tri-*O*-benzyl-2-deoxy-2-nitro-D-glucopyranoside (215 mg, 0.43 mmol) was dissolved in ethanol (5 mL) and placed in an oven-dried 25 mL round-bottom flask equipped with a magnetic stir bar and septum inlet. Raney nickel (slurry in water, ~1 mL) was then added *via* pipette and the mixture was allowed to stir at room temperature until TLC showed consumption of starting material (overnight). The Raney Nickel was then filtered from the reaction and was washed with ethanol (3 x 5 mL). The resulting ethanol/water mixture was then reduced to yield an oily water solution, which was then poured into methylene chloride (20 mL) and washed with water (20 mL). The methylene chloride extracts were dried over anhydrous magnesium sulfate, filtered and reduced to give a yellow syrup (170 mg, crude). The crude syrup was used in the next step of the reaction immediately to avoid any decomposition.

Acetylation of crude methyl 2-amino-2-deoxy-3,4,6-tri-*O*-benzyl-D-glucopyranoside.

The crude reaction mixture (170 mg, 0.37 mmol) was dissolved in anhydrous pyridine (10 mL) and was placed in a flame-dried, nitrogen-flushed 25 mL round-bottom flask equipped with a magnetic stir bar and septum inlet. Acetic anhydride (2 mL, 21.2

mmol) was then added *via* syringe and the mixture was allowed to stir at room temperature until TLC showed consumption of starting material. The mixture was then poured over ice water (20 mL) and the product was extracted with methylene chloride (3 x 30 mL). The combined extracts were dried over anhydrous magnesium sulfate, filtered and reduced. The product was isolated *via* flash column using 10:1 hexanes/ethyl acetate, but the product did not come off the column until it was flushed with ethyl acetate. The column afforded 160 mg of methyl 2-acetamido-2-deoxy-3,4,6-tri-*O*-benzyl-D-glucopyranoside (**9**) (73% for both steps) as a white residue.

^{1}H NMR ($CDCl_3$): δ 7.18 – 7.34 (m, 15H, Ar-H), 5.50 (d, J = 7.87 Hz, 1H, NH-Ac), 4.81 (m, 1H, H-2), 4.70 (d, J = 7.67 Hz, 1H, H-1), 4.53 – 4.63 (m, 6H, 3 x $OC\underline{H}_2Ph$), 4.05 (t, J = 8.32 Hz, 1H, H-3), 3.74 (m, 3H, H-4, H-6, H-6'), 3.50 (m, 1H, H-5), 3.48 (s, 3H, $OC\underline{H}_3$), 1.86 (s, 3H, $C\underline{H}_3$).

^{13}C NMR ($CDCl_3$): δ 171.25, 139.32, 139.08, 138.94, 129.42, 129.34, 129.24, 129.16, 128.99, 128.86, 128.79, 128.65, 128.61, 101.95, 81.47, 80,76, 79.54, 76.01, 75.80, 74.87, 74.59, 71.14, 57.81, 25.51.

m/z calculated: 505.60 *m/z* (ESI) observed: 504.60

_t_-Butyldiphenylsilyl protection of the primary hydroxyl of D-glucal (2).

D-Glucal (**2**) (1.51 g, 10.3 mmol) and imidazole (1.43 g, 21.0 mmol) were placed in a flame dried 100 mL round-bottom flask equipped with a magnetic stir bar and septum inlet. D-Glucal (**2**) and imidazole were then dissolved in anhydrous dimethylformamide (45 mL) and allowed to stir at room temperature. *t*-Butyl-diphenylsilyl chloride (2.35 mL, 9.0 mmol) was then added *via* syringe and the mixture

was allowed to stir at room temperature until TLC (100% ethyl acetate, R_f = 0.66) no longer showed evidence of starting material. The mixture was then reduced and the product was collected *via* flash column (2:1 hexanes/ethyl acetate). The combined fractions afforded 3.03 g of protected glucal **10** as a clear syrup (76%).

^{1}H NMR (D_6-DMSO): δ 7.67 – 7.62 (m, 5H, Ar-H), 7.44 – 7.39 (m, 5H, Ar-H), 6.34 (dd, J = 7.69, 4.39 Hz, 1H, H-1), 5.23 (d, J = 5.68 Hz, 1H, OH), 4.95 (d, J = 5.49, 1H, OH), 4.59 – 4.57 (m, 1H, H-2), 3.96 (m, 1H, H-4), 3.90 (d, J = 3.66 Hz, 2H, H-6, H-6'), 3.72 (m, 1H, H-5), 3.45 (m, 1H, H-3), 0.97 (s, 9H, $C(C\underline{H}_3)_3$).

^{13}C NMR (D_6-DMSO): δ 144.3, 136.57, 134.54, 131.23, 129.28, 105.9, 80.5, 70.3, 70.0, 64.4, 28.3, 20.6.

m/z calculated: 384.54 *m/z* (ESI) observed: 383.20

Benzylation of 6-*O*-*t*-butyldiphenylsilyl-D-glucal (10).

TBDPS-protected D-glucal (**10**) (1.74 g, 4.6 mmol) was dissolved in anhydrous tetrahydrofuran and placed in a flame-dried 100 mL round-bottom flask equipped with a magnetic stir bar. Sodium hydride (60% dispersion) (1.36 g, 33.8 mmol) was then added slowly while the solution stirred at room temperature. After allowing the solution to stir for 15 minutes, benzyl bromide (3.39 mL, 28.5 mmol) was added *via* syringe. The solution was then refluxed until TLC (5:1 hexanes/ethyl acetate, R_f = 0.66) indicated consumption of the starting material (~3 hrs). The reaction mixture was then poured over ice water (75 mL) and washed with 5% sulfuric acid (10 mL). The product was then extracted with methylene chloride (3 x 100 mL) and the combined organic extracts were dried over anhydrous magnesium sulfate, filtered and reduced. Pure product was then

isolated *via* flash column using hexanes to flush the excess benzyl bromide and ethyl acetate to elute the product. The column afforded 4.97 g of **11** as an orange syrup (98%).

^{1}H NMR ($CDCl_3$): δ 7.67 – 7.71 (m, 5H, Ar-H), 7.21 – 7.46 (m, 15H, Ar-H), 6.23 (dd, J = 7.32, 5.13 Hz, 1H, H-1), 4.86 (m, 1H, H-2), 4.51 – 4.70 (m, 4H, 2 x $OC\underline{H}_2Ph$), 4.44 (m, 1H, H-5), 4.15 (m, 1H, H-3), 4.04 (m, 2H, H-6, H-6'), 3.74 (m, 1H, H-4), 1.06 (s, 9H, $C(C\underline{H}_3)_3$).

^{13}C NMR ($CDCl_3$): δ 144.7, 139.31, 139.22, 136.83, 134.54, 130.69, 129.43, 129.36, 129.21, 129.00, 128.90, 128.82, 128.70, 103.5, 76.87, 75.50, 74.92, 74.32, 71.86, 69.66, 28.20, 20.59.

m/z calculated: 564.79 *m/z* (APCI, + H_2O) observed: 582.33

Deprotection of the primary hydroxyl in 3,4-di-*O*-benzyl-6-*t*-butyldiphenylsilyl-D-glucal (11) using tetra-*N*-butyl ammonium fluoride.

The protected sugar **11** (4.85 g, 8.6 mmol) was dissolved in anhydrous tetrahydrofuran (100 mL) and placed in a 250 mL flame-dried round-bottom flask equipped with a magnetic stir bar and septum inlet. Tetra-*N*-butylammonium fluoride in THF (1M, 8.6 mL, 8.6 mmol) was then added *via* syringe and the solution was allowed to stir at room temperature until starting material was no longer evident by TLC (2:1 hexanes/ethyl acetate, R_f = 0.48). The solution was then reduced and the pure product was isolated *via* flash column using 4:1 hexanes/ethyl acetate. The combined fractions afforded 2.15 g of the **12** as a light-brown syrup (77%).

^{1}H NMR ($CDCl_3$): δ 7.26 – 7.38 (m, 10H, Ar-H), 6.41 (td, J = 13.36, 10.44, 1.46 Hz, 1H, H-1), 4.91 (m, 1H, H-2), 4.56 – 4.80 (m, 5H, 2 x OC<u>H</u>$_2$Ph, OH), 4.24 (m, 1H, H-3), 3.97 (m, 1H, H-5), 3.81 (m, 2H, H-6, H-6'), 3.69 (m, 1H, H-4).

^{13}C NMR ($CDCl_3$): δ 145.5, 139.18, 138.97, 129.53, 129.46, 129.06, 128.97, 128.95, 128.80, 103.8, 76.64, 75.63, 74.92, 71.68, 70.21, 62.93.

m/z calculated: 326.39 *m/z* (ESI) observed: 327.29

Preparation of 3,4-di-*O*-benzyl-6-*O*-imidazolyl-D-glucal (13).

3,4-Di-*O*-benzyl-D-glucal (**12**) (385 mg, 1.2 mmol) was dissolved in anhydrous tetrahydrofuran (7 mL) and placed in a flame-dried 25 mL round-bottom flask equipped with a septum inlet and magnetic stir bar. *N,N*-Thiocarbonyldiimidazole (502 mg, 2.4 mmol) was then added and the mixture was allowed to stir at room temperature under a nitrogen atmosphere until TLC (2:1 hexanes/ethyl acetate, R_f = 0.33) showed consumption of starting material (overnight). Upon completion of the reaction, the reaction mixture was reduced and the product was isolated *via* flash column (3:1 hexanes/ethyl acetate). The combined fractions from the column afforded 380 mg of **13** as a clear yellow syrup (74%).

^{1}H NMR ($CDCl_3$): δ 8.22 (s, 1H, NC<u>H</u>=N), 7.52 (s, 1H, NC<u>H</u>=C), 7.21 – 7.37 (m, 10H, Ar-H), 7.01 (s, 1H, NC<u>H</u>=C), 6.40 (dd, J = 7.32 Hz, 5.13, 1H, H-1), 4.98 (m, 1H, H-2), 4.78 – 4.89 (m, 5H, H-5, 2 x OC<u>H</u>$_2$Ph), 4.68 (m, 1H, H-3), 4.27 (m, 2H, H-6, H-6'), 3.78 (m, 1H, H-4).

^{13}C NMR ($CDCl_3$): δ 184.6, 145.1, 138.8, 138.2, 137.9, 131.8, 129.54, 129.52, 129.3, 129.0, 128.9, 128.8, 118.43, 101.2, 76.1, 75.2, 74.4, 73.9, 72.2, 71.8.

m/z calculated: 436.52 *m/z* (ESI) observed: 437.20

Attempted tri-*n*-butyltin hydride reduction of 3,4-di-*O*-benzyl-6-*O*-imidazolyl-D-glucal (13).

In a flame-dried 100 mL three-necked round-bottom flask equipped with a magnetic stir bar and septum inlets, a solution of anhydrous toluene (30 mL) and tri-*n*-butyltin hydride (0.21 mL, 0.77 mmol) was refluxed under an inert atmosphere. 3,4-Di-*O*-benzyl-6-*O*-imidazolyl-D-glucal (**13**) (200 mg, 0.5 mmol) was dissolved in anhydrous toluene (10-15 mL) and was added dropwise to the toluene / *n*-Bu_3SnH solution over a 20 minute period. The mixture was allowed to reflux until TLC showed consumption of starting material (~5 hrs). The solution was then reduced to a brown residue and the product was extracted using hot acetonitrile (3 x 50 mL). The combined extracts were washed with hexanes (4 x 50 mL) to remove any tin containing compounds and the clean acetonitrile extracts were reduced to yield a brown syrup. The product was further purified *via* flash column using 5:1 hexanes/ethyl acetate. Upon review of the NMR data, it was determined that the desired product was not produced using this method. Unconsumed starting material was the main component observed in the ^1H NMR spectrum.

Tosylation of 3,4-di-*O*-benzyl-D-glucal (12).

3,4-Di-*O*-benzyl-D-glucal (**12**) (650 mg, 2.0 mmol) was dissolved in anhydrous pyridine (20 mL) and placed in a flame-dried 25 mL round-bottom flask equipped with a magnetic stir bar and septum inlet. *p*-Toluensulfonyl chloride (1.0 g, 5.2 mmol) was then

added and the mixture was allowed to stir at room temperature. After TLC (4:1 hexanes/ethyl acetate, R_f = 0.37) no longer showed evidence of starting material, water (1-2 mL) was added to the solution and the mixture was allowed to stir for 1 hour. The mixture was then poured into water (35 mL) and the organic product was extracted with methylene chloride (3 x 30 mL). The combined extracts were dried over anhydrous magnesium sulfate and then reduced. The product was further purified by flash column in 6:1 hexanes/ethyl acetate to afford 906 mg of **15** as a clear syrup (95%).

^{1}H NMR ($CDCl_3$): δ 7.83 (dd, J = 8.24, 4.76 Hz, 2H, Ar-H), 7.23 – 7.35 (m, 12H, Ar-H, Ar-H), 6.26 (dd, J = 7.51, 4.94 Hz, 1H, H-1), 4.86 (m, 1H, H-2), 4.48 – 4.82 (m, 4H, 2 x O$\underline{CH_2}$Ph), 4.35 (m, 1H, H-5), 4.26 (m, 1H, H-3), 4.14 (m, 2H, H-6, H-6'), 3.73 (m, 1H, H-4), 2.42 (s, 3H, $C\underline{H_3}$).

^{13}C NMR ($CDCl_3$): δ 145.8, 145.0, 138.97, 138.62, 130.79, 129.47, 129.21, 129.14, 129.02, 128.98, 128.93, 128.78, 128.73, 101.4, 75.78, 75.56, 74.68, 74.38, 71.50, 69.17, 22.9.

m/z calculated: 480.57 *m/z* (APCI, + H_2O) observed: 498.36

Reduction of tosylated dibenzyl-D-glucal (15) *via* lithium aluminum hydride.

Lithium aluminum hydride (50 mg, 1.3 mmol) was dissolved in anhydrous tetrahydrofuran (8 mL) and placed in a flame-dried, nitrogen-flushed 25 mL round-bottom flask equipped with a magnetic stir bar and septum inlet. Tosylated dibenzyl glucal (**15**) (150 mg, 0.3 mmol) was then dissolved in anhydrous tetrahydrofuran (2 mL) and added dropwise *via* syringe. The solution was then refluxed while maintaining an inert atmosphere until TLC (4:1 hexanes/ethyl acetate, R_f = 0.86) showed complete

consumption of starting material. Upon completion, the lithium aluminum hydride was quenched by adding 1 mL of water, 3 mL of 15% sodium hydroxide and 1 mL of water sequentially. The reaction mixture was then filtered to remove the aluminum salts, and was then poured over water (15 mL) and the product was extracted with methylene chloride (3 x 20 mL). The combined extracts were dried over anhydrous magnesium sulfate, filtered and reduced. The product was further purified *via* flash column using 10:1 hexanes/ethyl acetate to afford 80 mg of **14** as a yellow syrup (83%).

^{1}H NMR ($CDCl_3$): δ 7.26 – 7.38 (m, 10H, Ar-H), 6.36 (dd, J = 7.51, 4.94 Hz, 1H, H-1), 4.87 (m, 1H, H-2), 4.56 – 4.72 (m, 4H, 2 x O$\underline{CH_2}$Ph), 4.21 (m, 1H, H-5), 3.96 (m, 1H, H-3), 3.48 (m, 1H, H-4), 1.38 (d, J = 6.41 Hz, 3H, $\underline{CH_3}$).

^{13}C NMR ($CDCl_3$): δ 145.7, 139.34, 139.20, 129.59, 129.44, 129.00, 128.78, 128.67, 128.01, 101.21, 80.61, 77.54, 75.24, 75.10, 71.70, 18.8.

m/z calculated: 310.40 *m/z* (ESI, + H_2O) observed: 328.26

Preparation of 1-*O*-acetyl-3,4-di-*O*-benzyl-2,6-dideoxy-2-nitro-α-D-glucopyranoside (16) from 3,4-di-*O*-benzyl rhamnal (14).

In a flame-dried 25 mL round-bottom flask equipped with a magnetic stir bar and septum inlet, concentrated nitric acid (0.35 mL, 8.3 mmol) was added to acetic anhydride (3.2 mL) at –10 °C under a nitrogen atmosphere over 30 minutes. The solution was then further cooled to –42 °C and 3,4-di-*O*-benzyl-D-rhamnal (**14**) (390 mg, 1.3 mmol) in acetic anhydride (1 mL) was added dropwise over 15 minutes. The mixture was then allowed to stir at –42 °C until TLC showed consumption of starting material. The reaction mixture was then brought to 0 °C and was poured over ice water (10 mL),

diluted with saturated sodium chloride (20 mL) and extracted with diethyl ether (3 x 20 mL). The combined organic extracts were dried over magnesium sulfate, filtered and reduced. The reduced extracts yielded 500 mg of crude yellow syrup. Literature reported a greater yield in other examples when using the crude product directly in the next step.

Preparation of 3,4-di-*O*-benzyl-2-nitro-D-rhamnal (17) from crude 1-*O*-acetyl-3,4-di-*O*-benzyl-2,6-dideoxy-2-nitro-α-D-glucopyranoside (16).

In a flame dried 25 mL round-bottom flask equipped with a magnetic stir bar and septum inlet, triethylamine (0.25 mL, 1.8 mmol) was added slowly to a stirred solution of the crude 1-*O*-acetyl-3,4-di-*O*-benzyl-2,6-dideoxy-2-nitro-α-D-glucopyranoside (**16**) (500 mg, 1.2 mmol) in freshly distilled methylene chloride (8 mL) at 0 °C under a nitrogen atmosphere. After adding the base, the cold bath was removed and the mixture was allowed to stir at room temperature until TLC showed consumption of starting material (~4 hrs). The solution was then further diluted with methylene chloride (20 mL) and washed with water (1 x 30 mL), 1M HCl (1 x 30 mL), saturated sodium bicarbonate (1 x 30 mL) and saturated sodium chloride (1 x 30 mL). The organic product was extracted with methylene chloride and the combined extracts were dried over magnesium sulfate. After reducing the extracts, the product was isolated *via* flash column in 10:1 hexanes/ethyl acetate to yield 170 mg of 3,4-di-*O*-benzyl-2-nitro-D-rhamnal (**17**) as a yellow syrup (37% for both steps).

^{1}H NMR ($CDCl_3$): δ 8.21 (s, 1H, H-1), 7.22 – 7.43 (m, 10H, Ar-H), 4.70 – 4.82 (m, 4H, 2 x O$C\underline{H}_2$Ph), 4.62 (m, 1H, H-5), 4.57 (m, 1H, H-5), 4.52 (d, J = 11.9 Hz, 1H, H-3), 4.41 (d, J = 11.9 Hz, 1H, H-4), 1.40 (d, J = 7.14 Hz, 3H, $C\underline{H}_3$).

^{13}C NMR ($CDCl_3$): δ 155.56, 138.70, 138.38, 130.79, 129.65, 129.51, 129.23, 129.08, 129.04, 90.87, 77.28, 75.65, 74.25, 72.81, 69.49, 17.42.

Preparation of methyl 3,4-di-*O*-benzyl-2,6-dideoxy-2-nitro-D-glucopyranoside (18) from 3,4-di-*O*-benzyl-2-nitro-D-rhamnal (17).

In a flame-dried 10 mL vial equipped with a magnetic stir bar and septum inlet, a mixture of methanol (0.343 mL, 6.6 mmol) and triethylamine (0.914 mL, 6.3 mmol) were allowed to stir at room temperature under a nitrogen atmosphere. A solution of 3,4-di-*O*-benzyl-2-nitro-D-rhamnal (**17**) (150 mg, 0.421 mmol) in anhydrous tetrahydrofuran (3 mL) was added dropwise over 15 minutes. The mixture was allowed to stir until TLC showed consumption of starting material (~5 hrs). The solution was reduced and the product was collected *via* flash column (10:1 hexanes/ethyl acetate) to give 110 mg of methyl 3,4-di-*O*-benzyl-2,6-dideoxy-2-nitro-D-glucopyranoside (**18**) as a yellow syrup (67%).

^{1}H NMR ($CDCl_3$): δ 7.30 – 7.42 (m, 10H, Ar-H), 4.86 (m, 1H, H-2), 4.70 (d, J = 8.06 Hz, 1H, H-1), 4.65 – 4.76 (m, 4H, 2 x OC$\underline{H}_2$Ph), 4.51 (m, 1H, H-4), 4.23 (m, 1H, H-3), 3.49 (s, 3H, OC$\underline{H}_3$), 1.34 (d, J = 6.21 Hz, 3H, C$\underline{H}_3$).

^{13}C NMR ($CDCl_3$): δ 138.37, 137.86, 129.59, 129.52, 129.26, 129.15, 128.97, 128.72, 101.65, 91.04, 84.19, 82.43, 76.69, 73.04, 72.86, 27.85, 18.88.

m/z calculated: 387.43 m/z (ESI, + H_2O) observed: 405.35

Raney nickel reduction of methyl 3,4-di-*O*-benzyl-2,6-dideoxy-2-nitro-D-gluco-pyranoside (18).

Methyl 3,4-di-*O*-benzyl-2,6-dideoxy-2-nitro-D-glucopyranoside (**18**) (100 mg, 0.25 mmol) was dissolved in ethanol (5 mL) and placed in an oven-dried 25 mL round-bottom flask equipped with a magnetic stir bar and septum inlet. Raney nickel (slurry in water, ~1 mL) was then added *via* pipette and the mixture was allowed to stir at room temperature until TLC showed consumption of starting material. The Raney nickel was then filtered from the reaction and was washed with ethanol (3 x 5 mL). The resulting ethanol/water mixture was then reduced to yield an oily water solution, which was then poured into methylene chloride (20 mL) and washed with water (20 mL). The methylene chloride extracts were dried over anhydrous magnesium sulfate, filtered and reduced to give a yellow syrup (90 mg, crude). The crude syrup was used in the next step of the reaction immediately to prevent decomposition.

Acetylation of crude methyl 3,4-di-*O*-benzyl-2,6-dideoxy-2-amino-D-gluco-pyranoside to afford methyl *N*-acetyl-3,4-di-*O*-benzyl quinavosamine (19).

The crude reaction mixture from the previous experiment (90 mg, 0.25 mmol) was dissolved in anhydrous pyridine (8 mL) and was placed in a flame-dried, nitrogen flushed 25 mL round-bottom flask equipped with a magnetic stir bar and septum inlet. Acetic anhydride (2 mL, 21.2 mmol) was then added *via* syringe and the mixture was allowed to stir at room temperature until TLC showed consumption of starting material. The mixture was then poured over ice water (20 mL) and the product was extracted with methylene chloride (3 x 30 mL). The combined extracts were dried over anhydrous

magnesium sulfate, filtered and reduced. The product was isolated *via* flash column in 2:1 hexanes/ethyl acetate, but the product did not come off the column until it was flushed with methanol. The column afforded 20 mg of methyl *N*-acetyl-3,4-di-*O*-benzyl quinavosamine (**19**) (19% for both steps combined) as a white residue.

^{1}H NMR ($CDCl_3$): δ 7.25 – 7.36 (m, 10H, Ar-H), 5.46 (d, J = 7.51 Hz, 1H, N-H), 4.84 (m, 2H, 1 x OC$\underline{H}_2$Ph), 4.69 (m, 1H, H-2), 4.68 (d, J = 8.06 Hz, 1H, H-1), 4.65 (m, 2H, 1 x OC$\underline{H}_2$Ph), 4.03 (dd, J = 8.79, 1.28 Hz, 1H, H-5), 3.46 (s, 3H, OC$\underline{H}_3$), 3.37 (m, 1H, H-3), 3.21 (m, 1H, H-4), 1.86 (s, 3H, C(O)C$\underline{H}_3$), 1.32 (d, J = 6.23 Hz, 3H, C$\underline{H}_3$).

^{13}C NMR ($CDCl_3$): δ 171.39, 139.34, 138.96, 129.52, 129.49, 129.09, 128.95, 128.89, 128.85, 101.74, 85.62, 81.68, 76.27, 76.11, 72.26, 58.52, 30.97, 25.01, 19.24.

m/z calculated: 399.48 *m/z* (ESI) observed: 398.49

Preparation of D-galactal (21) from tri-*O*-acetyl-D-galactal (20).

In a flame-dried round-bottom flask equipped with a magnetic stir bar and septum inlet, tri-*O*-acetyl-D-galactal (**20**) (400 mg, 1.5 mmol) was dissolved in methanol (10 mL). A catalytic amount of sodium (1 mg, 0.037 mmol) was then added and the mixture was allowed to stir until TLC (100% ethyl acetate, R_f = 0.19) showed consumption of starting material (~5 hrs). To quench the reaction, carbon dioxide in the form of dry ice (2.0 g) was added to the solution and the mixture was allowed to stir. The solution was then reduced to give a clear syrup. The pure product was then extracted from the syrup using hot ethyl acetate (6 x 25 mL). The combined extracts were reduced to yield 215

mg of D-galactal (**21**) as a white powder (73%). Melting point 103-104 °C, literature melting point 104 °C.[31]

^{1}H NMR (D_6-DMSO): δ 6.23 (dd, J = 7.87, 4.39 Hz, 1H, H-1), 4.72 (t, J = 5.86 Hz, 1H, OH), 4.61 (d, J = 6.59 Hz, 1H, OH), 4.45 (m, 1H, H-2), 4.37 (d, J = 4.39 Hz, 1H, OH), 4.16 (m, 1H, H-5), 3.72 (m, 2H, H-3, H-4), 3.54 (m, 2H, H-6, H-6').

^{13}C NMR (D_6-DMSO): δ 144.6, 105.2, 79.1, 65.9, 65.1, 61.8.

m/z calculated: 146.14 *m/z* (ESI) observed: 145.00

Preparation of 6-*O*-*t*-butyldiphenylsilyl-D-galactal (22).

In a flame-dried 25 mL round-bottom flask equipped with a magnetic stir bar and septum inlet, D-galactal (**21**) (140 mg, 0.96 mmol) was dissolved in anhydrous dimethylformamide (8 mL) under nitrogen. Imidazole (136 mg, 2.0 mmol) was then added to the mixture and was dissolved at room temperature. *t*-Butyldiphenylsilyl chloride (0.23 mL, 0.9 mmol) was then added *via* syringe and the mixture was allowed to stir until TLC (100% ethyl acetate, R_f = 0.60) showed consumption of starting material (~3 hrs). The mixture was then reduced and the product was collected *via* flash column with 3:1 hexanes/ethyl acetate to afford 330 mg of **22** as a clear syrup (90%).

^{1}H NMR (D_6-DMSO): δ 7.61 – 7.64 (m, 5H, Ar-H), 7.39 – 7.45 (m, 5H, Ar-H), 6.23 (dd, J = 8.06, 4.39 Hz, 1H, H-1), 4.67 (d, J = 6.41 Hz, 1H, OH), 4.52 (d, J = 4.21 Hz, 1H, OH), 4.49 (m, 1H, H-2), 4.17 (m, 1H, H-5), 3.95 (m, 1H, H-3), 3.84 (m, 1H, H-4), 3.75 (m, 2H, H-6, H-6'), 0.97 (s, 9H, C(C$\underline{H}_3$)$_3$).

^{13}C NMR (D_6-DMSO): δ 144.21, 136.56, 134.37, 131.32, 129.35, 105.22, 78.70, 65.94, 64.65, 64.43, 28.34, 20.53.

m/z calculated: 384.54 *m/z* (ESI) observed: 383.65

Benzylation of *t*-butyldiphenylsilyl protected D-galactal (22).

In a flame-dried nitrogen-flushed 100 mL round-bottom flask equipped with a magnetic stir bar and septum inlet was added a solution of TBDPS-protected galactal (**22**) (1.7 g, 4.4 mmol) dissolved in anhydrous tetrahydrofuran (40 mL). Sodium hydride (60% dispersion) (0.78 g, 19.4 mmol) was then added slowly to prevent bubbling and the mixture was allowed to stir at room temperature for 15 minutes. Benzyl bromide (3.21 mL, 27.9 mmol) was added *via* syringe and the solution was refluxed until TLC (4:1 hexanes/ethyl acetate, R_f = 0.94) showed consumption of starting material (~3 hrs). Upon completion, the reaction mixture was poured over ice water (50 mL) and was washed with 5% sulfuric acid (20 mL). The aqueous layer was extracted with methylene chloride (3 x 50 mL) and the combined extracts were dried over anhydrous magnesium sulfate. The solution was then filtered, the filtrate was reduced, and the product was isolated *via* flash column chromatography (20:1 hexanes/ethyl acetate) to afford 2.47 g of **23** as a yellow syrup (99%).

^{1}H NMR ($CDCl_3$): δ 7.70 – 7.73 (m, 5H, Ar-H), 7.63 – 7.65 (m, 5H, Ar-H), 7.20 – 7.44 (m, 10H, Ar-H), 6.27 (dd, J = 7.87, 4.58 Hz, 1H, H-1), 4.81 (m, 1H, H-2), 4.57 – 4.66 (m, 4H, 2 x OC$\underline{H}_2$Ph), 4.20 (m, 1H, H-5), 4.08 (m, 1H, H-3), 4.03 (m, 1H, H-4), 3.94 (d, J = 6.77 Hz, 2H, H-6, H-6'), 1.07 (s, 9H, C(C$\underline{H}_3$)$_3$).

^{13}C NMR ($CDCl_3$): δ 145.22, 139.50, 139.24, 136.65, 134.39, 130.71, 129.45, 129.36, 129.24, 128.87, 128.69, 128.50, 128.40, 101.45, 73.26, 73.21, 72.34, 71.88, 71.81, 63.09, 28.11, 20.52.

m/z calculated: 564.79 *m/z* (ESI, + H_2O) observed: 582.46

Deprotection of 3,4-di-*O*-benzyl-6-*t*-butyldiphenylsilyl-D-galactal (23) using tetra-*N*-butyl ammonium fluoride.

The protected sugar (**23**) (2.3 g, 4.1 mmol) was dissolved in anhydrous tetrahydrofuran (40 mL) and placed in a 100 mL flame-dried round-bottom flask equipped with a magnetic stir bar and septum inlet. 1M Tetra-*N*-butyl ammonium fluoride in THF (4.1 mL, 4.1 mmol) was then added *via* syringe and the solution was allowed to stir at room temperature until starting material was no longer evident by TLC (2:1 hexanes/ethyl acetate, R_f = 0.39). The solution was then reduced and the pure product was isolated *via* flash column using 4:1 hexanes/ethyl acetate. The combined fractions afforded 570 mg of **24** as a light-brown syrup (44%).

^1H NMR ($CDCl_3$): δ 7.29 – 7.37 (m, 10H, Ar-H), 6.41 (dd, J = 7.32, 5.13Hz, 1H, H-1), 4.85 – 4.88 (m, 2H, H-2, OH), 4.63 – 4.74 (m, 4H, 2 x O$\underline{CH_2}$Ph), 4.18 (m, 1H, H-5), 4.13 (m, 1H, H-3), 3.98 (m, 2H, H-6, H-6'), 3.75 (m, 1H, H-4).

^{13}C NMR ($CDCl_3$): δ 145.82, 139.09, 138.89, 129.52, 129.47, 129.16, 129.00, 128.76, 128.60, 99.70, 76.75, 73.70, 73.07, 72.29, 70.52, 62.43.

m/z calculated: 326.39 *m/z* (ESI, + H_2O) observed: 344.13

Tosylation of 3,4-di-*O*-benzyl-D-galactal (24).

3,4-Di-*O*-benzyl-D-galactal (**24**) (500 mg, 1.5 mmol) was dissolved in anhydrous pyridine (15 mL) and placed in a flame-dried 25 mL round-bottom flask equipped with a magnetic stir bar and septum inlet. *p*-Toluenesulfonyl chloride (1.23 g, 3.9 mmol) was then added and the mixture was allowed to stir at room temperature. After TLC (5:1 hexanes/ethyl acetate, R_f = 0.18) no longer showed evidence of starting material, water (1-2 mL) was added to the solution and the mixture was allowed to stir for 1 hour. The mixture was then poured into water (25 mL) and the organic product was extracted with methylene chloride (3 x 30 mL). The combined extracts were dried over anhydrous magnesium sulfate and then reduced. Because of the purity of the crude product, a flash column was not necessary. The reduced extracts provided 800 mg of **25** as a light brown syrup (99%).

^{1}H NMR ($CDCl_3$): δ 7.74 (d, J = 8.42 Hz, 2H, Ar-H), 7.26 – 7.37 (m, 12H, Ar-H,), 6.18 (d, J = 6.23 Hz, 1H, H-1), 4.85 (m, 1H, H-2), 4.48 – 4.65 (m, 4H, 2 x OC$\underline{H}_2$Ph), 4.45 (m, 1H, H-5), 4.27 (m, 2H, H-6, H-6'), 4.03 (m, 1H, H-3), 3.88 (m, 1H, H-4), 2.42 (s, 3H, C$\underline{H}_3$).

^{13}C NMR ($CDCl_3$): δ 148.20, 144.64, 139.25, 138.62, 133.81, 129.88, 129.45, 129.41, 129.11, 128.93, 128.84, 128.64, 128.50, 100.77, 74.68, 73.59, 73.38, 72.26, 72.19, 69.29, 23.03.

m/z calculated: 480.57 *m/z* (ESI, + H_2O) observed: 498.29

Reduction of tosylated dibenzyl-D-galactal (25) with lithium aluminum hydride.

Lithium aluminum hydride (120 mg, 3.15 mmol) was dissolved in anhydrous tetrahydrofuran (10 mL) and placed in a flame-dried, nitrogen flushed 25 mL round-bottom flask equipped with a magnetic stir bar and septum inlet. Tosylated dibenzyl galactal (0.9 mmol, 420 mg) was then dissolved in anhydrous tetrahydrofuran (2 mL) and added dropwise *via* syringe. The solution was then refluxed while maintaining an inert atmosphere until TLC (2:1 hexanes/ethyl acetate, R_f = 0.70) showed complete consumption of starting material. Upon completion, the lithium aluminum hydride was quenched by adding 1 mL of water, 3 mL 15% of sodium hydroxide, and 1 mL of water sequentially. The solution was then filtered and poured over water (15 mL). The product was extracted with methylene chloride (3 x 20 mL). The combined extracts were dried over anhydrous magnesium sulfate, filtered and reduced. The product was further purified *via* flash column in 10:1 hexanes/ethyl acetate to afford 20 mg of **26** as a yellow syrup (7%).

^{1}H NMR ($CDCl_3$): δ 7.22 – 7.40 (m, 10H, Ar-H), 6.37 (dd, J = 7.87, 4.76 Hz, 1H, H-1), 4.85 (m, 1H, H-2), 4.55 – 4.75 (m, 4H, 2 x O$C\underline{H}_2$Ph), 4.05 (q, J = 6.59 Hz, 1H, H-5), 3.70 (m, 1H, H-3), 3.65 (m, 1H, H-4), 1.28 (d, J = 6.59 Hz, 3H, $C\underline{H}_3$).

^{13}C NMR ($CDCl_3$): δ 145.63, 139.53, 139.31, 130.86, 129.38, 129.27, 128.94, 128.84, 128.65, 100.64, 76.29, 74.20, 73.25, 71.04, 69.88, 17.85.

m/z calculated: 310.156894 m/z (ESI) observed: 310.156894

Direct 6-*O*-tosylation of D-glucal (2).

In a flame-dried 25 mL round-bottom flask equipped with a magnetic stir bar and septum inlet was placed D-glucal (**2**) (500 mg, 3.4 mmol). The sugar was then dissolved in anhydrous pyridine (10 mL) and dry methylene chloride (10 mL). The solution was cooled to 0 °C and *p*-toluenesulfonyl chloride (972 mg, 5.1 mmol) was added. The mixture was allowed to stir until TLC (100% ethyl acetate, R_f = 0.47) showed consumption of starting material (2.5 hrs). Water (2 mL) was then added to the reaction and the solution was allowed to stir for 30 minutes. The mixture was then poured over water (20 mL) and extracted with methylene chloride (3 x 30 mL). The combined extracts were then further washed with aqueous copper (II) sulfate (30 mL), saturated sodium chloride (30 mL) and water (30 mL). The combined organic layers were then dried over anhydrous magnesium sulfate, filtered and reduced. Crude **27** (780 mg) was used directly in the next step.

^{1}H NMR ($CDCl_3$): δ 7.81 (d, J = 8.42 Hz, 2H, Ar-H), 7.35 (d, J = 8.06 Hz, 2H, Ar-H), 6.28 (dd, J = 7.87, 4.57 Hz, 1H, H-1), 4.70 (m, 1H, H-2), 4.36 (m, 1H, H-5), 4.27 (m, 2H, H-6, H-6'), 4.13 (m, 1H, H-3), 3.94 (m, 1H, H-4), 2.45 (s, 3H, $C\underline{H}_3$).

^{13}C NMR ($CDCl_3$): δ 152.26, 146.13, 138.86, 130.95, 130.13, 104.32, 76.65, 72.66, 70.76, 69.47, 22.91.

m/z calculated: 300.33 *m/z* (APCI) observed: 301.01

Reduction of 6-*O*-tosyl-D-glucal (27) with lithium aluminum hydride.

The crude tosylated glucal (750 mg, 2.5 mmol) was dissolved in anhydrous tetrahydrofuran (10 mL) and placed in a flame-dried 25 mL round-bottom flask equipped with a magnetic stir bar and septum inlet. The solution was cooled to 0 °C and a 0.9 M solution of lithium aluminum hydride in THF (283 mg $LiAlH_4$, 7.5 mmol in 8.4 mL THF) was added dropwise *via* syringe. Upon completion of the addition, the solution was heated to reflux and was allowed to stir go completion (1 hr) using TLC (100% ethyl acetate, R_f = 0.47) as a monitoring method. The reaction mixture was then quenched with water (1 mL), 15 % NaOH (2 mL), and water (1 mL). The aluminum salts were then filtered and the solution was washed with sodium bicarbonate (30 mL) and extracted with diethyl ether (3 x 30 mL). The combined extracts were dried over anhydrous magnesium sulfate, filtered and reduced. The crude syrup was purified *via* flash column (1:1 hexanes/ethyl acetate) to afford 201 mg of D-rhamnal (**28**) as a white residue (45% for both steps combined).

^{1}H NMR ($CDCl_3$): δ 6.22 (dd, J = 7.87, 4.21 Hz, 1H, H-1), 5.19 (d, J = 5.49 Hz, 1H, OH), 4.85 (d, J = 5.49 Hz, 1H, OH), 4.55 (m, 1H, H-2), 3.88 (m, 1H, H-5), 3.62 (m, 1H, H-3), 3.06 (m, 1H, H-4), 1.20 (d, J = 6.02 Hz, 3H, C$\underline{H}_3$).

^{13}C NMR ($CDCl_3$): δ 144.5, 106.6, 76.3, 75.7, 70.3, 19.2.

Direct tosylation of D-galactal (21).

In a flame-dried 25 mL round-bottom flask equipped with a magnetic stir bar and septum inlet was placed D-galactal (**21**) (450 mg, 3.1 mmol). The sugar was then dissolved in anhydrous pyridine (9 mL) and dry methylene chloride (9 mL). The solution

was cooled to 0 °C and *p*-toluenesulfonyl chloride (875 mg, 4.6 mmol) was added. The mixture was allowed to stir until TLC (100% ethyl acetate, R_f = 0.49) showed consumption of starting material (2.5 hrs). Water (2 mL) was then added to the reaction and the solution was allowed to stir for 30 minutes. The mixture was poured over water (20 mL) and extracted with methylene chloride (3 x 30 mL). The combined extracts were then further washed with aqueous copper (II) sulfate (30 mL), sodium chloride (30 mL) and water (30 mL). The combined organic layers were then dried over anhydrous magnesium sulfate, filtered and reduced. Crude **29** (840 mg) was used in the next synthetic step.

^{1}H NMR ($CDCl_3$): δ 7.81 (d, J = 8.42 Hz, 2H, Ar-H), 7.35 (d, J = 8.06 Hz, 2H, Ar-H), 6.28 (dd, J = 7.87, 4.57 Hz, 1H, H-1), 4.70 (m, 1H, H-2), 4.36 (m, 1H, H-5), 4.27 (m, 2H, H-6, H-6'), 4.13 (m, 1H, H-3), 3.94 (m, 1H, H-4), 2.45 (s, 3H, $C\underline{H}_3$).

^{13}C NMR ($CDCl_3$): δ Decomposition of the product prevented collection of data.

Attempted reduction of 6-*O*-tosylated-D-galactal with lithium aluminum hydride.

The crude tosylated galactal (750 mg, 2.6 mmol) was dissolved in anhydrous tetrahydrofuran (10 mL) and placed in a flame-dried 25 mL round-bottom flask equipped with a magnetic stir bar and septum inlet. The solution was cooled to 0 °C and a 0.9 M solution of lithium aluminum hydride in THF (304 mg, 7.7 mmol $LiAlH_4$ in 8.5 mL THF) was added dropwise *via* syringe. Upon completion of the addition, the solution was heated to reflux and was allowed to stir until completion (1 hr). The reaction mixture was then quenched with water (1 mL), 15 % NaOH (2 mL), and water (1 mL). The

aluminum salts were then filtered and the solution was dried over anhydrous magnesium sulfate, filtered and reduced. Isolation of the product was attempted *via* flash column in 3:1 hexanes/ethyl acetate but NMR spectra did not show presence of the **30**, but rather, a mixture of **30** and tosylated byproduct.

Preparation of 3,4-di-*O*-benzyl-1-*O*-acetyl-6-*O*-*t*-butyldiphenylsilyl-2-deoxy-2-nitro-α-D-galactopyranoside from 3,4-di-*O*-benzyl-6-*O*-*t*-butyldiphenylsilyl-D-galactal (23).

In a flame-dried 25 mL round-bottom flask equipped with a magnetic stir bar and septum inlet, concentrated nitric acid (0.56 mL, 9.1 mmol) was added to acetic anhydride (7 mL) at –10 °C under a nitrogen atmosphere over 30 minutes. The solution was then further cooled to –42 °C and 3,4-di-*O*-benzyl-6-*O*-*t*-butyldiphenylsilyl-D-galactal (**23**) (1.35 g, 2.4 mmol) in acetic anhydride (3 mL) was added dropwise over 15 minutes. The mixture was then allowed to stir at –42 °C until TLC showed consumption of starting material. The reaction mixture was then brought to 0 °C and was poured over ice water (30 mL), diluted with saturated sodium chloride (35 mL) and extracted with diethyl ether (3 x 30 mL). The combined organic extracts were dried over magnesium sulfate, filtered and reduced. The reduced extracts yielded 2.5 g of crude yellow syrup. Literature reported a greater yield for similar compounds when using the crude product directly in the next step.

Preparation of 3,4-di-*O*-benzyl-6-*O*-*t*-butyldiphenylsilyl-2-nitro-D-galactal (31) from crude 1-*O*-acetyl-6-*O*-*t*-butyldiphenylsilyl-3,4-di-*O*-benzyl-2-deoxy-2-nitro-α-D-galactopyranoside.

In a flame-dried 50 mL round-bottom flask equipped with a magnetic stir bar and septum inlet, triethylamine (0.697 mL, 5.0 mmol) was added slowly to a stirred solution of the crude 3,4-di-*O*-benzyl-1-*O*-acetyl-6-*O*-*t*-butyldiphenylsilyl-2-deoxy-2-nitro-α-D-galactopyranoside (2.5 g, 3.7 mmol) in freshly distilled methylene chloride (25 mL) at 0 °C under a nitrogen atmosphere. After adding the base, the cold bath was removed and the mixture was allowed to stir at room temperature until TLC (100% toluene, $R_f = 0.49$) showed consumption of starting material (~ 4 hrs). The solution was then further diluted with methylene chloride (20 mL) and washed with water (50 mL), 1M HCl (50 mL), saturated sodium bicarbonate (50 mL) and saturated sodium chloride (50 mL). The organic product was extracted with methylene chloride (3 x 35 mL) and the combined extracts were dried over magnesium sulfate. After reducing the extracts, the product was isolated *via* flash column using 10:1 hexanes/ethyl acetate to yield 670 of mg 3,4-di-*O*-benzyl-6-*O*-*t*-butyldiphenylsilyl-2-nitro-D-galactal (**31**) as a yellow syrup (46% for both steps).

^{1}H NMR ($CDCl_3$): δ 7.77 (s, 1H, H-1), 7.59 – 7.62 (m, 5H, Ar-H), 7.20 – 7.42 (m, 15H, Ar-H), 4.74 (m, 1H, H-3), 4.49 – 4.69 (m, 4H, 2 x O$\underline{CH_2}$Ph), 4.12 – 4.24 (m, 3H, H-5, H-6, H-6'), 3.81 (m, 1H, H-4), 1.06 (s, 9H, C($\underline{CH_3}$)$_3$).

^{13}C NMR ($CDCl_3$): δ 166.88, 138.97, 138.61, 136.68, 131.01, 135.33, 129.75, 129.53, 129.40, 129.21, 129.06, 128.86, 128.66, 88.79, 83.39, 75.77, 74.45, 69.97, 63.46, 54.27, 30.97, 15.25.

Preparation of methyl 3,4-di-*O*-benzyl-6-*O*-*t*-butyldiphenylsilyl-2-deoxy-2-nitro-D-galactopyranoside (32).

Methanol (0.48 mL, 9.24 mmol) and triethylamine (1.28 mL, 8.82 mmol) were placed in a flame-dried, nitrogen-flushed 25 mL round-bottom flask equipped with a magnetic stir bar and septum inlet. A solution of 3,4-di-*O*-benzyl-6-*O*-*t*-butyldiphenylsilyl-2-nitro-D-galactal (**31**) (422 mg, 0.70 mmol) in anhydrous tetrahydrofuran (5 mL) was added to the solution dropwise over a 15 minute period. The mixture was then allowed to react until TLC (10:1 hexanes/ethyl acetate, R_f = 0.34) showed consumption of starting material (~3 hrs). The solution was then reduced and the product was isolated *via* flash column using 15:1 hexanes/ethyl acetate to provide 260 mg of **32** as a yellow syrup (44%).

^{1}H NMR ($CDCl_3$): δ 7.61 – 7.65 (m, 5H, Ar-H), 7.22 – 7.48 (m, 15H, Ar-H), 4.90 (d, J = 8.24 Hz, 1H, H-1), 4.88 (m, 1H, H-2), 4.56 – 4.65 (m, 6H, 3 x O$\underline{CH_2}$Ph), 4.10 (m, 1H, H-5), 3.83 (m, 2H, H-6, H-6'), 3.75 (m, 1H, H-3), 3.54 (m, 1H, H-4), 3.43 (s, 3H, O$\underline{CH_3}$), 1.09 (s, 9H, C(C$\underline{H_3}$)$_3$).

^{13}C NMR ($CDCl_3$): δ 138.86, 138.34, 136.58, 133.97, 130.95, 130.70, 130.31, 130.04, 129.65, 129.26, 128.89, 128.70, 102.14, 88.50, 81.07, 76.87, 76.29, 74.74, 62.92, 58.29, 31.19, 28.50, 20.45.

m/z calculated: 641.28 *m/z* observed: 640.32

Attempted Raney nickel reduction and acetylation of methyl 3,4-di-*O*-benzyl-6-*O*-*t*-butyldiphenylsilyl-2-deoxy-2-nitro-D-galactopyranoside (32).

In 25 mL round-bottom flask equipped with a magnetic stir bar and septum inlet was placed methyl 3,4-di-*O*-benzyl-6-*O*-*t*-butyldiphenylsilyl-2-deoxy-2-nitro-D-galactopyranoside (**32**) (260 mg, 0.4 mmol) dissolved in ethanol (5 mL). Raney nickel (~1 mL) was then added to the solution and the mixture was allowed to stir at room temperature overnight. The reaction mixture was then suction filtered to remove the Raney nickel and the filtrate was reduced to remove the ethanol to yield an oily water mixture. The oil was poured into methylene chloride (15 mL) and washed with water (20 mL). The aqueous layers were extracted with methylene chloride (3 x 15 mL) and the combined organic extracts were dried over anhydrous magnesium sulfate. The extracts were filtered and reduced to afford 190 mg of crude product.

The crude product (190 mg, 0.4 mmol) was dissolved in anhydrous pyridine (8 mL) and placed in a flame-dried, nitrogen-flushed 25 mL round-bottom flask equipped with magnetic stir bar and septum inlet. The mixture was then treated with acetic anhydride (2 mL) *via* syringe and the reaction was allowed to stir at room temperature overnight. The reaction mixture was then poured over ice water (15 mL) and extracted with methylene chloride (3 x 20 mL). The combined organic extracts were dried over anhydrous magnesium sulfate, filtered and reduced. Isolation of the pure product was attempted with a flash column using 10:1 hexanes/ethyl acetate, but the desired product was never characterized.

Attempted *S*-glycosylation of 3,4,6-tri-*O*-benzyl-2-nitro-D-glucal (7) with benzyl mercaptan.

To a stirred solution of triethylamine (1.92 mL, 13.2 mmol) and benzyl mercaptan (1.63 mL, 13.9 mmol) at 0 °C under a nitrogen atmosphere in a flame-dried 25 mL round-bottom flask equipped with a magnetic stir bar and septum inlet, was added a solution of 3,4,6-tri-*O*-benzyl-2-nitro-D-glucal (**7**) (400 mg, 0.86 mmol) in anhydrous tetrahydrofuran (6.6 mL) dropwise over 20 minutes. The reaction was allowed to run at room temperature until TLC (5:1 hexanes/ethyl acetate, $R_f = 0.33$) showed consumption of starting material. Upon completion, the solution was poured over dilute 0.1 M NaOH (30 mL) and extracted with methylene chloride (3 x 30 mL). The combined extracts were dried over anhydrous magnesium sulfate, filtered and reduced. Isolation of the suspected product was achieved *via* flash column chromatography (10:1 hexanes/ethyl acetate). Upon examination of mass spectrometer data, it was concluded that **34** was not formed.

Attempted *C*-glycosylation of 3,4,6-tri-*O*-benzyl-2-nitro-D-glucal (7) with diethyl malonate.

In a flame-dried, nitrogen-flushed 25 mL round-bottom flask equipped with magnetic stir bar and septum inlet was placed diethyl malonate (0.304 mL, 2.0 mmol). A suspension of sodium hydride (77 mg, 2.0 mmol) in anhydrous tetrahydrofuran (5 mL) was then added to the solution *via* syringe slowly to allow evolution of hydrogen gas. The mixture was then cooled to 0 °C and a solution of 3,4,6-tri-*O*-benzyl-2-nitro-D-glucal (**8**) (250 mg, 0.54 mmol) in anhydrous THF (3 mL) was added dropwise. The reaction was allowed to stir at room temperature until TLC (3:1 hexanes/ethyl acetate, $R_f = 0.51$)

showed consumption of starting material. The mixture was then poured over saturated ammonium chloride (30 mL) and extracted with methylene chloride (3 x 30 mL). The combined extracts were dried over anhydrous magnesium sulfate, filtered and reduced. The suspected product was isolated *via* flash column using 3:1 hexanes/ethyl acetate to afford 190 mg of yellow syrup. Upon investigation of spectral data, ^{1}H NMR and mass spectral data agreed with the formation of **35**, but ^{13}C NMR data did not afford a signal for the two equivalent carbonyl carbons. Further investigation of the reaction must be done to positively identify the desired product.

_N_-glycosylation of 3,4,6-tri-_O_-benzyl-2-nitro-D-glucal (7) with benzyl amine.

In a flame-dried, nitrogen-flushed 25 mL round-bottom flask equipped with magnetic stir bar and septum inlet was placed triethylamine (1.12 mL, 7.7 mmol) and benzyl amine (0.88 mL, 8.1 mmol). The solution was cooled to 0 °C and 2-nitro-3,4,6-tri-*O*-benzyl-D-glucal (**7**) (250 mg, 0.5 mmol) dissolved in anhydrous THF (5 mL) was added slowly *via* syringe. Upon complete addition, the mixture was stirred at room temperature until TLC (3:1 hexanes/ethyl acetate, R_f = 0.27) showed consumption of starting material. The solution was then poured over saturated ammonium chloride (25 mL) and the organic products were extracted with methylene chloride (3 x 30 mL). The combined extracts were then dried over anhydrous magnesium sulfate, filtered and reduced. The *N*-glycosylated product was isolated *via* flash column in 3:1 hexanes/ethyl acetate to provide 140 mg of **36** as a white residue (46%, mix of α/β).

^{1}H NMR ($CDCl_3$): δ 7.17 – 7.36 (m, 20H, Ar-H), 5.16 (d, J = 2.38 Hz, 1H, N-H), 4.53 (m, 1H, H-2), 4.49 (m, 1H, H-1), 4.31 – 4.41 (m, 8H, 4 x C$\underline{H}_2$Ph), 4.26 (m, 1H, H-5), 4.09 (m, 2H, H-6, H-6'), 3.73 (m, 1H, H-3), 3.62 (m, 1H, H-4).

^{13}C NMR ($CDCl_3$): δ 150.40, 138.75, 138.15, 137.58, 136.74, 130.22, 130.13, 130.01, 129.78, 129.67, 129.60, 129.50, 129.39, 129.04, 128.80, 128.68, 128.58, 79.91, 75.84, 75.41, 74.69, 73.33, 72.14, 71.24, 69.64, 54.57.

m/z calculated: 568.66 *m/z* (ESI) observed: 569.35

Deacetylation of 3,4-di-*O*-acetyl-L-fucal (37) to yield L-fucal (40).

In a flame-dried 25 mL round-bottom flask equipped with a magnetic stir bar and septum inlet was placed 3,4-di-*O*-acetyl-L-fucal (**37**) (0.500g, 2.3 mmol). The sugar was then dissolved in methanol (10 mL) and a catalytic amount of sodium (spheres, 2 mg) was added. The reaction mixture was allowed to stir at room temperature under a nitrogen atmosphere until TLC (100% ethyl acetate, R_f = 0.48) showed consumption of starting material (~ 1hr). The solution was then quenched with CO_2 in the form of dry ice (3 g) and the mixture was reduced. L-Fucal was isolated by extracting the crude mixture with hot ethyl acetate (4 x 25 mL) to yield 290 mg of **40** as a light-brown syrup (95%).

^{1}H NMR (D_6-DMSO): δ 6.21 (dd, J = 8.06, 4.39 Hz, 1H, H-1), 4.43 (m, 1H, H-2), 4.18 (m, 1H, H-5), 3.88 (q, J = 6.59 Hz, 1H, H-4), 3.46 (d, J = 4.39 Hz, 1H, H-3), 1.17 (d, J = 6.59 Hz, 3H, C$\underline{H}_3$).

^{13}C NMR (D_6-DMSO): δ 144.7, 104.8, 74.1, 68.6, 65.3, 18.6.

Preparation of 3,4-di-*O*-*t*-butyldiphenylsilyl-L-fucal (41).

In a flame-dried, argon-flushed 25 mL round-bottom flask equipped with a magnetic stir bar and septum inlet was placed L-fucal (**40**) (190 mg, 1.5 mmol) and imidazole (450 mg, 6.6 mmol). Anhydrous *N,N*-dimethylformamide (10 mL) was then added *via* syringe and the mixture was allowed to stir under argon until the sugar and imidazole were completely dissolved. After addition of *t*-butylchlorodiphenylsilane (0.86 mL, 3.3 mmol), the solution was allowed to stir at room temperature until TLC (4:1 hexanes/ethyl acetate, R_f = 0.72) showed consumption of starting material (~ 4hrs). The mixture was then poured over water (25 mL) and extracted with methylene chloride (3 x 25 mL). The combined organic extracts were dried over anhydrous magnesium sulfate, filtered and reduced. Isolation of the product was achieved *via* flash column using 15:1 hexanes ethyl acetate eluent to afford 664 mg of **41** as a clear syrup (75%).

^{1}H NMR ($CDCl_3$): δ 7.67 – 7.79 (m, 10H, Ar-H), 7.31 – 7.48 (m, 10H, Ar-H), 6.30 (d, J = 5.86 Hz, 1H, H-1), 4.45 (m, 2H, H-2, H-5), 3.80 (q, J = 6.41 Hz, 1H, H-4), 3.55 (dd, J = 4.94, 2.01 Hz, 1H, H-3), 1.36 (d, J = 6.77 Hz, 3H, C$\underline{H}_3$), 1.10 (s, 9H, C(C$\underline{H}_3$)$_3$), 1.07 (s, 9H, C(C$\underline{H}_3$)$_3$).

^{13}C NMR ($CDCl_3$): δ 145.63, 136.13, 135.86, 134.14, 134.00, 131.08, 130.70, 128.89, 128.74, 102.53, 73.78, 69.07, 67.50, 27.94, 27.86, 20.49, 20.31, 18.18.

Preparation of 1-*O*-acetyl-3,4-di-*O*-*t*-butyldiphenylsilyl-2-deoxy-2-nitro-L-fuco-pyranoside (42).

In a flame-dried 25 mL round-bottom flask equipped with a magnetic stir bar and septum inlet, concentrated nitric acid (0.12 mL, 2.7 mmol) was added to acetic anhydride

(1.5 mL) at –10 °C under a nitrogen atmosphere over 30 minutes. The solution was then further cooled to –42 °C and 3,4-di-*O*-t-butyldiphenylsilyl-L-fucal (**41**) (280 mg, 0.5 mmol) in acetic anhydride (1 mL) was added dropwise over 15 minutes. After stirring at –42 °C until TLC (5:1 hexanes/ethyl acetate, R_f = 0.49) showed consumption of starting material (~1 hour), the mixture was poured over ice water (20 mL), washed with saturated sodium chloride (25 mL), and extracted with methylene chloride (3 x 20 mL). The combined organic extracts were dried over magnesium sulfate, filtered and reduced. The reduced extracts yielded 310 mg of crude yellow syrup, which was used directly in the next step.

Preparation of 3,4-di-*O*-*t*-butyldiphenylsilyl-2-nitro-L-fucal (38).

In a flame-dried 25 mL round-bottom flask equipped with a magnetic stir bar and septum inlet, triethylamine (0.127 mL, 0.91 mmol) was added slowly to a stirred solution of the crude 1-*O*-acetyl-3,4-di-*O*-*t*-butyldiphenylsilyl-2-deoxy-2-nitro-L-fucopyranoside (**42**) (400 mg, 0.56 mmol) in freshly distilled methylene chloride (10 mL) at 0 °C under a nitrogen atmosphere. After adding the base, the cold bath was removed and the mixture was allowed to stir at room temperature until TLC (4:1 hexanes/ethyl acetate, R_f = 0.55) showed consumption of starting material (~ 4 hrs). The solution was then further diluted with methylene chloride (20 mL) and washed with water (30 mL), 1M HCl (30 mL), saturated sodium bicarbonate (30 mL) and saturated sodium chloride (30 mL). The organic product was extracted with methylene chloride (3 x 25 mL) and the combined extracts were dried over magnesium sulfate. After reducing the extracts, the product was

isolated *via* flash column using 10:1 hexanes/ethyl acetate to yield 160 mg of 3,4-di-*O*-*t*-butyldiphenylsilyl-2-nitro-L-fucal (**38**) as a yellow syrup (46% for both steps).

^{1}H NMR ($CDCl_3$): δ 8.16 (s, 1H, H-1), 7.65 – 7.72 (m, 10H, Ar-H), 7.30 – 7.46 (m, 10H, Ar-H), 5.16 (m, 1H, H-3), 4.87 (t, J = 1.83 Hz, 1H, H-4), 4.68 (q, J = 7.14 Hz, 1H, H-5), 1.66 (d, J = 7.14 Hz, 3H, $C\underline{H}_3$), 1.10 (s, 9H, $C(C\underline{H}_3)_3$), 1.05 (s, 9H, $C(C\underline{H}_3)_3$).

^{13}C NMR ($CDCl_3$): δ 154.6, 136.82, 136.22, 134.52, 133.98, 131.60, 131.11, 129.72, 128.75, 99.98, 79.64, 74.09, 62.71, 28.74, 27.82, 24.38, 24.44, 18.20.

Preparation of methyl 3,4-di-*O*-*t*-butyldiphenylsilyl-2-deoxy-2-nitro-L-fuco-pyranoside (43).

In a flame-dried, argon-flushed 25 mL round-bottom flask equipped with a magnetic stir bar and septum inlet was placed triethylamine (0.41 mL, 2.9 mmol) and methanol (0.122 mL, 3.0 mmol). To the stirred solution was added dropwise 3,4-di-*O*-*t*-butyldiphenylsilyl-2-nitro-L-fucal (**38**) (150 mg, 0.23 mmol) dissolved in anhydrous tetrahydrofuran (5 mL). The solution was allowed to stir at room temperature under argon until TLC showed consumption of the starting material (overnight). Upon completion, the reaction mixture was reduced and the product was isolated *via* flash column using 12:1 hexanes/ethyl acetate as eluent. The column afforded 140 mg of (**43**) as a yellow syrup (89%).

^{1}H NMR ($CDCl_3$): δ 7.66 – 7.77 (m, 10H, Ar-H), 7.35 – 7.48 (m, 10H, Ar-H), 4.96 (m, 1H, H-2), 4.73 (m, 1H, H-5), 4.50 (d, J = 8.06 Hz, 1H, H-1), 4.28 (m,

1H, H-3), 3.46 (s, 3H, OC$\underline{H}_3$), 3.26 (m, 1H, H-4), 1.72 (d, J = 7.14 Hz, 3H, C$\underline{H}_3$), 1.11 (s, 9H, C(C$\underline{H}_3$)$_3$), 1.09 (s, 9H, C(C$\underline{H}_3$)$_3$).

^{13}C NMR ($CDCl_3$): δ The dilute nature of the sample did not allow for characterization of the product spectrum.

m/z calculated: 683.31 *m/z* (ESI, + H_2O, - Ph_2t-Bu) observed: 510.75

Attempted reduction and acetylation of methyl 3,4-di-*O*-*t*-butyldiphenylsilyl-2-deoxy-2-nitro-L-fucopyranoside (43).

In an oven-dried 25 mL round-bottom flask equipped with magnetic stir bar and septum inlet was placed methyl 3,4-di-*O*-*t*-butyldiphenylsilyl-2-deoxy-2-nitro-L-fuco-pyranoside (100 mg, 0.15 mmol) dissolved in ethanol (8 mL). To the solution was added Raney nickel (~ 1 pipette) and the solution was allowed to stir under argon for 48 hours. Upon completion, the reaction mixture was filtered *via* vacuum filter to provide an oily water mixture. The oil was then reduced to remove the ethanol. After reduction, the resulting oil was poured into water (30 mL) and the organic products were extracted using methylene chloride (3 x 30 mL). The combined organic extracts were dried over magnesium sulfate, filtered and reduced to afford 60 mg of crude product.

The crude mixture was then dissolved in pyridine (5 mL) and placed in a flame-dried 25 mL round-bottom flask. Acetic anhydride (1 mL) was then added *via* syringe and the mixture was allowed to stir at room temperature overnight. Upon completion, the solution was poured over ice water (20 mL) and extracted with methylene chloride (3 x 20 mL). The combined organic extracts were dried over magnesium sulfate, filtered and reduced to afford 60 mg of crude product. The main product was then isolated using

preparative TLC utilizing 3:1 hexanes/ethyl acetate as eluent. Upon examination of ^{1}H NMR spectra, **44** was not formed. NMR data indicated possible decomposition.

References

1. Iowa State University Extension Food Safety Project. www.exnet.iastate.edu/Pages/families/fs/staph.html
2. US Center for Disease Control and Prevention. www.cdc.gov/ncidod/ARESIST/visa.htm
3. National Center for Health Statistics, US Center for Disease Control and Prevention. www.cdc.gov/nchs/data/lcwkl.pdf
4. Lee, J. C., "The Prospects for Developing a Vaccine Against *Staphylococcus Aureus,*" *Trends in Microbiology*. **1996**, *4*, 162-166.
5. Smith, T. L., Jarvis, W. R. "Antimicrobial Resistance in *Staphylococcus aureus*." *Microbes. Infect*. **1999**, *1*, 795-805.
6. File, T. M., Jr. "Overview of Resistance in the 1990's," *Chest*. **1999**, *115*, 35-85
7. Nicolaou, K. C., Cho, S. Y., Hughes, R., Winssinger, N., Smethurst, C., Labischinski, H., Endermann, R. "Solid- and Solution-Phase Synthesis of Vancomycin and Vancomycin Analogues with Activity against Vancomycin-Resistant Bacteria," *Chem. Eur. J.* **2001**, *7*, 3798-3823.
8. Lee, J. C., "The Prospects for Developing a Vaccine Against *Staphylococcus Aureus,*" *Trends in Microbiology*. **1996**, *4*, 162-166.
9. Herscovics, A. "Importance of Glycosidases in Mammalian Glycoprotein Biosynthesis," *Biochim. Biophys. Acta*. **1999**, *1473*, 96-107.
10. Cacan, R, Duvet, S., Kmiecik, D, Labiau, O., Mir, A. M., Verbert, A. "Glyco-deglyco' Processes During the Synthesis of *N*-Glycoproteins," *Biochimie*. **1998**, *80*, 59-68.

11. Lamzin, V. S., Dauter, Z., Wilson, K. S. "How Nature Deals with Stereoisomers," *Curr. Opin. Struct. Biol.* **1995**, *5*, 830-836.

12. Collins, P., Ferrier, R., "Monosaccharides: Their Chemistry and Their Roles in Natural Products." Wiley: New York, New York, **1995**.

13. "Industrial Gums: Polysaccharides and Their Derivatives, 3rd Ed." Whistler, R. L., and BeMiller, J. N., Eds. Academic Press: San Diego, CA, **1993**.

14. Severian, D. "Polysaccharides in Medicinal Applications." Marcel Dekker Inc.: New York, NY, **1996**.

15. Nicolaou, K. C., Pihko, A. J., Koskinen, A. M. P. "An Expedient Synthesis of D-Callipeltose," *Tet:Assymetry*. **2001**, *12*, 937-942.

16. Litjens, R., Leeuwenburgh, M. A., van der Marcel, G. A., van Boom, J. H. "A Novel Approach Towards the Stereoselective Synthesis of 2-Azido-2-deoxy-β-D-Mannosides," *Terahedron. Lett.* **2001**, *42*, 8693-8696.

17. Williams, L. J., Harris, C. R., Glunz, P. W., Danishefsky, S. J. "In Pursuit of an Anticancer Vaccine: A Monomolecular Construct Containing Multiple Carbohydrate Antigens," *Tetrahedron. Lett.* **2000**, *41*, 9505-9508.

18. Campbell, M. K., "Biochemistry." Harcourt Brace, New York, **1991**, 96-125.

19. *Methods Carbohydr. Chem.* **1962**, *1*, 242.

20. *Carb. Res.* **1970**, *14*, 231.

21. Lemieux, R. U., Ratcliffe, R. M. "The Azidonitration of Tri-*O*-acetyl-D-galactal," *Can. J. Chem.* **1979**, *57*, 1244-1251.

22. Nicolaou, K. C., Baran, P. S., Zhong, Y. L., Vega, J. A. "Novel IBX-Mediated Processes for the Synthesis of Amino Sugars and Libraries Thereof," *Angew. Chem. Int. Ed.* **2000**, *39*, 2525-2529.

23. Kan, C., Long, C. M., Moushumi, P., Ring, C. M., Tully, S. E., Rojas, C. M. *Org. Lett.* **2001**, *3*, 381-384.

24. Di Bussolo, V., Liu, J., Huffman, L. G., Gin, D. Y., "Acetamidoglycosylation with Glycal Donors: A One-Pot Glycosidic Coupling with Direct Installation of the Natural C(2)-*N*-Acetylamino Functionality," *Angew. Chem. Int. Ed.* **2000**, *39*, 204-207.

25. Das, J., Schmidt, R. R., "Convenient Glycoside Synthesis of Amino Sugars: Michael Type Addition to 2-Nitro-D-galactal," *Eur. J. Org. Chem.* **1998**, 1609-1613.

26. Winterfeld, G. A., Das, J., Schmidt, R. R. "Convenient Synthesis of Nucleosides of 2-Deoxy-2-nitro-D-galactose and *N*-Acetyl-D-galactosamine," *Eur. J. Org.* Chem. **2000**, 3047-3050.

27. Winterfeld, G. A., Schmidt, R. R. "Nitroglycal Concatenation: A Broadly Applicable and Efficient Approach to the Synthesis of Complex *O*-Glycans," *Angew. Chem. Int. Ed.* **2001**, *40*, 2654-2657.

28. Winterfeld, G. A., Ito, Y., Ogawa, T., Schmidt, R. R. "A Novel and Efficient Route Towards α-GalNAc-Thr Building Blocks for Glycopeptide Synthesis," *Eur. J. Org. Chem.* **1999**, 1167-1171.

29. Hanessian, S., editor. "Preparative Carbohydrate Chemistry." Marcel Dekker, New York, **1997**, 154.

30. Larock, R. C., "Comprehensive Organic Transformations, 2nd edition." Wiley-VCH, New York, **1999**, 48.

31. Whistler, R. L, editor. "Methods in Carbohydrate Chemistry, Volume 2." Academic Press, New York, **1962**, 405-410.

32. "Aldrich: Catalog Handbook of Fine Chemicals." Sigma-Aldrich Company, **1998-1999**, 1630.

Appendix

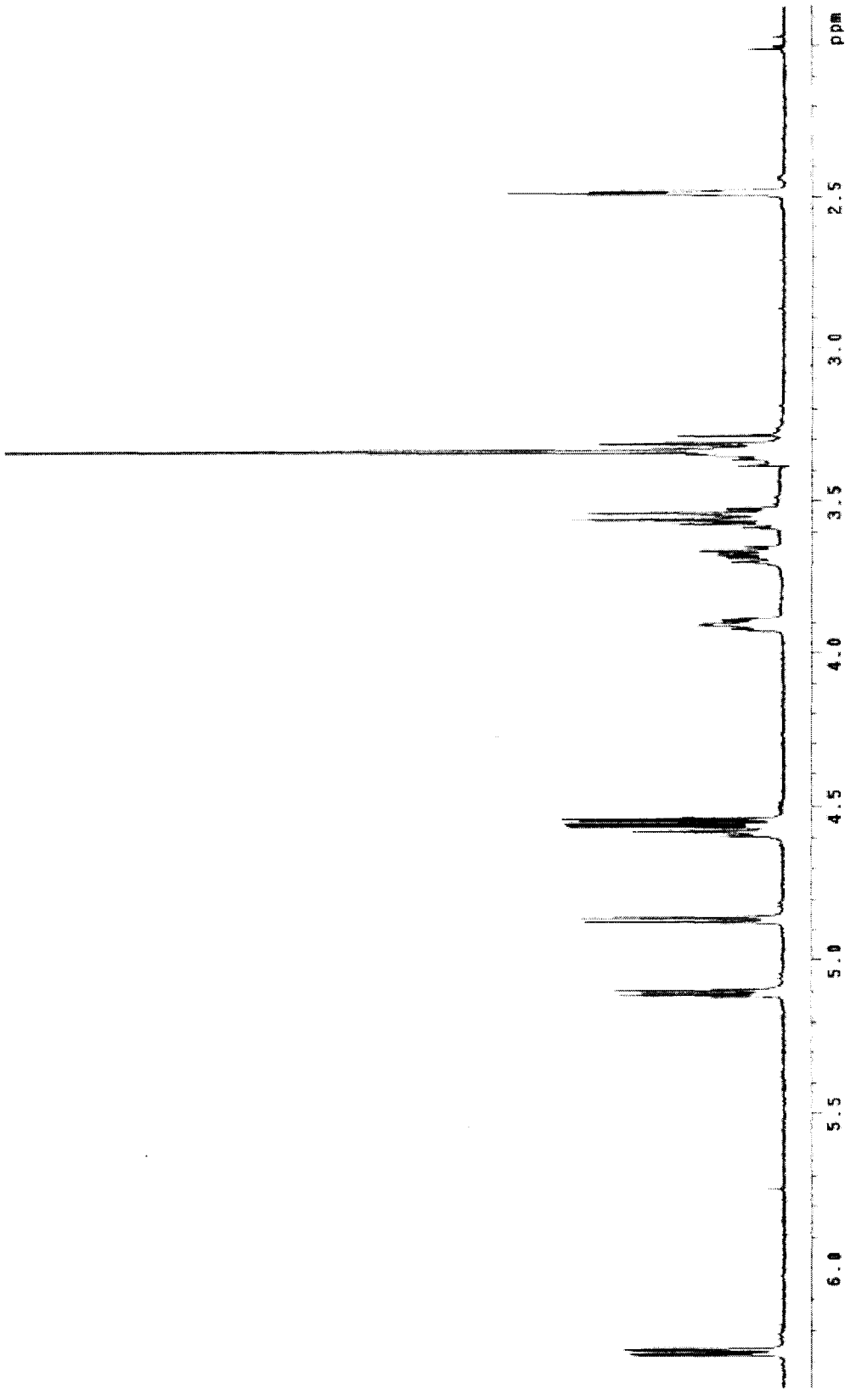

Figure 15: ^{1}H NMR spectrum of **2**

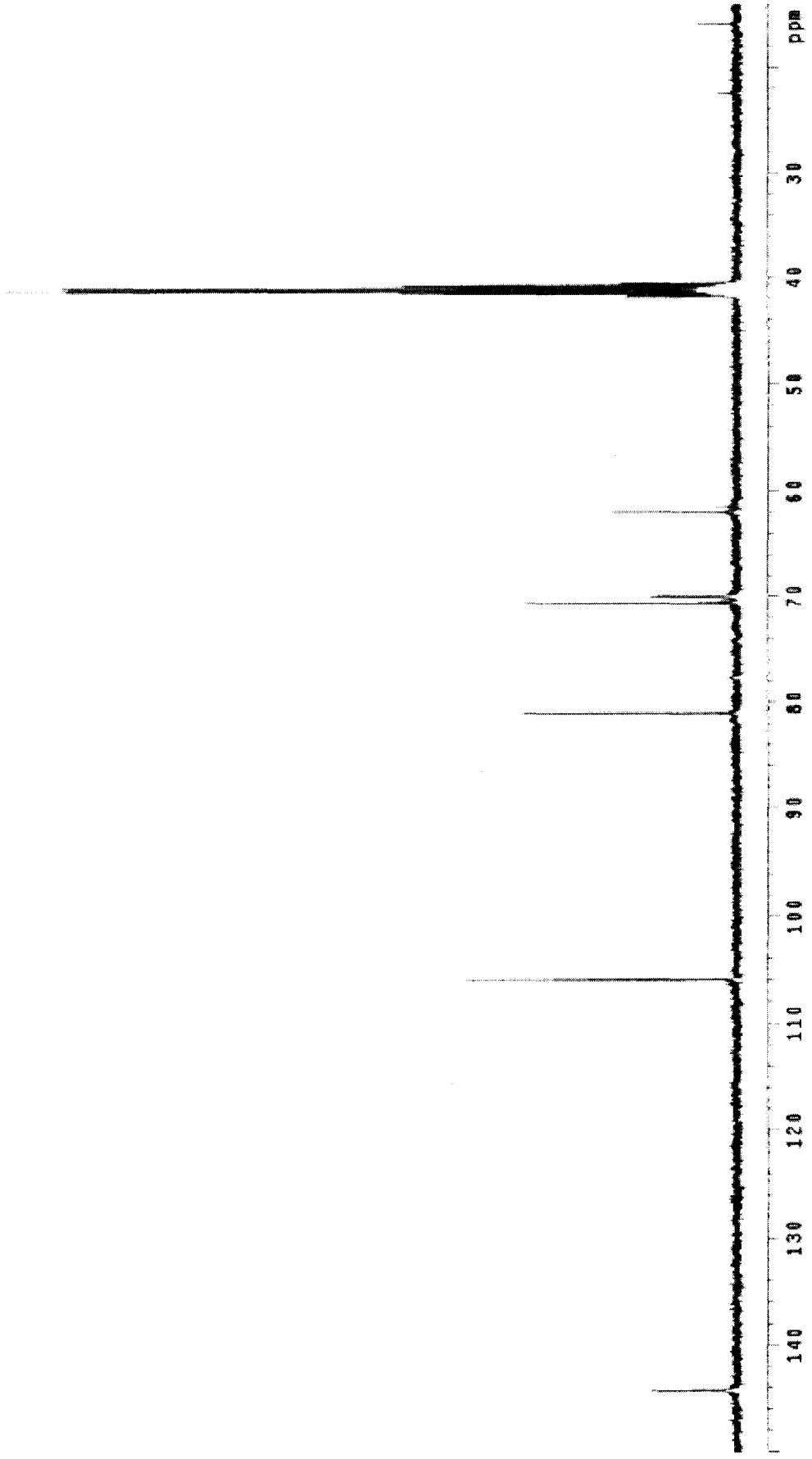

Figure 16: ^{13}C NMR spectrum of **2**

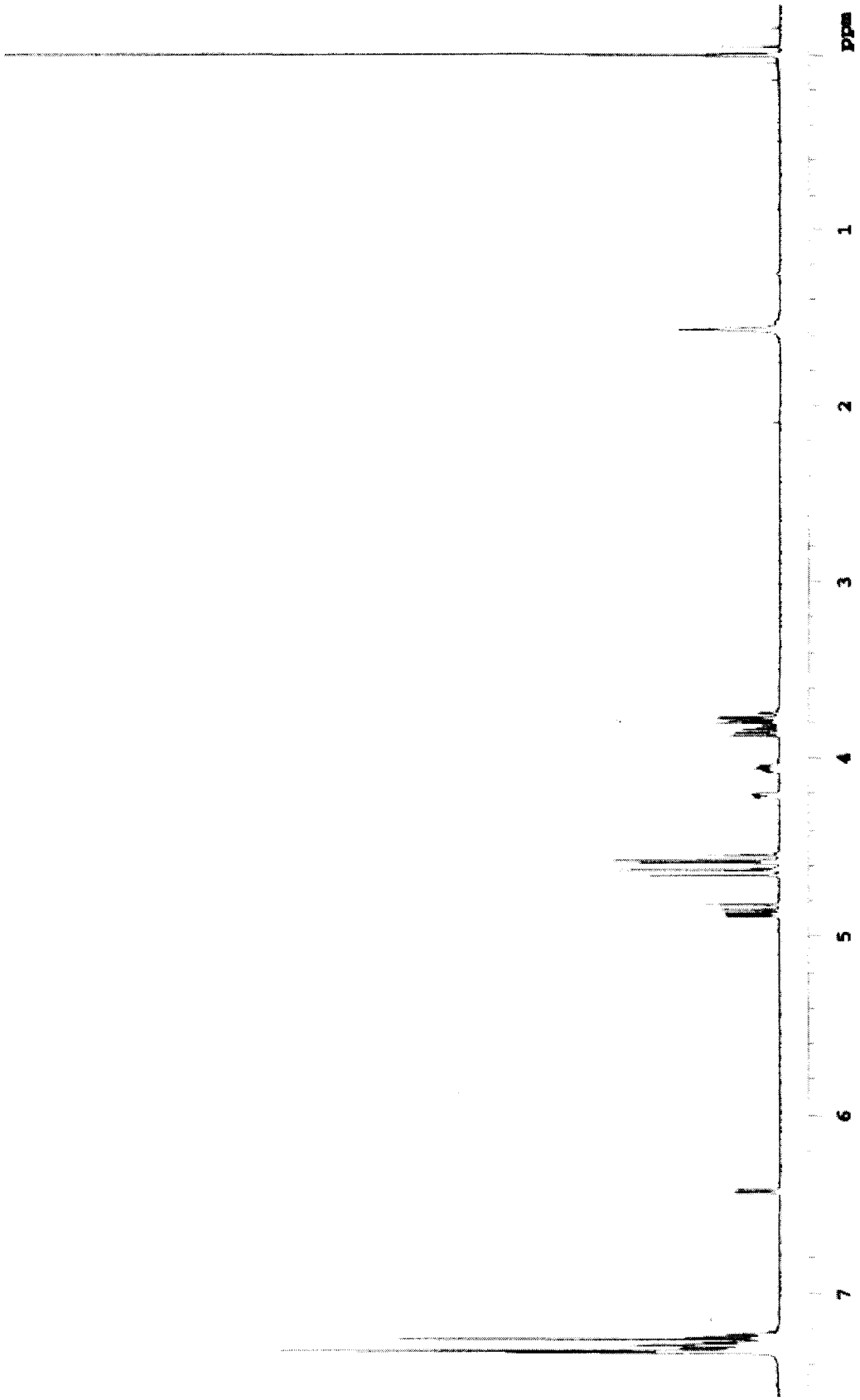

Figure 17: ^{1}H NMR spectrum of **3**

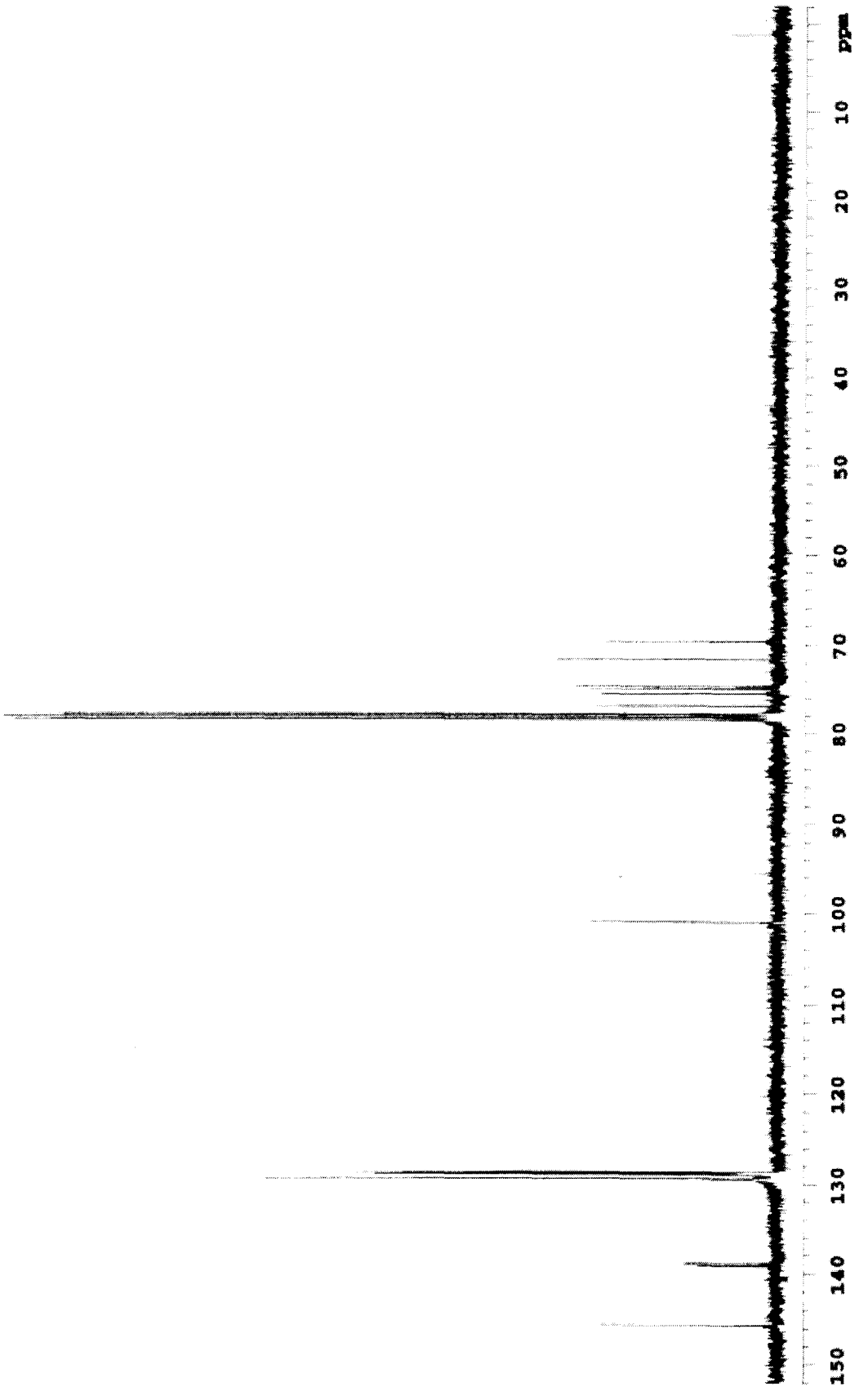

Figure 18: ^{13}C NMR spectrum of **3**

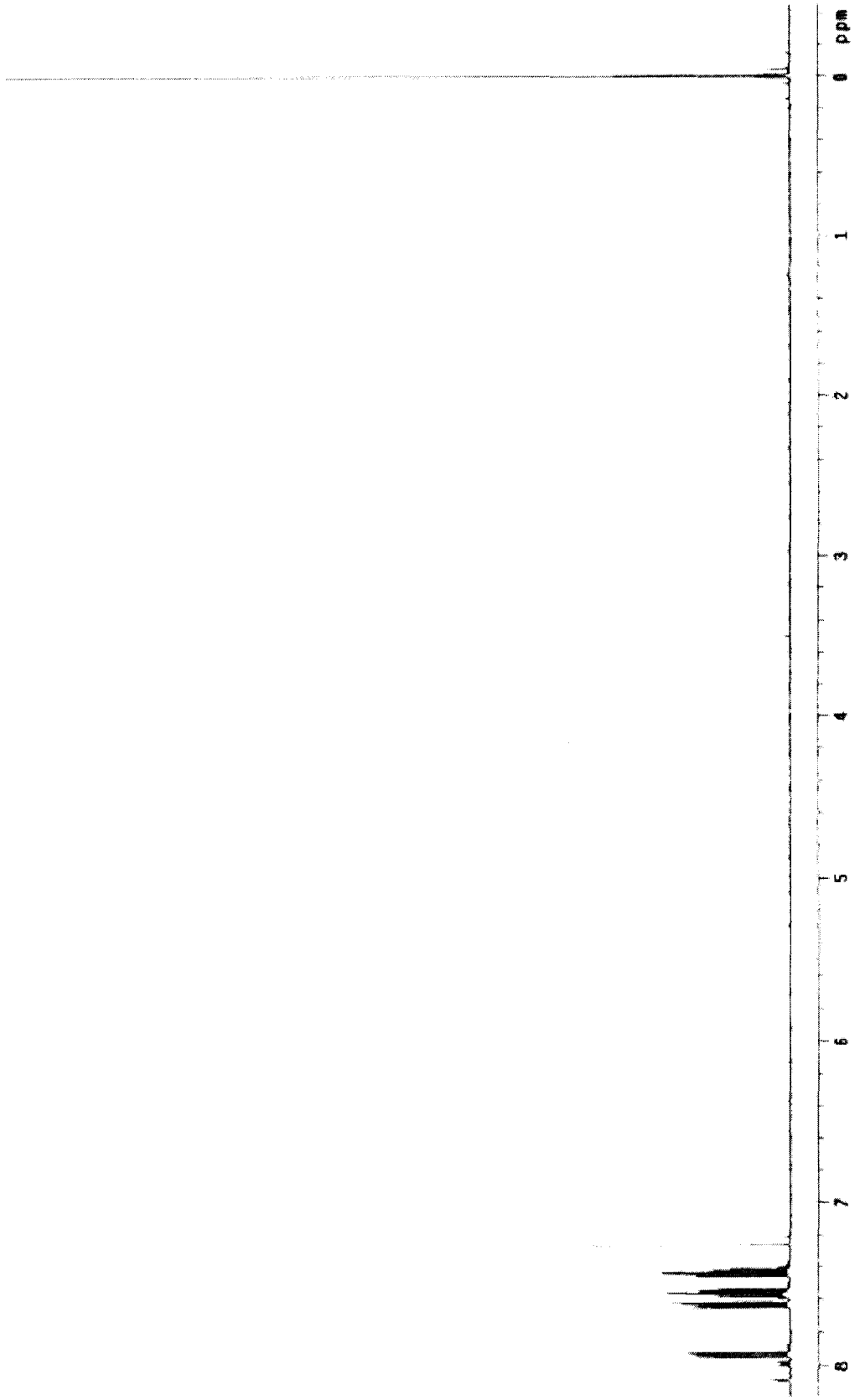

Figure 19: ^{1}H NMR spectrum of **5**

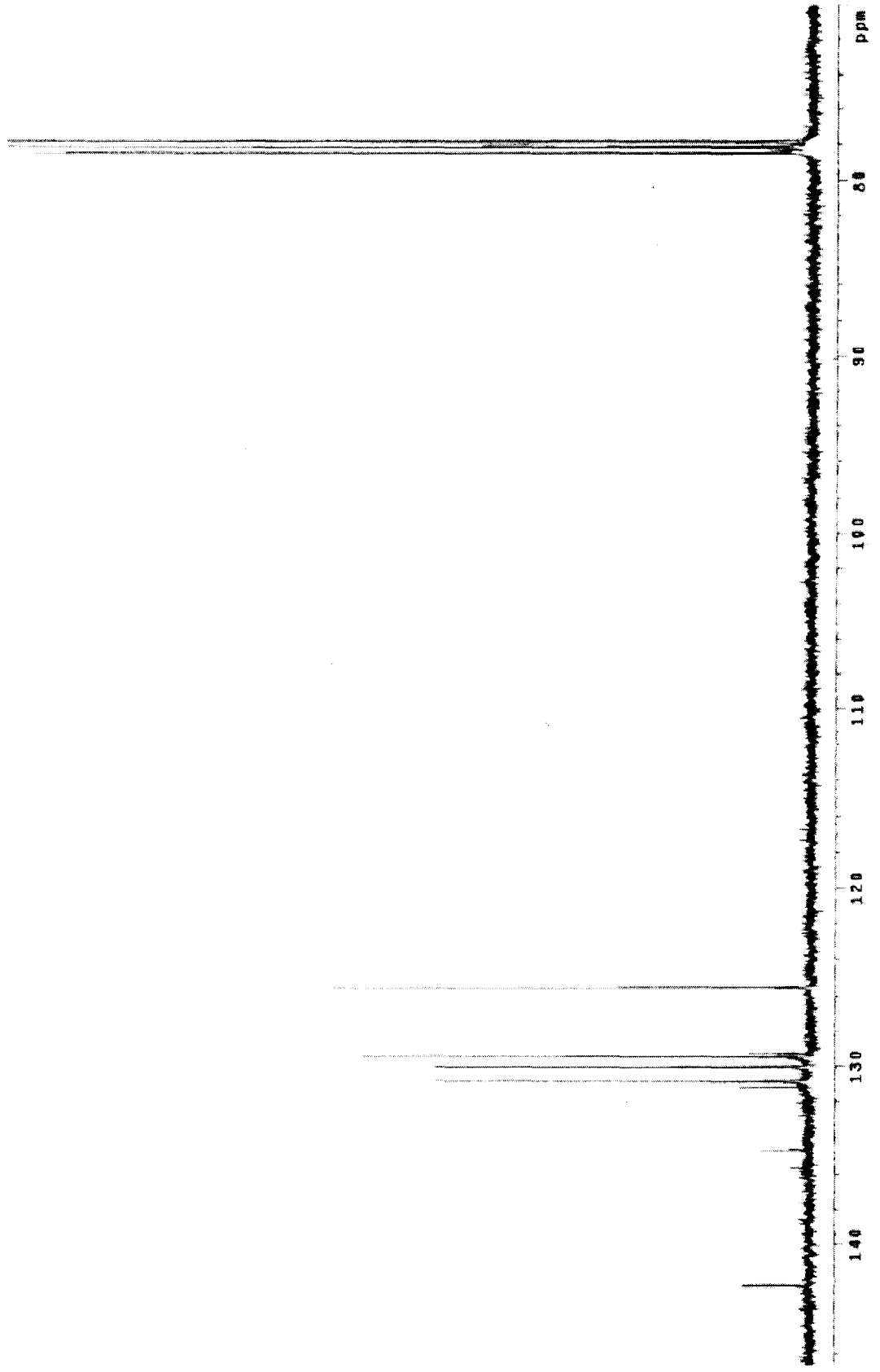

Figure 20: ^{13}C NMR spectrum of **5**

Acquisition Parameter:

Source	: APCI	Polarity	: Positive
Mode	: Std/Normal		
CapExit	: 86.7 Volt	Skim 1	: 16.0 Volt
Scan Range	: 15.00 - 2200.00 m/z	Trap Drive	: 45
Accum.time	: 4040 µs	Summation	: 10 Spectra
MS/MS	:		

Profile Spectrum, No.: 1, Time: 0 min

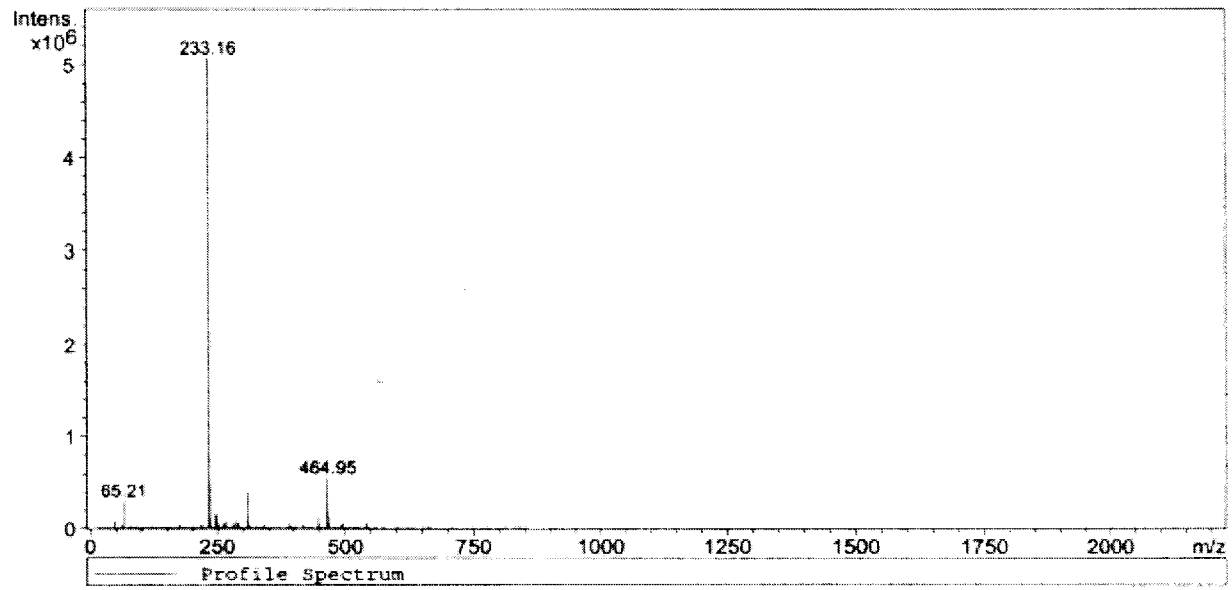

MS Peak List (Profile Spectrum):

Mass	Intensity	Width	Mass	Intensity	Width	Mass	Intensity	Width
47.21	79605	0.30	262.13	51609	0.30	391.35	52277	0.30
65.21	312261	0.20	263.19	57456	0.30	446.29	126838	0.40
233.16	5071002	0.30	266.09	85916	0.30	447.31	59837	0.20
233.92	969352	0.30	281.12	66228	0.20	464.95	563256	0.30
235.04	489427	0.30	288.21	88728	0.30	465.92	195791	0.30
236.09	75401	0.40	291.22	58695	0.30	466.92	125822	0.40
245.24	154391	0.30	309.21	408900	0.30	540.86	54713	0.70
249.13	145853	0.30	310.17	93431	0.30			
250.14	61195	0.30	311.17	69220	0.30			

Figure 21: Mass spectrum of **5**

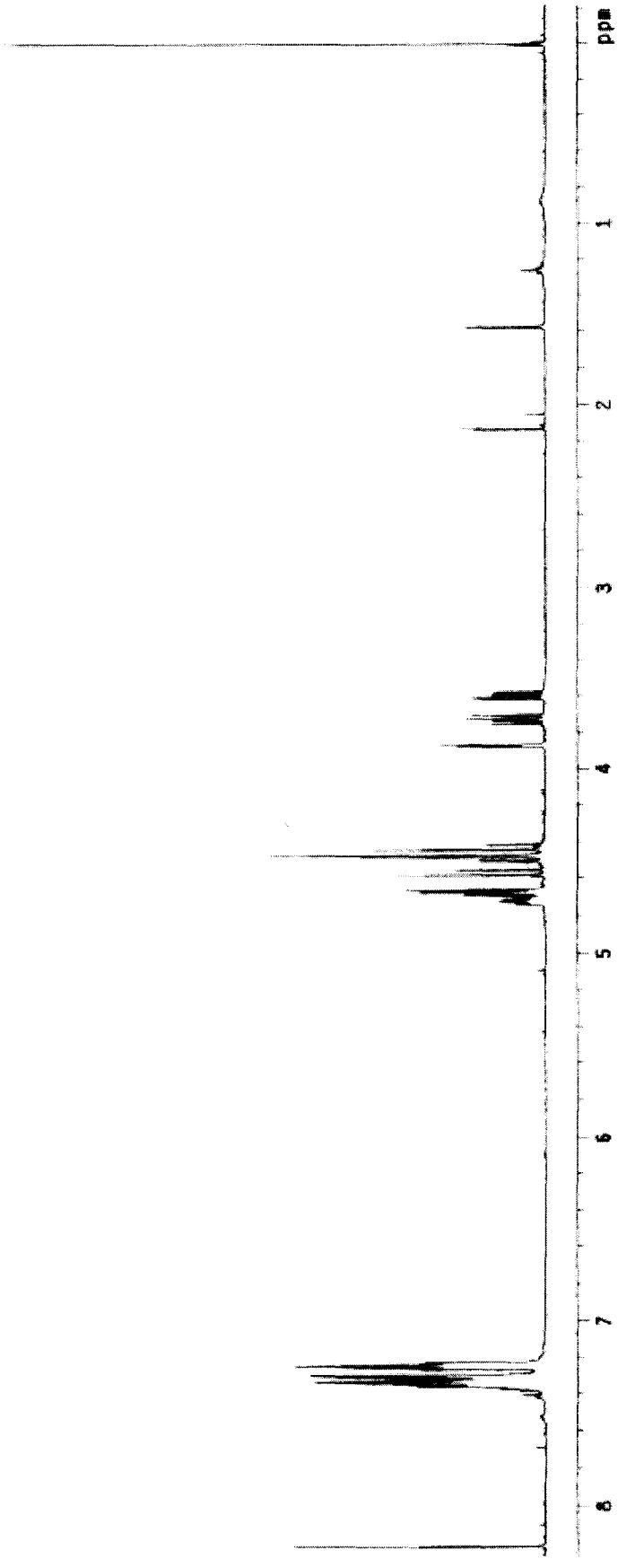

Figure 22: ^{1}H NMR spectrum of **7**

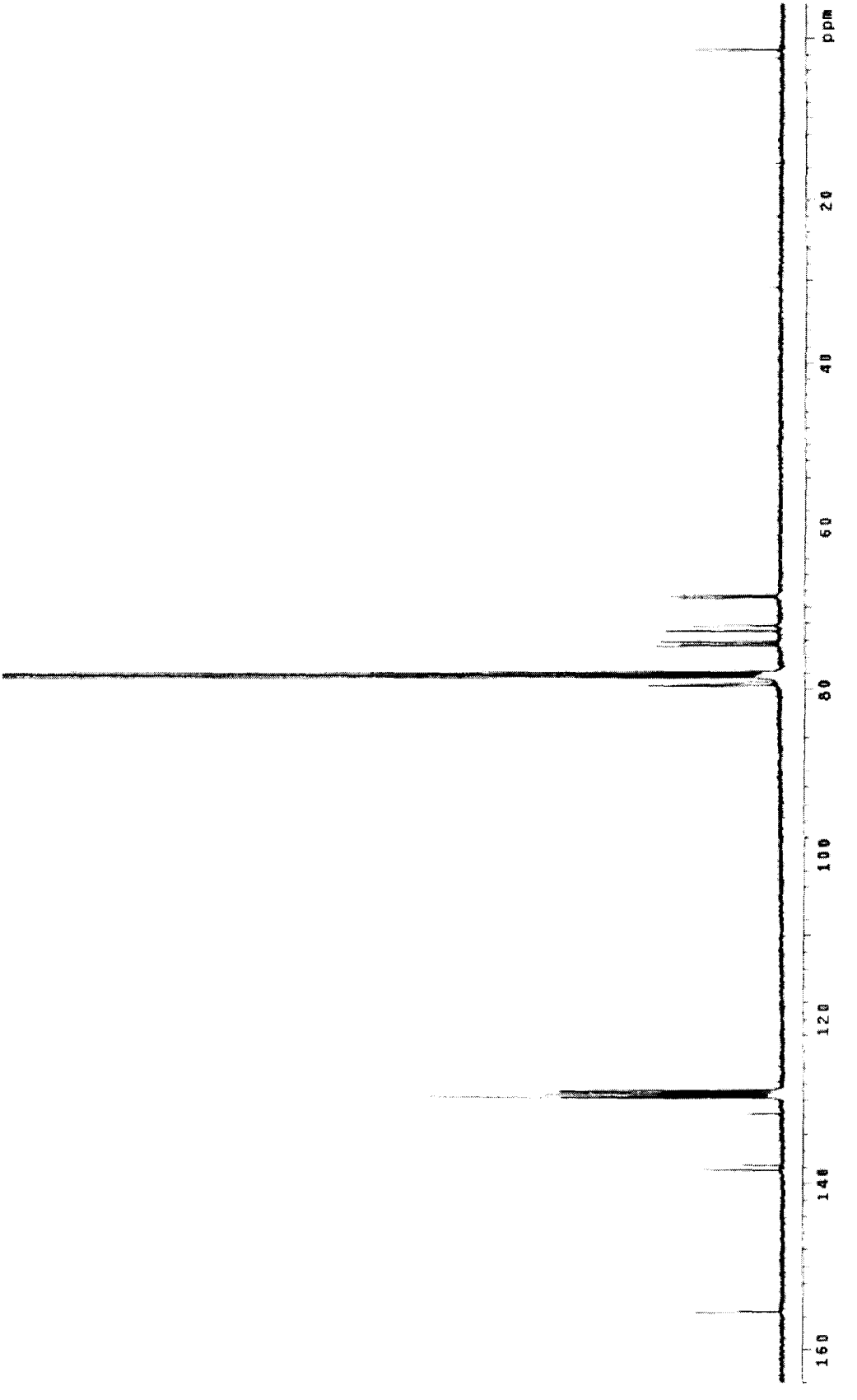

Figure 23: ^{13}C NMR spectrum of **7**

Acquisition Parameter

Ion Source Type	ESI	Ion Polarity	Positive		
Mass Range Mode	Std/Normal	Scan Begin	15.00 m/z	Scan End	2200.00 m/z
Skim 1	30.9 Volt	Cap Exit Offset	77.0 Volt	Trap Drive	49.5
Accumulation Time	2370 µs	Averages	10 Spectra		

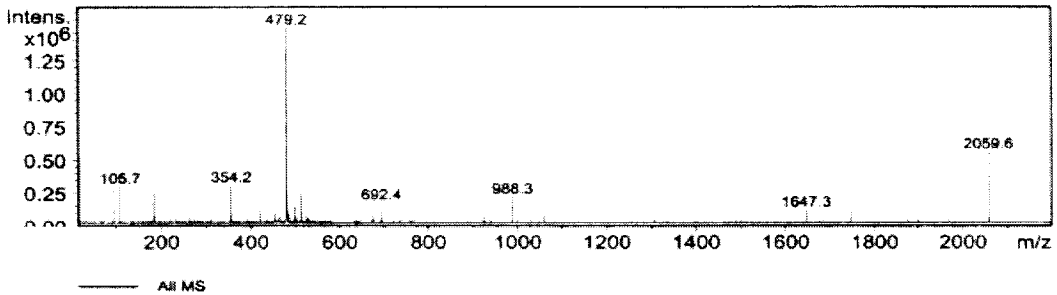

Index	Mass	Intensity	Width	S/N
1	91.16	288333.00	0.34	308.61
2	105.71	303596.00	0.21	349.17
3	181.14	251232.00	0.34	288.95
4	354.16	315178.00	0.41	362.49
5	355.14	83083.00	0.45	95.56
6	419.48	114031.00	0.15	131.15
7	452.20	81156.00	0.54	93.34
8	477.64	67240.00	0.29	77.33
9	479.22	1639766.00	0.49	1885.92
10	480.15	545521.00	0.38	627.41
11	481.23	110273.00	0.53	126.83
12	484.19	76303.00	0.46	87.76
13	497.27	133412.00	0.42	153.44
14	511.40	248806.00	0.37	286.16
15	512.20	95825.00	0.36	110.32
16	673.06	74705.00	0.15	85.92
17	673.34	65728.00	0.34	75.59
18	692.43	164732.00	0.14	189.46
19	988.34	213708.00	0.18	245.79
20	1647.33	100921.00	0.20	116.07
21	1747.32	95873.00	0.08	110.38
22	2059.62	594756.00	0.09	684.04

Figure 24: Mass spectrum of **7**

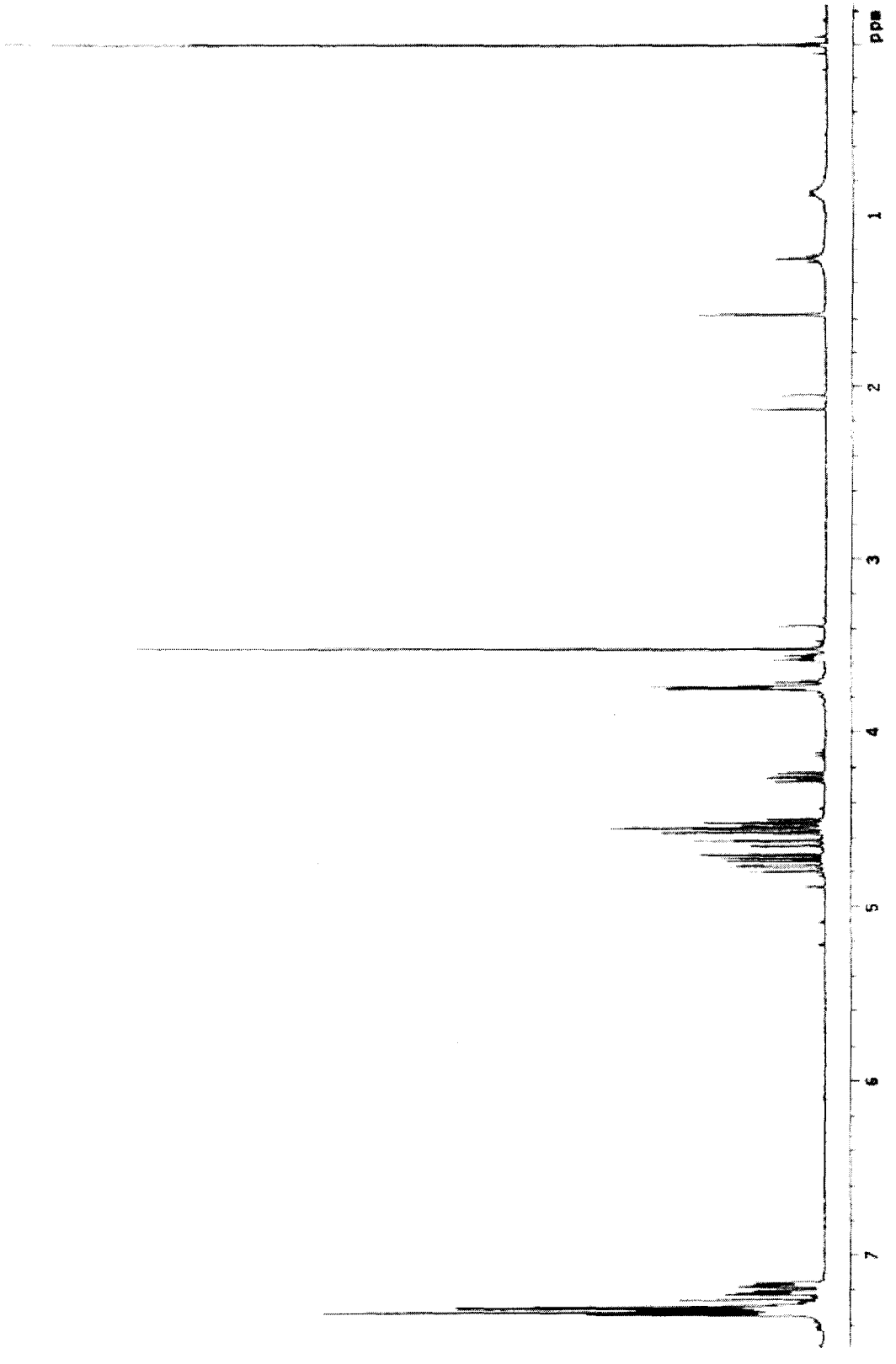

Figure 25: ^{1}H NMR spectrum of **8**

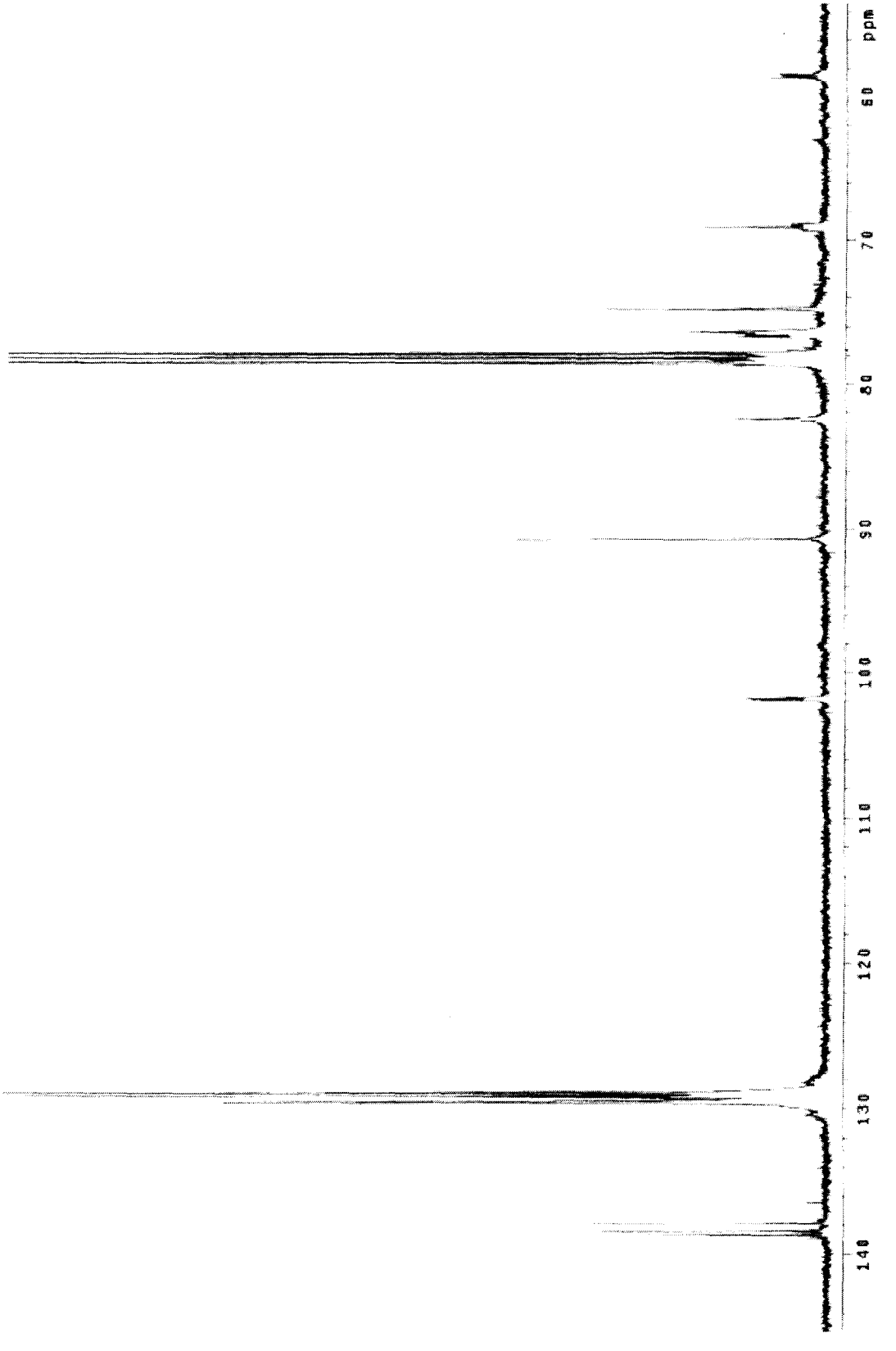

Figure 26: ^{13}C NMR spectrum of **8**

Acquisition Parameter

Ion Source Type	ESI	Ion Polarity	Positive		
Mass Range Mode	Std/Normal	Scan Begin	15.00 m/z	Scan End	2200.00 m/z
Skim 1	25.0 Volt	Cap Exit Offset	77.0 Volt	Trap Drive	40.0
Accumulation Time	1925 µs	Averages	10 Spectra		

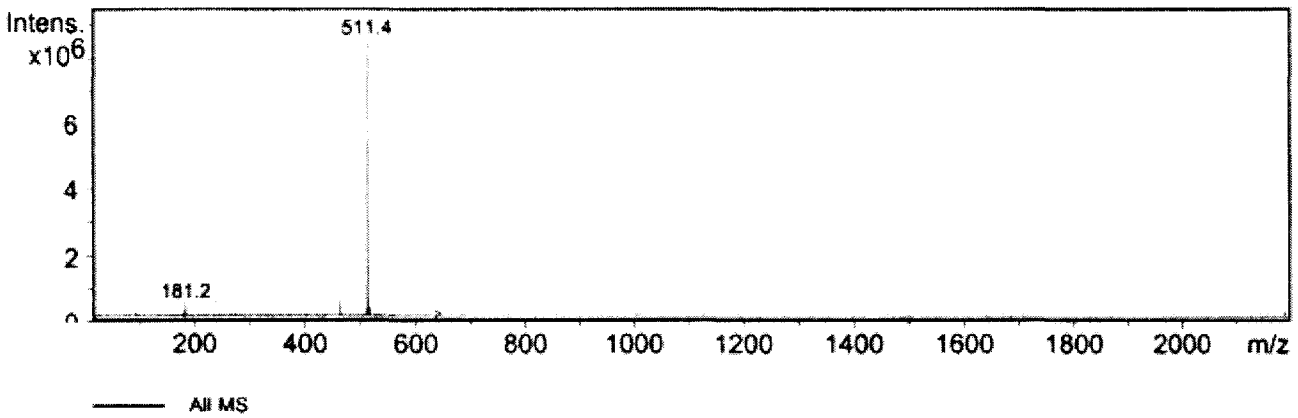

Index	Mass	Intensity	Width	S/N
1	181.22	463927.00	0.39	443.16
2	462.34	558829.00	0.57	533.81
3	463.32	215309.00	0.23	205.67
4	511.44	9420358.00	0.56	8998.69
5	512.91	569907.00	0.45	544.40
6	516.41	251166.00	0.37	239.92

Figure 27: Mass spectrum of **8**

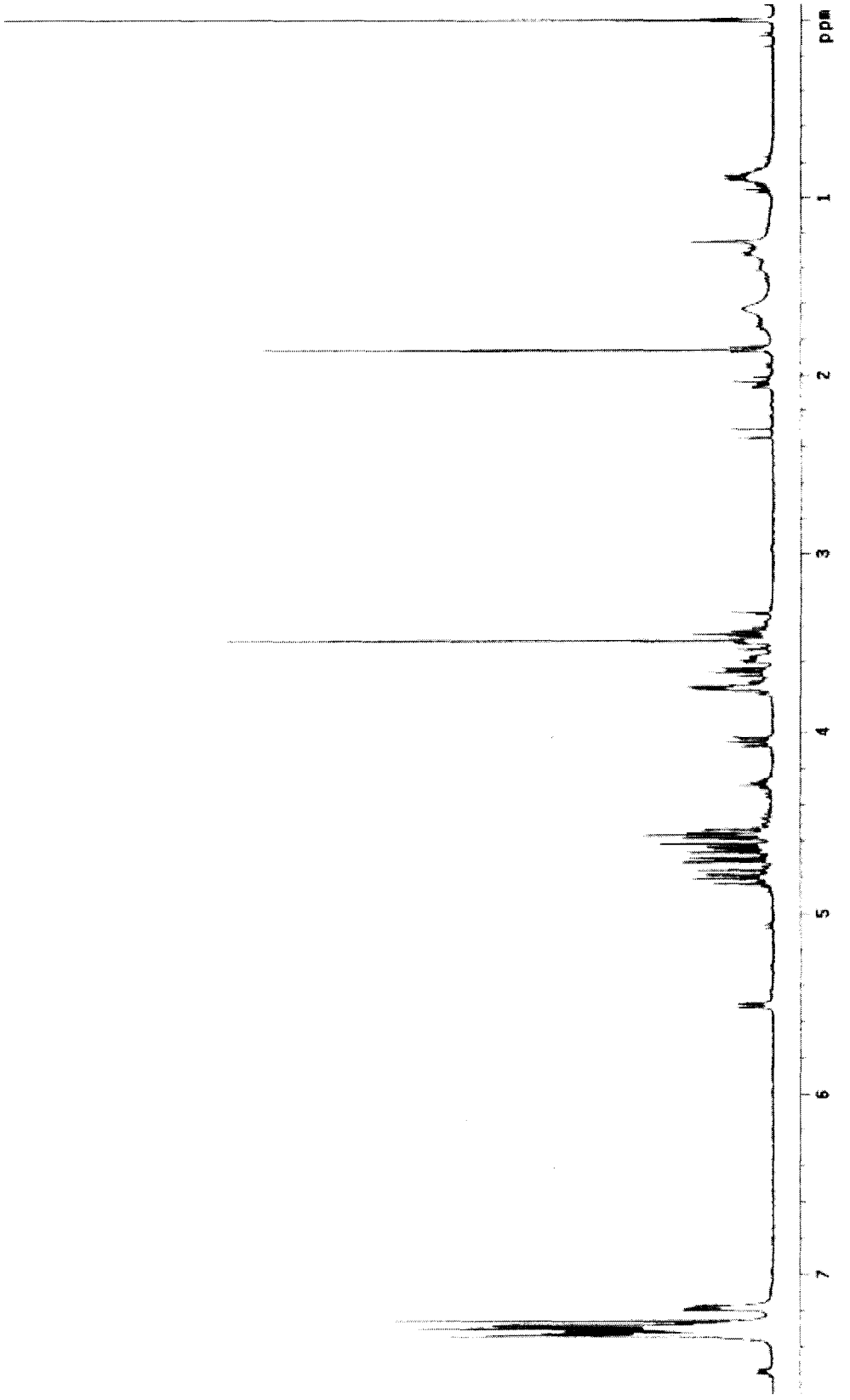

Figure 28: ^{1}H NMR spectrum of **9**

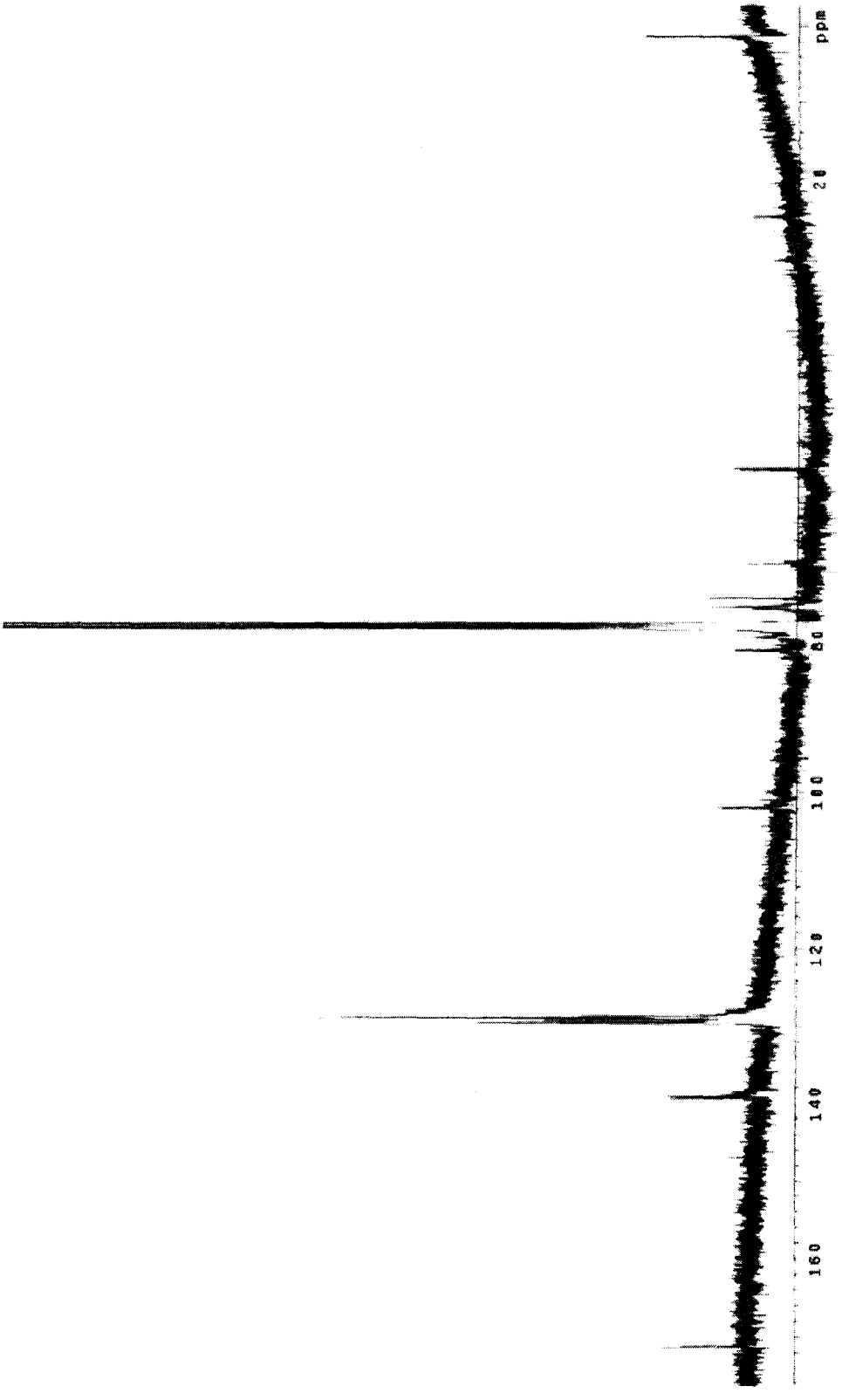

Figure 29: ^{13}C NMR spectrum of **9**

Acquisition Parameter

Ion Source Type	ESI	Ion Polarity	Negative		
Mass Range Mode	Std/Normal	Scan Begin	15.00 m/z	Scan End	2200.00 m/z
Skim 1	-30.0 Volt	Cap Exit Offset	-77.0 Volt	Trap Drive	45.0
Accumulation Time	20000 µs	Averages	10 Spectra		

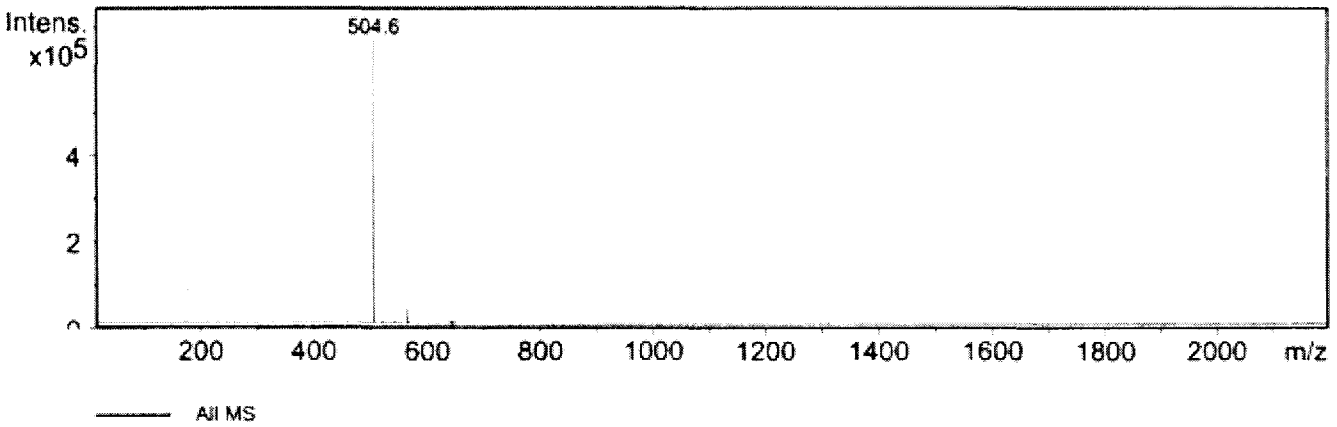

Index	Mass	Intensity	Width	S/N
1	504.60	738929.00	0.30	14011.58
2	564.38	41445.00	0.35	785.88
3	565.08	15915.00	0.37	301.78

Figure 30: Mass spectrum of **9**

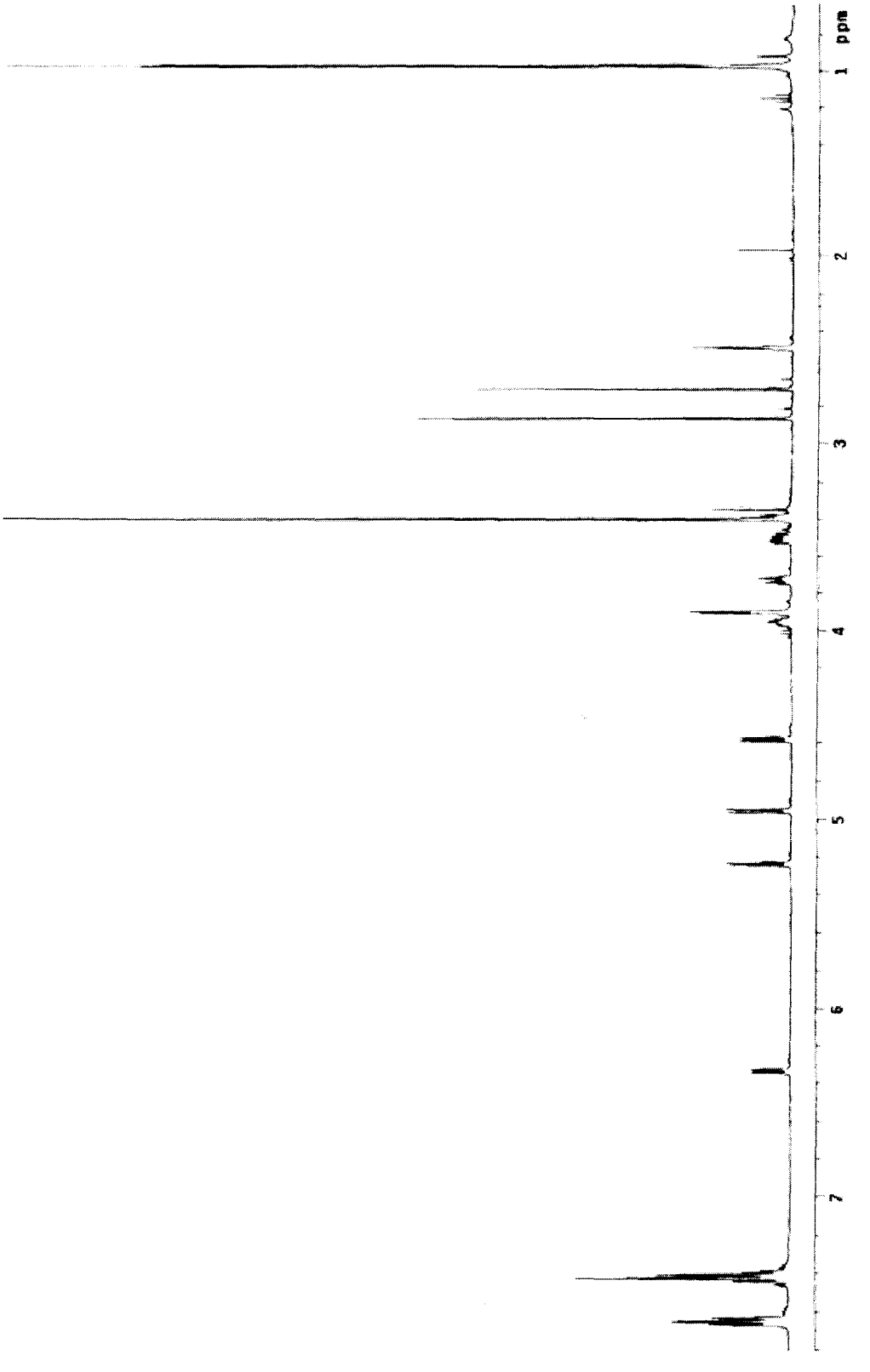

Figure 31: ^{1}H NMR spectrum of **10**

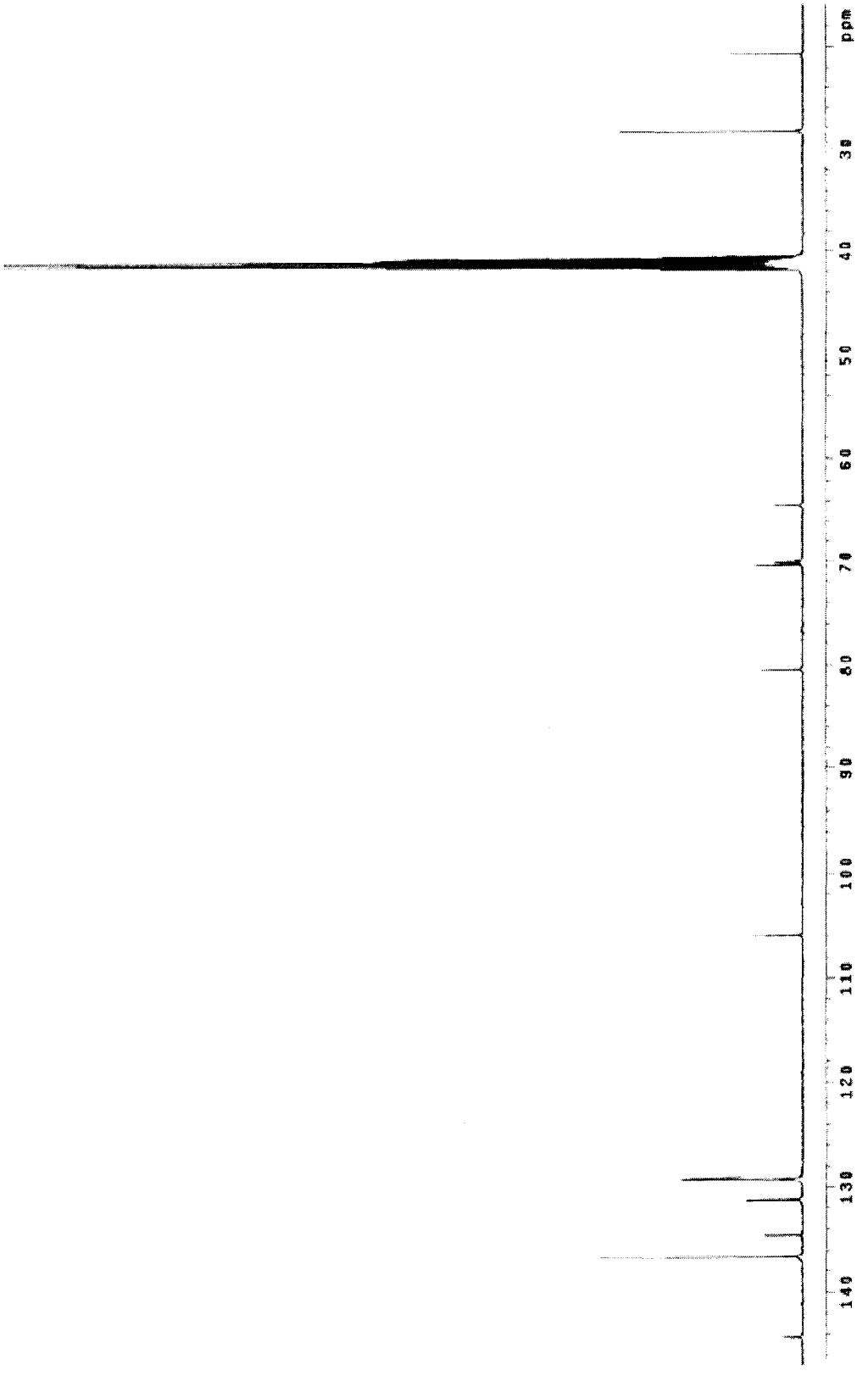

Figure 32: ^{13}C NMR spectrum of **10**

Acquisition Parameter:

Source	: ESI	Polarity	: Negative
Mode	: Std/Normal		
CapExit	: -108.7 Volt	Skim 1	: -38.0 Volt
Scan Range	: 15.00 - 2200.00 m/z	Trap Drive	: 45
Accum.time	: 20000 µs	Summation	: 10 Spectra
MS/MS	:		

Profile Spectrum, No.: 1, Time: 0 min

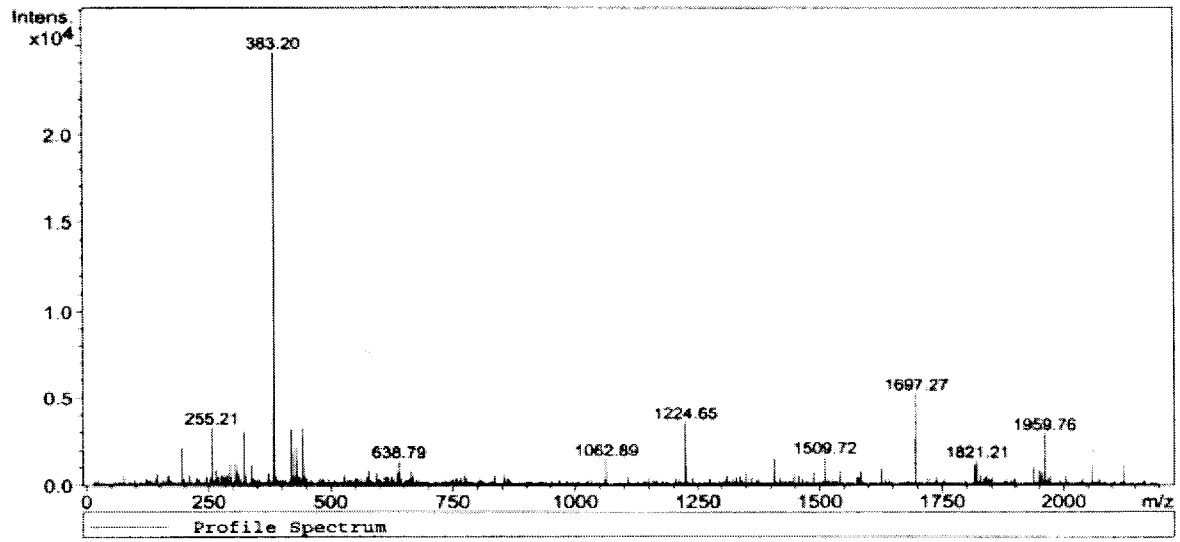

MS Peak List (Profile Spectrum):

Mass	Intensity	Width	Mass	Intensity	Width	Mass	Intensity	Width
195.09	2146	0.40	420.14	1177	0.40	1405.93	1519	0.20
255.21	3263	0.20	421.17	1889	0.40	1509.72	1613	0.20
293.19	1225	0.20	429.18	2138	0.40	1697.27	5218	0.20
305.16	1279	0.30	443.23	3264	0.30	1816.33	1181	0.20
323.17	3018	0.30	444.17	1263	0.30	1821.21	1379	0.20
337.20	1201	0.20	638.79	1364	0.20	1938.06	1038	0.20
383.20	24603	0.40	639.11	1285	0.70	1959.76	2916	0.20
384.17	8190	0.30	1062.89	1483	0.20	2060.03	2250	0.20
385.18	2805	0.20	1224.65	3551	0.20	2124.15	1153	0.20
419.15	3202	0.40	1225.95	1553	0.20			

Figure 33: Mass spectrum of **10**

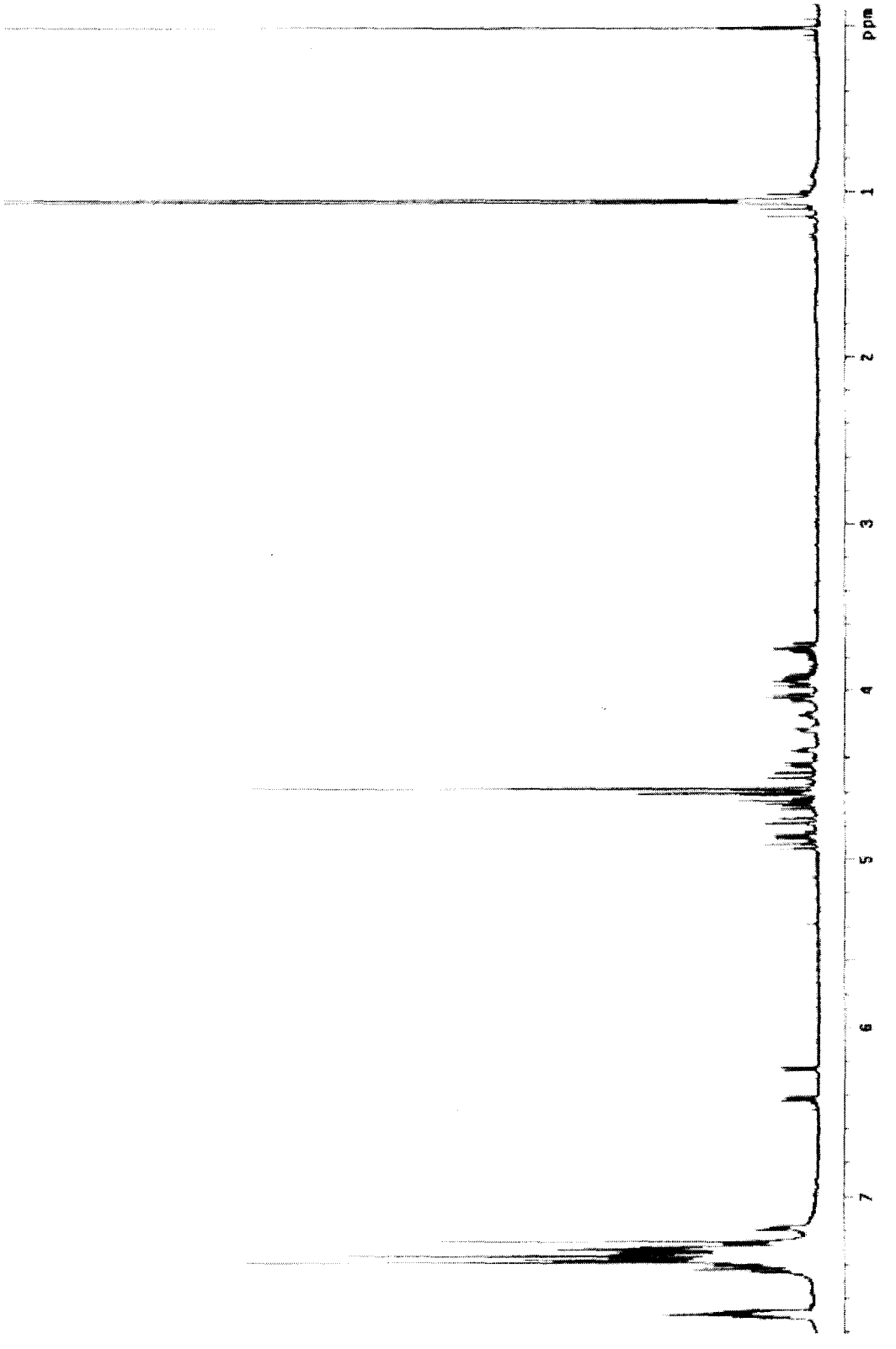

Figure 34: ^{1}H NMR spectrum of **11**

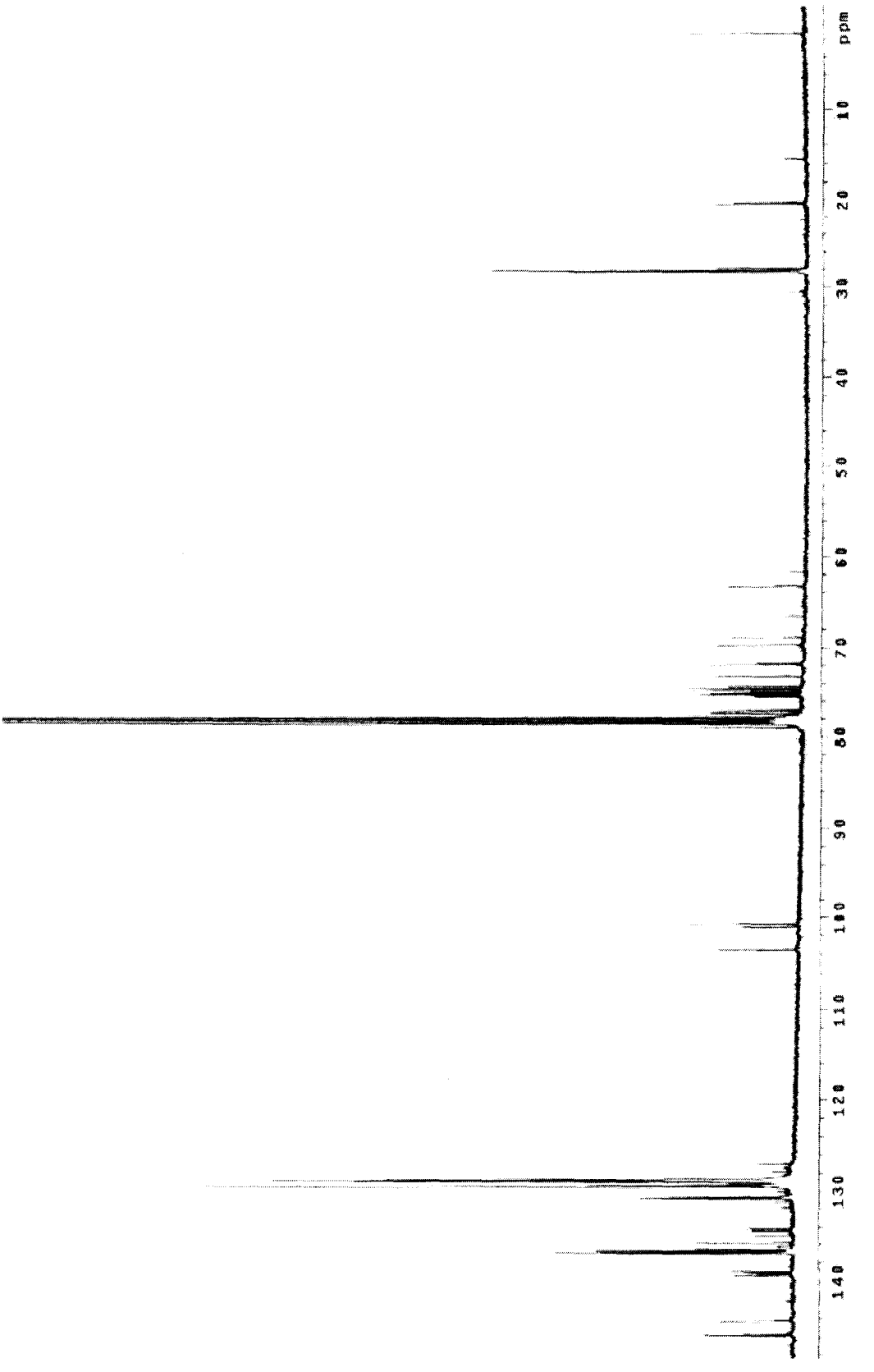

Figure 35: ^{13}C NMR spectrum of **11**

Acquisition Parameter:

Source	: APCI	Polarity	: Positive
Mode	: Std/Normal		
CapExit	: 100.7 Volt	Skim 1	: 30.0 Volt
Scan Range	: 15.00 - 2200.00 m/z	Trap Drive	: 45
Accum.time	: 1128 µs	Summation	: 10 Spectra
MS/MS	:		

Profile Spectrum, No.: 1, Time: 0 min

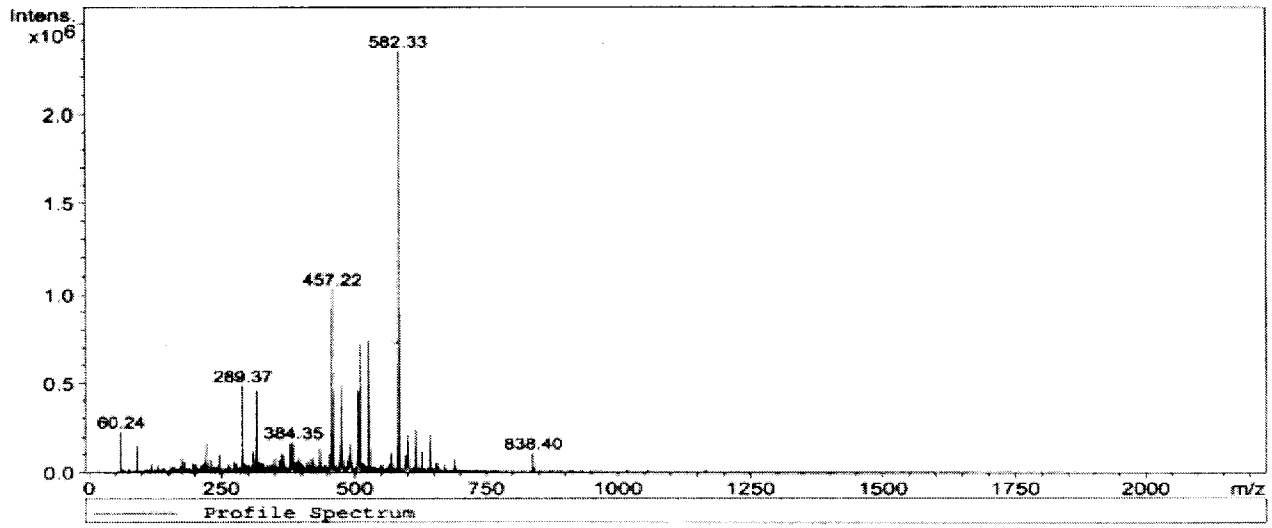

MS Peak List (Profile Spectrum):

Mass	Intensity	Width	Mass	Intensity	Width	Mass	Intensity	Width
60.24	230074	0.30	457.22	1033586	0.60	528.31	136621	0.20
91.25	153356	0.30	458.11	476244	0.30	568.38	112828	0.60
221.37	166318	0.60	459.16	181780	0.40	582.33	2346741	0.30
245.44	101652	0.50	473.28	132253	0.40	583.14	889941	0.40
289.37	487438	0.40	474.25	482196	0.30	584.13	278370	0.50
290.29	133029	0.20	475.20	201213	0.40	597.00	102348	0.20
309.45	123875	0.50	476.29	141648	0.60	600.23	213476	0.40
316.42	455285	0.40	490.25	103072	0.50	614.31	235638	0.30
317.33	171756	0.40	492.27	159492	0.50	615.28	143400	0.20
363.44	103591	0.30	506.32	453787	0.40	626.24	117143	0.60
365.36	104143	0.40	507.33	203283	0.30	642.26	211581	0.80
379.26	167052	0.50	509.34	724934	0.30	643.20	118884	0.50
384.35	172394	0.60	510.30	307836	0.40	838.40	114336	0.30
434.30	140990	0.30	526.38	742830	0.40			
453.34	104977	0.40	527.32	366522	0.30			

Figure 36: Mass spectrum of **11**

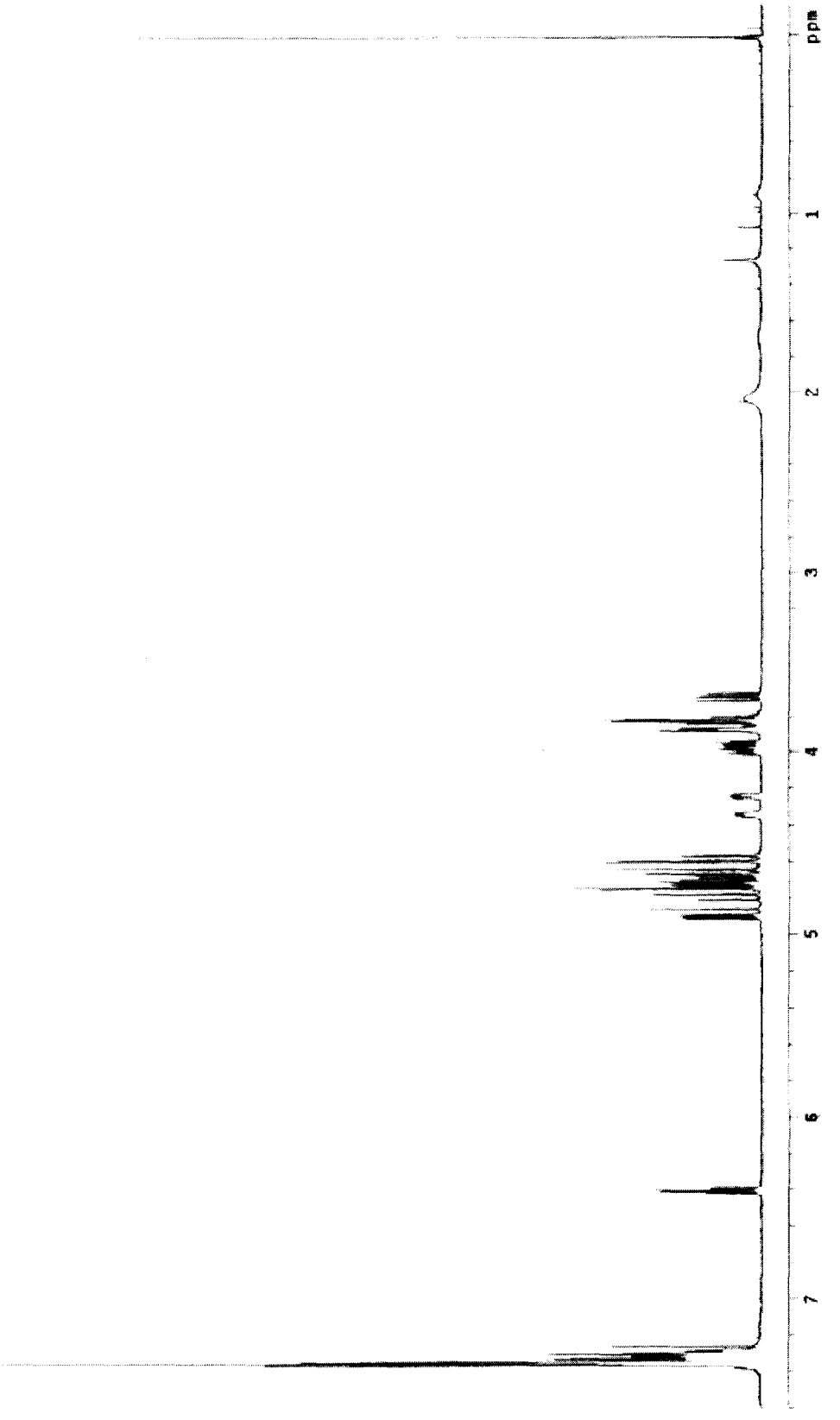

Figure 37: ^{1}H NMR spectrum of **12**

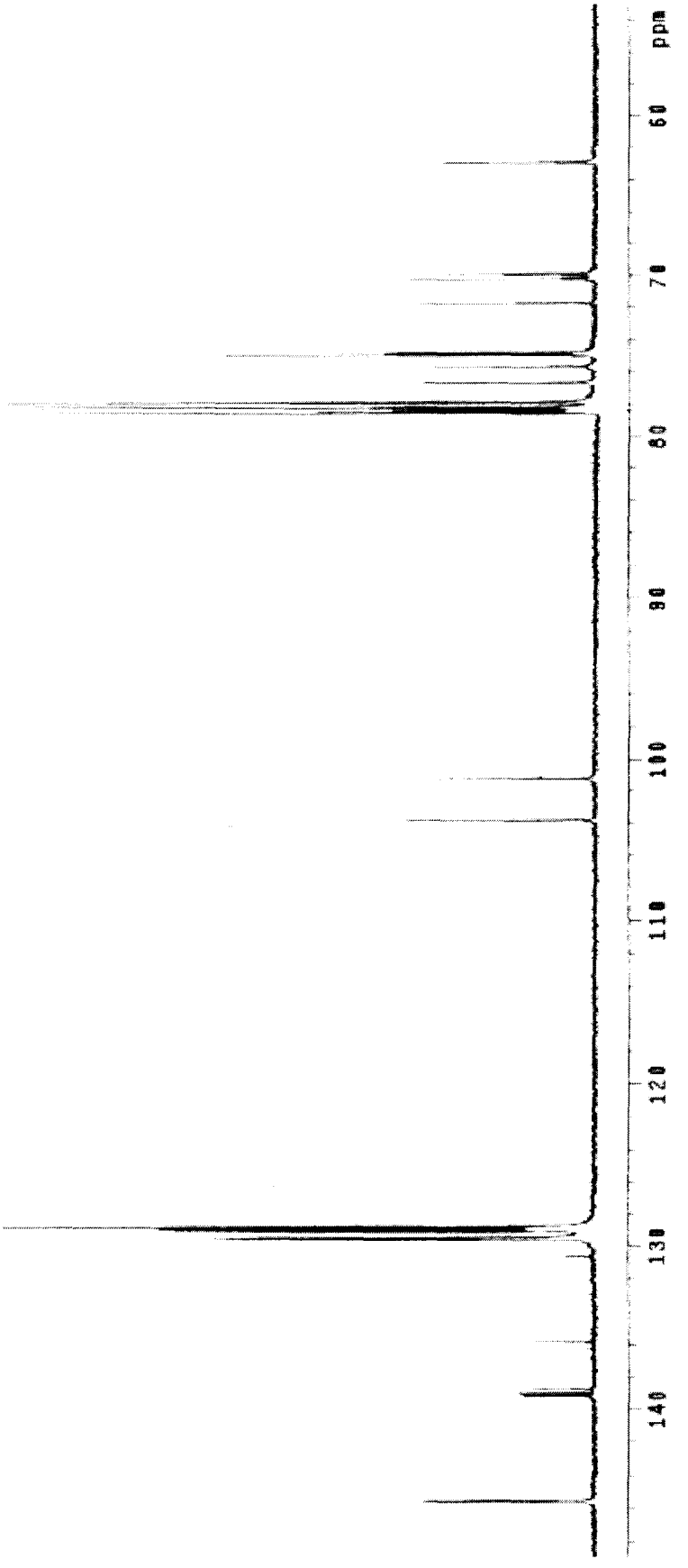

Figure 38: ^{13}C NMR spectrum of **12**

Acquisition Parameter:

Source	: APCI	Polarity	: Positive
Mode	: Std/Normal		
CapExit	: 86.7 Volt	Skim 1	: 16.0 Volt
Scan Range	: 15.00 - 1000.00 m/z	Trap Drive	: 40
Accum.time	: 20000 µs	Summation	: 10 Spectra
MS/MS	: 344.3 u		

Profile Spectrum, No.: 1, Time: 0 min

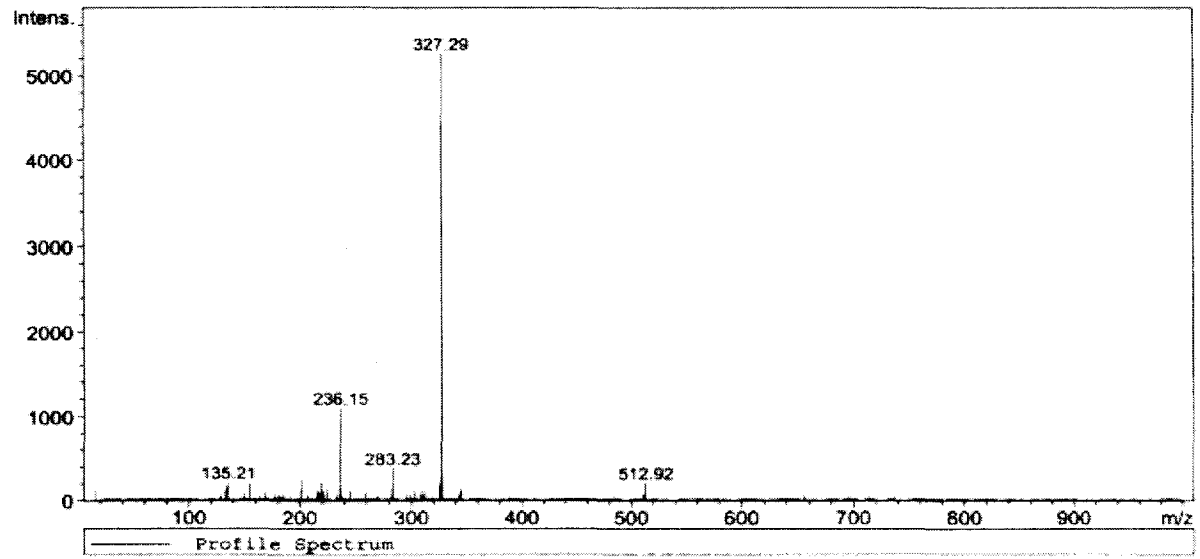

MS Peak List (Profile Spectrum):

Mass	Intensity	Width	Mass	Intensity	Width	Mass	Intensity	Width
133.15	170	0.30	236.15	1100	0.30	325.39	161	0.20
135.21	217	0.20	237.16	124	0.30	326.24	210	0.30
155.05	194	0.30	245.24	112	0.30	326.65	138	0.10
201.19	251	0.30	282.32	145	0.20	327.29	5258	0.30
215.32	125	0.20	283.23	386	0.20	328.27	324	0.20
219.13	215	0.20	303.21	119	0.20	345.46	146	0.20
221.17	119	0.30	309.19	118	0.40	512.92	215	0.20
224.08	135	0.20	312.29	112	0.40			

Figure 39: Mass spectrum of **12**

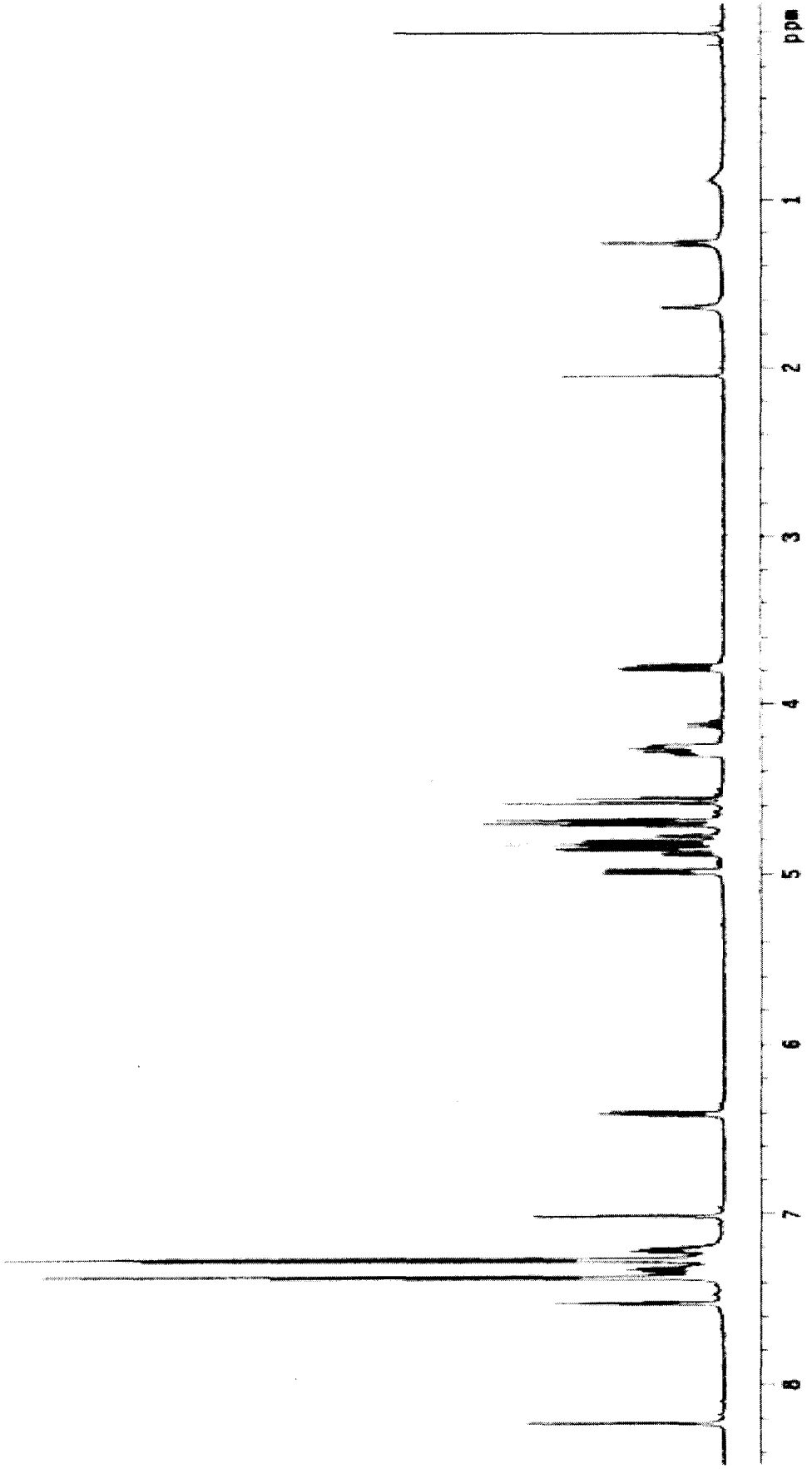

Figure 40: ^{1}H NMR spectrum of **13**

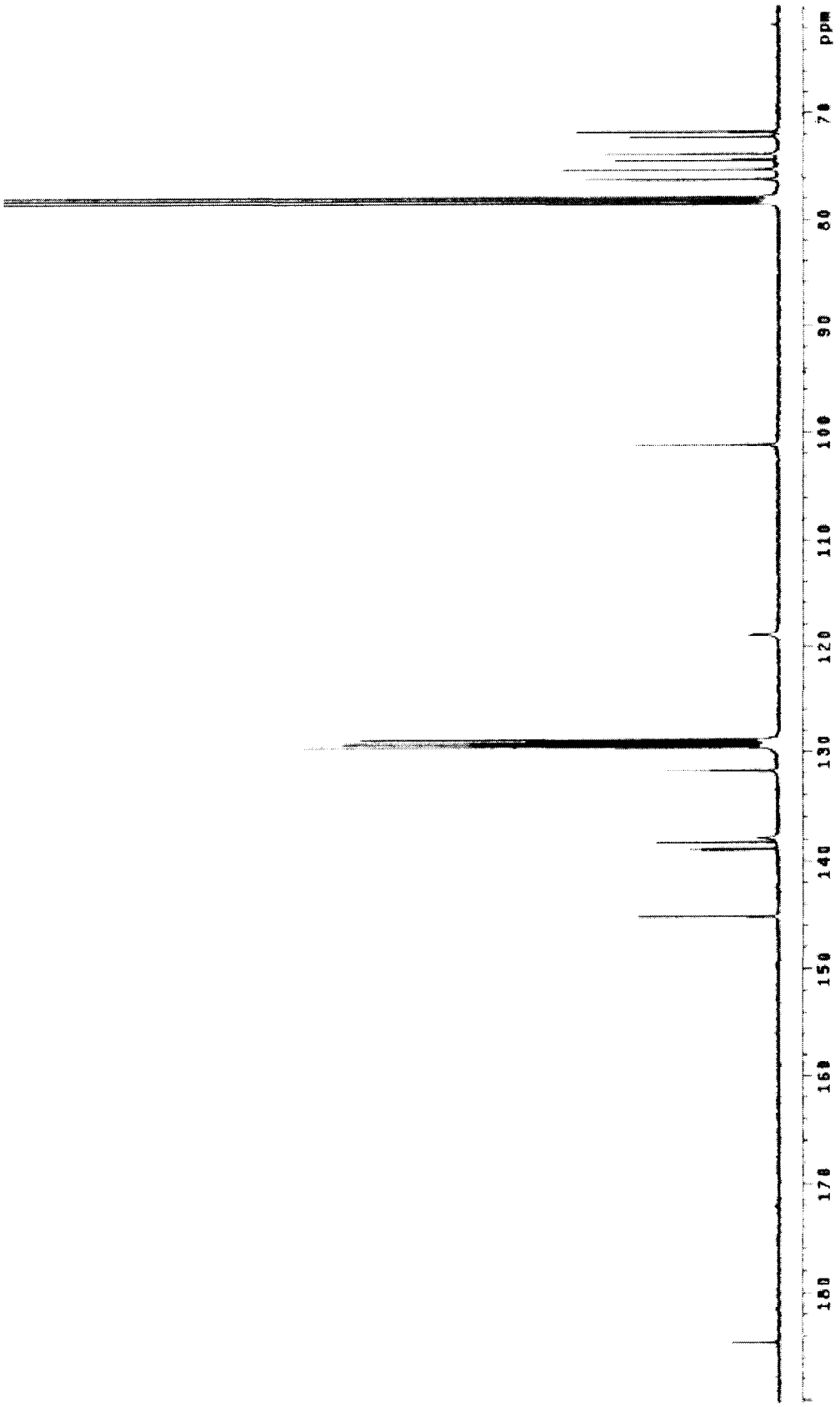

Figure 41: ^{13}C NMR spectrum of **13**

Acquisition Parameter

Ion Source Type	ESI	Ion Polarity	Positive		
Mass Range Mode	Std/Normal	Scan Begin	15.00 m/z	Scan End	2200.00 m/z
Skim 1	25.0 Volt	Cap Exit Offset	77.0 Volt	Trap Drive	40.0
Accumulation Time	1679 µs	Averages	10 Spectra		

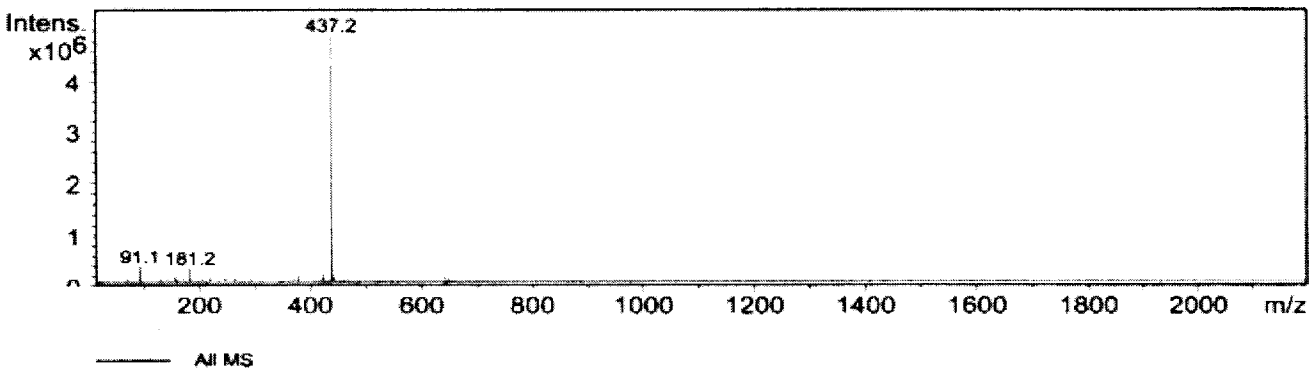

Index	Mass	Intensity	Width	S/N
1	91.15	321563.00	0.32	278.69
2	155.13	113158.00	0.32	98.07
3	181.16	282484.00	0.35	244.82
4	245.16	120124.00	0.37	104.11
5	377.18	123124.00	0.40	106.71
6	421.21	211033.00	0.42	182.90
7	437.23	5368861.00	0.39	4653.02
8	438.00	1534555.00	0.38	1329.95
9	439.07	478970.00	0.38	415.11

Figure 42: Mass spectrum of **13**

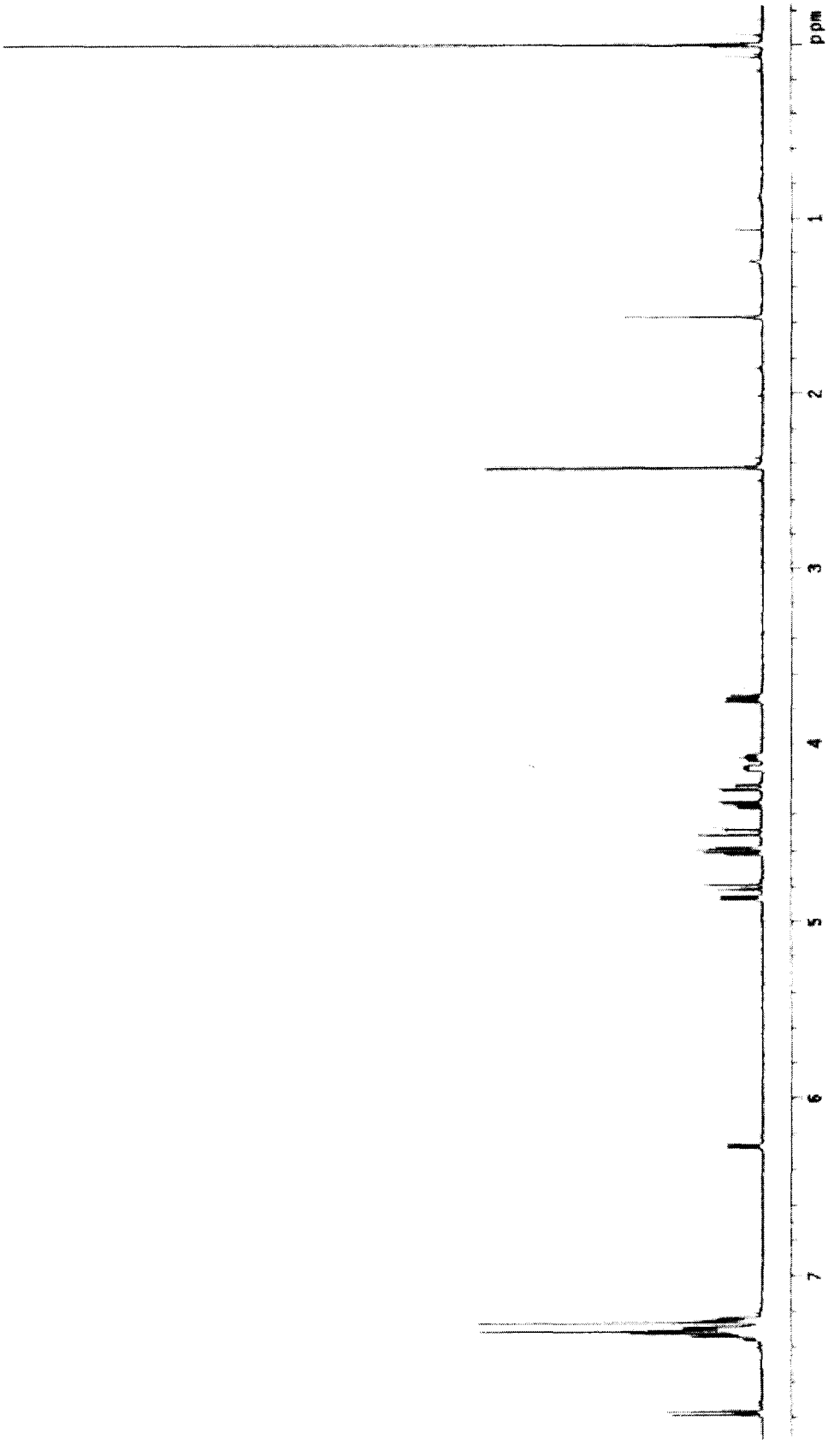

Figure 43: ^{1}H NMR spectrum of **15**

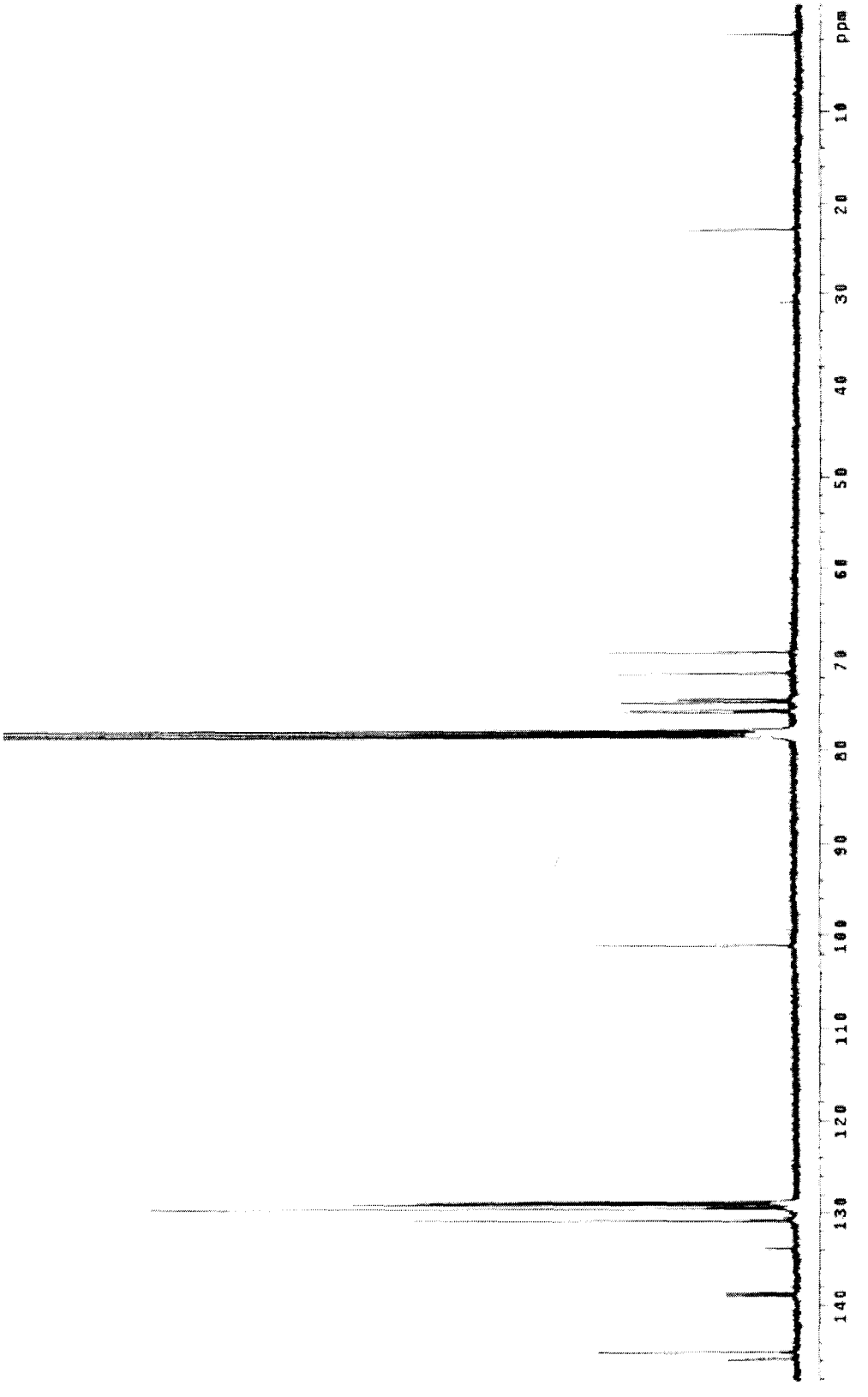

Figure 44: ^{13}C NMR spectrum of **15**

Acquisition Parameter:

Source	: ESI	Polarity	: Positive
Mode	: Std/Normal		
CapExit	: 88.7 Volt	Skim 1	: 18.0 Volt
Scan Range	: 15.00 - 2200.00 m/z	Trap Drive	: 45
Accum.time	: 2861 µs	Summation	: 10 Spectra
MS/MS	:		

Profile Spectrum, No.: 1, Time: 0 min

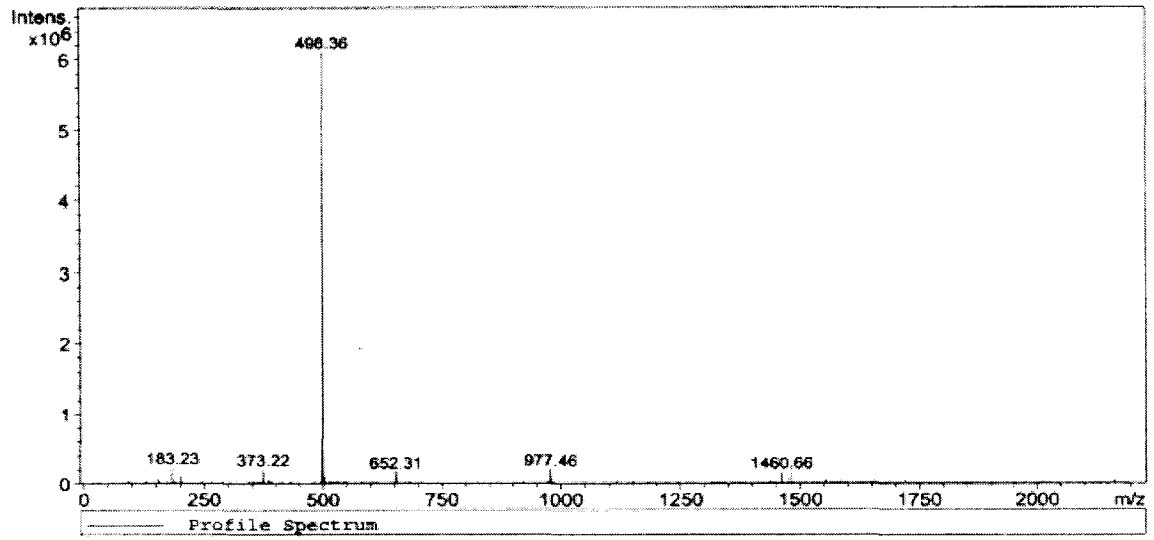

MS Peak List (Profile Spectrum):

Mass	Intensity	Width	Mass	Intensity	Width	Mass	Intensity	Width
155.20	64012	0.20	500.05	491872	0.30	979.20	64718	0.20
183.23	229626	0.30	501.15	128417	0.30	1117.73	51715	0.20
201.26	113848	0.30	503.34	78043	0.40	1460.66	158601	0.20
373.22	201901	0.50	652.31	162572	0.60	1478.83	153244	0.20
374.15	59662	0.40	653.31	70104	0.50	1552.84	52669	0.20
498.36	6108542	0.30	977.46	199765	0.40	1720.42	54167	0.20
498.99	1870232	0.30	978.26	145214	0.40	2165.03	63431	0.20

Figure 45: Mass spectrum of **15**

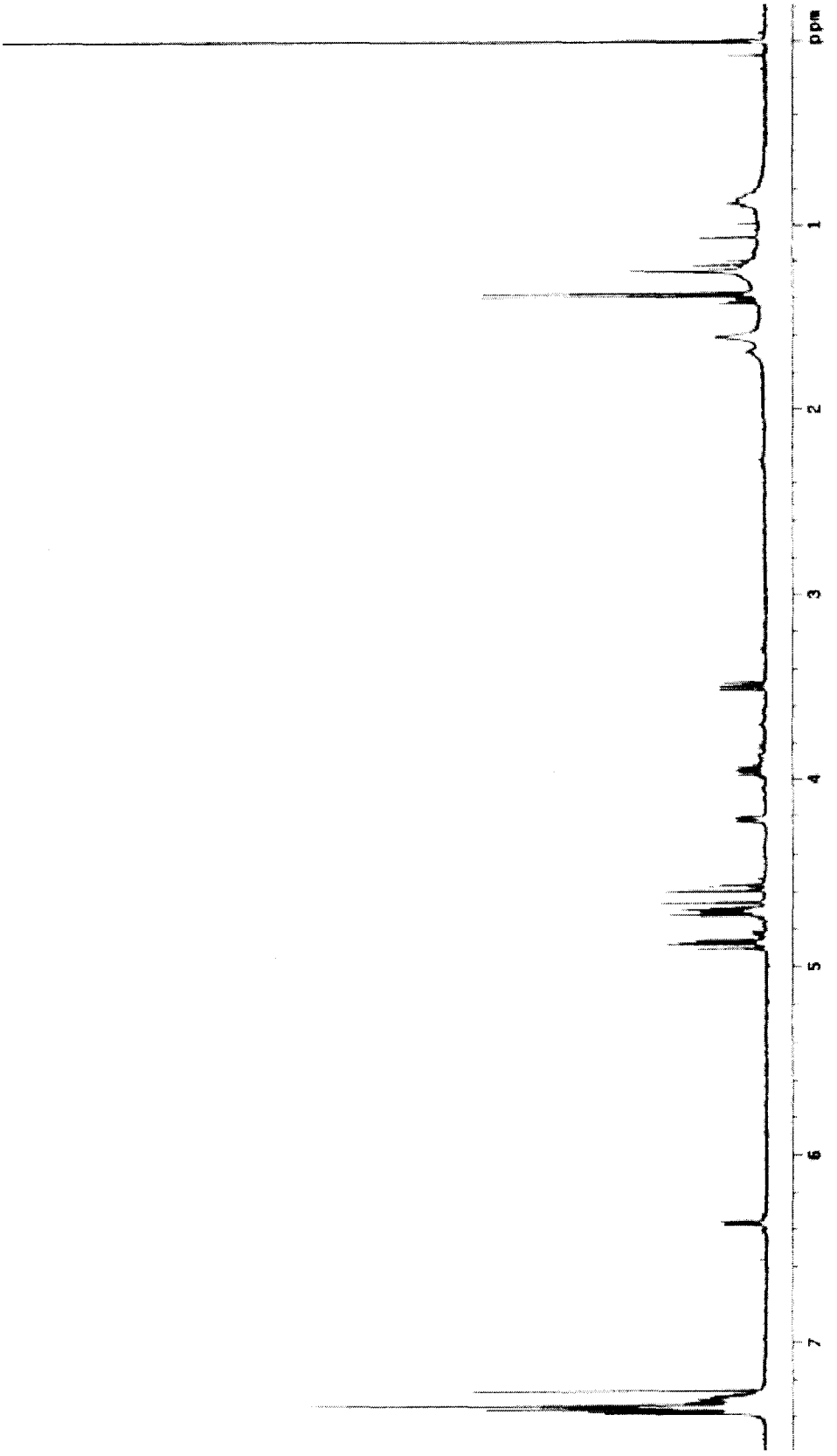

Figure 46: ^{1}H NMR spectrum of **14**

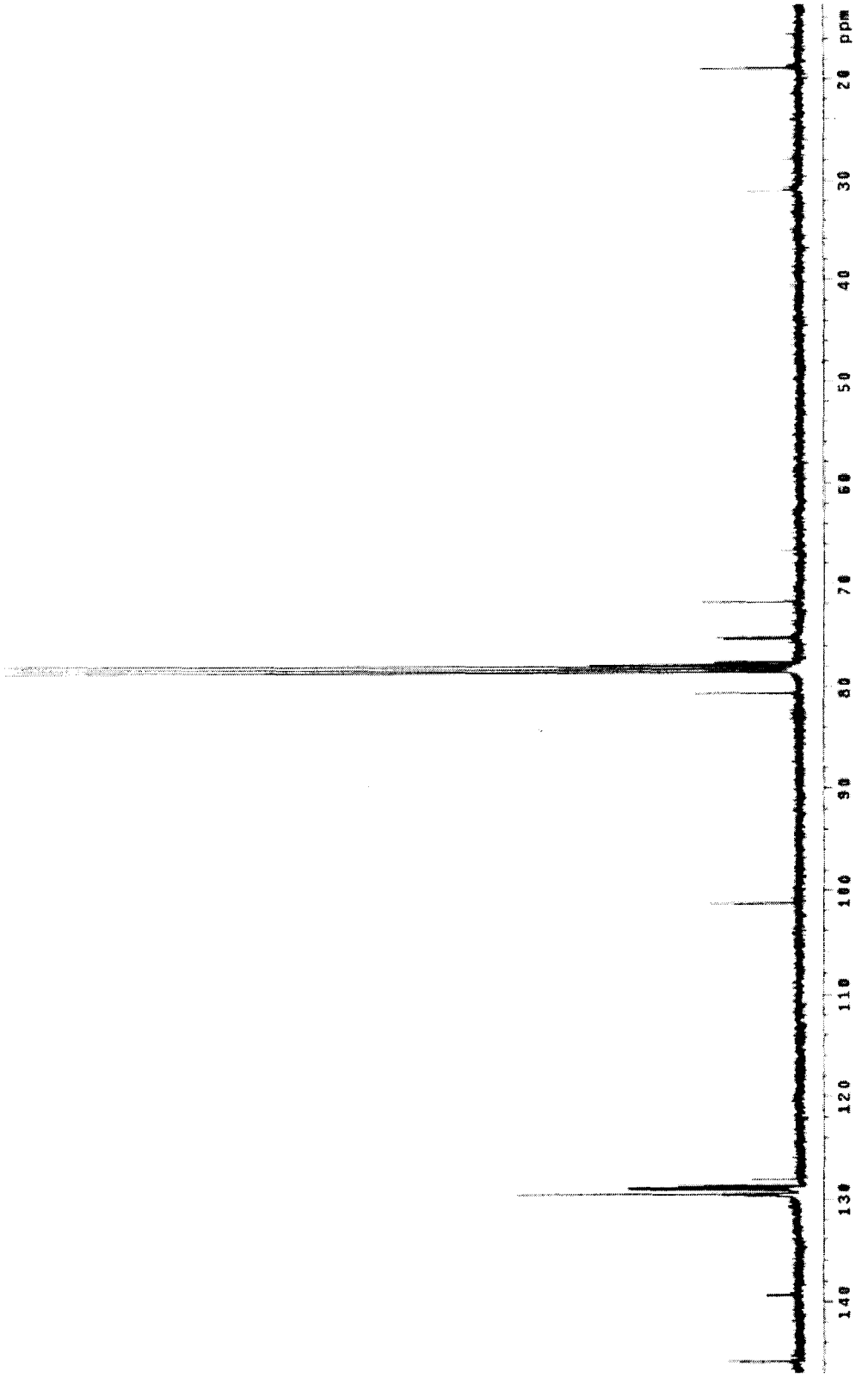

Figure 47: ^{13}C NMR spectrum of **14**

Acquisition Parameter:

Source	: ESI	Polarity	: Positive
Mode	: Std/Normal		
CapExit	: 88.7 Volt	Skim 1	: 18.0 Volt
Scan Range	: 15.00 - 2200.00 m/z	Trap Drive	: 35
Accum.time	: 5830 µs	Summation	: 10 Spectra
MS/MS	:		

Profile Spectrum, No.: 1, Time: 0 min

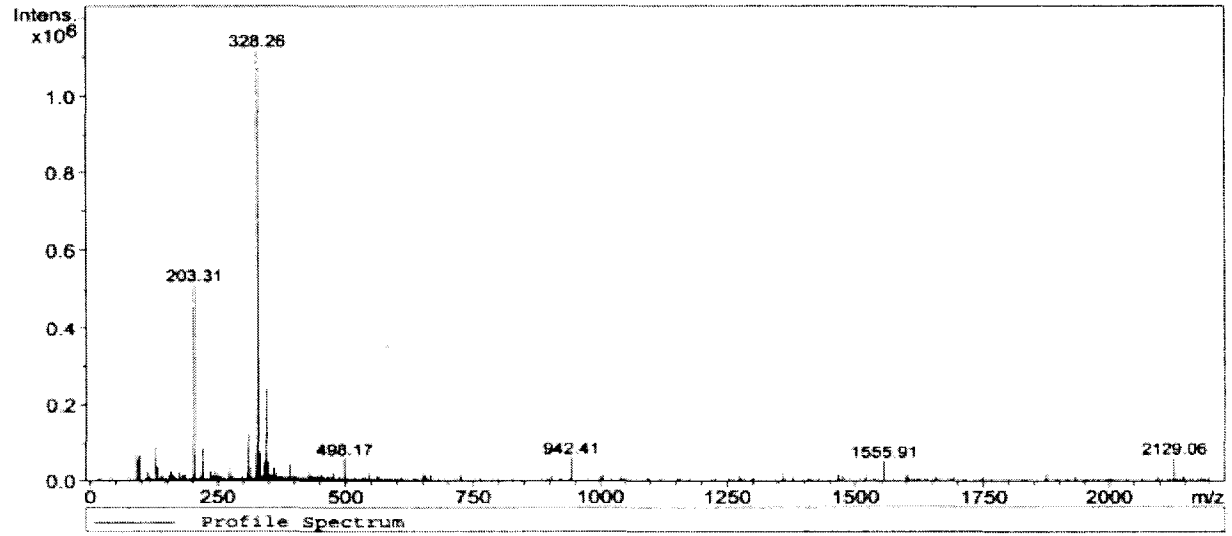

MS Peak List (Profile Spectrum):

Mass	Intensity	Width	Mass	Intensity	Width	Mass	Intensity	Width
91.26	69994	0.30	312.27	32402	0.30	344.18	240487	0.40
97.30	67542	0.40	328.26	1115399	0.30	345.18	56498	0.40
129.28	92431	0.40	329.12	318432	0.30	349.23	50271	0.30
131.31	36126	0.40	330.18	59200	0.30	360.26	32674	0.30
203.31	512306	0.30	332.35	31896	0.30	391.36	41934	0.30
204.24	77828	0.30	333.25	75174	0.30	498.17	58578	0.30
220.31	85873	0.40	341.21	45414	0.30	942.41	61893	0.20
272.82	33351	0.20	342.18	45272	0.30	1555.91	52540	0.20
311.26	120393	0.30	343.20	49999	0.50	2129.06	61200	0.20

Figure 48: Mass spectrum of **14**

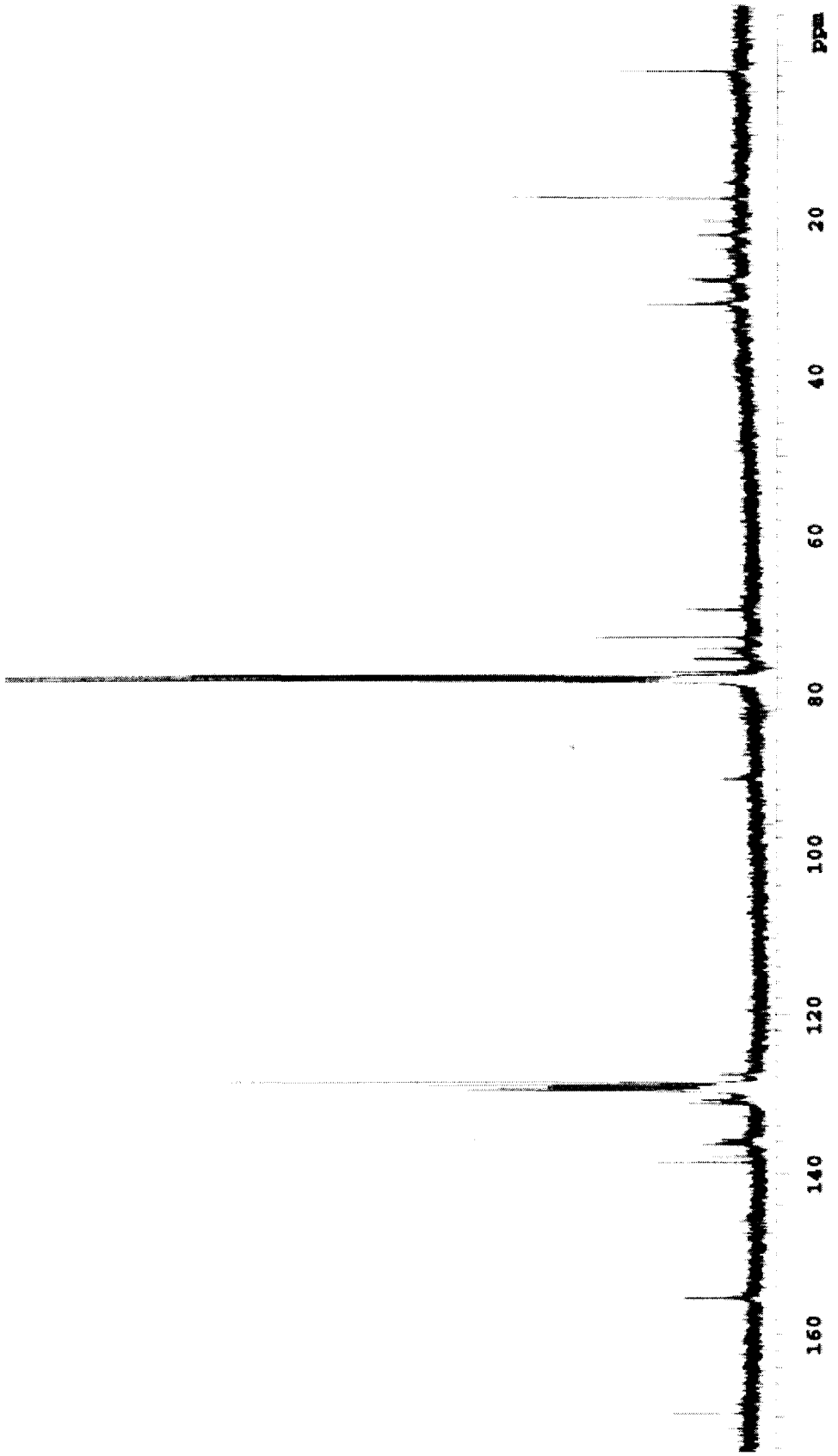

Figure 50: ^{13}C NMR spectrum of **17**

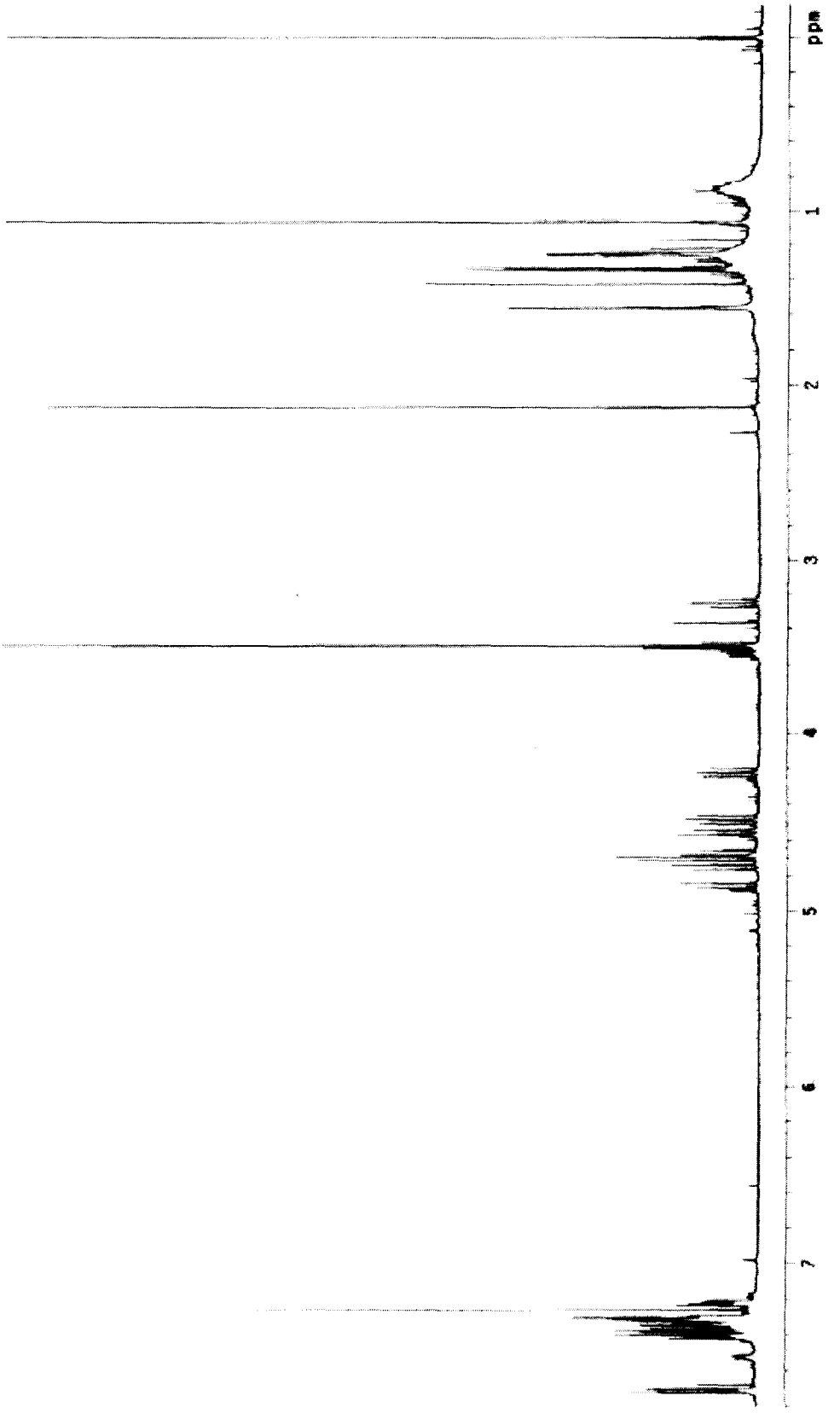

Figure 51: ^{1}H NMR spectrum of **18**

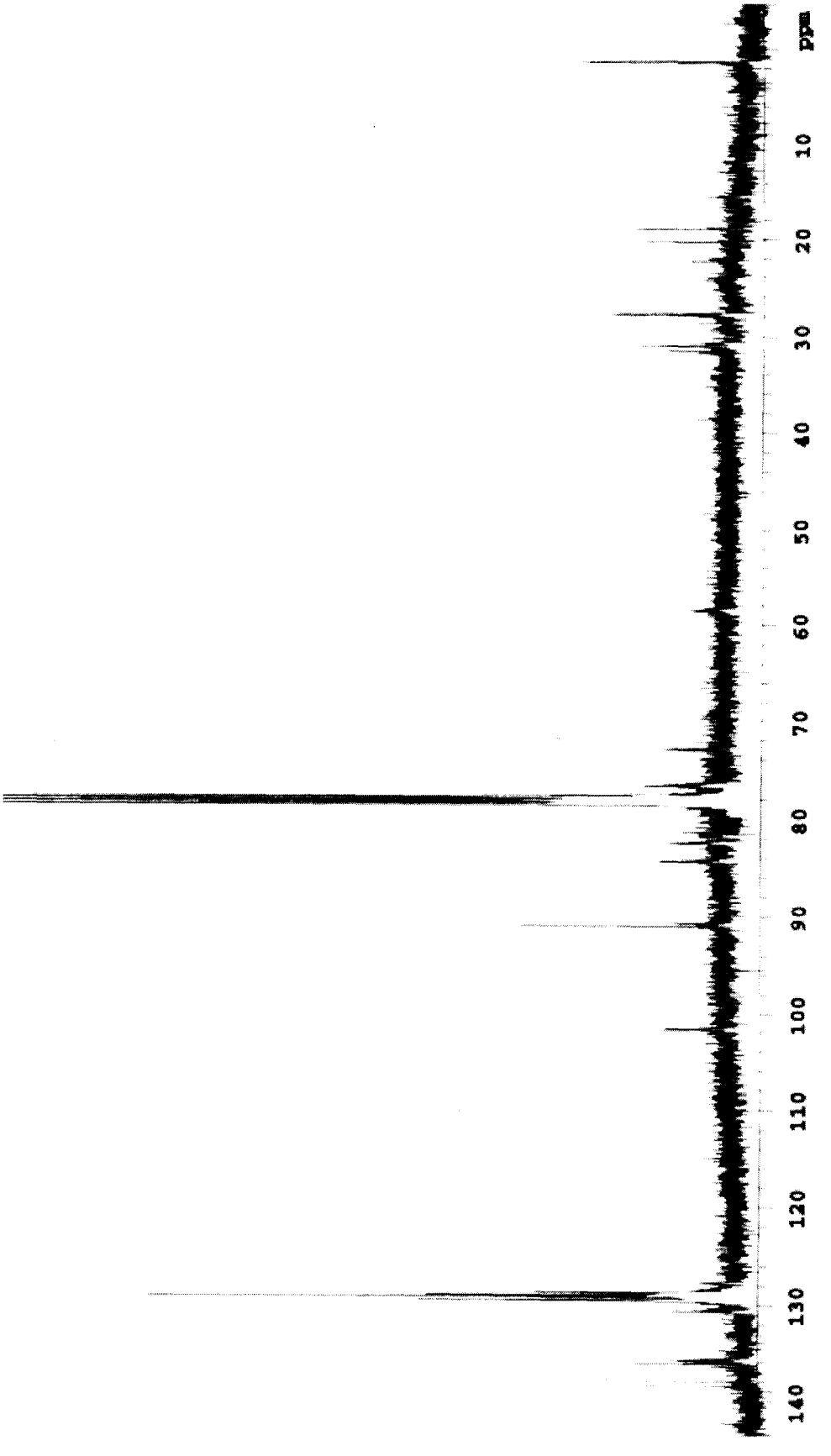

Figure 52: ^{13}C NMR spectrum of **18**

Acquisition Parameter

Ion Source Type	ESI	Ion Polarity	Positive		
Mass Range Mode	Std/Normal	Scan Begin	15.00 m/z	Scan End	2200.00 m/z
Skim 1	25.0 Volt	Cap Exit Offset	70.2 Volt	Trap Drive	40.0
Accumulation Time	4451 µs	Averages	10 Spectra		

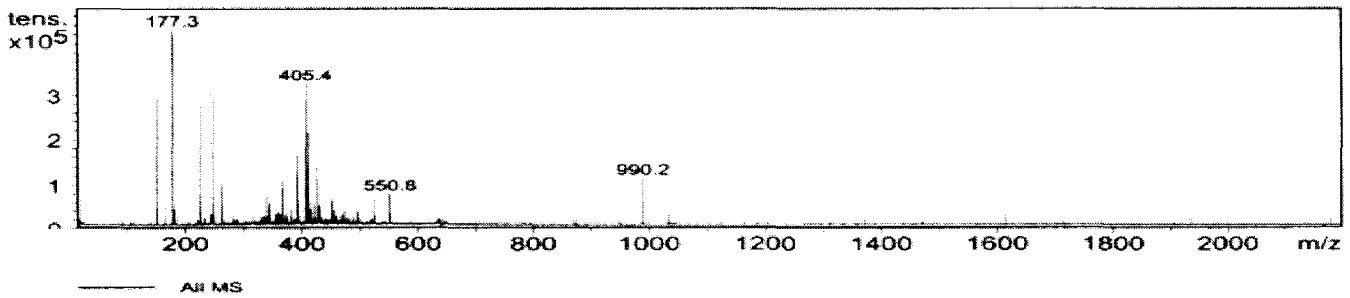

Index	Mass	Intensity	Width	S/N
1	149.22	318764.00	0.44	196.38
2	177.26	494457.00	0.45	304.62
3	178.25	60039.00	0.37	36.99
4	223.29	306992.00	0.46	189.13
5	245.26	348885.00	0.47	214.94
6	246.21	54965.00	0.35	33.86
7	261.21	106518.00	0.44	65.62
8	337.25	79433.00	0.43	48.94
9	343.24	59057.00	0.54	36.38
10	365.30	114545.00	0.47	70.57
11	391.38	175527.00	0.47	108.14
12	405.35	357984.00	0.48	220.54
13	406.32	98041.00	0.39	60.40
14	410.30	231919.00	0.42	142.88
15	411.26	61679.00	0.39	38.00
16	419.34	55907.00	0.49	34.44
17	426.19	147334.00	0.44	90.77
18	429.29	50185.00	0.48	30.92
19	450.25	64828.00	0.47	39.94
20	522.80	72506.00	0.43	44.67
21	550.83	80840.00	0.43	49.80
22	990.22	118558.00	0.03	73.04

Figure 53: Mass spectrum of **18**

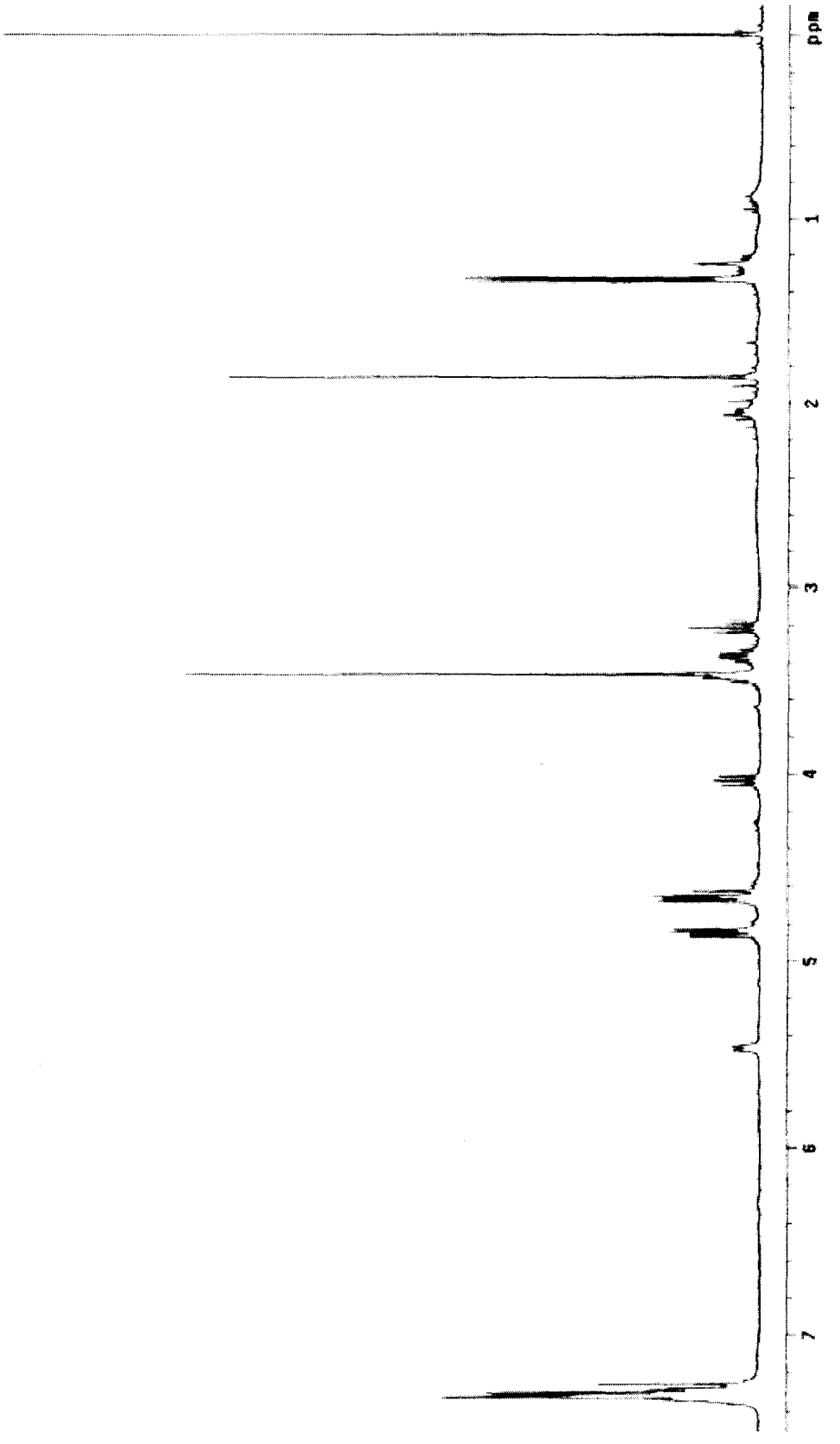

Figure 54: ^{1}H NMR spectrum of **19**

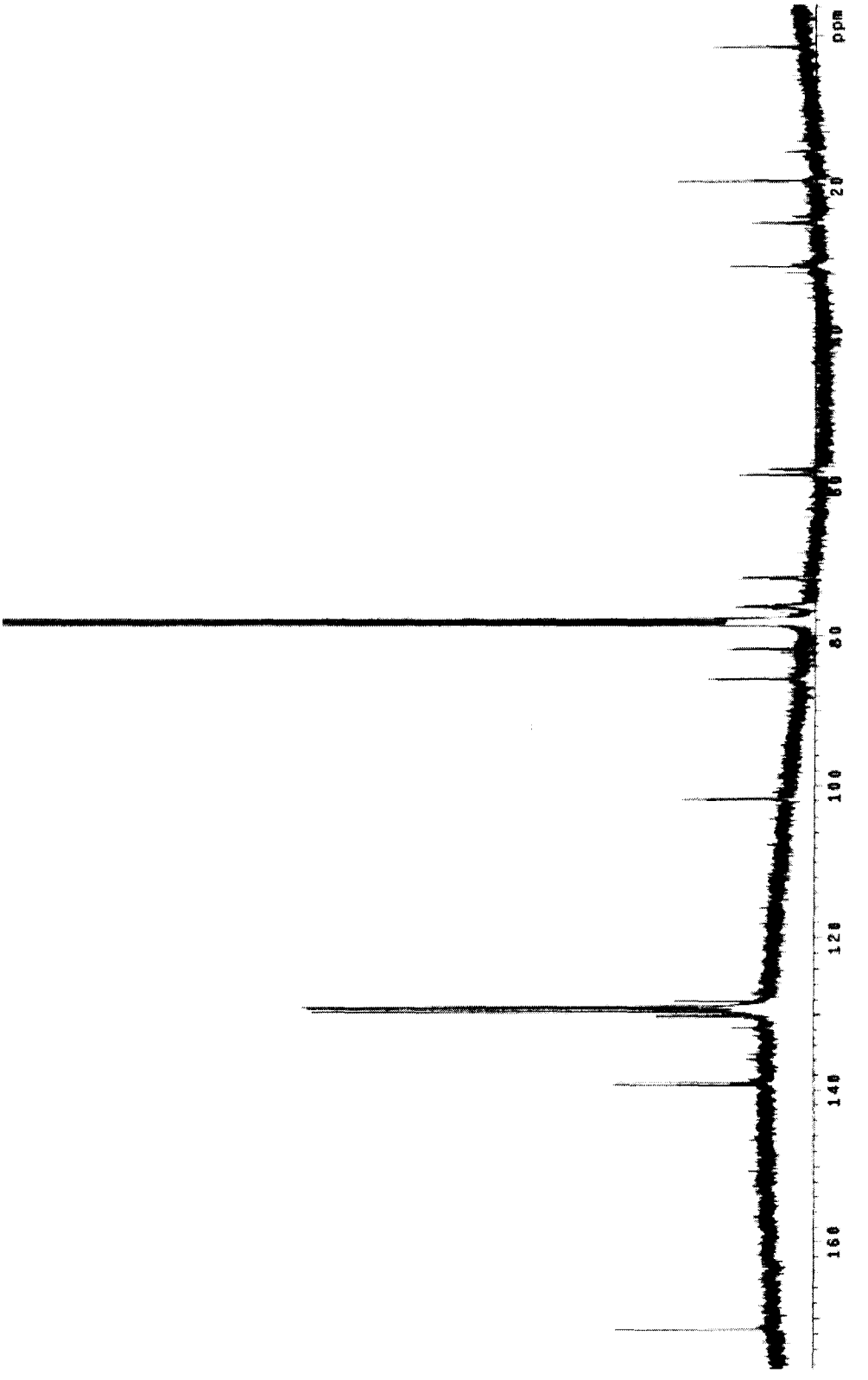

Figure 55: ^{13}C NMR spectrum of **19**

Acquisition Parameter

Ion Source Type	ESI	Ion Polarity	Negative		
Mass Range Mode	Std/Normal	Scan Begin	15.00 m/z	Scan End	2200.00 m/z
Skim 1	-26.0 Volt	Cap Exit Offset	-77.0 Volt	Trap Drive	45.0
Accumulation Time	15732 µs	Averages	10 Spectra		

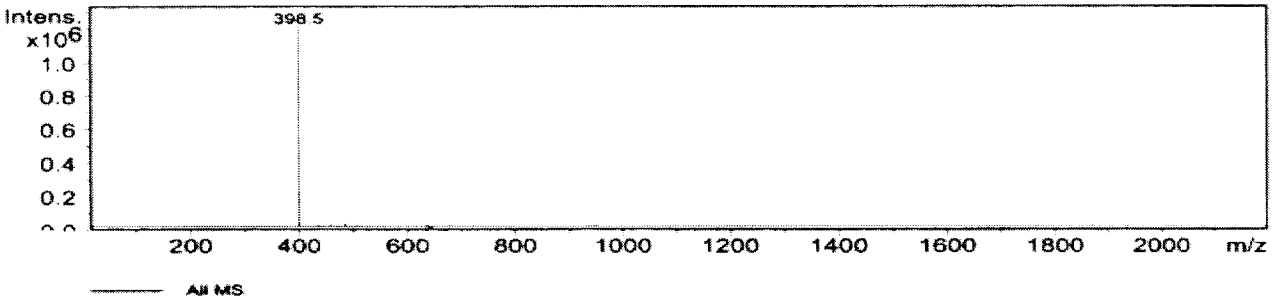

Index	Mass	Intensity	Width	S/N
1	375.48	2502.00	0.22	24.38
2	398.49	1326354.00	0.29	12923.91
3	412.25	2873.00	0.46	27.99
4	414.26	2625.00	0.36	25.58
5	434.23	9321.00	0.36	90.82
6	435.17	4492.00	0.40	43.77
7	436.15	3720.00	0.36	36.25
8	441.18	2828.00	0.39	27.56
9	456.19	13791.00	0.36	134.38
10	457.15	4342.00	0.34	42.31
11	458.15	4499.00	0.37	43.84
12	469.28	4758.00	0.34	46.36
13	483.26	22044.00	0.38	214.80
14	484.22	9350.00	0.31	91.11
15	504.26	5531.00	0.37	53.89
16	505.28	2952.00	0.30	28.76
17	555.29	2617.00	0.35	25.50
18	654.30	3759.00	0.65	36.63
19	950.64	7892.00	0.23	76.90
20	1718.93	4781.00	0.08	46.59
21	1871.92	5147.00	0.04	50.15

Figure 56: Mass spectrum of **19**

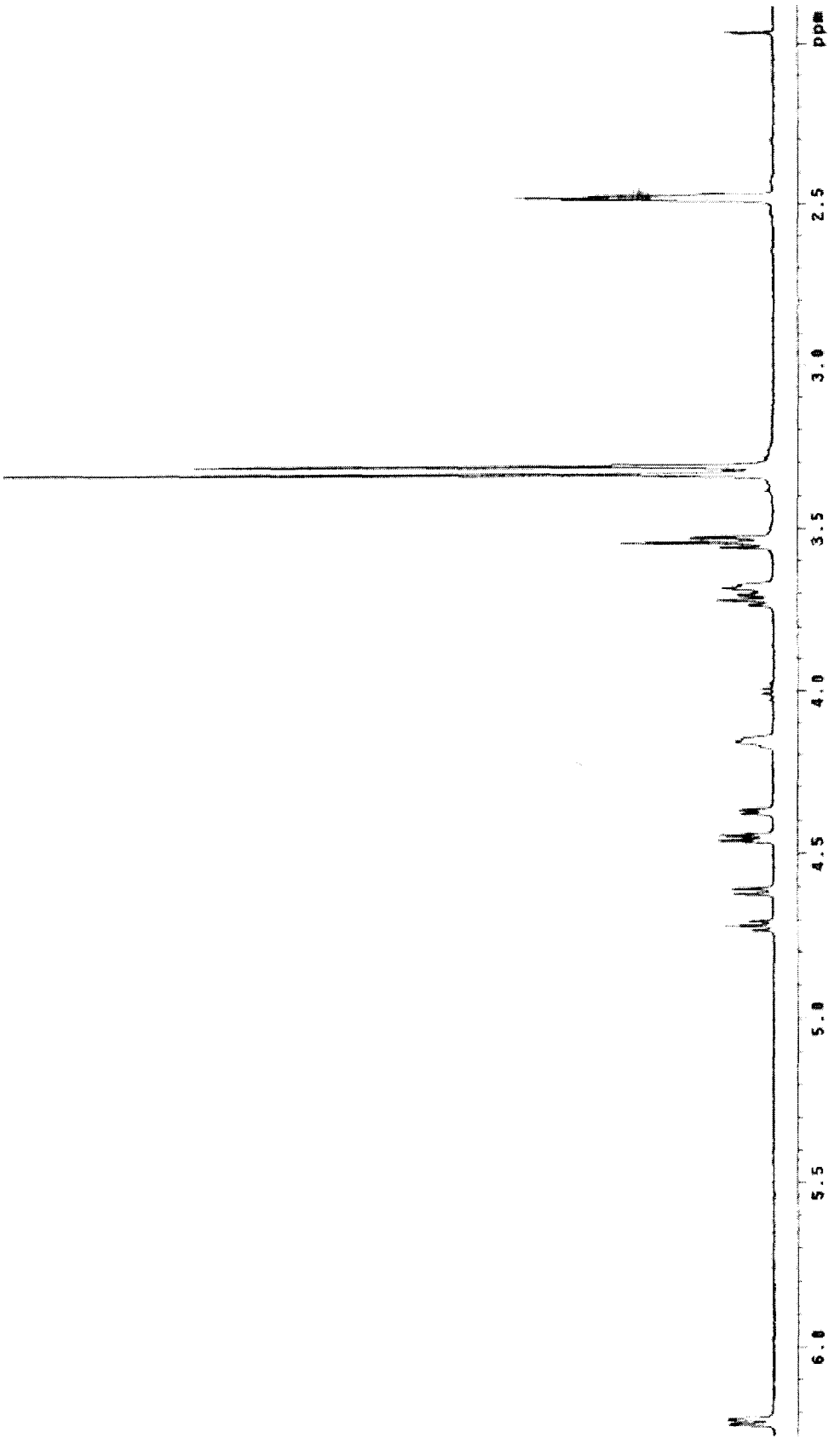

Figure 57: ^{1}H NMR spectrum of **21**

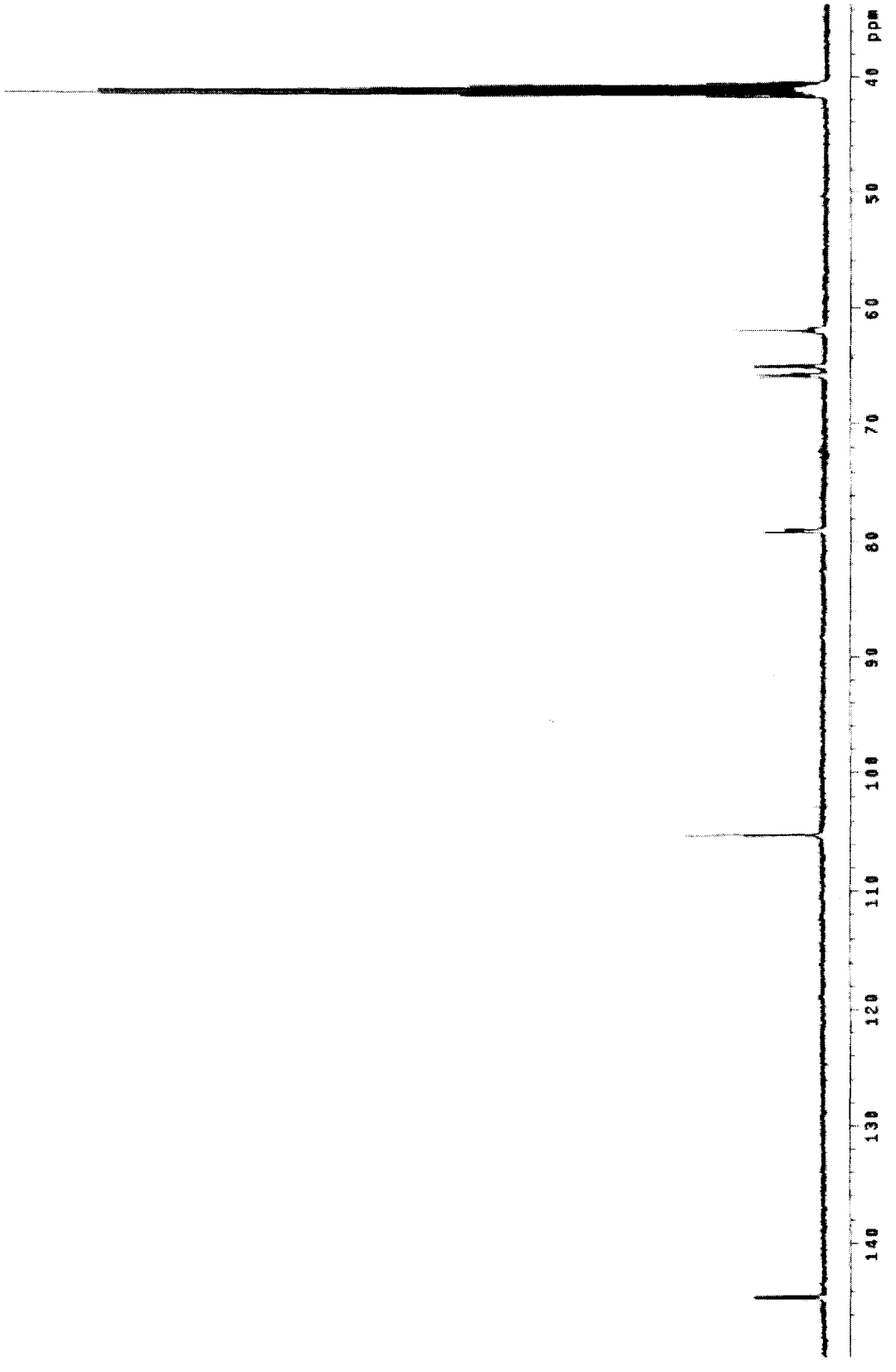

Figure 58: ^{13}C NMR spectrum of **21**

Acquisition Parameter

Ion Source Type	ESI	Ion Polarity	Negative		
Mass Range Mode	Std/Normal	Scan Begin	15.00 m/z	Scan End	2200.00 m/z
Skim 1	-21.0 Volt	Cap Exit Offset	-67.2 Volt	Trap Drive	25.0
Accumulation Time	20000 µs	Averages	10 Spectra		

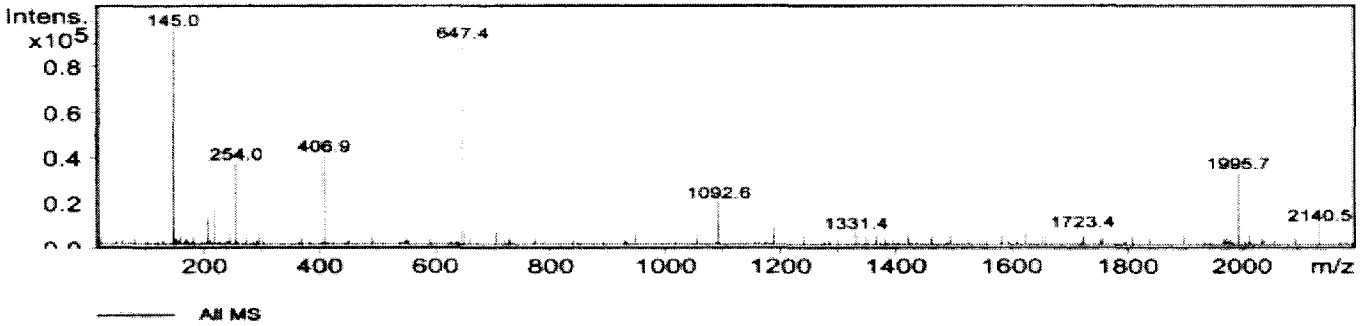

Index	Mass	Intensity	Width	S/N
1	144.99	106601.00	0.33	1365.74
2	145.97	7428.00	0.29	95.17
3	204.97	13709.00	0.34	175.64
4	216.85	16842.00	0.20	215.77
5	243.27	5233.00	0.20	67.04
6	254.02	39978.00	0.07	512.19
7	292.26	5001.00	0.23	64.07
8	406.86	43822.00	0.22	561.44
9	647.43	100188.00	0.08	1283.58
10	704.06	5887.00	0.24	75.42
11	1092.62	20946.00	0.04	268.35
12	1188.93	8040.00	0.10	103.01
13	1331.42	5492.00	0.03	70.36
14	1624.95	5519.00	0.20	70.71
15	1723.43	6067.00	0.08	77.73
16	1995.74	35312.00	0.18	452.41
17	2140.47	9475.00	0.20	121.39

Figure 59: Mass spectrum of **21**

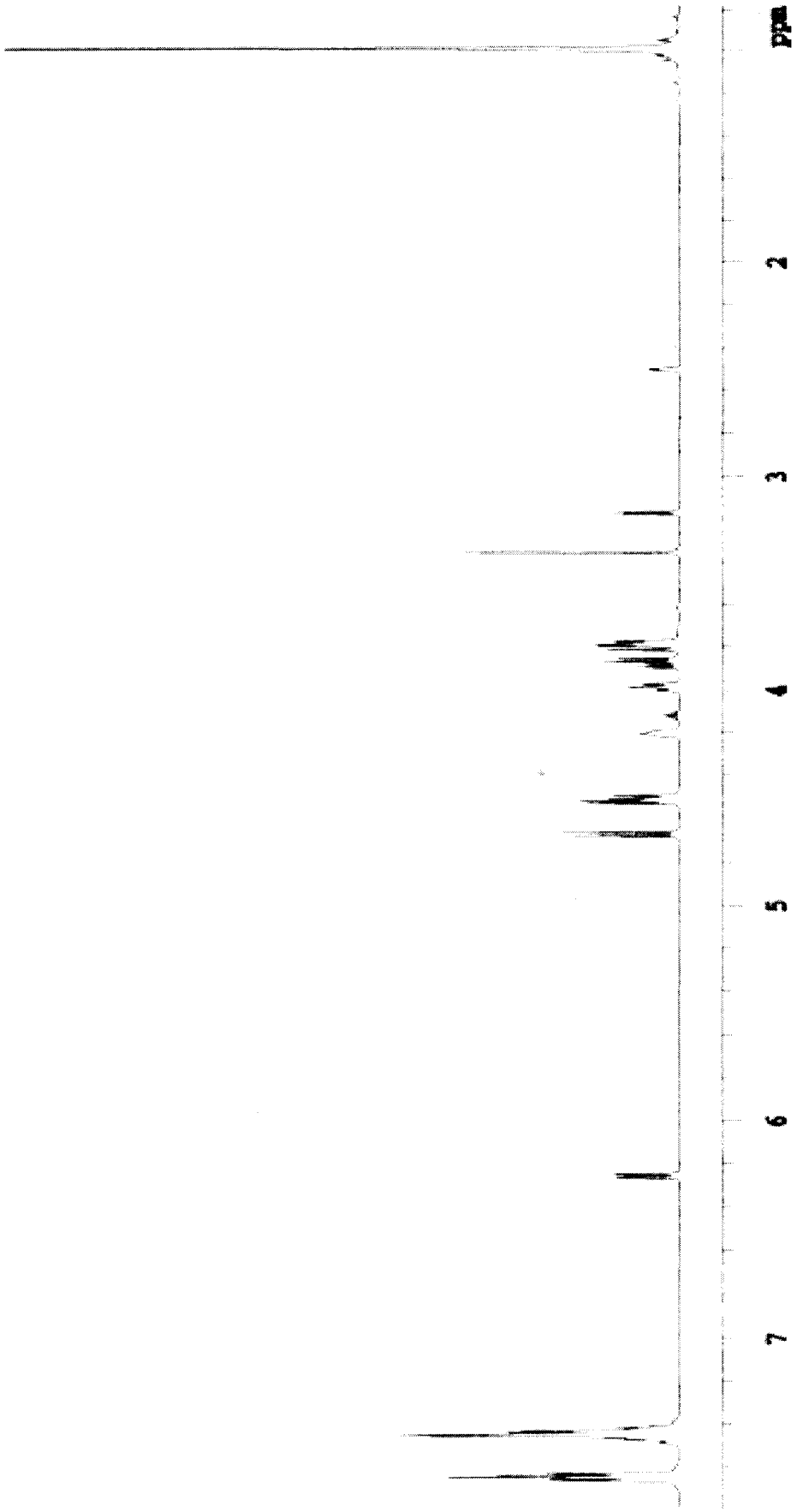

Figure 60: ^{1}H NMR spectrum of **22**

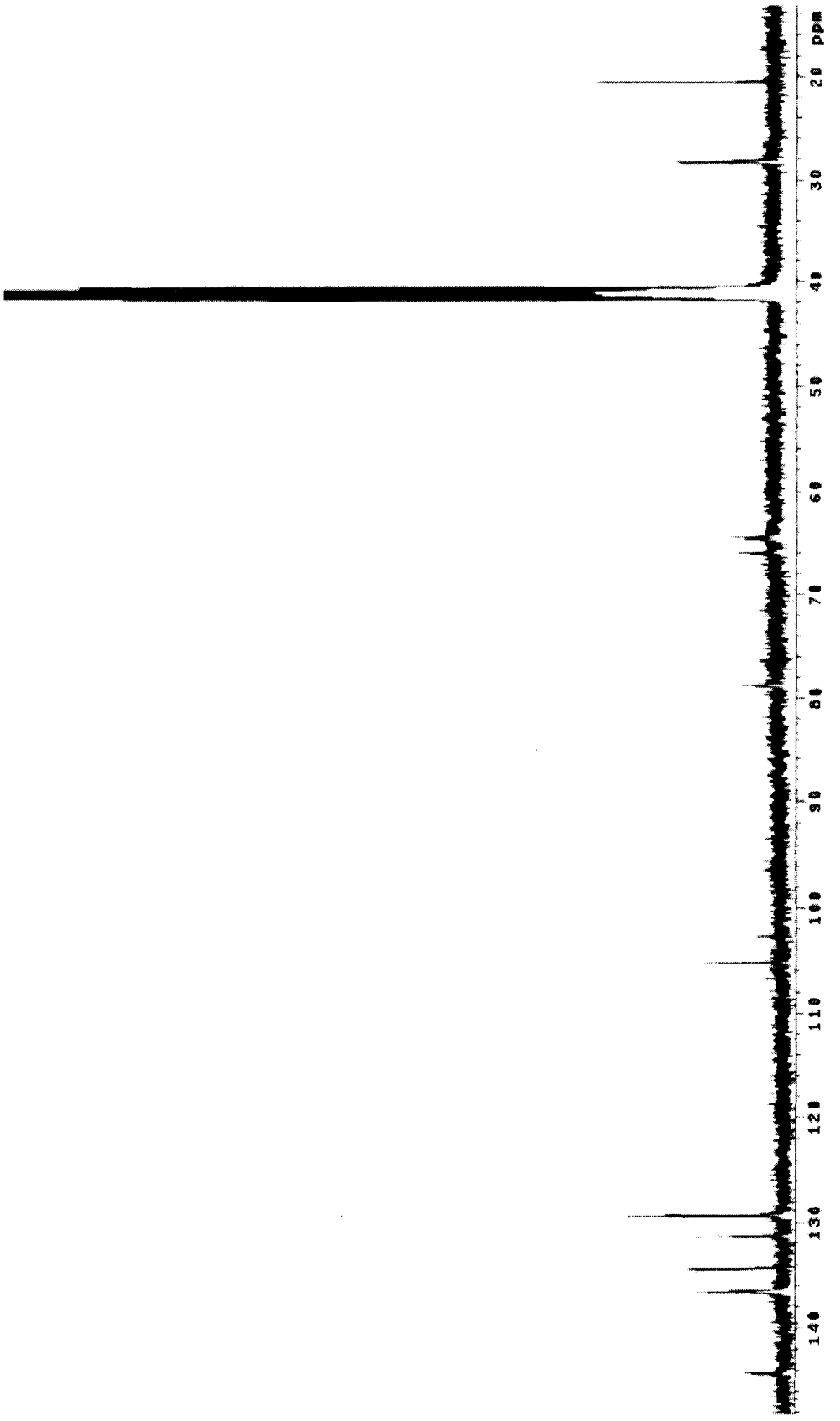

Figure 61: ^{13}C NMR spectrum of **22**

Acquisition Parameter

Ion Source Type	ESI	Ion Polarity	Negative		
Mass Range Mode	Std/Normal	Scan Begin	15.00 m/z	Scan End	2200.00 m/z
Skim 1	-25.3 Volt	Cap Exit Offset	-70.6 Volt	Trap Drive	45.5
Accumulation Time	20000 µs	Averages	10 Spectra		

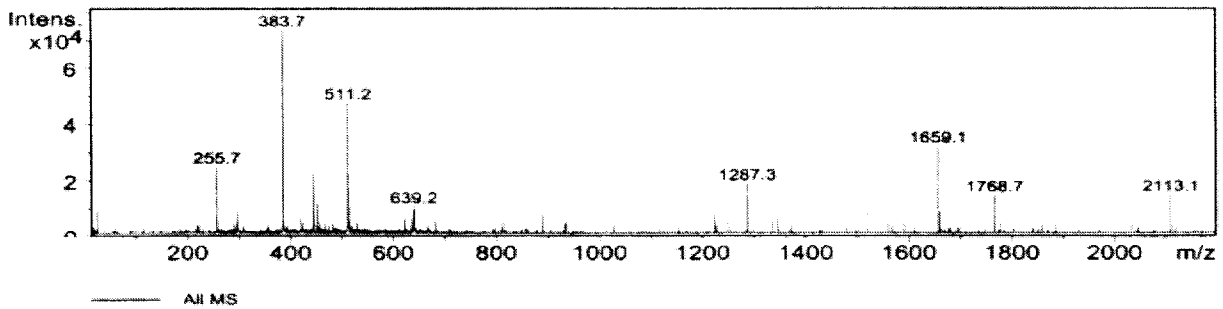

Index	Mass	Intensity	Width	S/N
1	24.13	8963.00	0.11	95.86
2	255.75	26512.00	0.38	283.56
3	294.44	8358.00	0.34	89.39
4	294.93	8190.00	0.16	87.60
5	383.65	81120.00	0.43	867.62
6	384.17	77446.00	0.47	828.33
7	443.38	23607.00	0.35	252.49
8	444.06	11652.00	0.29	124.62
9	451.23	12122.00	0.34	129.65
10	510.40	10445.00	0.20	111.71
11	511.17	51598.00	0.54	551.87
12	512.11	24210.00	0.52	258.94
13	513.06	10087.00	0.39	107.89
14	638.94	8652.00	0.32	92.54
15	639.24	10577.00	0.28	113.13
16	640.53	9293.00	0.18	99.39
17	1287.33	19831.00	0.12	212.10
18	1522.57	9575.00	0.18	102.41
19	1592.86	9999.00	0.22	106.94
20	1659.06	34637.00	0.22	370.46
21	1660.23	8140.00	0.32	87.06
22	1660.58	8387.00	0.16	89.70

Figure 62: Mass spectrum of **22**

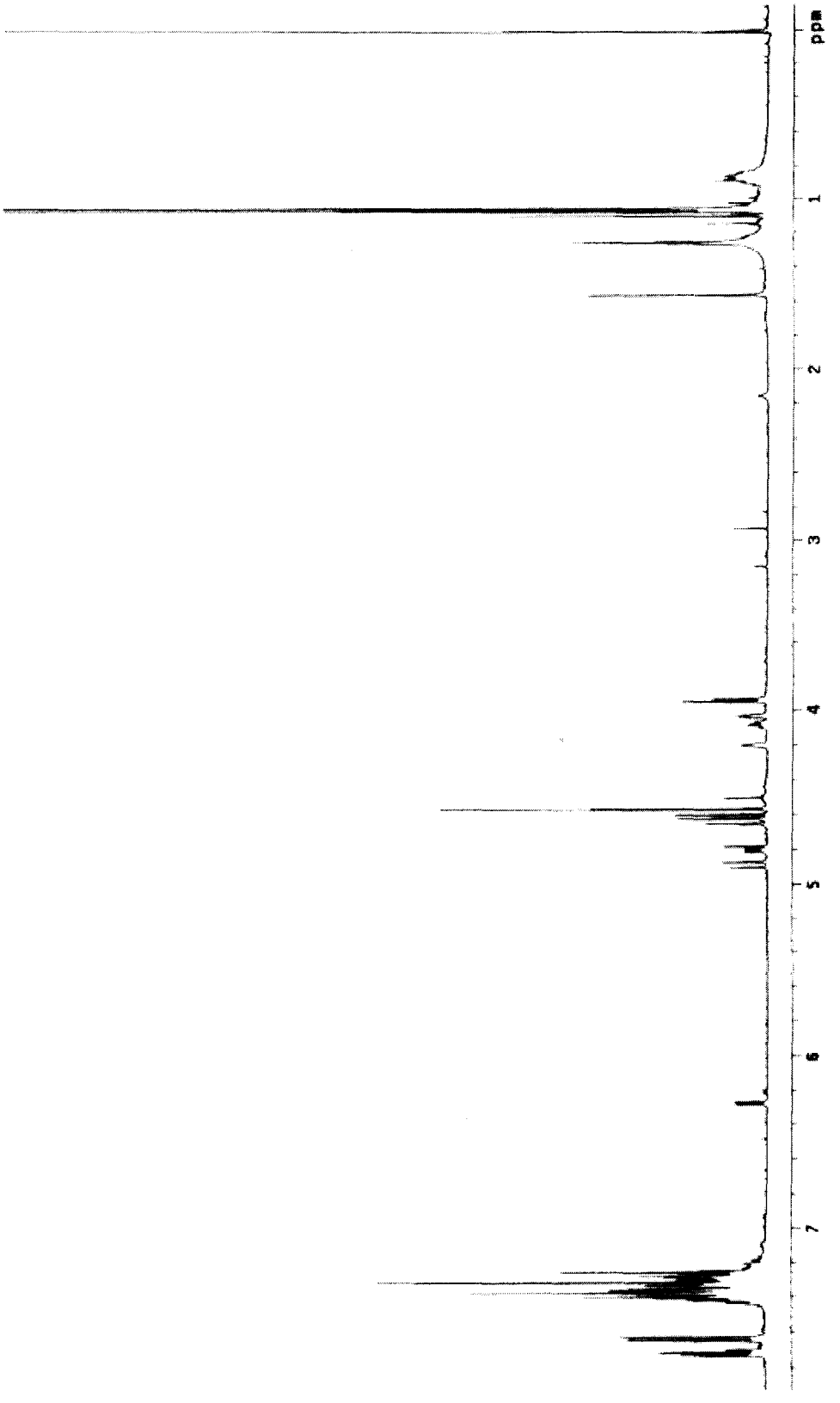

Figure 63: ^{1}H NMR spectrum of **23**

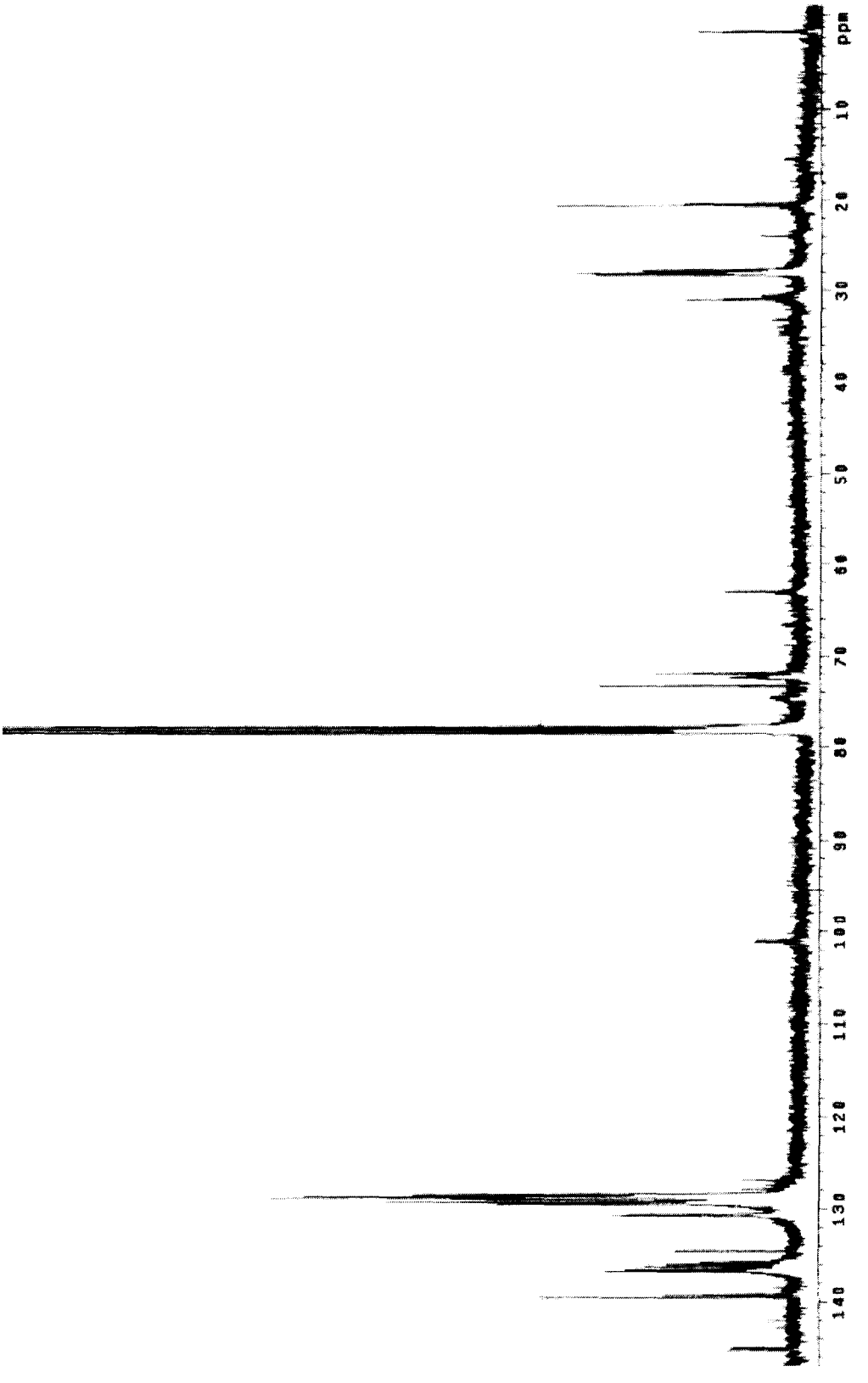

Figure 64: ^{13}C NMR spectrum of **23**

Acquisition Parameter

Ion Source Type	ESI	Ion Polarity	Negative		
Mass Range Mode	Std/Normal	Scan Begin	15.00 m/z	Scan End	2200.00 m/z
Skim 1	-25.3 Volt	Cap Exit Offset	-70.6 Volt	Trap Drive	45.5
Accumulation Time	20000 µs	Averages	10 Spectra		

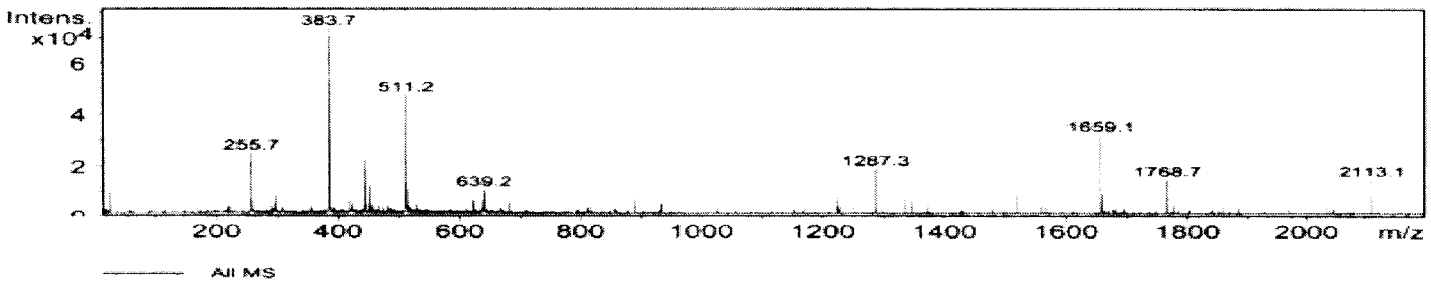

Index	Mass	Intensity	Width	S/N
1	24.13	8963.00	0.11	95.86
2	255.75	26512.00	0.38	283.56
3	294.44	8358.00	0.34	89.39
4	294.93	8190.00	0.16	87.60
5	383.65	81120.00	0.43	867.62
6	384.17	77446.00	0.47	828.33
7	443.38	23607.00	0.35	252.49
8	444.06	11652.00	0.29	124.62
9	451.23	12122.00	0.34	129.65
10	510.40	10445.00	0.20	111.71
11	511.17	51598.00	0.54	551.87
12	512.11	24210.00	0.52	258.94
13	513.06	10087.00	0.39	107.89
14	638.94	8652.00	0.32	92.54
15	639.24	10577.00	0.28	113.13
16	640.53	9293.00	0.18	99.39
17	1287.33	19831.00	0.12	212.10
18	1522.57	9575.00	0.18	102.41
19	1592.86	9999.00	0.22	106.94
20	1659.06	34637.00	0.22	370.46
21	1660.23	8140.00	0.32	87.06
22	1660.58	8387.00	0.16	89.70

Figure 65: Mass spectrum of **23**

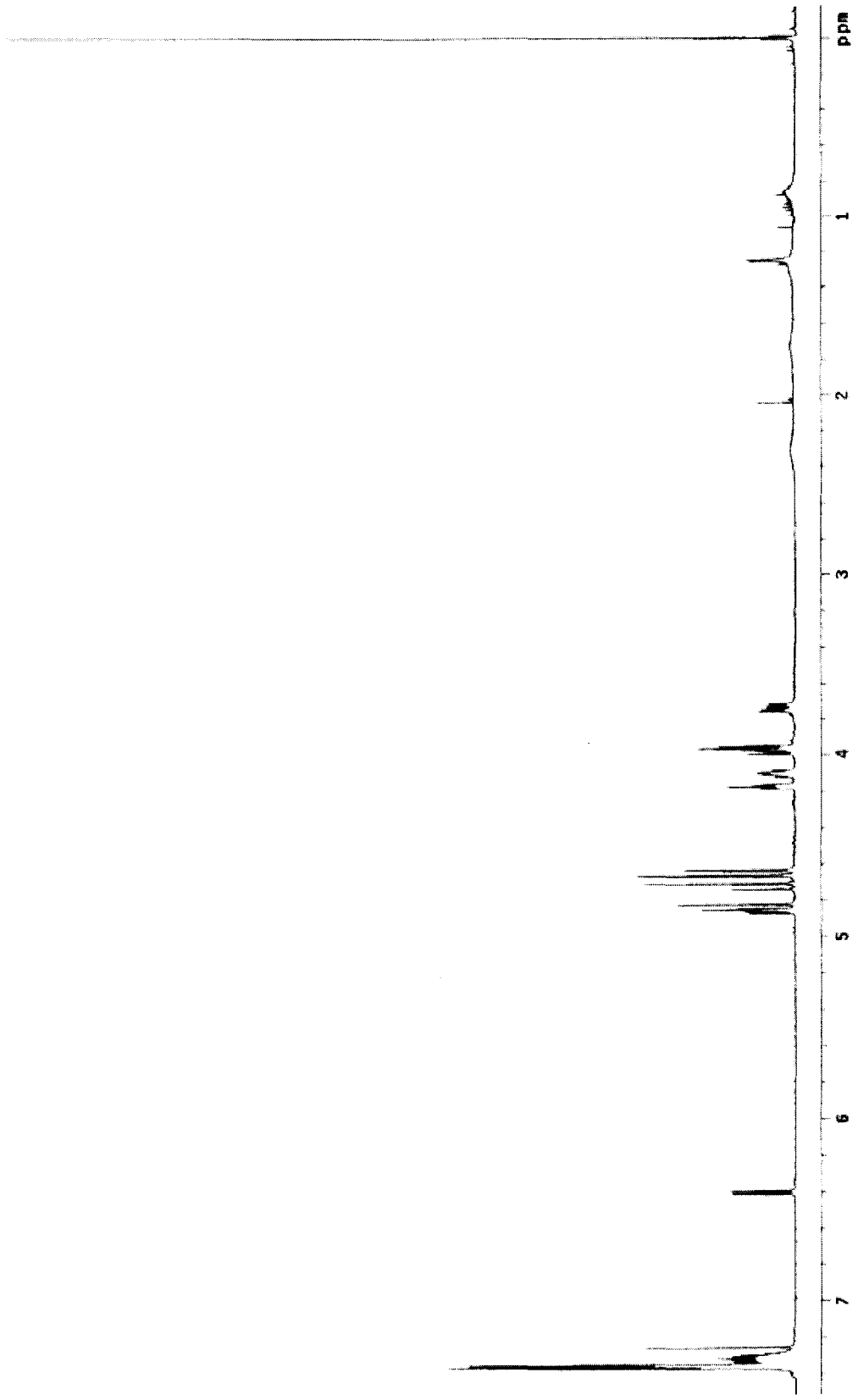

Figure 66: ^{1}H NMR spectrum of **24**

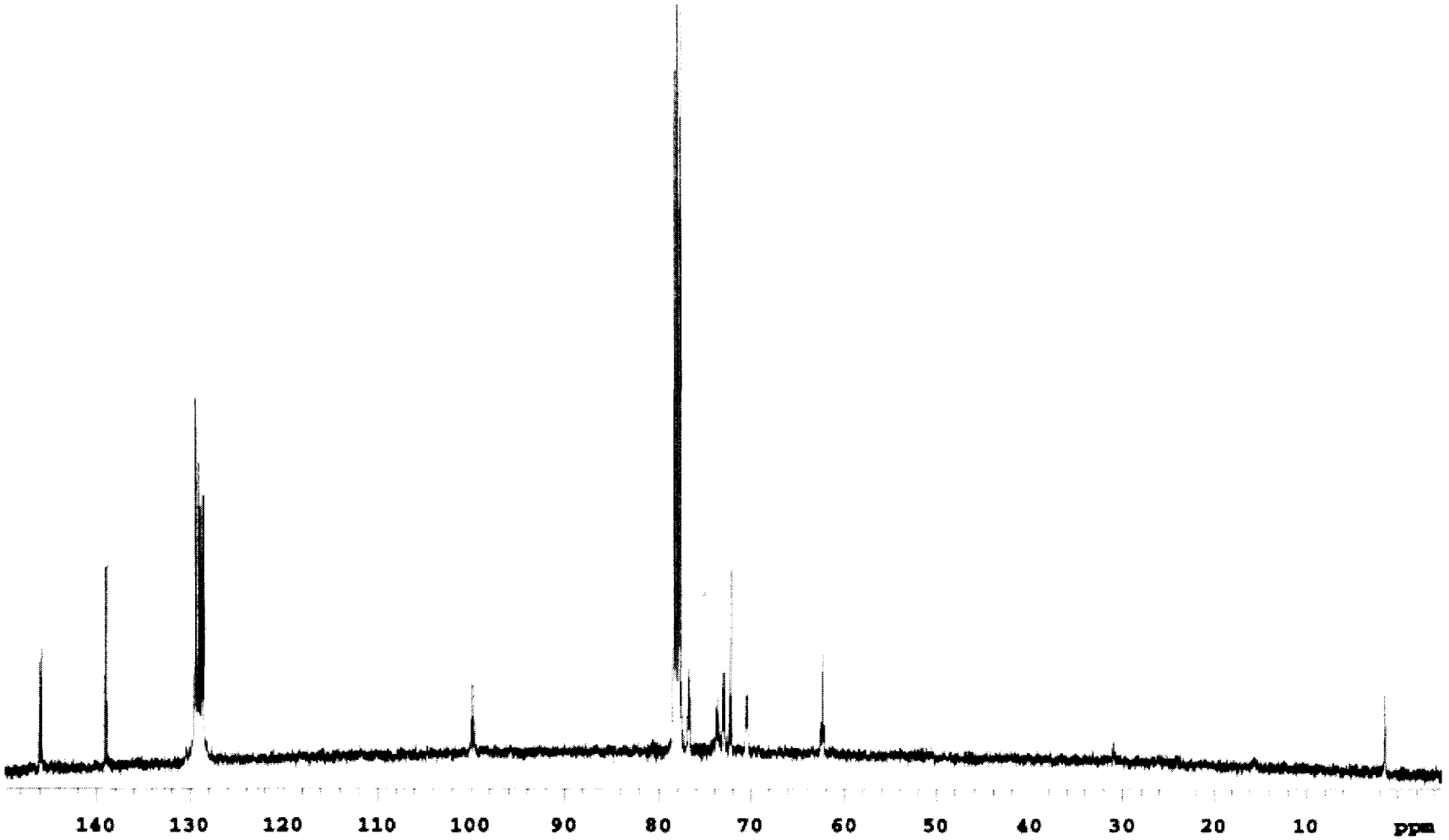

Figure 67: ^{13}C NMR spectrum of **24**

Acquisition Parameter

Ion Source Type	ESI	Ion Polarity	Positive		
Mass Range Mode	Std/Normal	Scan Begin	15.00 m/z	Scan End	2200.00 m/z
Skim 1	25.0 Volt	Cap Exit Offset	76.0 Volt	Trap Drive	41.0
Accumulation Time	1947 µs	Averages	10 Spectra		

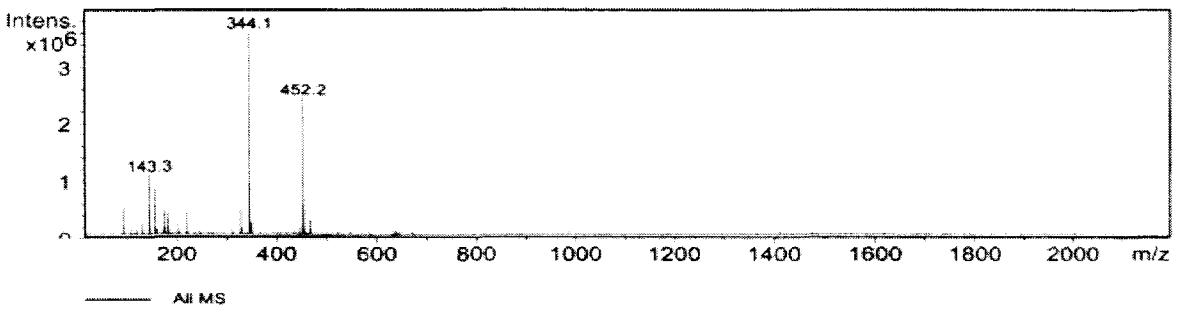

Index	Mass	Intensity	Width	S/N
1	91.32	536215.00	0.37	314.85
2	129.28	202096.00	0.42	118.66
3	143.27	1155931.00	0.40	678.73
4	144.25	161185.00	0.37	94.64
5	145.26	164962.00	0.41	96.86
6	155.23	897285.00	0.38	526.86
7	173.26	494558.00	0.39	290.39
8	181.24	406802.00	0.38	238.86
9	183.17	154992.00	0.38	91.01
10	201.23	268902.00	0.36	157.89
11	219.18	469805.00	0.37	275.85
12	327.15	595039.00	0.44	349.39
13	344.13	3978651.00	0.45	2336.14
14	344.99	993401.00	0.36	583.29
15	349.16	239789.00	0.34	140.78
16	445.32	192974.00	0.18	113.31
17	452.16	2662878.00	0.55	1563.56
18	453.04	811600.00	0.40	476.55
19	454.04	155033.00	0.40	91.03
20	486.14	273089.00	0.45	160.35

Figure 68: Mass spectrum of **24**

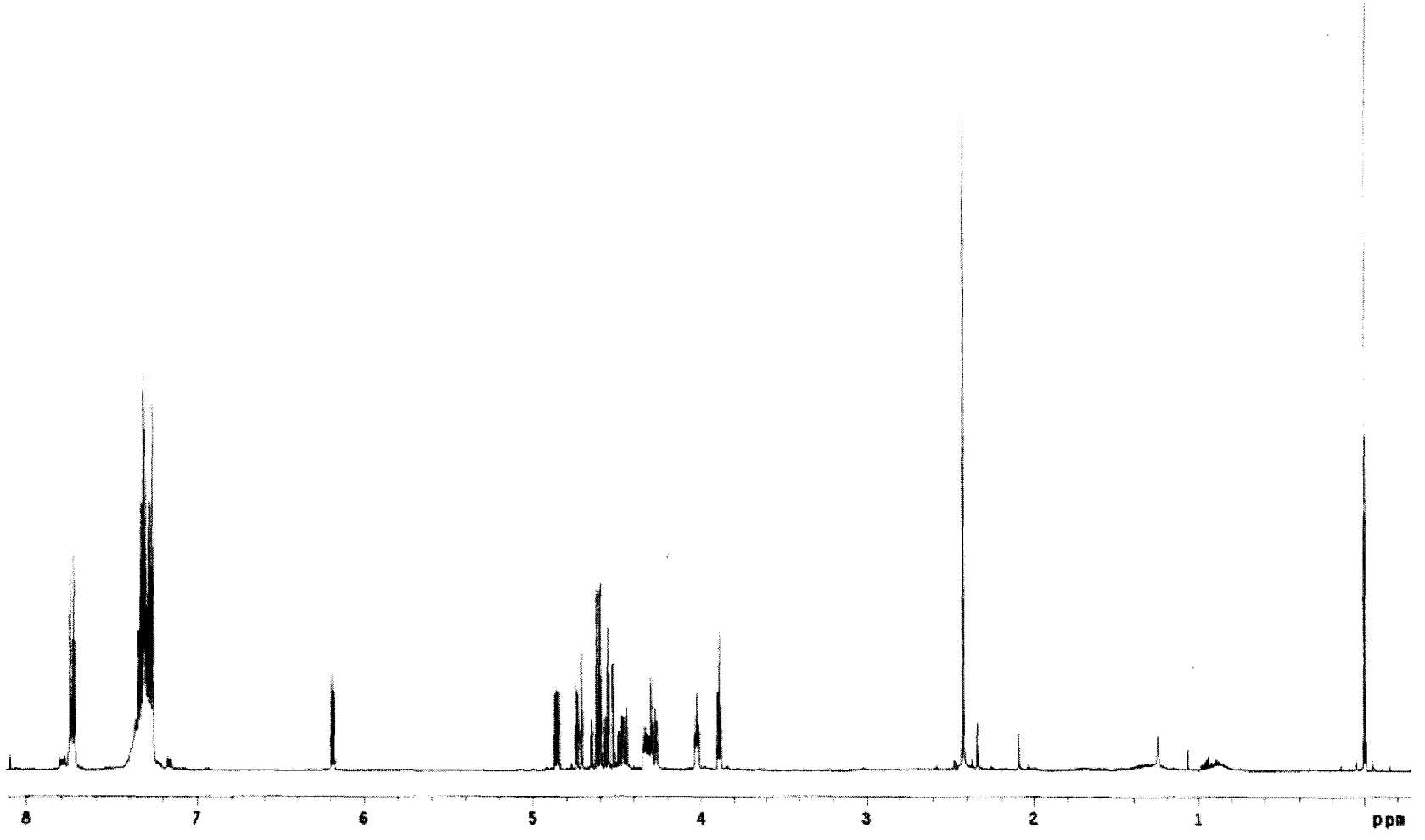

Figure 69: ^{1}H NMR spectrum of **25**

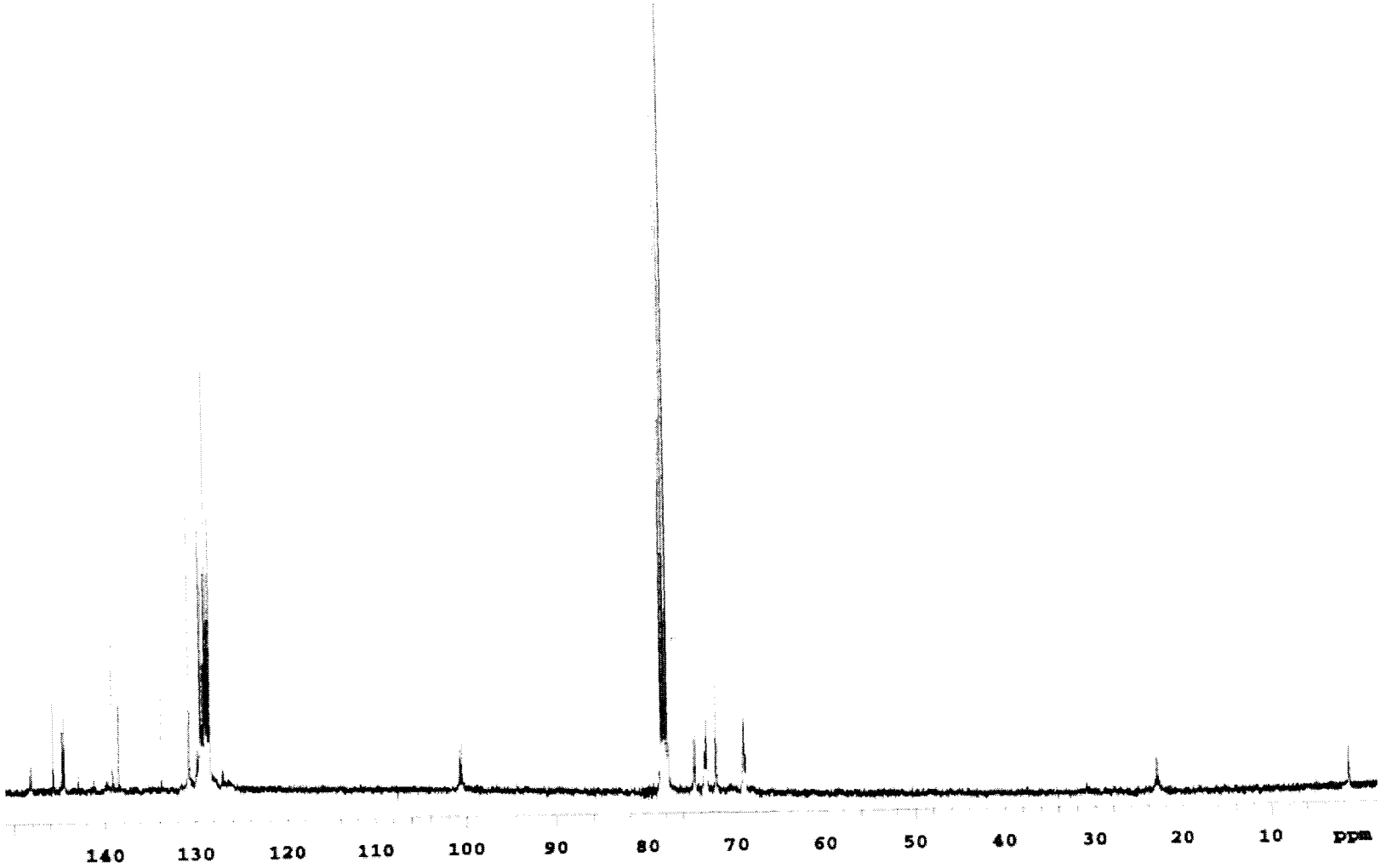

Figure 70: ^{13}C NMR spectrum of **25**

Acquisition Parameter

Ion Source Type	ESI	Ion Polarity	Positive		
Mass Range Mode	Std/Normal	Scan Begin	15.00 m/z	Scan End	2200.00 m/z
Skim 1	21.0 Volt	Cap Exit Offset	77.0 Volt	Trap Drive	40.0
Accumulation Time	471 µs	Averages	10 Spectra		

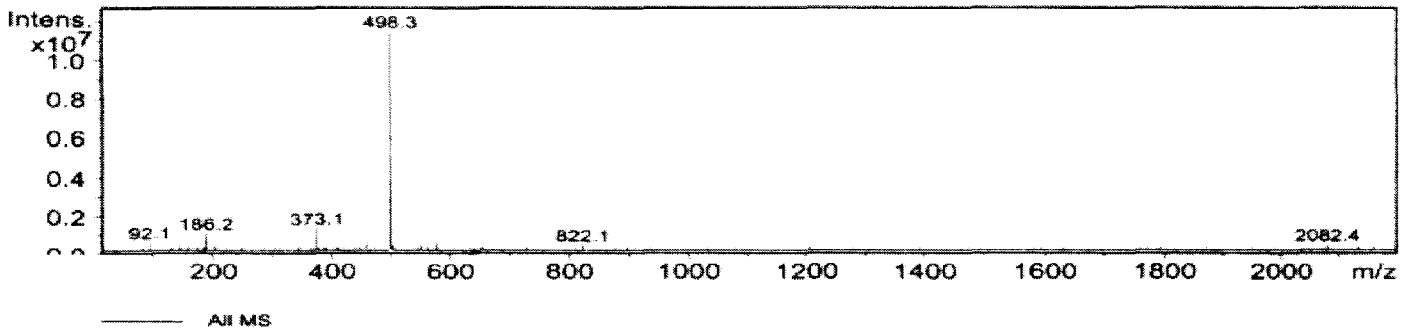

Index	Mass	Intensity	Width	S/N
1	92.07	458819.00	0.24	19.07
2	143.07	280723.00	0.33	11.67
3	186.24	992684.00	0.35	41.26
4	343.05	280782.00	0.20	11.67
5	373.11	1289129.00	0.38	53.59
6	374.13	276051.00	0.36	11.47
7	456.32	477431.00	0.05	19.85
8	498.29	12610374.00	0.40	524.18
9	499.16	3979201.00	0.37	165.41
10	500.19	1323573.00	0.37	55.02
11	501.21	320712.00	0.35	13.33
12	549.27	303654.00	0.44	12.62
13	560.28	316347.00	0.45	13.15
14	576.31	485386.00	0.38	20.18
15	822.13	287815.00	0.11	11.96
16	2082.38	304191.00	0.17	12.64

Figure 71: Mass spectrum of **25**

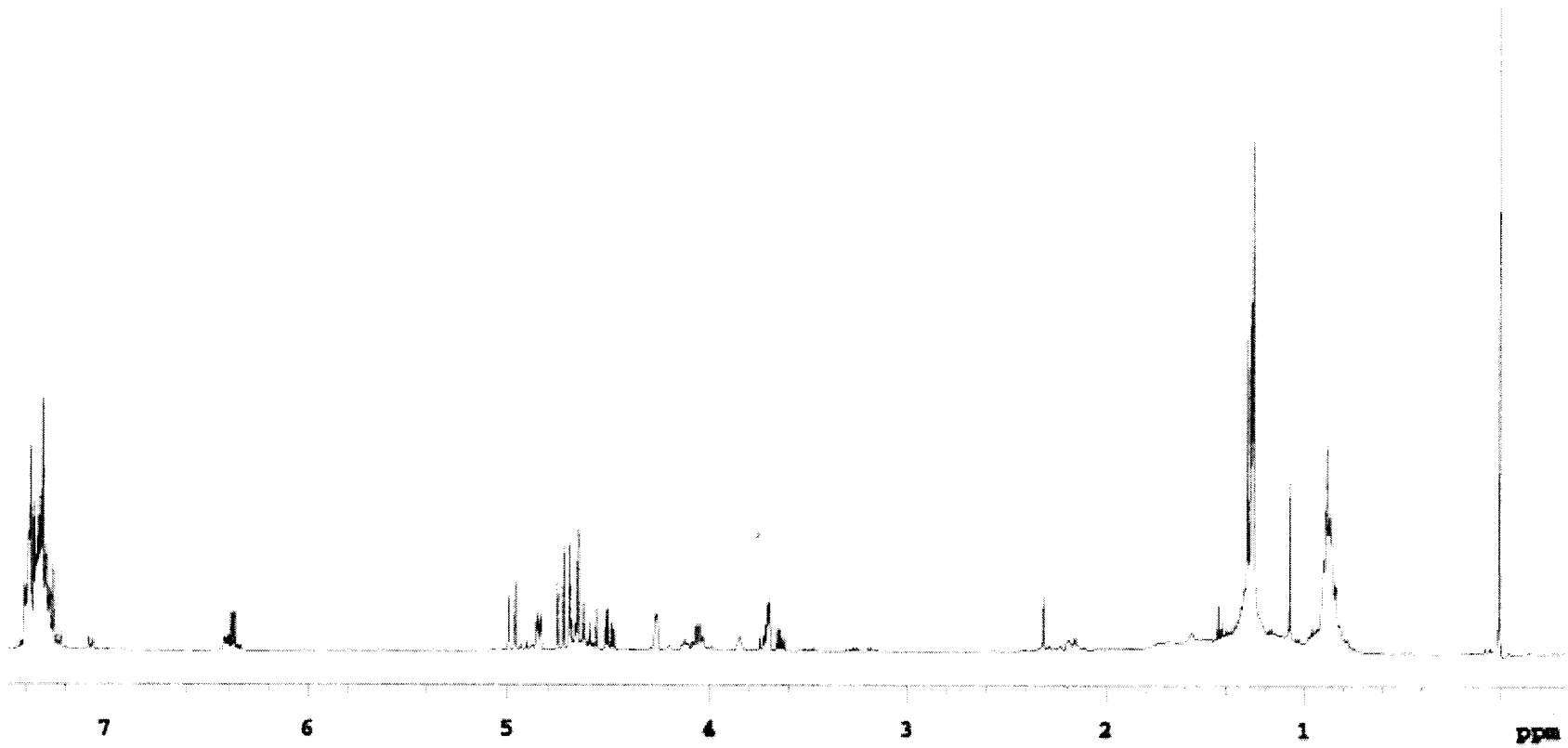

Figure 72: ^{1}H NMR spectrum of **26**

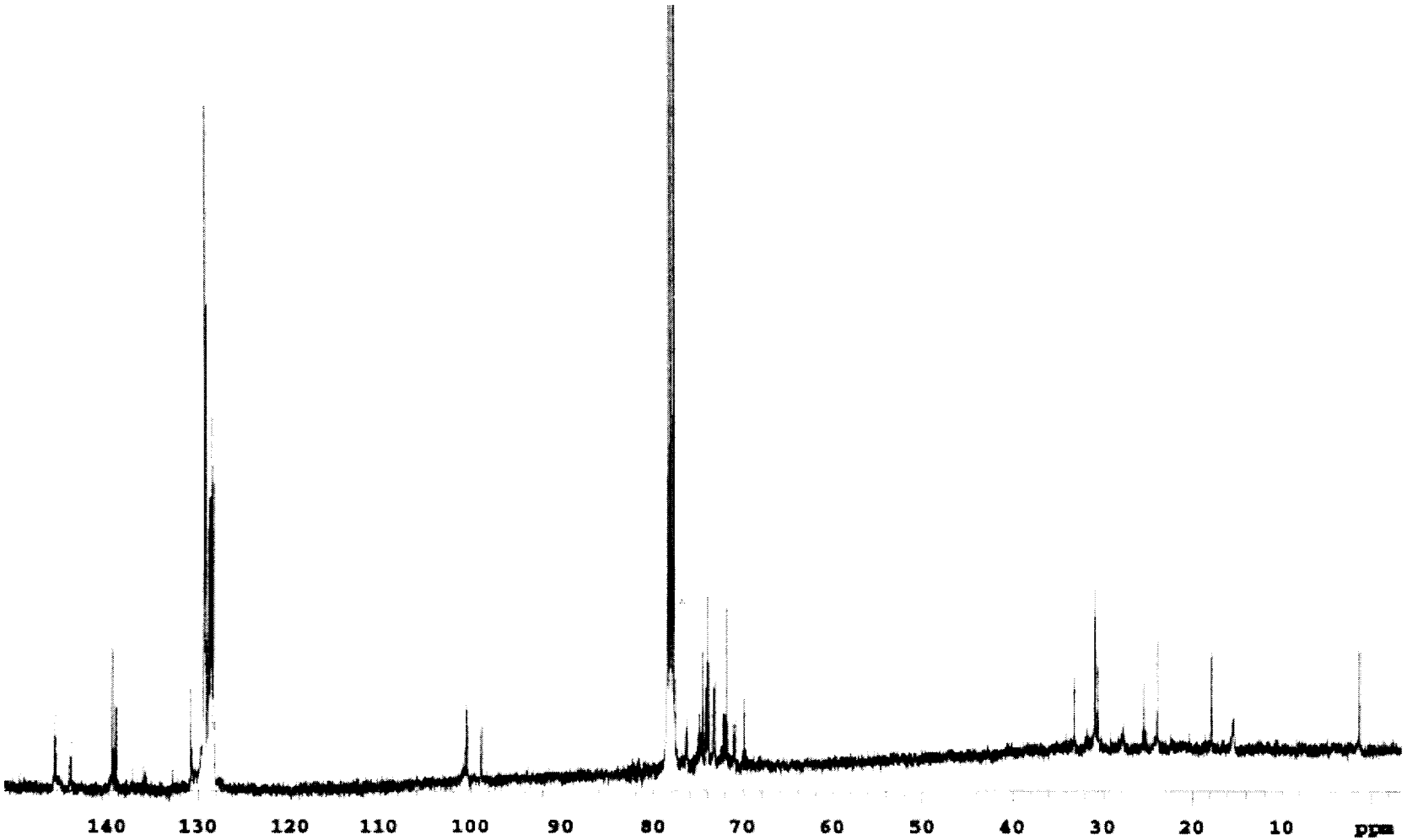

Figure 73: ^{13}C NMR spectrum of **26**

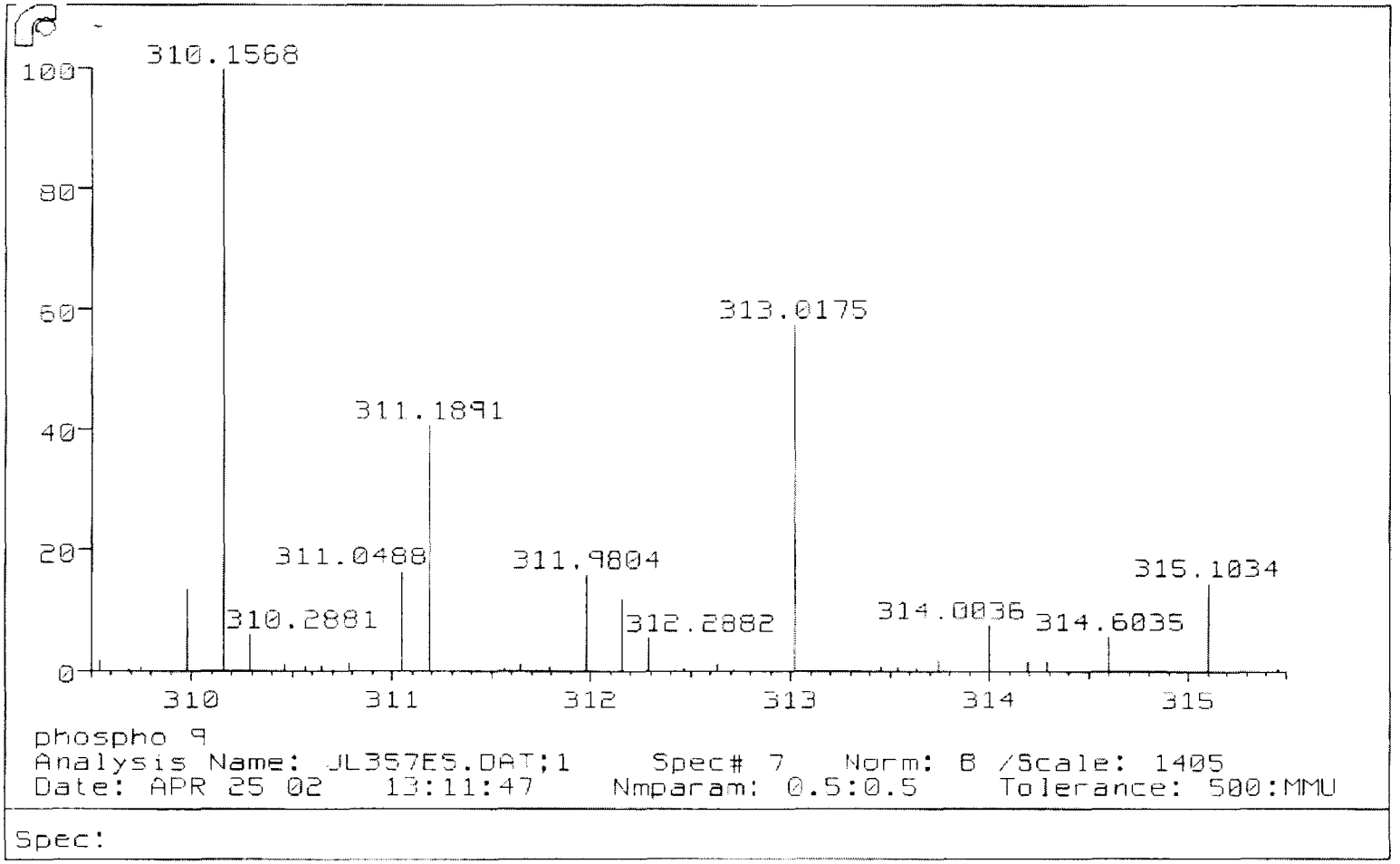

Figure 74: Mass spectrum of **26**

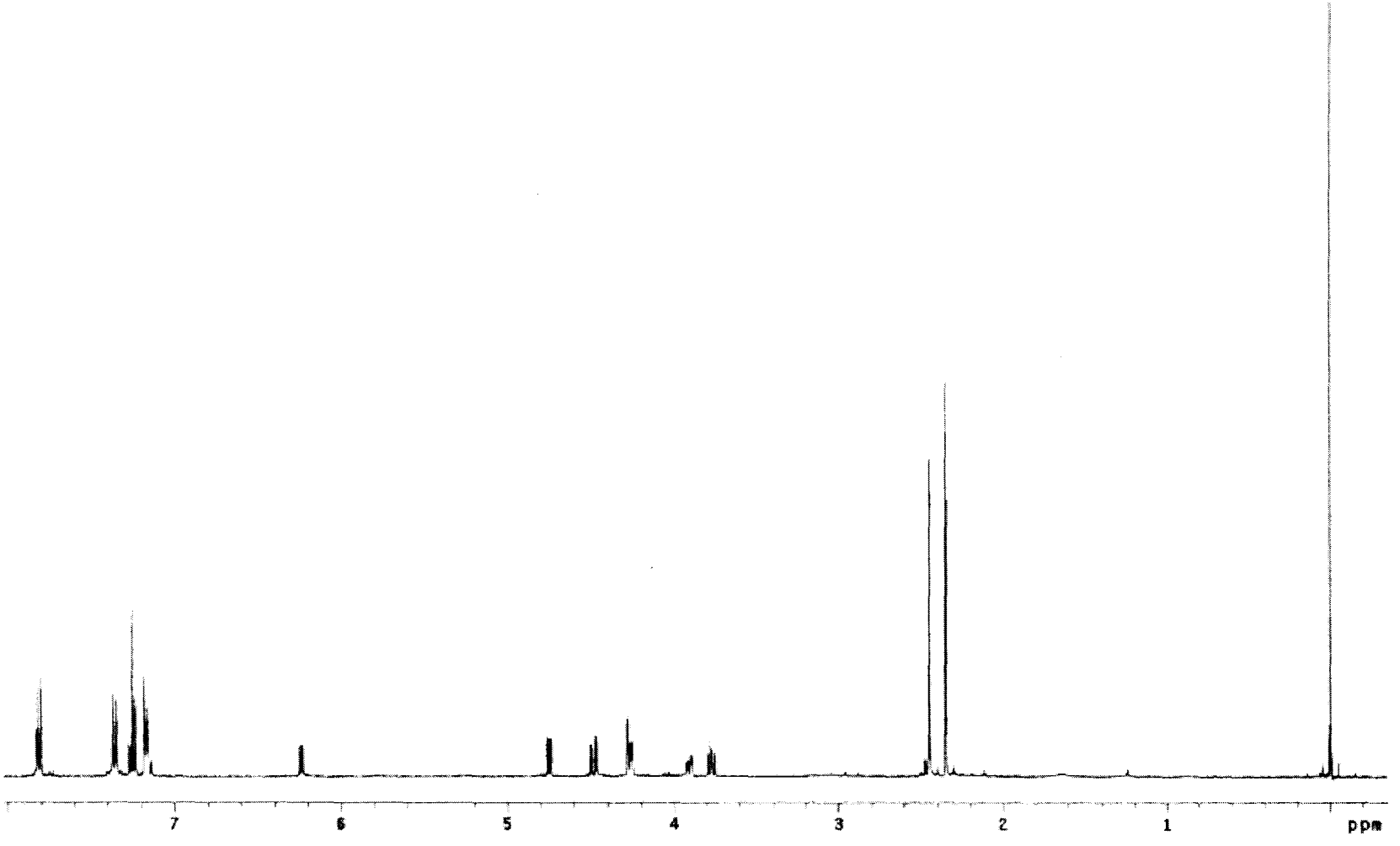

Figure 75: ^{1}H NMR spectrum of **27**

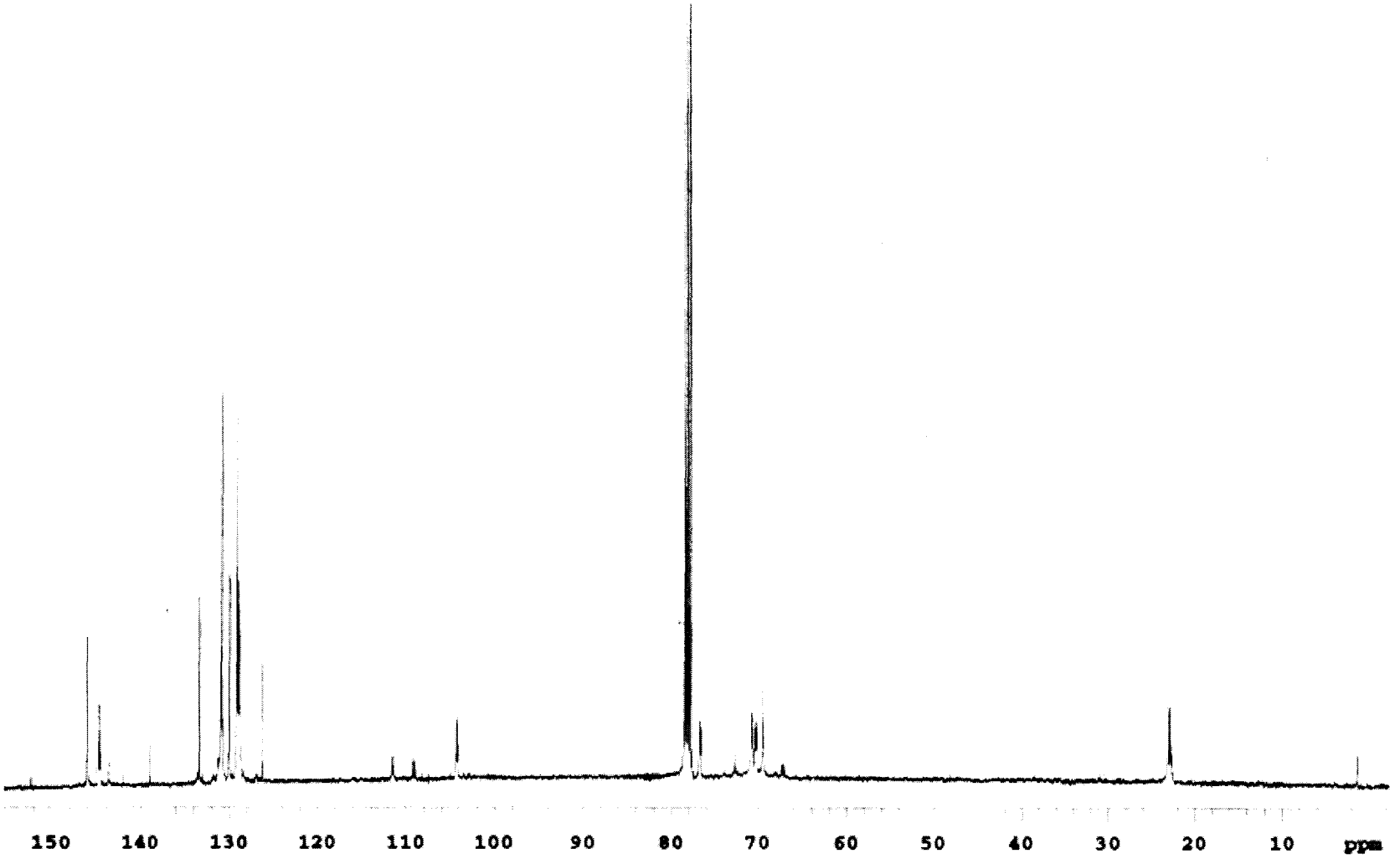

Figure 76: ^{13}C NMR spectrum of **27**

Acquisition Parameter

Ion Source Type	APCI	Ion Polarity	Positive		
Mass Range Mode	Std/Normal	Scan Begin	15.00 m/z	Scan End	2200.00 m/z
Skim 1	20.0 Volt	Cap Exit Offset	77.0 Volt	Trap Drive	30.0
Accumulation Time	20000 µs	Averages	10 Spectra		

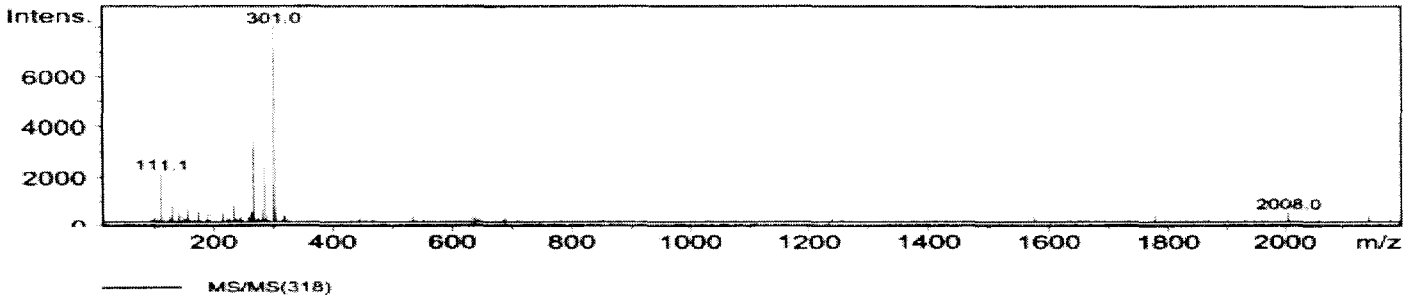

Index	Mass	Intensity	Width	S/N
1	111.09	2225.00	0.16	49.88
2	129.06	715.00	0.23	16.03
3	139.02	391.00	0.07	8.77
4	145.15	354.00	0.21	7.94
5	155.02	608.00	0.04	13.63
6	173.22	455.00	0.03	10.20
7	190.01	404.00	0.27	9.06
8	213.92	449.00	0.03	10.07
9	232.94	779.00	0.18	17.46
10	261.21	448.00	0.05	10.04
11	264.43	784.00	0.12	17.58
12	265.03	3711.00	0.25	83.19
13	266.18	466.00	0.27	10.45
14	281.86	521.00	0.31	11.68
15	283.02	2506.00	0.31	56.22
16	300.08	1716.00	0.19	38.47
17	301.01	8799.00	0.31	197.25
18	301.96	661.00	0.23	14.82
19	319.22	303.00	0.05	6.79
20	2008.02	437.00	0.03	9.80

Figure 77: Mass spectrum of **27**

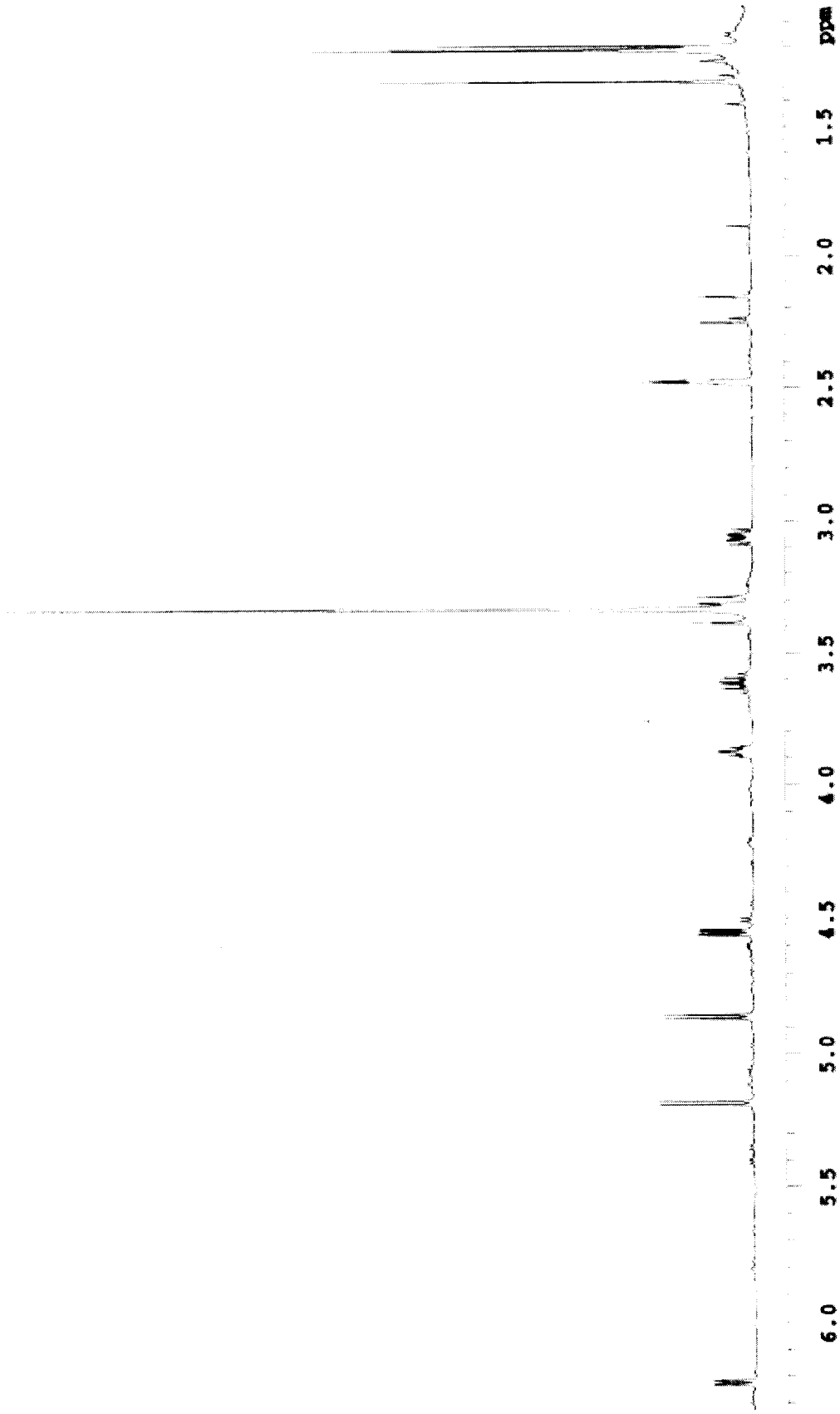

Figure 78: ^{1}H NMR spectrum of **28**

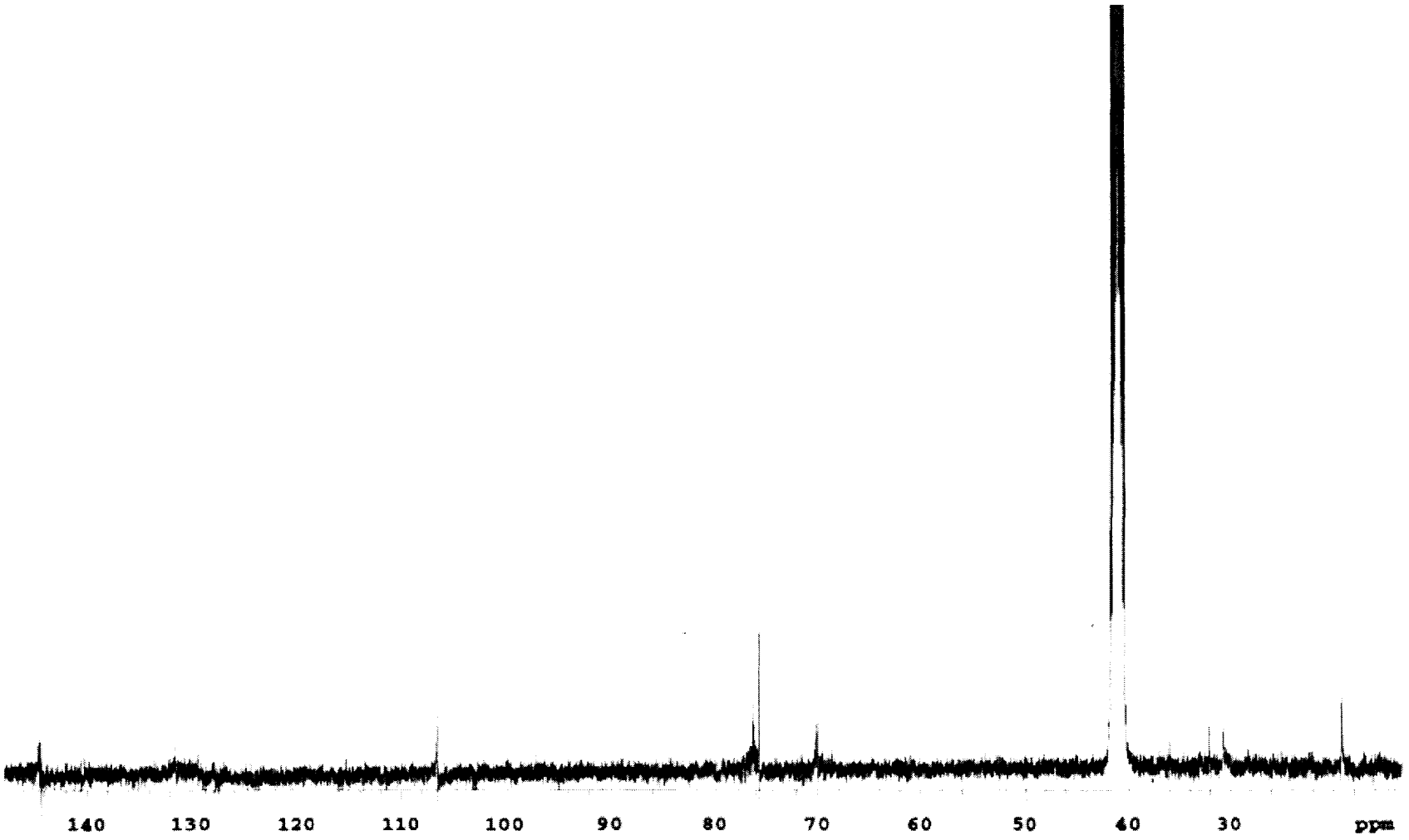

Figure 79: ^{13}C NMR spectrum of **28**

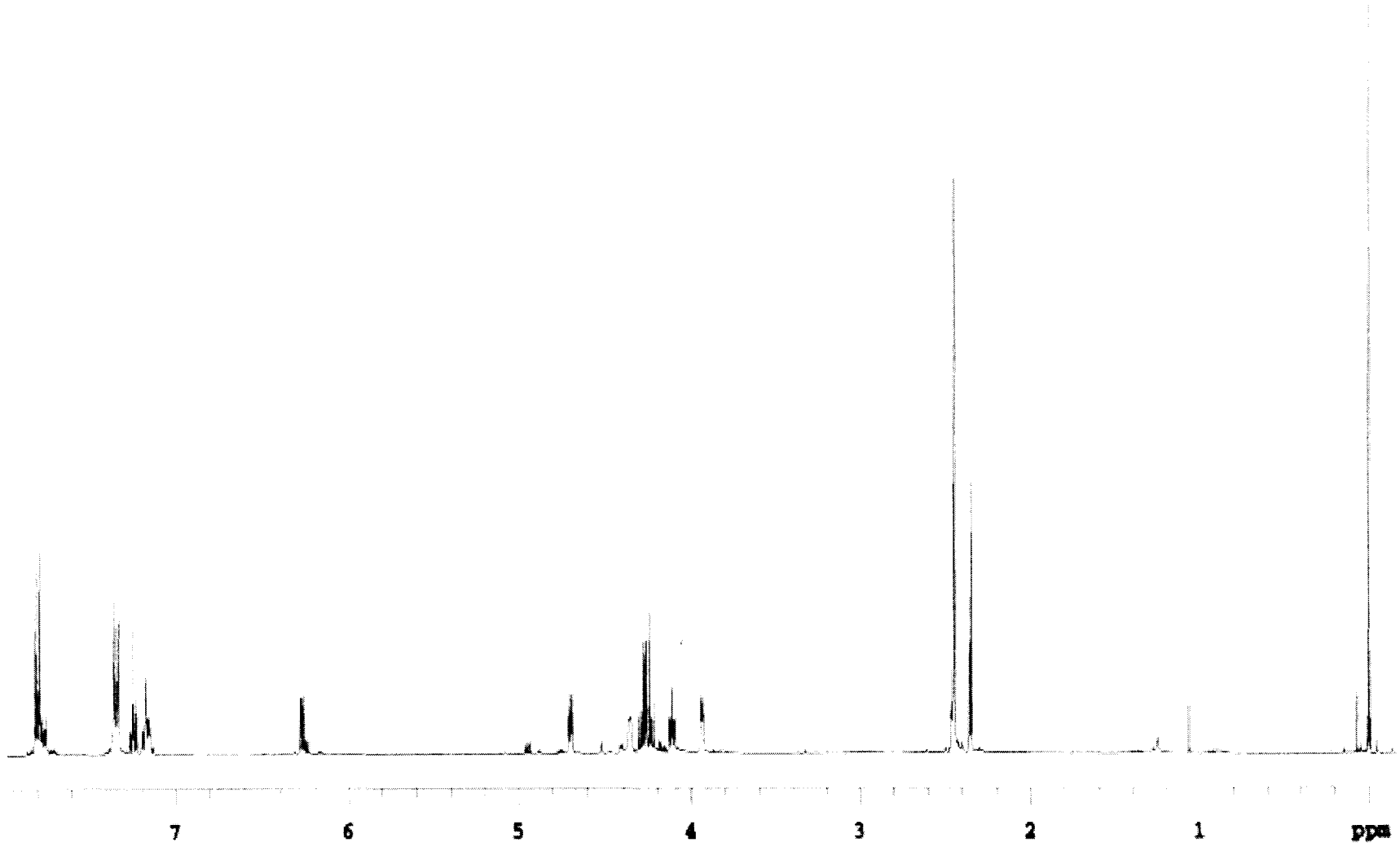

Figure 80: ^{1}H NMR spectrum of **29**

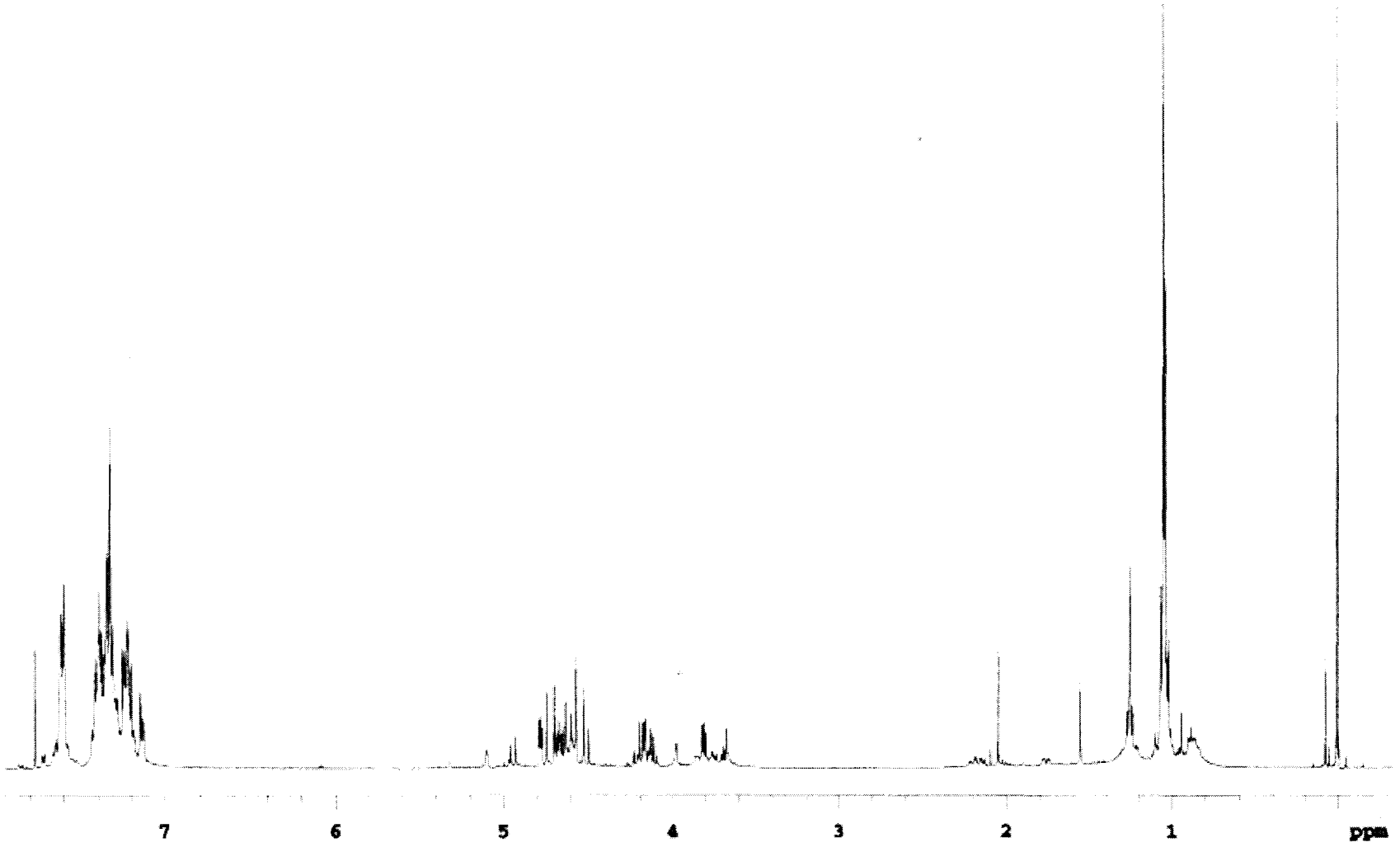

Figure 81: ^{1}H NMR spectrum of **31**

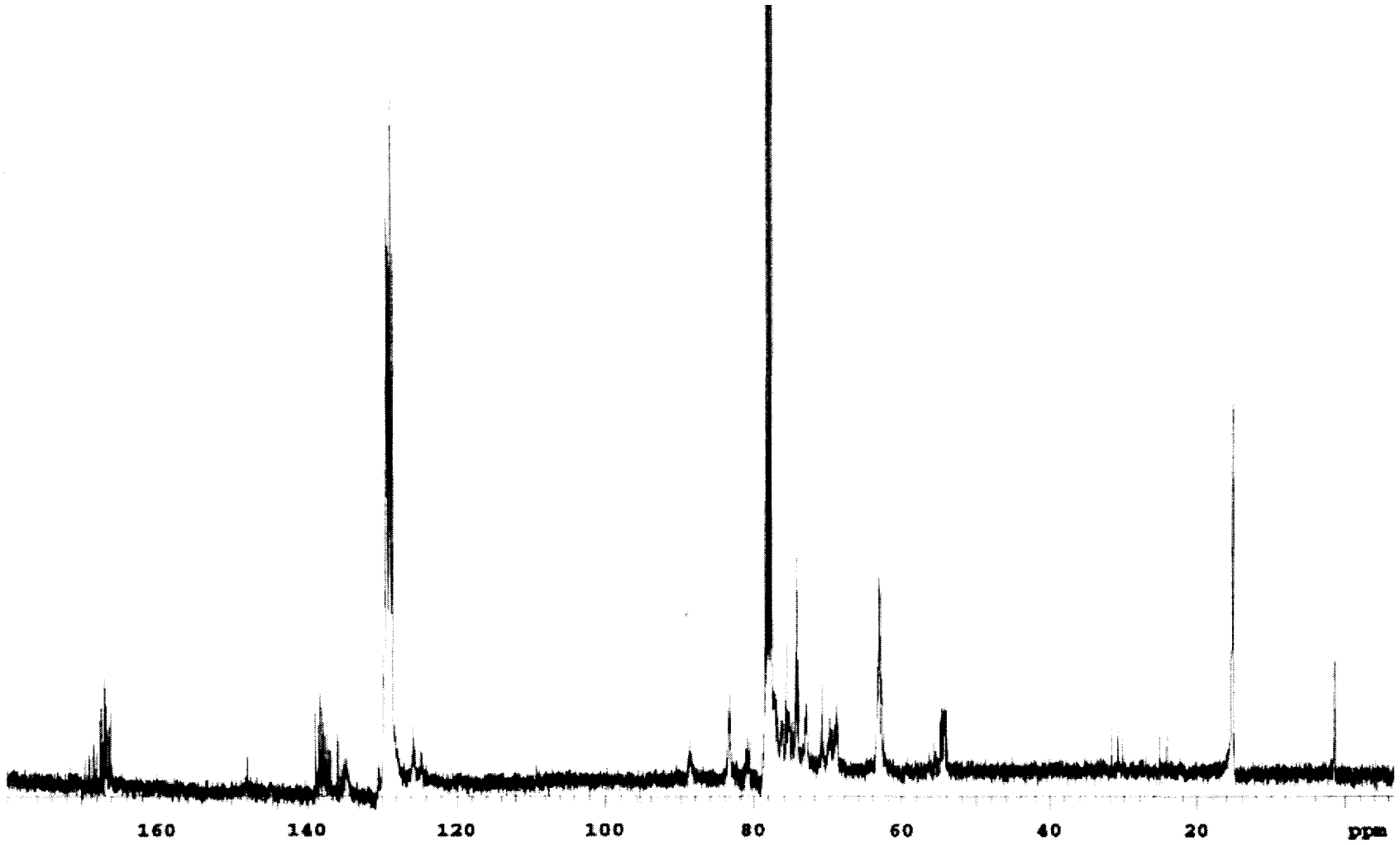

Figure 82: ^{13}C NMR spectrum of **31**

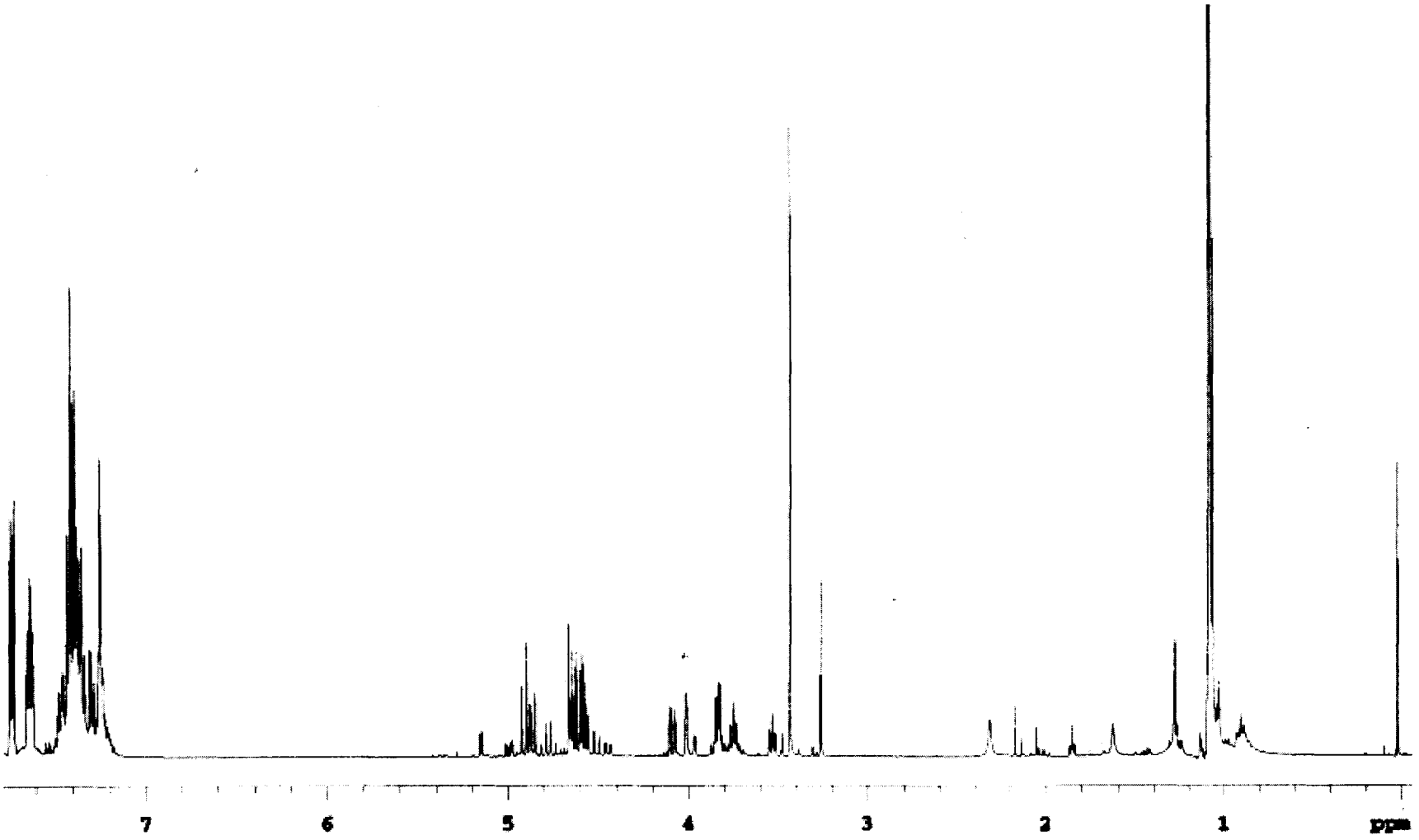

Figure 83: ^{1}H NMR spectrum of **32**

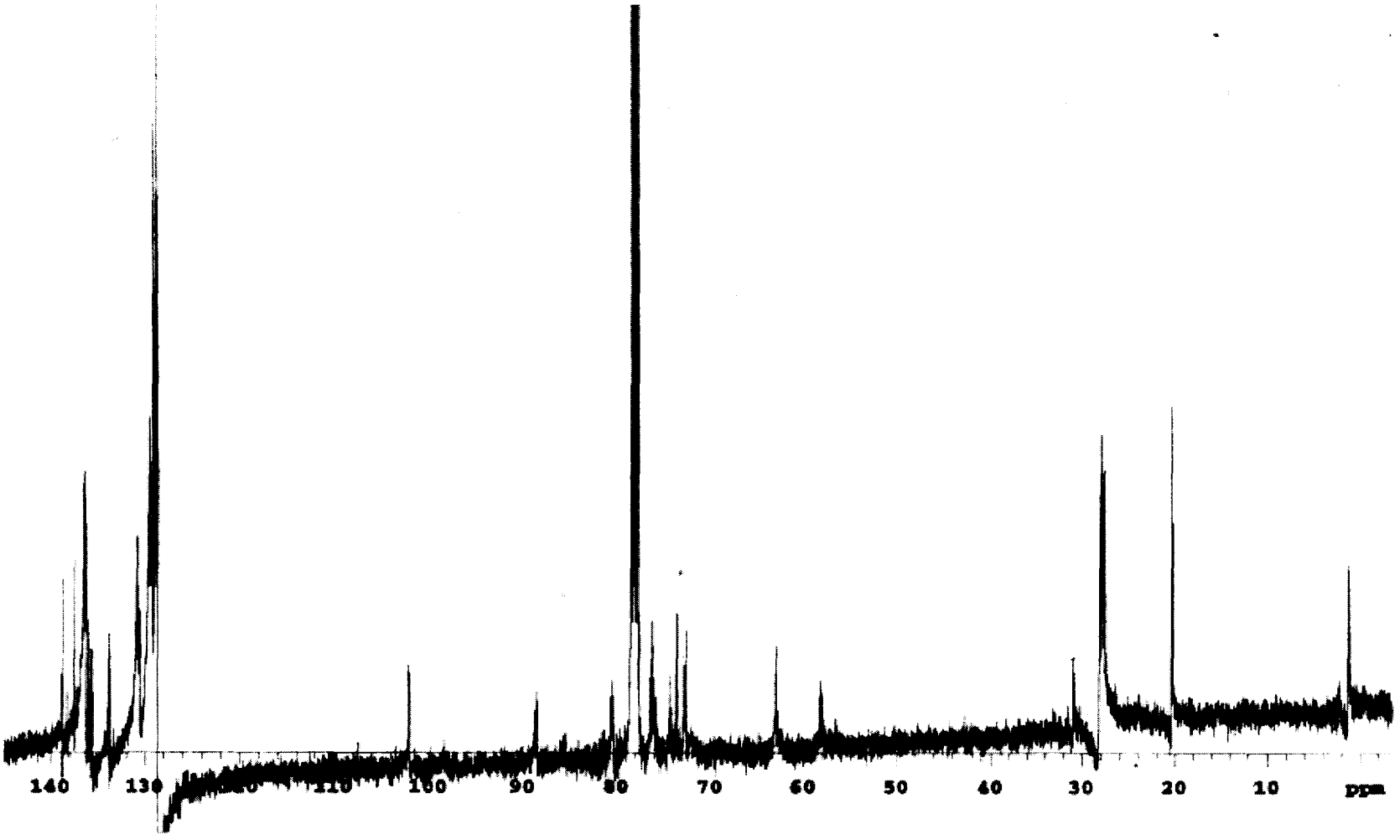

Figure 84: ^{13}C NMR spectrum of **32**

Acquisition Parameter

Ion Source Type	ESI	Ion Polarity	Positive		
Mass Range Mode	Std/Normal	Scan Begin	15.00 m/z	Scan End	2200.00 m/z
Skim 1	25.0 Volt	Cap Exit Offset	77.0 Volt	Trap Drive	40.0
Accumulation Time	1925 µs	Averages	10 Spectra		

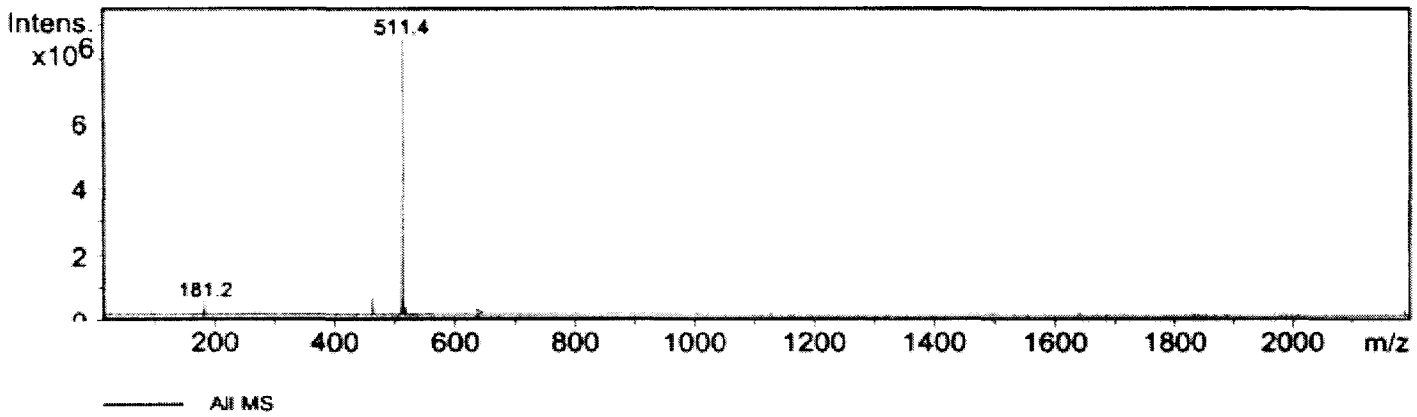

Index	Mass	Intensity	Width	S/N
1	181.22	463927.00	0.39	443.16
2	462.34	558829.00	0.57	533.81
3	463.32	215309.00	0.23	205.67
4	511.44	9420358.00	0.56	8998.69
5	512.91	569907.00	0.45	544.40
6	516.41	251166.00	0.37	239.92

Figure 85: Mass spectrum of **32**

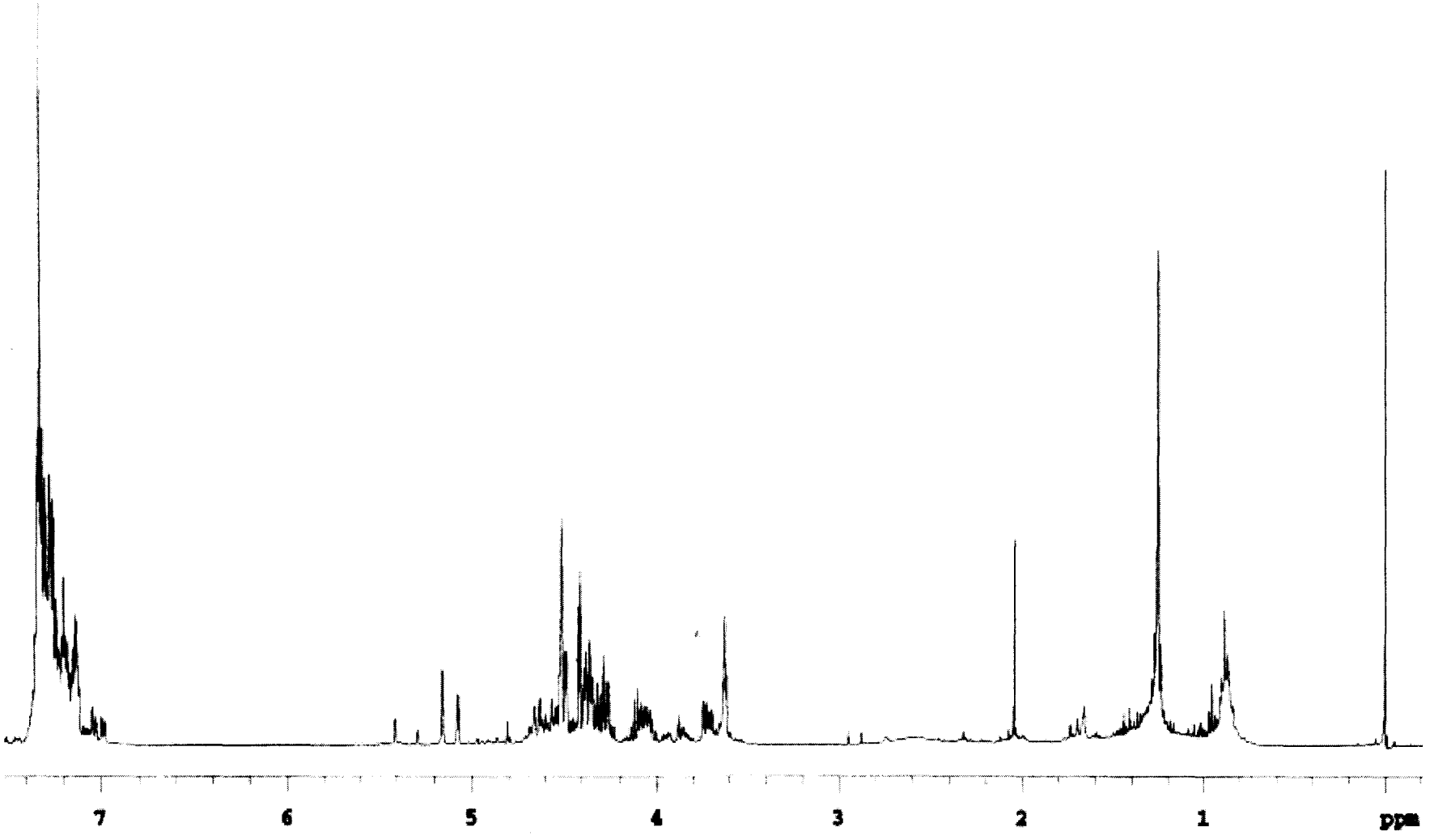

Figure 86: ^{1}H NMR spectrum of **36**

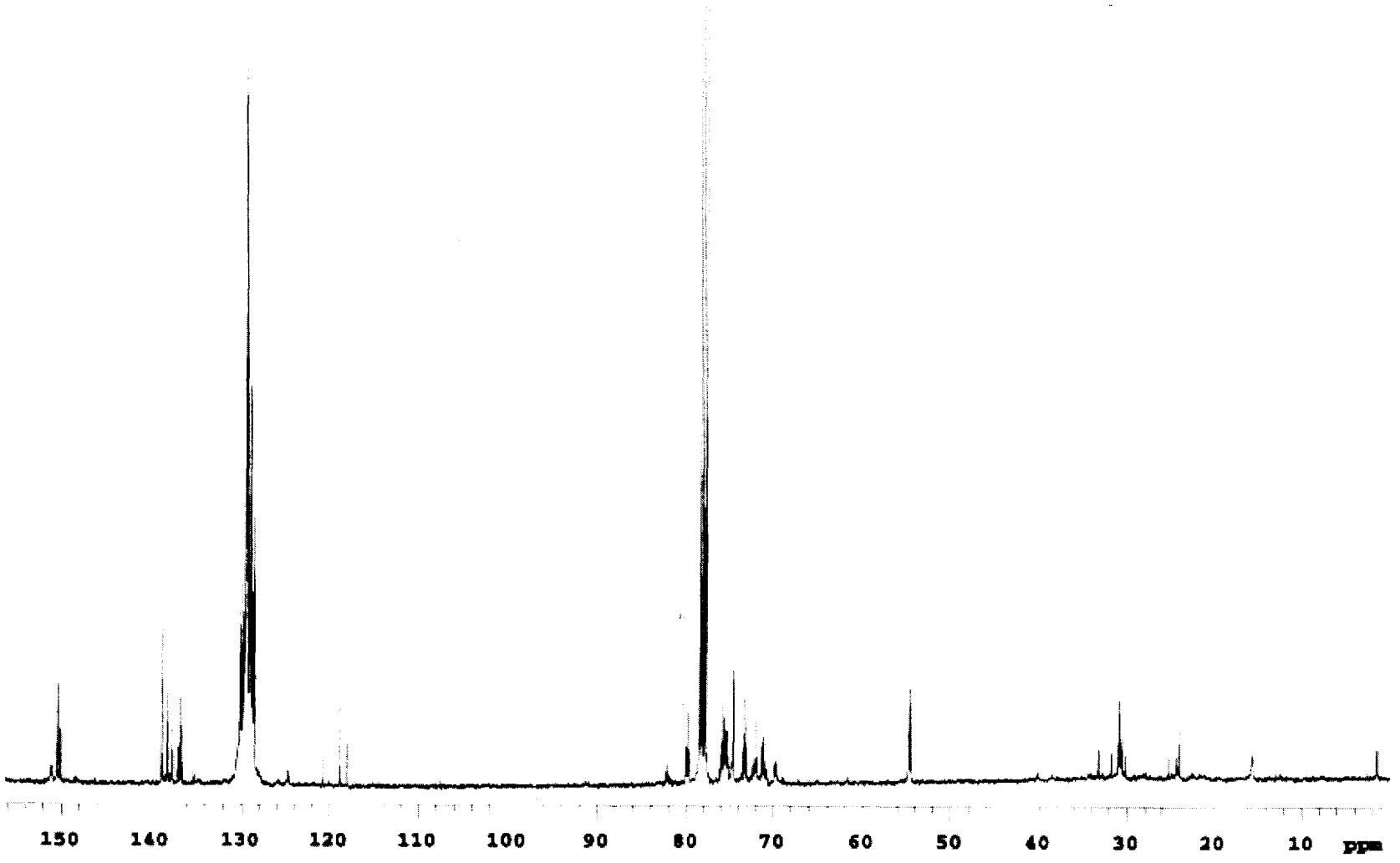

Figure 87: ^{13}C NMR spectrum of **36**

Acquisition Parameter

Ion Source Type	ESI	Ion Polarity	Positive		
Mass Range Mode	Std/Normal	Scan Begin	15.00 m/z	Scan End	2200.00 m/z
Skim 1	32.0 Volt	Cap Exit Offset	77.0 Volt	Trap Drive	45.0
Accumulation Time	1369 µs	Averages	10 Spectra		

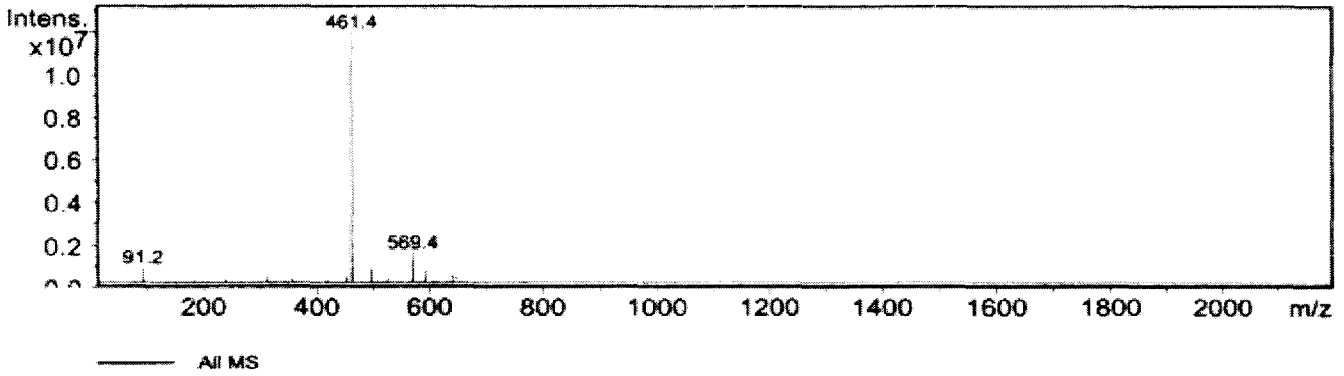

Index	Mass	Intensity	Width	S/N
1	91.25	819320.00	0.34	533.47
2	451.79	326916.00	0.52	212.86
3	461.36	13158106.00	0.34	8567.37
4	461.95	3839944.00	0.31	2500.22
5	463.01	722844.00	0.37	470.65
6	496.27	802052.00	0.35	522.22
7	569.35	1600507.00	0.39	1042.11
8	570.25	605493.00	0.35	394.24
9	591.38	637452.00	0.35	415.05
10	592.36	267393.00	0.36	174.10

Figure 88: Mass spectrum of **36**

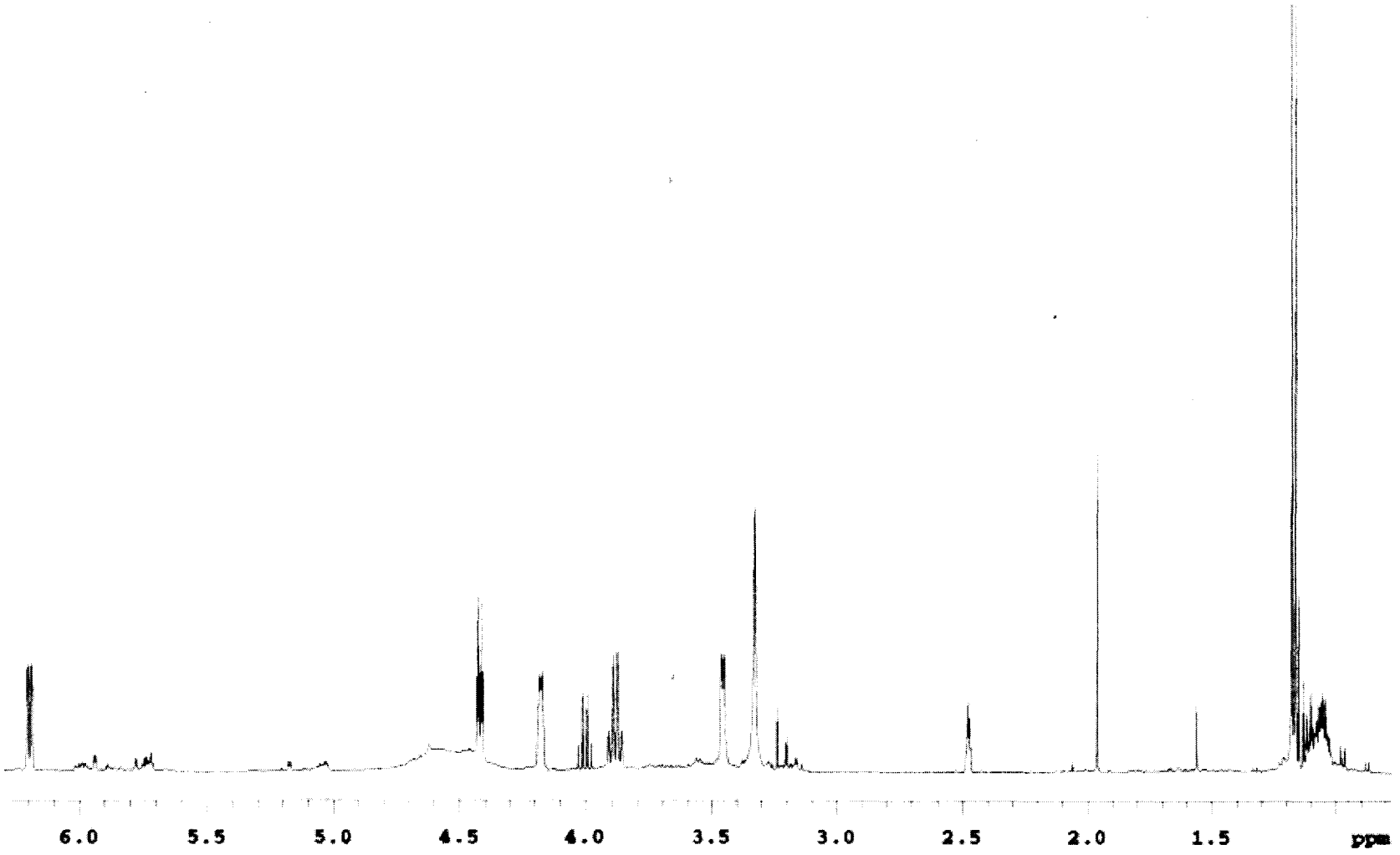

Figure 89: ^{1}H NMR spectrum of **40**

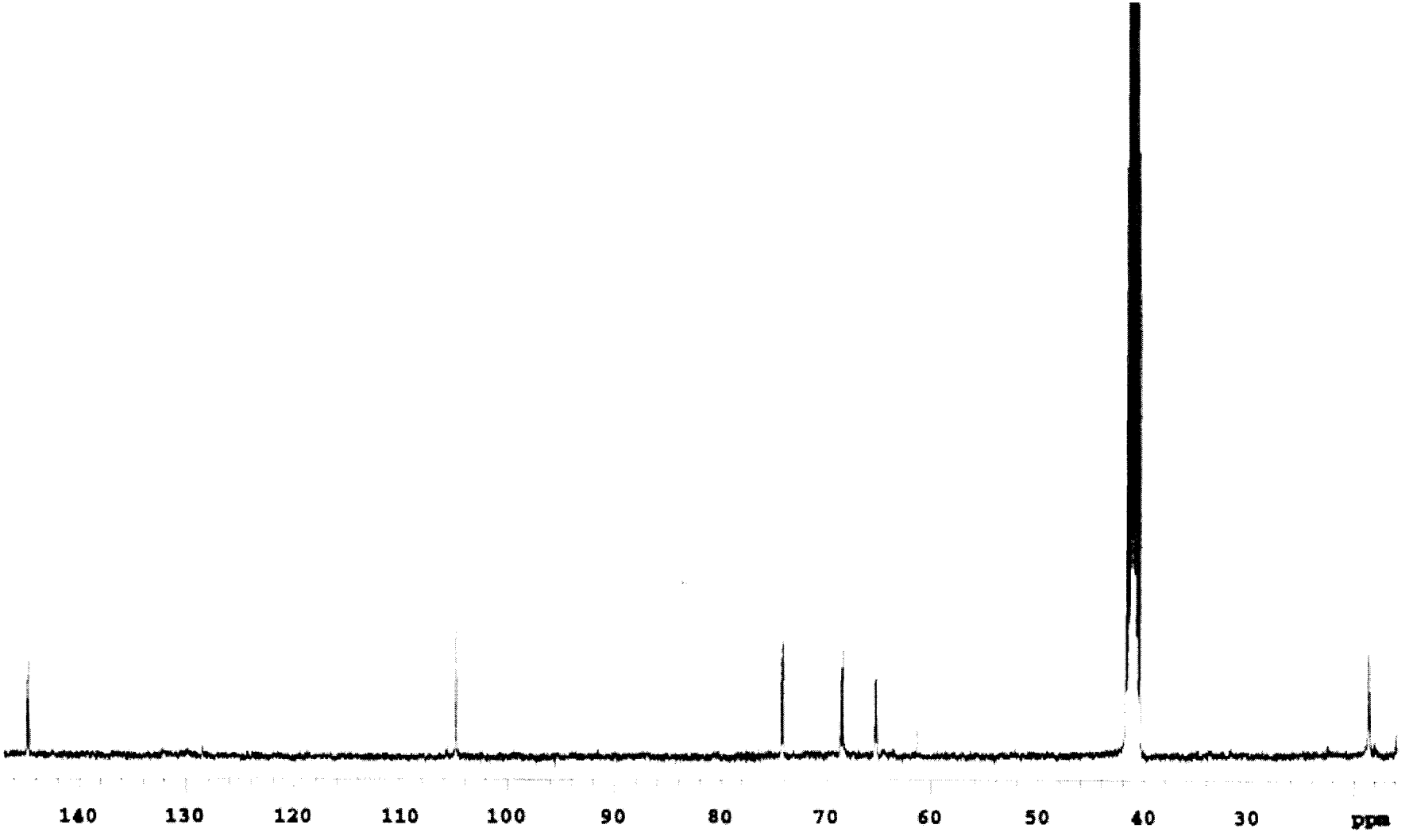

Figure 90: ^{13}C NMR spectrum of **40**

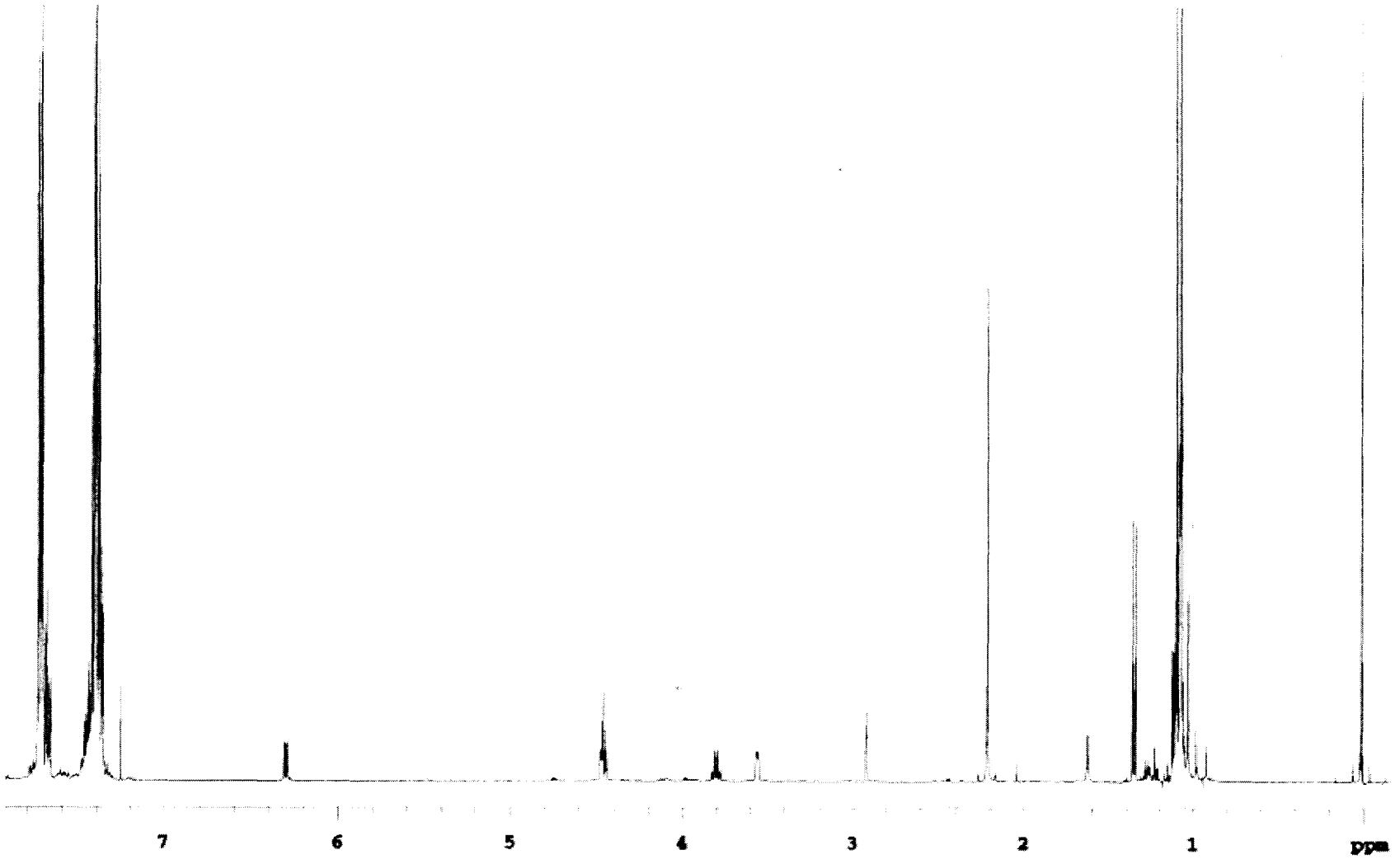

Figure 91: ^{1}H NMR spectrum of **41**

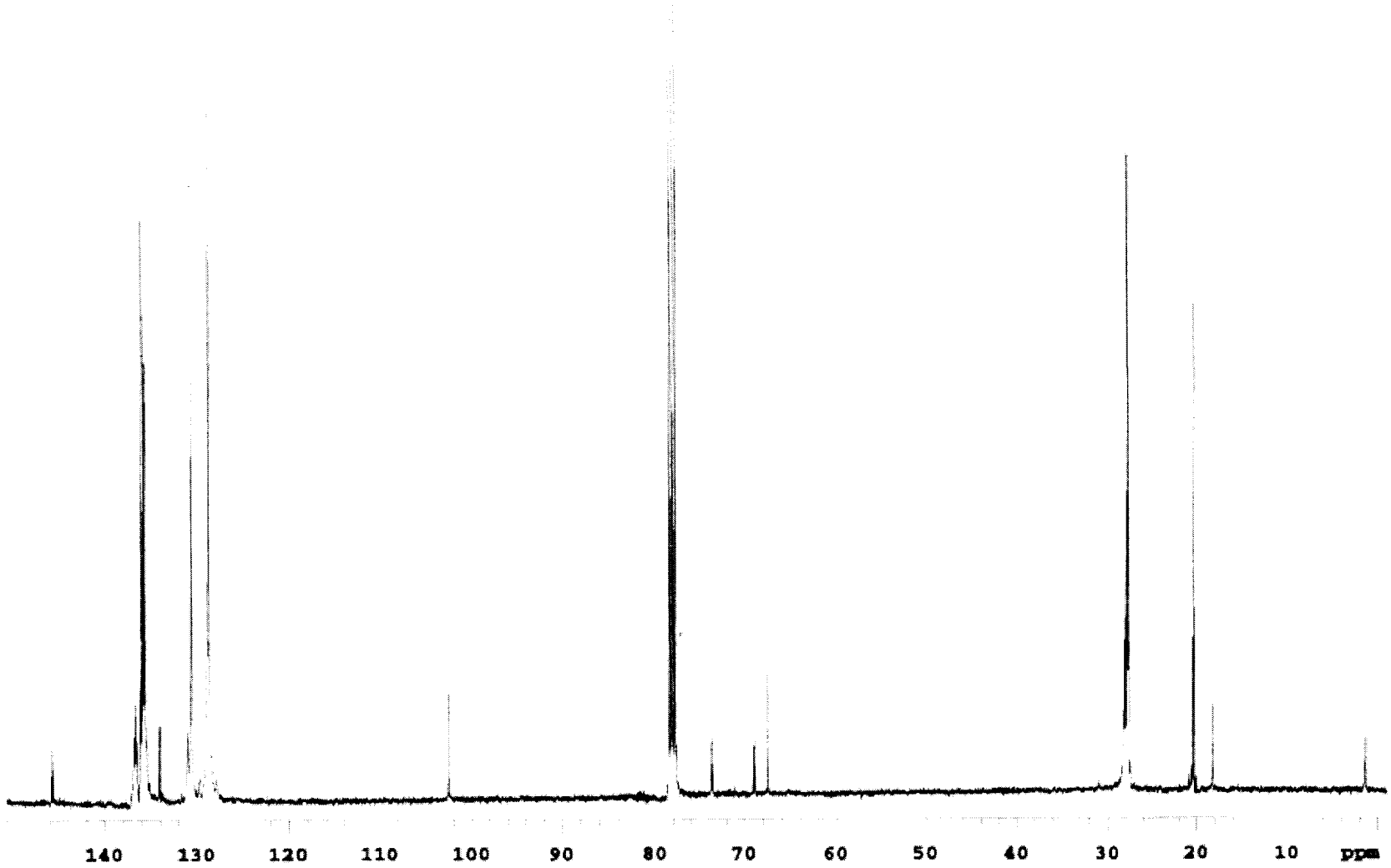

Figure 92: ^{13}C NMR spectrum of **41**

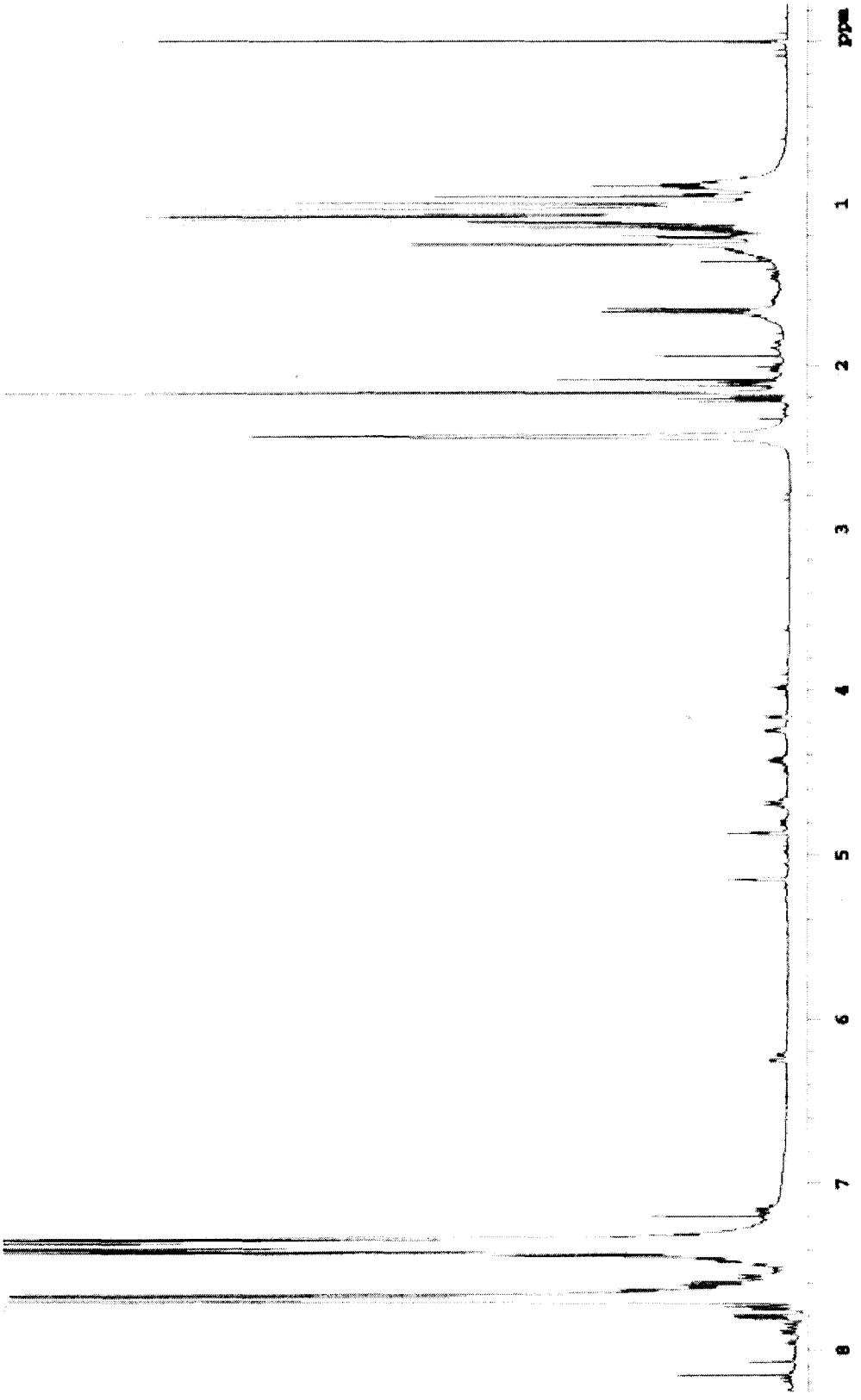

Figure 93: ^{1}H NMR spectrum of **38**

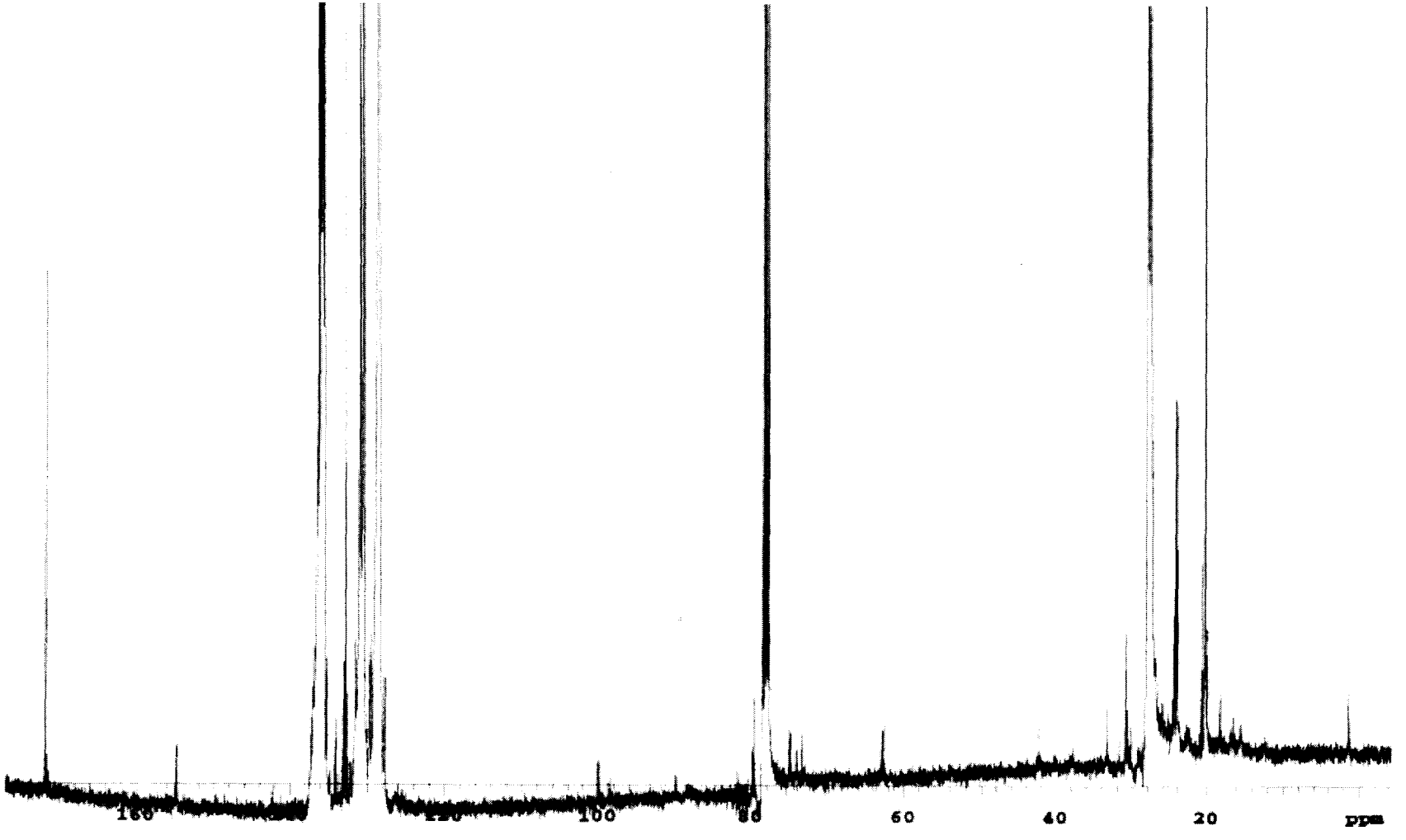

Figure 94: ^{13}C NMR spectrum of **38**

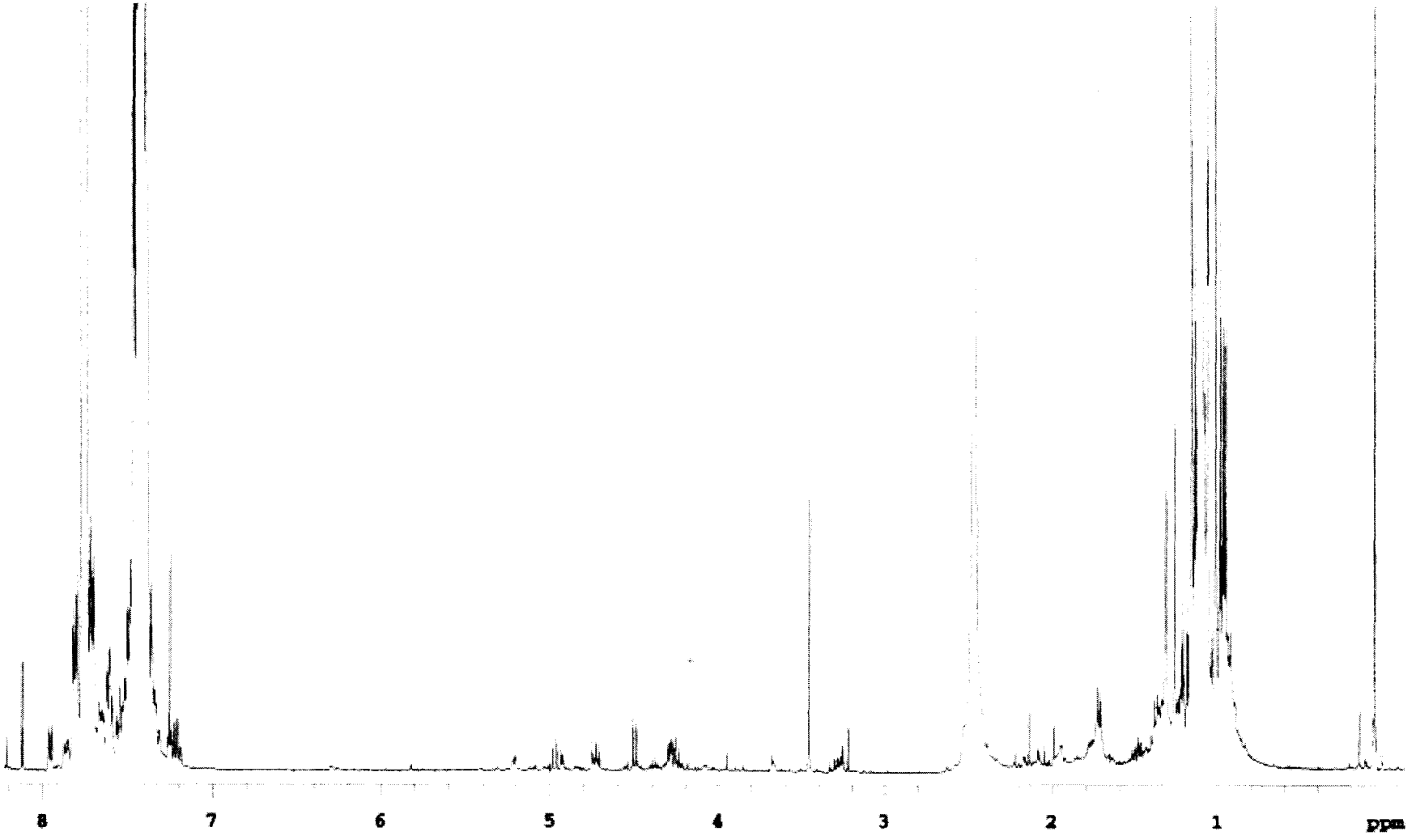

Figure 95: ^{1}H NMR spectrum of **43**

Acquisition Parameter

Ion Source Type	ESI	Ion Polarity	Negative		
Mass Range Mode	Std/Normal	Scan Begin	15.00 m/z	Scan End	2200.00 m/z
Skim 1	-17.0 Volt	Cap Exit Offset	-73.3 Volt	Trap Drive	50.0
Accumulation Time	20000 µs	Averages	10 Spectra		

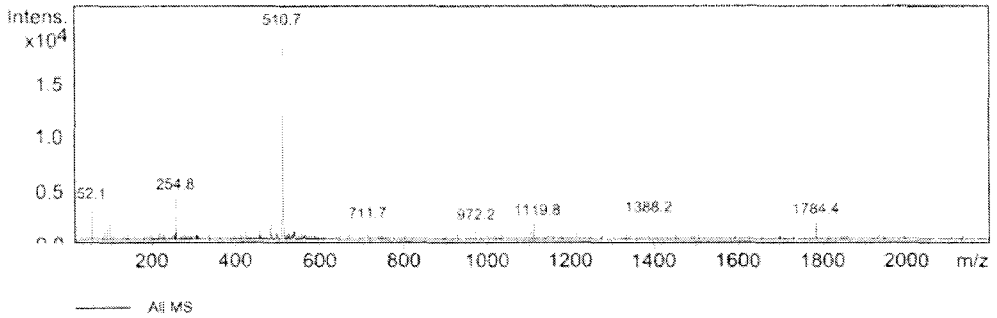

Index	Mass	Intensity	Width	S/N
1	52.12	3903.00	0.03	58.12
2	96.02	2162.00	0.08	32.20
3	254.75	4890.00	0.37	72.82
4	482.66	1773.00	0.25	26.40
5	509.02	1885.00	0.75	28.07
6	510.75	22073.00	0.64	328.79
7	511.65	9861.00	0.48	146.85
8	512.71	4783.00	0.33	71.23
9	513.65	1439.00	0.24	21.43
10	536.60	1446.00	0.20	21.53
11	536.90	1914.00	0.12	28.50
12	711.73	1782.00	0.08	26.54
13	972.22	1636.00	0.03	24.36
14	1035.76	1334.00	0.22	19.87
15	1112.35	1448.00	0.21	21.56
16	1119.83	2103.00	0.12	31.32
17	1318.85	1367.00	0.20	20.36
18	1388.16	2460.00	0.22	36.63
19	1784.43	2276.00	0.14	33.89
20	1786.03	1835.00	0.03	27.33

Figure 96: Mass spectrum of **43**